Vol. 127, June 1, 1981
Complete in one issue

ISSN 0003-2670

ANALYTICA CHIMICA ACTA

International journal devoted to all branches of analytical chemistry

ELSEVIER SCIENTIFIC PUBLISHING COMPANY

ANALYTICA CHIMICA ACTA

International journal devoted to all branches of analytical chemistry
Revue internationale consacrée à tous les domaines de la chimie analytique
Internationale Zeitschrift für alle Gebiete der analytischen Chemie

PUBLICATION SCHEDULE FOR 1981 (incorporating the section on Computer Techniques and Optimization)

	J	F	M	A	M	J	J	A	S	O	N	D
Analytica Chimica Acta	123	124/1	124/2	125	126	127	128	129	130/1	130/2	131	132
Section on Computer Techniques and Optimization		133/1			133/2			133/3			133/4	

Scope. *Analytica Chimica Acta* publishes original papers, short communications, and reviews dealing with ever aspect of modern chemical analysis, both fundamental and applied. The section on *Computer Techniques an Optimization* is devoted to new developments in chemical analysis by the application of computer techniques and b interdisciplinary approaches, including statistics, systems theory and operation research. The section deals with th following topics: Computerized acquisition, processing and evaluation of data. Computerized methods for th interpretation of analytical data including chemometrics, cluster analysis, and pattern recognition. Storage and retrieva systems. Optimization procedures and their application. Automated analysis for industrial processes and qualit control. Organizational problems.

Submission of Papers. Manuscripts (three copies) should be submitted as designated below for rapid and efficien handling:

Papers from the Americas to: Professor Harry L. Pardue, Department of Chemistry, Purdue University, West Lafayette IN 47907, U.S.A.

Papers from all other countries to: Dr. A. M. G. Macdonald, Department of Chemistry, The University, P.O. Box 363 Birmingham B15 2TT, England.

For the section on *Computer Techniques and Optimization:* Dr. J. T. Clerc, Universität Bern, Pharmazeutisches Institut Sahlistrasse 10, CH-3012 Bern, Switzerland.

American authors are recommended to send manuscripts and proofs by INTERNATIONAL AIRMAIL.

Submission of an article is understood to imply that the article is original and unpublished and is not being considered for publication elsewhere. Upon acceptance of an article by the journal, the author(s) resident in the U.S.A. will be asked to transfer the copyright of the article to the publisher. This transfer will ensure the widest dissemination of information under the U.S. Copyright Law.

Information for Authors. Papers in English, French and German are published. There are no page charges. Manuscripts should conform in layout and style to the papers published in this Volume. Authors should consult Vol. 121, p. 353 for detailed information. Reprints of this information are available from the Editors or from: Elsevier Editorial Services Ltd., Mayfield House, 256 Banbury Road, Oxford OX2 7DE (Great Britain).

Reprints. Fifty reprints will be supplied free of charge. Additional reprints (minimum 100) can be ordered. An order form containing price quotations will be sent to the authors together with the proofs of their article.

Advertisements. Advertisement rates are available from the publisher.

Subscriptions. Subscriptions should be sent to: Elsevier Scientific Publishing Company, P.O. Box 211, 1000 AE Amsterdam, The Netherlands. The section on *Computer Techniques and Optimization* can be subscribed to separately.

Publication. *Analytica Chimica Acta* (including the section on *Computer Techniques and Optimization*) appears in 11 volumes in 1981. The subscription for 1981 (Vols. 123–133) is Dfl. 1639.00 plus Dfl. 198.000 (postage) (total approx. U.S. $942.00). The subscription for the *Computer Techniques and Optimization* section only (Vol. 133) is Dfl. 149.00 plus Dfl. 18.00 (postage) (total approx. U.S. $86.00). Journals are sent automatically by airmail to the U.S.A. and Canada at no extra cost and to Japan, Australia and New Zealand for a small additional postal charge. All earlier volumes (Vols. 1–121) except Vols. 23 and 28 are available at Dfl. 164.00 (U.S. $84.00), plus Dfl. 13.00 (U.S. $6.50) postage and handling, per volume.

Claims for issues not received should be made within three months of publication of the issue, otherwise they cannot be honoured free of charge.

Customers in the U.S.A. and Canada who wish to obtain additional bibliographic information on this and other Elsevier journals should contact Elsevier/North Holland Inc., Journal Information Center, 52 Vanderbilt Avenue, New York, NY 10017. Tel: (212) 867-9040.

ANALYTICA CHIMICA ACTA
VOL. 127 (1981)

ANALYTICA CHIMICA ACTA

International journal devoted to all branches of analytical chemistry

ELSEVIER SCIENTIFIC PUBLISHING COMPANY

Anal. Chim. Acta, Vol. 127 (1981)

Printed in The Netherlands.

Analytica Chimica Acta, 127 (1981) 1—21
Elsevier Scientific Publishing Company, Amsterdam — Printed in The Netherlands

Special Report

RECENT DEVELOPMENTS IN pH STANDARDISATION AND MEASUREMENT FOR DILUTE AQUEOUS SOLUTIONS

ARTHUR K. COVINGTON

Electrochemistry Research Laboratories, Department of Physical Chemistry, School of Chemistry, University of Newcastle, Newcastle upon Tyne, NE1 7RU (Gt. Britain)

(Received 27th October 1980)

SUMMARY

The preparation of standard specifications at national and international level on pH measurement has stimulated new experimental work on this important subject, which is reviewed here against the background of continuing international deliberations and controversy about the definition of the pH scale in terms of a single primary standard or multi-primary standards.

The concept of pH, first introduced by Sørensen [1] as

$$pH = -\log c_{H^+} \quad (1)$$

where c_{H^+} is the hydrogen ion concentration (in mol dm^{-3}), was subsequently modified [2] in terms of hydrogen ion activity, a_{H^+}, to

$$pH = -\log a_{H^+} \quad (2)$$

This can only be a notional definition of this quantity, for pH is unique amongst physicochemical quantities in that it involves a single ion activity and, defined in terms of eqn. (2) alone, it is immeasurable. It is thus customary to refer to the definition of pH as an operational one, i.e., it is defined in terms of the operation or method used to measure it. Essentially, this is done by means of the so-called operational cell (I).

$$Hg\ |Hg_2Cl_2|\ KCl\ (\lessdot 3.5\ mol\ dm^{-3})\ \vdots\vdots\ Solution\ |H_2|\ Pt \quad (I)$$

or minor variants of it. The dotted lines indicate a liquid—liquid junction. The cell is standardised by a solution, or solutions, of assigned pH value, and so

$$Hg\ |Hg_2Cl_2|\ KCl\ \vdots\vdots\ X\ |H_2|\ Pt \quad (II)$$

and

$$Hg\ |Hg_2Cl_2|\ KCl\ \vdots\vdots\ S\ |H_2|\ Pt \quad (III)$$

where X represents an unknown (test) solution and S a solution of assigned value, pH(S).

The pH of the unknown, pH(X), is then given by

$$pH(X) = pH(S) - (E_X - E_S)/k - (E_{J(X)} - E_{J(S)})/k \quad (3)$$

where E_X and E_S are the e.m.f. values of cells II and III, respectively; $E_{J(X)}$ and $E_{J(S)}$ are the liquid junction potential contributions arising in cells II and III, and $k = RTF^{-1}$ (ln 10). The measurement of pH is therefore a comparative method as seen by combining cells II and III as cell IV

$$Pt\ |H_2|\ S \overset{\vdots}{\underset{E_{J(S)}}{\vdots}} KCl\ (<3.5\ mol\ dm^{-3}) \overset{\vdots}{\underset{E_{J(X)}}{\vdots}} X\ |H_2|\ Pt \quad (IV)$$

The last term in eqn. (3) is usually referred to as the residual liquid junction potential term, and to evaluate pH(X) from eqn. (3) it is assumed to be zero. This will never be strictly true but it may be a reasonable approximation the more similar are X and S in composition and concentration. As seen more clearly from cell IV, $E_{J(X)}$ is then equal and opposite to $E_{J(S)}$ in its contribution to the e.m.f. of cell IV.

The assignment of pH values to a standard reference solution, or solutions, is done by means of cell V without liquid junction

$$Pt\ |H_2|\ Buffer, Cl^-(m)\ |AgCl|\ Ag \quad (V)$$

in four stages. First, from the Nernst equation for cell V in terms of its e.m.f. (E), the quantity

$$-\log m_H \gamma_H \gamma_{Cl} = (E - E^0)\, k^{-1} + \log m \quad (4)$$

is calculated, where m is the molality (in mol kg^{-1}), γ_H and γ_{Cl} are single ion activity coefficients of hydrogen and chloride ions, respectively, and E^0 is the e.m.f. of the cell

$$Pt\ |H_2|\ HCl\ (a = 1)\ |AgCl|\ Ag \quad (VI)$$

Secondly, the value of $-\log m_H \gamma_H \gamma_{Cl}$ is extrapolated to $m = 0$, usually a small linear extrapolation, to remove the effect of the added chloride; this value may be referred to as $-\log (m_H \gamma_H \gamma_{Cl})^0 = p(a_H \gamma_{Cl})^0$. Thirdly, the introduction of a convention for the single ion activity coefficient of the chloride ion allows pH, as defined notionally be eqn. (2), to be obtained

$$pH(S) = p(a_H \gamma_{Cl})^0 + \log \gamma_{Cl} \quad (5)$$

The convention agreed [3] is referred to as the Bates—Guggenheim convention in which a form of the Debye—Hückel equation is used

$$-\log \gamma_{Cl} = AI^{1/2}(1 + 1.5I^{1/2})^{-1} \quad (6)$$

where I is the ionic strength of the buffer, which should not exceed 0.1 mol kg^{-1} if eqn. (6) is to be valid, and A is the value of the Debye—Hückel limiting slope.

The fourth stage is to repeat the measurements on cell V, which requires also measurements of cell VI, over a temperature range at 5-K intervals.

Values of pH(S) at these temperatures are then fitted to convenient smoothing equations in T (K) such as

$$\mathrm{pH(S)} = AT^{-1} + \mathrm{B} + CT + \mathrm{D}T^2 \quad (7)$$

or

$$\mathrm{pH(S)} = \mathrm{pH(S)}_{298} + \mathrm{b}(T - 298) + \mathrm{c}(T - 298)^2 \quad (8)$$

With the assignment of pH(S) values to several primary standard reference solutions, this method constitutes the multi-primary standard approach [4] pioneered by the National Bureau of Standards (NBS, USA) in the period 1943—69. Most national pH scale recommendations are based on this multi-standard system. Notably different is the British Standard (BS) pH scale [5] which, in contrast, recommends only one primary reference standard but assigns pH(S) values, determined by the operational cell IV, to a number of secondary reference standards. The basis for this different approach, which was initiated by Guggenheim, is the argument that, to define the pH scale (i.e., to define the line of operational cell e.m.f. versus pH), only one point, one primary reference standard, is required, the other parameter being the theoretical slope factor, k. The use of several primary standards constitutes over-definition and must lead to inconsistencies, although these are usually small. It must be emphasized that the definition of pH scales is quite distinct from the measurement of pH with glass—reference electrode—pH meter assemblies where several standards are necessary in order to compensate for possible deficiencies in electrode and meter performance.

At this stage it is convenient to review the historical development of the NBS and BS approaches.

DEVELOPMENT OF THE MULTI-STANDARD (NBS) SCALE

Only post-1944 developments are considered here. Earlier attempts to establish pH scales, notably by Hitchcock and Taylor [6] and MacInnes et al. [7], have been reviewed by Bates [4]. In 1942 Bates et al. [8] presented a list of 17 standard buffers for the calibration of pH meter assemblies at 20, 25 and 30°C. They expressed the hope that pure crystalline buffer salts would ultimately be available to cover the useful pH range in steps of 0.2 in pH. A year later Bates and Acree [9] published pH(S) values for 0.025 mol kg^{-1} equimolal phosphate buffer from 0 to 60°C and this became the first standard buffer. The period 1944—6 saw the work of Hamer et al. [10, 11] on potassium hydrogenphthalate and a third buffer, 0.01 mol kg^{-1} borax, was added in 1946 [12]. Attempts to extend the pH scale downwards led in 1951—3 to the fourth standard, potassium hydrogentartrate, [13] and to the fifth, potassium tetraoxalate [14], but this latter was later relegated to a secondary standard. Similarly, work in 1956 on calcium hydroxide [15] was described as being on the sixth standard but this too was relegated to secondary standard status. The so-called "blood pH" or physiological phosphate

buffer (1:3.5) was then regarded as the fifth standard [16], and Staples and Bates [17] added potassium hydrogencitrate and 0.025 mol kg^{-1} equimolal carbonate—hydrogencarbonate as the sixth and seventh standards.

In 1957 Bower and Bates [18] studied the existing buffers at 60—95°C and in 1962 Bates [19] revised all the previous values in line with the recently agreed convention [3] for the single ion activity coefficient of the chloride ion, and extended the values of pH(S) to three decimal places.

It is pertinent to enquire what leads to a distinction between primary and secondary standard status on the NBS approach. Amongst the criteria are pH between 3 and 11, salts available in highly pure form with good keeping qualities of solution (e.g., not prone to mould growth), but also the expectancy of a small residual liquid junction potential. Thus Tris buffer [tris-(hydroxymethyl)aminomethane], which is known to show abnormal liquid junction potential contributions with certain types of commercial reference electrode junctions [20], is regarded by Bates as a secondary buffer [4]. This feature also precludes selection of similar nitrogenous base substances such as piperazine phosphate [21] and probably tricine [tris(hydroxymethyl)methylglycine [22]] from selection as primary standards (see below). Bates [4] also mentions a second kind of secondary standard, useful for checking performance of pH meter assemblies, with values assigned by operational cell measurements. Examples given include 0.05 mol kg^{-1} borax and 0.1 mol kg^{-1} hydrochloric acid.

DEVELOPMENT OF THE BRITISH STANDARD pH SCALE

Moves to establish a British Standard pH scale began in 1948 when the Royal Society called a special conference of interested parties chaired by the then Director of the National Physical Laboratory (NPL), Sir Charles Darwin. This led to the formation of a British Standards Institution Technical Committee (C34) with Professor E. A. Guggenheim as chairman. British Standard BS1647 based on potassium hydrogenphthalate as the single primary standard, with values based on recalculations of the work of Hamer et al. [10, 11], was published in 1950 [5]. The specification also listed secondary buffers, the pH values of which were established by reference to the primary standard using the operational cell (I), and which were to be used for calibrating pH meter assemblies. The secondary pH values used were those of Hitchcock and Taylor [6] and MacInnes et al. [7]. In 1960, work was initiated on the determination of secondary standard values and was subsequently published [23] but has only recently been incorporated in the revised British Standard. In 1961, BS1647 was revised [24] to take into account the agreement reached by Bates and Guggenheim [3] on the convention for single ion chloride activity and the then recently published values of pH extending the scale from 60 to 95°C [18].

Since 1977, a revision of BS1647 has been in progress based on a redetermination of values of pH(S) for potassium hydrogenphthalate and a sup-

plementation and checking of the results of Alner et al. [23] for the determination of secondary standard values by the operational cell [25]. The operational cell (VI) is used with hydrogen electrodes and the liquid junctions formed with essential cylindrical symmetry [26] within 1 mm capillary tubes using the vessel shown in Fig. 1. Values are now available for 16 secondary standard reference solutions as shown in Table 1. In italics below each entry in Table 1 are given differences (which are nearly always larger) from the NBS values [4] (cell V) in terms of 10^{-3} pH. Some comment is required on these differences which arise not just from residual liquid junction potentials. For phthalate, the differences arise because NBS data are based on the results of Hamer et al. [10, 11] which are slightly in error (see below). Subtraction of these phthalate values from others at each temperature gives values which can be ascribed to residual liquid junction potentials. Strictly, these should be called conventional residual liquid junction potentials (l.j.p.), because their evaluation is based on the adoption of the Bates—Guggenheim convention [3] which led to the NBS assigned values.

Thus, for the 0.025 equimolal phosphate buffer at 25°C, the value of 0.008 is made up of 0.005 residual l.j.p. and 0.003, which is the difference between Hamer's [10, 11] and the new value (4.008—4.005) for phthalate buffer. Likewise at 37°C, 0.007 + 0.006 = 0.013. For the tartrate, the two

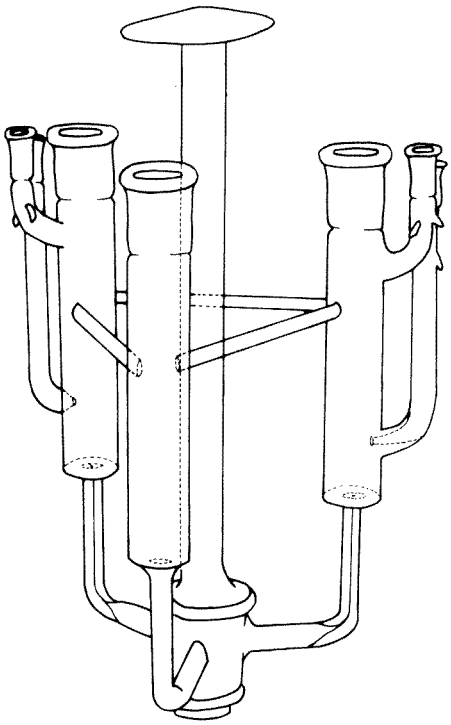

Fig. 1. Cell vessel for operational cell determinations of pH values of secondary reference standards with two liquid junctions formed in 1 mm internal diameter capillary tubing.

TABLE 1

Primary and secondary pH buffers for use in calibrating glass electrode—pH meter assemblies

Buffer	Temp. (°C)												
	0	10	20	25	30	37	40	50	60	70	80	90	95
0.1 mol kg^{-1} Potassium tetraoxalate	—	—	1.475	1.479	1.483	1.490	1.493	1.503	1.513	1.52	1.53	1.53	1.53
0.05 mol kg^{-1} Potassium tetraoxalate	—	1.638	1.644	1.646	1.648	1.649	1.650	1.653	1.660	1.671	1.689	1.72	1.73
		32	*31*	*33*	*35*	*42*	*44*	*54*	*63*	*72*	*77*	*72*	*76*
0.05 mol kg^{-1} Sodium hydrogendiglycolate	—	3.470	3.484	3.492	3.502	3.519	3.527	3.558	3.595	—	—	—	—
		11	*15*	*17*	*18*	*18*	*21*	*22*	*24*				
Saturated potassium hydrogentartrate	—	—	—	3.556	3.549	3.544	3.542	3.544	3.553	3.570	3.596	3.627	3.649
				1	*3*	*4*	*5*	*5*	*7*	*10*	*15*	*23*	
0.05 mol kg^{-1} Potassium hydrogenphthalate	4.000	3.997	4.000	4.005	4.011	4.022	4.027	4.050	4.080	4.116	4.159	4.208	4.235
	3	*1*	*2*	*3*	*4*	*6*	*8*	*10*	*11*	*10*	*5*	*−3*	*−8*
0.1 mol l^{-1} Acetic acid +0.1 mol l^{-1}	4.664	4.652	4.645	4.644	4.643	4.647	4.650	4.663	4.684	4.713	4.75	4.80	4.83
sodium acetate	*19*	*13*	*11*	*10*	*11*	*11*	*11*	*12*					
0.01 mol l^{-1} Acetic acid +0.01 mol l^{-1}	4.729	4.717	4.712	4.713	4.715	4.722	4.726	4.743	4.768	4.800	4.839	4.88	4.91
sodium acetate	*8*	*8*	*8*	*7*	*7*	*5*	*4*	*2*					
0.02 mol kg^{-1} Piperazine phosphate	—	6.419	6.310	6.259	6.209	6.143	6.116	6.030	5.952	—	—	—	—
		34	*28*	*25*	*25*	*24*	*24*	*28*					
0.025 mol kg^{-1} Disodium hydrogenphosphate	6.961	6.912	6.873	6.857	6.843	6.828	6.823	6.814	6.817	6.830	6.86	6.90	6.92
+0.025 mol kg^{-1} potassium dihydrogenphosphate	*19*	*11*	*8*	*8*	*10*	*13*	*15*	*19*	*19*	*15*	*−1*	*−23*	*−34*
0.03043 mol kg^{-1} Disodium hydrogenphosphate	7.506	7.460	7.423	7.406	7.390	7.369	—	—	—	—	—	—	—
+0.008695 mol kg^{-1} potassium dihydrogenphosphate	*23*	*12*	*6*	*7*	*10*	*16*							
0.04 mol kg^{-1} Disodium hydrogenphosphate	—	7.488	7.445	7.428	7.414	7.404	—	—	—	—	—	—	—
+0.01 mol kg^{-1} potassium dihydrogenphosphate													
0.05 mol kg^{-1} Tris hydrochloride	8.399	8.083	7.788	7.648	7.513	7.332	7.257	7.018	6.794	—	—	—	—
+0.01667 mol kg^{-1} Tris	*72*	*58*	*52*	*52*	*50*	*50*	*52*	*52*					
0.05 mol kg^{-1} Borax	9.475	9.347	9.233	9.182	9.134	9.074	9.051	8.983	8.932	8.898	8.88	8.84	8.89
	35	*17*	*12*	*12*	*15*	*19*	*20*	*25*	*24*				
0.01 mol kg^{-1} Borax	9.451	9.329	9.225	9.179	9.138	9.086	9.066	9.009	8.965	9.932	8.91	8.90	8.89
	13	*4*	*0*	*1*	*1*	*−5*	*2*	*2*	*−3*	*−11*			
0.025 mol kg^{-1} Sodium hydrogencarbonate	10.273	10.154	10.045	9.995	9.948	9.889	9.866	9.800	9.753	9.728	9.725	9.75	9.77
+0.025 mol kg^{-1} sodium carbonate	*54*	*25*	*17*	*17*	*18*	*14*	*23*	*28*					
Saturated calcium hydroxide	13.360	12.965	12.602	12.431	12.267	12.049	11.959	11.678	11.423	11.192	10.984	10.80	10.71
	63	*38*	*25*	*23*	*22*	*−6*	*25*	*27*	*26*				

acetate buffers, the two phosphate buffers and 0.01 mol kg^{-1} borax the differences only affect pH measurements of the highest accuracy (±0.003). Buffers of pH <3.5 and >9.5, including the 0.05 mol kg^{-1} borax buffer, show larger differences and this is also true of Tris and the other amine-type buffers. Factors contributing to high conventional l.j.p.'s include high ionic mobilities, high ionic strength and unsuspected formation of new species which could affect the validity of the Bates—Guggenheim convention [3]. Conventional l.j.p.'s at 25°C are plotted in Fig. 2. There is good agreement with previous work of Paabo and Bates [27].

OTHER NATIONAL STANDARD ORGANISATION RECOMMENDATIONS

A recent survey for IUPAC Commission I4 [28] shows that the number of primary standards adopted nationally varies; for example, France recommends 3, Roumania 5, Poland and Hungary 7 and G.F.R. 9. Those that are not regarded as primary standards are secondary standards and obviously the NBS criteria are either accepted or excluded. Table 2 summarizes the situation from the recent survey [28] and further information. The situation regarding the Japanese standard [29] is unclear but potassium hydrogenphthalate is singled out for special mention.

CRITIQUE OF THE MULTI-STANDARD AND SINGLE PRIMARY STANDARD APPROACHES

A summary of the two approaches to the definition of pH scale is shown in Table 3. An essential point of difference between the two approaches is that, with the use of more than one primary standard, a plot of operational cell e.m.f. against assigned pH(S) values, dependent on which primary standards are selected and how many, may not have experimentally the theo-

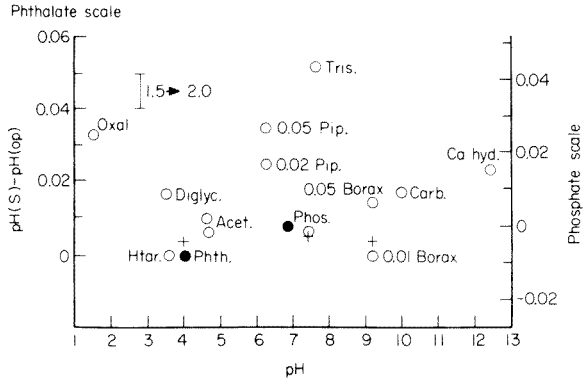

Fig. 2. Plot of pH(S) — pH(operational) vs. pH for some buffer solutions at 25°C. These are values of conventional liquid junction potential; (+) values from Paabo and Bates [27]; (•) reference values.

TABLE 2

Comparison of national pH scale recommendations [28][a]

	Ox.	Tart.	Cit.	Phth.	Acet.	1:1 Phos.	1:3.5 Phos.	Borax	Carb.	Ca Hyd.
France	S	S	—	P	—	P	S	P	S	—
G.F.R.	P	P	P	P	—	P	P	P	P	P
Hungary	P	P	—	P	—	P	P	P	P	—
India	P	P	—	P	—	P	P	P	—	P
Japan	R	—	—	ST	—	R	—	R	R	—
Poland	P	P	—	P	—	P	P	P	—	P
Roumania	—	P	—	P	—	P	P	P	—	—
U.K.	S	—	—	P	S	S	—	S	S	—
U.S.A.	S	P	P	P	—	P	P	P	P	S
U.S.S.R.	P	—	—	P	—	P	—	P	—	—

[a]P = primary; S = secondary; R = reference; ST = standard.

retical slope factor, k. The deviation may be small, as will the deviations of the points themselves from the straight line. Again, it must be emphasized that the experimental method is the operational cell with hydrogen electrodes and liquid junctions formed with cylindrical symmetry and not commercial glass-reference electrode operational cell measurements. The deviations from the best straight line or theoretical line are principally due to residual liquid junction potentials and Fig. 2 is essentially another way of showing this. A smaller effect arises from the use of the Bates—Guggenheim convention [3] for every primary buffer. The effect of a change, at 0.1 mol kg^{-1} ionic strength level, of the denominator factor from 1.5 to 2.0 is shown in Fig. 2. The Bates—Guggenheim convention is a reasonable one judged by our knowledge of simple mixed electrolytes containing, e.g., HCl + KCl. In the complex buffer solutions selected as primary standards, there may be doubts as to its inherent applicability, not least in terms of the well-known deficiencies of the Debye—Hückel theory itself.

A corollary of the fact that the slope of the operational cell e.m.f. vs. pH(S) plot is not theoretical is that a measured pH(X) will depend on which standard buffer is used (eqn. 3), even if the measurement is made with hydrogen electrodes and liquid junctions with cylindrical symmetry. Measurements with commercial glass—reference electrode—pH meter assemblies will only confuse the issue. The differences will be small, fortunately, of the order of ±0.02 in pH in most cases. This situation cannot arise if a single primary standard scale is accepted. All measurements are then traceable back to the single primary standard in terms of secondary standards with pH(S) values assigned through the operational cell IV. By definition, therefore, the plot of operational cell e.m.f. against pH(S) is a perfect straight line of theoretical slope when hydrogen electrodes and cylindrical liquid junctions are employed. The slope may be less than theoretical when commercial glass—reference electrode—pH meter assemblies are used. Use of the bracketing

TABLE 3

Summary of the two approaches to pH scales and measurement

	Multi-standard	Single standard
Number of primary standards	5—7	1
Number of secondary standards	Some at high and low pH	Infinity in principle, including high ionic strength buffers
Determination of $pa_H\gamma_{Cl}$	Harned cell for all primary standards	Harned cell for single primary standard
Bates—Guggenheim convention for γ_{Cl}	Applied to all primary standards at all T	Applied to single primary standard at all T
Determination of secondary standards (S_2)	Harned cell (pa_H) or operational cell	Operational cell with liquid junction formed with cylindrical symmetry
E_H versus pH(S)	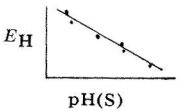 Points may scatter and best slope may not be theoretical depending on number and which standards used	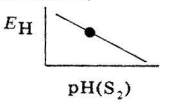 Single point, slope defined as theoretical
Determination of pH(X) with glass—calomel cell with liquid junction	Operational cell with one or two primary standards	Operational cell with one secondary standard, or two secondary standards (primary standard can be one of these)
Inconsistency Test	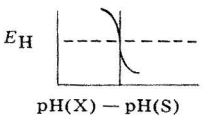 Inconsistency arises from residual liquid junction potential or ion-size incorrectly given	Cannot be inconsistent but pH(X) incorporates any residual liquid junction potential between S and X.
Advantages	2 or more primary standards can be used to check glass electrodes. Primary standards available as SRM's.	Defined by single substance. High-purity specification required on one substance only. 2 or more secondary standards can be used to check g.e. Secondary standards consistent, available as SRM's or user-determined. Easy to change to different primary standard (additive correction) and to special pH scales. Requires no changes to take advantage of improvements in measurement.
Disadvantages	Primary standards are inconsistent when measured in operational cell. Disagreement about number of primary standards. Uncertainty for accuracy class 0.02 (0.003 pH) depending on which primary standard used. Residual liquid junction potential incorporated in pH(X).	Residual liquid junction potential incorporated in pH(X) and pH(S).

procedure, whereby two standard buffers are chosen one on each side of the pH of the unknown X, is a valid procedure for practical pH measurements on both approaches. Use of bracketing with operational cell measurements with hydrogen electrodes and properly formed liquid junctions would lead essentially to the plot of operational cell e.m.f. versus pH(S) values on the multi-standard approach being a series of short intersecting straight lines, none necessarily of theoretical slope, and the dependence of pH(X) on selected buffer would thereby be avoided, provided it were agreed always to employ the next higher and next lower primary standard buffer of a rigidly agreed number of primary standards.

The intention behind the operational definition of pH is that it should yield numbers that are reproducible from place to place and at different times, but have as much significance in terms of hydrogen ion activity or concentration as possible. From a metrological point of view, a reproducible scale of numbers (i.e., not subject to which standard buffer is chosen) is essential. The inconsistencies of the NBS multi-standard scale are small only because the primary standards are selected from substances which show only small residual liquid junction effects; substituted amine-type substances are excluded from selection as primary standards.

It is generally agreed that a measured pH(X) can only be interpreted in terms of hydrogen ion activity (or concentration) when the properties of the unknown substance(s) in solution match those of the standard buffer in composition and concentration. Guggenheim wrote succinctly [30] about the single ion activity terms, that

$$\mathrm{pH} = -\log a_{\mathrm{H}^+} = -\log c_{\mathrm{H}^+} y_? \qquad (9)$$

where $y_?$ is a complicated function represented approximately by the mean ionic activity coefficient of a typical 1:1 electrolyte which places an uncertainty of ± 0.02 on pH, corresponding to 4.7% in hydrogen ion concentration. Most pH measurements, certainly in industry, are concerned with the reproducibility of the parameter pH and perhaps only 1 or 0.1% of pH measurements are made with a view to interpretation. Nearly all these are made by research workers who may be measuring pH when an alternative approach would be better. The vast majority of pH measurements, where only a reproducible scale of numbers is required, must not be subjugated to the requirements of a tiny minority of chemists who want to try to interpret pH measurements. It is essential that the reproducibility aspect of pH measurements is dominant. There are three special examples of applications where species concentrations are calculated from hydrogen ion concentrations obtained from pH measurements. All of these involve media of higher ionic strength. The complex-ion chemists have solved the problem in their own way [31]. The clinical biochemist and the oceanographer are particularly important users where special procedures are required; these will be discussed later in this report.

With the single primary standard approach, the number of secondary

standards available can be very large and added to as appropriate. In order to make a measurement of an "unknown", one selects the secondary standard closest to it in composition and pH (one is never entirely ignorant of the composition of an unknown). Under these conditions, the residual liquid junction potential in cell IV is likely to be small. There remains inherent in (built into) the measured pH(X), the liquid junction potential between potassium hydrogenphthalate and potassium chloride. The selection of potassium hydrogenphthalate as the single primary standard effectively takes with it a convention that this liquid junction potential is zero. Apart from Henderson [32] equation calculations (which are notoriously unreliable because of the assumption of constant mobilities across the junction), there are indications from Fig. 2 that this l.j.p. is small. The l.j.p. between equimolal phosphate and potassium chloride is almost the same, as seen in Fig. 2, and it is unlikely that two such dissimilar types of buffer substance would have similar values if they were not otherwise almost zero.

A further advantage of the selection of a single primary standard scale is that related scales of pH appropriate to, say, mixed aqueous media (e.g., 20% methanol—water) can be simply related to the dilute aqueous scale by the properties of one substance through its free energy of transfer between the two solvents, which, in principle at least, is measurable. The same is true if the other "solvent" is, in fact, a concentrated salt solution, e.g., $NaClO_4$ + H_2O, sea water, or isotonic saline.

The analogy between the single primary standard definition of pH scale and the definition of thermodynamic temperature in terms of one fixed point (the triple point of water) and the slope (273.15^{-1}) has been invoked and is worth exploring in detail since it has been criticised. Like most analogies it is good only up to a point. The fixed points of the thermodynamic temperature scale are established from the equation

$$T = \underset{P \to 0}{\mathrm{Lt}}\ PV(P_oV_o)^{-1}T_o \qquad (10)$$

where the subscript o refers to conditions at the triple point of water (273.16 K), and eqn. (10) refers to the use of a gas thermometer containing a real gas and the need to extrapolate to zero pressure to approximate to the properties of an ideal gas. A detailed comparison of the definition of temperature and its comparison with pH is given in Table 4. That pH is not a thermodynamic quantity is irrelevant to these considerations except that a non-thermodynamic convention is required to establish the single ion activity coefficients and it is the multiple use of this convention which is a contributory factor in the inconsistencies of the multi-point scale. There are three other differences: (a) the triple point of water is a uniquely obvious fixed point (primary standard) and no such obvious primary standard exists for pH; (b) at present, the values assigned to pH standards can vary with the source of the material; (c) the single primary standard approach utilises a different experimental method for secondary standard determination compared with that for primary standard value assignment.

TABLE 4

Comparison of approaches to the definition and measurement of temperature and pH

	T	pH
Definition of quantity	Second law of thermodynamics	$-\log a_{H^+}$
Definition of scales	Kelvin scale	
A) Fixed point	Triple point of water	pH of one primary standard
B) Slope	1/273.15	(RTF^{-1}) ln 10
C) Measurement	Gas thermometer (P → 0)	Harned cell (chloride → 0)
D) Convention	None	Bates—Guggenheim for γ_{Cl}
Secondary or reference standards: Measurement	Gas thermometer (P → 0)	*BS*: H_2|PS|KCl|SS|H_2 l.j. formed with cylindrical symmetry; *NBS*: as for primary standard
Number	6 including triple point	An infinite number in principle; 10
Practical measurement	International temperature scale 1927—1968	
A) Method/apparatus	Pt resistance thermometer Pt-Pt/Rh thermocouple Optical pyrometer	Glass—calomel electrodes—pH meter
B) Corrections	For interpolation errors	For errors of glass electrodes, sub-Nernstian slopes, residual l.j.p.

The definition of pH is an operational one but the operational cell is of paramount importance in pH measurements for definition and for measurement. However, the multi-standard approach accords much more significance to the cell without liquid junction, and it really would be more sensible on this approach to maintain that pH is defined operationally in terms of the cell without liquid junction but measured with the cell with liquid junction.

It has been suggested that the current situation whereby most nations accept the multi-standard approach has not caused difficulties and that tremendous costs and a chaotic situation would result in the interim with two systems in operation. This is not so. Costs to industry would be negligible as few industrial measurements would be affected. Manufacturers of pH equipment would also be unaffected; the latest pH meters with microprocessors and pH standard reference values in memory stores could easily be modified. Certification of standard reference materials will still be required but by a different procedure (cell IV instead of cell V) and the numbers on certificates will be slightly different. No chaotic situation need arise with the right publicity for the changes. As a counter to the argument that most national standards specifications would have to be changed, one must insist that no standard should be considered immutable since standards must encourage progress not preclude it. Further advances in accuracy and precision of pH measurements could follow from adoption of the single primary standard pH scale.

RECENT WORK ON POTASSIUM HYDROGENPHTHALATE

All national scales of pH include amongst their standard reference buffers the solution, with molality 0.05 mol kg^{-1}, of potassium hydrogenphthalate (KHPh), first suggested as a pH standard by Dodge [33] and studied by Hamer et al. [10, 11] at NBS. It is essential for a single primary standard pH scale that the purity requirements are well established and assigned pH(S) values are known accurately. A single substance for the preparation of a standard reference solution is preferable to a two-substance buffer such as phosphate, even though, since the pH of the latter is in the vicinity of the neutral point, the latter has its attractions. The phthalate buffer is probably the most studied of the buffer substances commonly available and yet there are some features about KHPh that have caused some to doubt its suitability. Some of these doubts arise from problems with its use as an acidimetric standard in Europe although it is widely used as such in the U.S.A. Secondly, measurements using cells without liquid junction for the certification of samples of standard reference material tend to be more variable than with other standard buffers to judge from the values given on NBS certificates (Table 5). Guggenheim, in recalculating the results of Hamer et al. [10, 11] and Bower and Bates [18] for BS1647, recognized that the two sets of data were inconsistent and fitted the data to two separate polynomials in temperature above and below 55°C.

Purity estimation

The adequate purity of a sample as a standard reference material is judged at NBS by measurements with the cell without liquid junction. No independent purity check was made apart from acidimetric estimation and the usual specification for recognized analytical-grade chemicals. The method for preparation of KHPh is catalytic oxidation of naphthalene or tetrahydronaphthalene to *o*-phthalic anhydride, which with water gives *o*-phthalic acid and on half-neutralisation by potassium carbonate, potassium hydrogen-*o*-

TABLE 5

Values of pH(S) for 0.05 mol kg^{-1} KHPh from NBS Certificates[a]

T (°C)	185c (1964)	185d (1967)	185e (1973)	T (°C)	185c (1964)	185d (1967)	185e (1973)
0	4.003	4.012	4.003	40	4.035	4.033	4.030
5	3.999	4.005	3.998	45	4.047	4.045	4.042
10	3.998	4.002	3.996	50	4.060	4.058	4.055
15	3.999	4.001	3.996	55	4.075	4.073	4.070
20	4.002	4.003	3.999	60	4.091	4.089	4.085
25	4.008	4.008	4.004	70	4.126	4.12	4.12
30	4.015	4.014	4.011	80	4.164	4.16	4.16
35	4.024	4.023	4.020	90	4.205	4.20	4.19
37/38	4.030	—	4.024	95	4.227	4.22	4.21

[a]Certificates prior to 1964 gave values to 0.01 only.

phthalate. Smith [34] showed that repeated recrystallisation of KHPh above 35°C was necessary to avoid co-crystallisation of phthalic acid from slightly acidic samples and this is the common commercial practice. Examination for likely impurities such as quinones and isomeric phthalic acids proved negative and recent work [35, 36] has shown that the commonest impurity of KHPh is phthalic acid which appears to be on the surface of the KHPh crystals rather than dispersed throughout the material. For this reason, it is inadvisable to grind the samples. Jee [35] and Covington and Utting [36] have recently devised methods of ether extraction of phthalic acid from KHPh samples and its estimation by u.v. spectrophotometry. The method is capable of detecting <0.003% (w/w) phthalic acid with a reproducibility of ±10% between samples. Free acid contents of 0.05% (w/w) are not uncommon, corresponding to a pH(S) error of −0.002. The phthalic acid contents of some samples are shown in Table 6. The use of the cell without liquid junction to establish the identity of samples of KHPh is a specialised and time-consuming procedure. A simpler method based on the cell

Pt $|H_2|$ Sample A ⁝ Sample B $|H_2|$ Pt (VII)

has been devised by Baucke [37], who was investigating the possible change in standard reference solutions on heat sterilisation. The cell vessel is a simple H-shape, with the two samples forming a liquid junction at a vertical sintered glass disc (porosity 4). Because samples will differ only slightly, no liquid junction potential is involved and any e.m.f. of cell VII indicates a difference in hydrogen ion concentration between samples. The technique is simpler than that with a potassium chloride bridge solution between the samples. It is, however, essential that the hydrogen leaving each hydrogen

TABLE 6

Comparison of KHPh samples by phthalic acid ether extraction and comparator cell methods

Sample	Phthalic acid concn. ($\times 10^{-4}$ %, w/w)	Cell (mV)[a]	
BDH Analar	4.8	Reference	
NBS 185c	4.5	−0.08	−0.03
NBS 84h	4.5	−0.05	−0.02
BDH pH standard	3.0	—	
BDH Analar (new sample)	3.0		Reference
BDH Analar (new sample) recryst. + K_2CO_3	2.1		−0.03, −0.04, −0.02
"Bad" sample	2.7×10^4		+5.8
"Bad" sample 1 × recryst. + K_2CO_3	210		
"Bad" sample 2 × recryst. + K_2CO_3	120		

[a]Plus sign indicates that sample is more acid than reference.

electrode compartment is taken to a common exit tube to ensure that the exit pressures are identical. By this method, as Table 6 shows, three U.K. samples (BDH Ltd. Poole, Dorset) were shown to be almost identical with NBS SRM 185c and 84h. Recrystallising a good sample, with addition of a trace of potassium carbonate, slightly improves the sample. A really bad sample containing 2.7% phthalic acid was improved by recrystallisation but even a second recrystallisation above 35°C was not sufficient to bring the phthalic acid to an acceptable level. A comparison between the ether extraction method and precise potentiometric titrations yielded a similar correlation of sample properties [35], but the use of cell VII is simpler. Few samples appear to be too alkaline, but if a sample shows no ether extraction of phthalic acid the presence of dipotassium phthalate should be suspected and may be confirmed with cell VII.

Redetermination of pH(S) values

Recently Bütikofer and Covington [38] redetermined pH(S) values for 0.05 mol kg^{-1} KHPh from 0 to 85°C. The material used was samples from BDH (Poole, Dorset), but a few measurements with NBS SRM 185c were not detectably different. The cell used was

$$\text{Pt} \mid \text{Pd} \mid \text{H}_2 \mid \text{KHPh, (0.05 mol kg}^{-1}\text{) KCl } (m) \mid \text{AgCl} \mid \text{Ag} \qquad \text{(VIII)}$$

with m = 0.005—0.05 mol kg^{-1}. The analysis was made with eqn. (4) combined with eqn. (8) by multilinear regression analysis [39]. A recent publication from NBS [40] in fact relates to a determination on SRM 185c in 1966, and more recent work on 185e by Etz has not been published [41]. The analysis [39] showed that the latest NBS work and that of Bütikofer and Covington [38] are in close agreement, as shown in Table 7 (columns six and seven).

Recalculation of previous work on pH(S) values of KHPh

The multilinear regression analysis [39] was used to re-analyse the results of Hamer et al. [10, 11], Bower and Bates [18] and Bates et al. [40] (kindly provided by Professor Bates), together with the most recent data of Etz (kindly provided by Drs. Durst and Etz) [41]. A particular problem in this re-analysis was knowing what value of E° (cell VI) to use in the calculations, bearing in mind that an uncertainty of 0.1 mV leads to an uncertainty of 0.001_7 in pH, which is only slightly temperature-dependent. At 0°C, E° is probably uncertain by as much as ±0.2 mV [39]. Results are shown in columns 3, 5 and 6 of Table 7, and plotted as a deviation function in Fig. 3.

Following the work of Hamer et al. [10, 11] on the acidimetric SRM 84a and its issue as pH SRM 185a, the procedure at NBS for certification of new batches of SRM has varied between a complete redetermination at three potassium chloride concentrations over a wide range of temperature (0—60°C), and a single-point determination at one temperature and one chloride concentration. In the latter case, the values given on the SRM certificate were

TABLE 7

Summary of recalculated pH(S) values for 0.05 mol kg^{-1} KHPh

T (°C)	NBS	Hamer et al.	Bower & Bates	Hetzer et al.	Etz	Bütikofer & Covington	Combined NBS
0	4.003	4.000	—	4.008	4.001	4.000	4.003
5	3.999	3.997	—	4.004	3.998	3.998	4.000
10	3.998	3.995	—	4.002	3.997	3.997	3.999
15	3.999	3.996	—	4.002	3.998	3.998	3.999
20	4.002	3.999	—	4.003	4.000	4.001	4.002
25	4.008	4.004	—	4.007	4.005	4.005	4.005
30	4.015	4.011	—	4.013	4.011	4.011	4.011
35	4.024	4.020	—	4.021	4.019	4.018	4.018
37	4.028	4.024	—	4.024	4.022	4.022	4.022
40	4.035	4.031	—	4.031	4.028	4.027	4.027
45	4.047	4.045	—	4.043	4.039	4.038	4.038
50	4.060	4.060	—	4.056	4.053	4.050	4.051
55	4.075	4.077	—	4.072	4.067	4.064	4.065
60	4.091	4.096[a]	4.082	4.090	4.084	4.080	4.081
65	4.108	4.118	—	4.110	4.102	4.097	4.099
70	4.126	4.141	4.124	4.132	4.122	4.116	4.119
75	4.145	4.166	—	4.156	4.144	4.137	4.140
80	4.164	4.194	4.162	4.183	4.168	4.159	4.163
85	4.184	4.223	—	4.211	4.193	4.183	4.188
90	4.205	4.255	4.202	4.241	4.220	4.208	4.215
95	4.227	4.289	4.231	4.273	4.249	4.236	4.243

[a](.....) Limit of experimental measurements.

calculated at other temperatures by reference to previous data. Table 8 summarizes the investigations made in 1944—73 as extracted from NBS notebooks kindly made available by Professor Bates. All data distinguished by an asterisk in Table 8 were subjected to the multilinear regression analysis [39], giving a total of 622 data points covering almost 30 years work and five different SRM samples. Where additional data existed, only those pertaining to three potassium chloride molalities (0.005, 0.010 and 0.015 mol kg^{-1}) were used. Data on acidimetric sample 85e were excluded when found to be discrepant. The results of this re-analysis are shown also in Table 7, last column. A plot of residuals versus temperature is shown in Fig. 4. It should be noted that the results of this re-analysis, the latest NBS data of Etz [41] and the new results of Bütikofer and Covington [38] are in excellent agreement (deviations between 0 and 60°C are no more than 0.003) but differ from the accepted NBS data [19] which are based on the work of Hamer et al. [10, 11], and its re-analysis. Further, the 60—90°C experimental results of Bower and Bates [18] (column 4 in Table 7) are consistent with later determinations [38, 41].

It is concluded that pH(S) values for KHPh (0.05 mol kg^{-1}) are now established to ±0.001 for material that can now be readily produced in a high

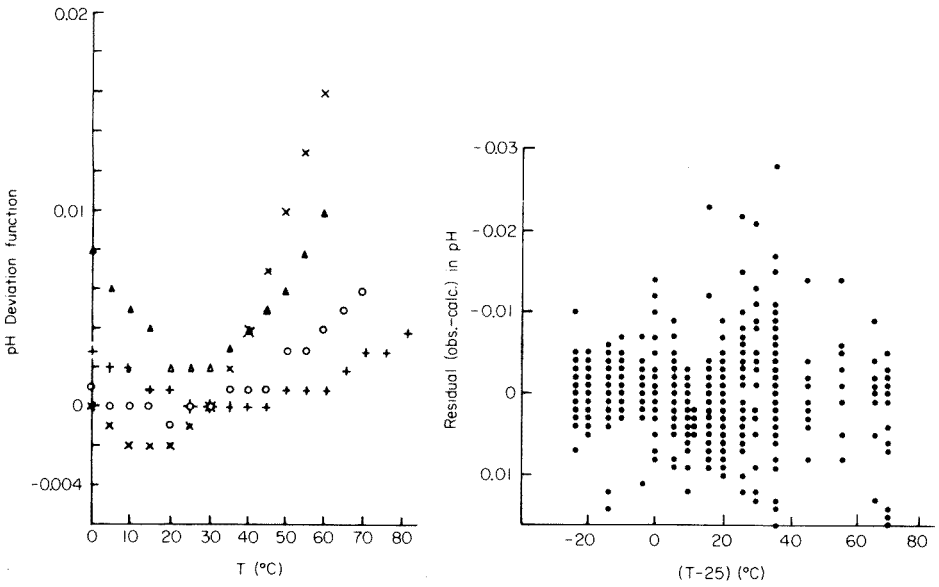

Fig. 3. pH deviation plot for recalculated results by multilinear regression [39]. The base line is the work of Bütikofer and Covington [38]. (×) Hamer and Acree [10]; (○) Etz [41]; (△) Hetzer et al. [21]; (+) combined NBS data.

Fig. 4. Computer multilinear regression analysis of combined NBS data.

TABLE 8

Summary of NBS determinations on 0.05 mol kg^{-1} KHPh

Data set	Date	SRM	KCl (mmol kg^{-1})	Temp. range	Worker(s)
1	1944	84a	1—50	0—60(5°)	Hamer & Acree
2	1946	84b	2—50	0—60(15°)	Hamer et al.
3[a]	7/52	185a	5, 10, 15	25, 30, 60, 50, 25	
4	11/54	185a	5, 10, 15	25, 60	Bower
5	4/54	185a	5, 10, 15	30, 60, 70, 80, 90, 95	Bower
6	4/55	185a	10	25, 40, 50, 60, 25	Bates
7[a]	6/55	85e	10	25, 0, 10—60, 25	
8	7/55	185b	10	25, 60, 25	Bates
9	7/55	84a	10	25, 60, 25	
10	8/58	185c	5, 10, 15	0—60	
11	9/58	185c	5, 10	25, 50, 55, 60, 25	
12[a]	2/64	185c	10	25	
13	1966	185d = 84g	5, 10, 15	0—35, 40—60	Hetzer
14[a]	1966	84a	10	25, 40—60	Hetzer
15	1973	185e	5, 10, 15	1—70	Etz

[a]Not included in the data re-analysis given in the last column of Table 7.

state of purity. KHPh is therefore highly suitable as the single primary reference solution. Its low buffer capacity is only a minor disadvantage.

PRACTICAL pH MEASUREMENTS

The single primary reference solution, like the original platinum bar metre standard in Paris, need never be used for practical measurements, If it is so used, it takes on the status of a secondary standard also. There seem to be some indications that glass electrodes after use in KHPh show longer response times. Even if this is so, it has no bearing on the suitability of KHPh as the single primary standard.

There is good evidence accumulated now that new glass electrodes follow closely the potential of hydrogen electrodes in alkali metal ion-free solutions in the pH range 1—12 [42—44]. Yet when glass-reference electrode pairs are calibrated in the operational cell using a variety of buffers with pH values assigned on either the multi-standard or single primary standard scales they show less than the theoretical slope (often described as sub-Nernstian behaviour). This behaviour is attributable to the behaviour of the reference electrode and depends on the method of forming the junction. Table 9 shows results with some different types of commercial junction [25]. Similar results have been obtained independently by Bates and White [45].

The medical biochemical field has already been mentioned as one where the interpretation of pH measurements is practised in order to obtain species concentrations in body fluids. The ionic strength of these fluids is high, 0.16 mol kg^{-1}, and beyond the range of applicability of the Bates—Guggenheim convention [3]. Only the two phosphate buffers (1:1 and 1:3.5, sometimes 1:4) are used in medical pH measurements. It so happens by coincidence that the phosphate buffers have a higher ionic strength (0.1 mol kg^{-1}) than most of the other commonly used buffers. Inconsistencies occur if buffers like Tris or tricine are used. Part of these inconsistencies can be removed if the ionic strength of other buffers is raised by the addition of sodium chloride [46] to the 0.16 level. Medical pH measurements are therefore a special

TABLE 9

Tests of the response of some types of reference electrode against the hydrogen electrode in buffers of pH 1.68—9.20 at 25°C

Type of junction	Slope (mV/pH)[a]
Ceramic plug	58.78 ± 0.07
Fibre plug	59.04 ± 0.05
Ground-glass sleeve	59.28 ± 0.13
Within 1-mm capillary tube	59.23 ± 0.10
(Theoretical)	59.16

[a]Based on NBS values of pH(S).

case akin to sea water [47] where it is appropriate to use buffers of ionic strength matched to those of the sample in order to reduce the residual liquid junction potential. For routine measurements of blood and blood serum, the use of the two-phosphate solutions is well established with high reproducibility [48] and is adequate because all that is required is a reproducible scale of numbers for routine clinical diagnosis. For sea water with ionic strength 0.7 mol kg^{-1} these problems are exacerbated and special sea-water pH scales have been suggested [49, 50].

CONCLUDING REMARKS

The adoption of the single primary standard pH scale represents a simplification of existing procedures and is the only correct one from a metrological point of view. Potassium hydrogenphthalate is the most suitable substance for use as the single primary standard at present. There will be no effect of change in the definition of the pH scale on the great majority of pH measurements and on virtually all industrial pH measurements. Multi-point standardisation of pH meter assemblies with standard reference materials supplied by manufacturers and national metrological institutes will still be the usual procedure.

Most of the arguments presented in this review have been rehearsed and developed during international discussions on pH scales and standards over the past three years and work on KHPh was stimulated by the revision of the British Standard BS1647 (1981) and subsequent international developments. The subject of pH scales has been discussed since 1977 in IUPAC Commissions I3 and V5 and this led to the holding of an IUPAC-sponsored conference of pH experts in Lisbon in June 1980 [51]. The International Standards Organisation (ISO) and International Electrotechnical Commission (IEC) currently have documents on pH in preparation and the Organisation for Legal Metrology has very recently approved a document on pH scales for dilute aqueous solutions. There are signs that the single primary standard scale is becoming increasingly accepted particularly by nations who are preparing their first national standards, while deep-rooted opposition exists in the U.S.A. and G.F.R. in particular. In the light of this controversy where agreement of the experts falls short of a consensus [51], it seemed appropriate to present the facts in this review for wider consideration.

In spite of the disagreements between experts, it is a pleasure to acknowledge the friendly atmosphere in which the various discussions have taken place. I am particularly indebted to Professor Roger Bates for his kind co-operation in providing original data for re-analysis. I am also grateful for the support given by members of British Standards Institution Technical Committee LBC/16, in particular by Dr. B. J. Birch, Mr. A. E. Bottom, Professor V. Gold, Dr. A. J. Head, Dr. J. Jackson, Dr. R. D. Jee, Dr. P. O. Kane and Mr. A. G. Smeeth.

REFERENCES

1 S. P. L. Sørensen, Biochem. Z., 21 (1909) 131, 201.
2 S. P. L. Sørensen and K. Linderstrøm-Lang, C. R. Trav. Lab. Carlsberg, 15 (1924) No. 6.
3 R. G. Bates and E. A. Guggenheim, Pure Appl. Chem., 1 (1960) 163.
4 R. G. Bates, Determination of pH. Theory and Practice, 2nd. edn., J. Wiley, New York, 1973, pp. 71, 73, 86, 89.
5 British Standards Institution, Specification for pH Scale BS1647 (1950).
6 D. I. Hitchcock and A. C. Taylor, J. Am. Chem. Soc., 59 (1937) 1812; 60 (1938) 2710.
7 D. A. MacInnes, D. Belcher and T. Shedlovsky, J. Am. Chem. Soc., 60 (1938) 1094.
8 R. G. Bates, W. J. Hamer, G. G. Manov and S. F. Acree, J. Res. Natl. Bur. Stand., 29 (1942) 183.
9 R. G. Bates and S. F. Acree, J. Res. Natl. Bur. Stand., 34 (1945) 373.
10 W. J. Hamer and S. F. Acree, J. Res. Natl. Bur. Stand., 32 (1944) 215; 35 (1945) 381.
11 W. J. Hamer, G. D. Pinching and S. F. Acree, J. Res. Natl. Bur. Stand., 35 (1945) 539; 36 (1946) 47.
12 G. G. Manov, N. J. DeLollis, P. W. Lindvall and S. F. Acree, J. Res. Natl. Bur. Stand., 36 (1946) 543.
13 R. G. Bates, V. E. Bower, R. G. Miller and E. R. Smith, J. Res. Natl. Bur. Stand., 47 (1951) 433.
14 V. E. Bower, R. G. Bates and E. R. Smith, J. Res. Natl. Bur. Stand., 51 (1953) 189.
15 R. G. Bates, V. E. Bower and E. R. Smith, J. Res. Natl. Bur. Stand., 56 (1956) 305.
16 V. E. Bower, M. Paabo and R. G. Bates, J. Res. Natl. Bur. Stand., 65A (1961) 267.
17 B. R. Staples and R. G. Bates, J. Res. Natl. Bur. Stand., 73A (1969) 37.
18 B. E. Bower and R. G. Bates, J. Res. Natl. Bur. Stand., 59 (1957) 261.
19 R. G. Bates, J. Res. Natl. Bur. Stand., 66A (1962) 179.
20 R. A. Durst and B. R. Staples, Clin. Chem., 18 (1972) 206.
21 H. B. Hetzer, R. A. Robinson and R. G. Bates, Anal. Chem., 40 (1968) 634.
22 R. G. Bates, R. N. Roy and R. A. Robinson, Anal. Chem., 45 (1973) 1663.
23 D. J. Alner, J. J. Greczek and A. B. Smeeth, J. Chem. Soc. (A), (1967) 1205.
24 British Standards Institution, Specification for pH Scale BS1647 (1961).
25 A. K. Covington and M. J. F. Rebelo, unpublished work, 1979.
26 E. A. Guggenheim, J. Am. Chem. Soc., 52 (1930) 1315.
27 M. Paabo and R. G. Bates, unpublished work, quoted in ref. 4, p. 85.
28 R. A. Durst and J. P. Cali, Pure Appl. Chem., 50 (1978) 1485.
29 Japanese Industrial Standard, Methods for Determination of pH of Aqueous Solutions, JIS Z8802 (1978).
30 E. A. Guggenheim, J. Phys. Chem., 34 (1930) 1758.
31 W. A. E. McBryde, Analyst, 94 (1969) 337.
32 P. Henderson, Z. Phys. Chem., 59 (1907) 118; 63 (1908), 325.
33 F. D. Dodge, J. Am. Chem. Soc., 42 (1920) 1655.
34 S. B. Smith, J. Am. Chem. Soc., 53 (1930) 3711.
35 R. D. Jee, Analyst, 105 (1980) 462.
36 A. K. Covington and A. J. Utting, Analyst, 105 (1980) 470.
37 F. G. K. Baucke, Chem. Eng. Technol., 49 (1977) 739.
38 H. P. Bütikofer and A. K. Covington, Anal. Chim. Acta, 108 (1979) 179.
39 H. P. Bütikofer, A. K. Covington and D. A. Evans, Electrochim. Acta, 24 (1979) 1071.
40 R. G. Bates, R. A. Durst, H. B. Hetzer and R. A. Robinson, J. Res. Natl. Bur. Stand., 81A (1977) 21.
41 E. Etz, unpublished work, 1973.
42 M. F. G. F. C. Camoes and A. K. Covington, Anal. Chem., 46 (1974) 1547.
43 A. K. Covington and M. I. A. Ferra, Anal. Chem., 49 (1977) 1363.

44 C. Mehrbach, C. H. Culberson, J. E. Hawley and R. M. Pytkowicz, Limnol. Oceanogr., 18 (1973) 897.
45 R. G. Bates and D. R. White, unpublished work, 1979.
46 R. G. Bates, C. A. Vega and D. R. White, Anal. Chem., 50 (1978) 1295.
47 K. H. Khoo, R. W. Ramette, C. H. Culberson and R. G. Bates, Anal. Chem., 49 (1977) 29.
48 B. D. Minty and J. F. Nunn, Ann. Clin. Biochem., 14 (1977) 245.
49 I. Hansson, Deep Sea Res., 20 (1973) 479.
50 T. Almgren, D. Dyrssen and M. Strandberg, Deep Sea Res., 22 (1975) 635.
51 Chemistry International, (1980) No. 6, p. 23.

Analytica Chimica Acta, 127 (1981) 23—38
Elsevier Scientific Publishing Company, Amsterdam — Printed in The Netherlands

REGRESSION DATA PROCESSING METHODS FOR PARALLEL ZERO- AND FIRST-ORDER PROCESSES APPLIED TO LACTATE DEHYDROGENASE SUBUNIT DETERMINATIONS

RICHARD S. HARNER[a] and HARRY L. PARDUE*
Department of Chemistry, Purdue University, W. Lafayette, IN 47907 (U.S.A.)
(Received 18th December 1980)

SUMMARY

Multipoint data-processing methods developed for parallel zero-order and first-order processes have been evaluated for the simultaneous determination of the heart and muscle subunits of lactate dehydrogenase. Conditions are adjusted such that pyruvate inhibition of heart and muscle subunits of the enzyme follows pseudo-first-order kinetics with apparent rate constants of $k_H \simeq 0.7\ s^{-1}$ and $k_M \simeq 1.4\ s^{-1}$ for the heart and muscle subunits, respectively. The influence of these first-order inhibition processes on the zero-order catalytic reaction is used to determine the two subunits in single- and two-component samples. Stopped-flow mixing is used and 250 data points collected during the early part of the reaction are fitted to four different mathematical models for the parallel process in order to determine initial velocity components resulting from each subunit present, and these velocity components are related to enzyme concentration. Enzymes in synthetic samples are determined in the 0—80 nmol l^{-1} range with uncertainties of about 1 nmol l^{-1} for single- and two-component samples prepared from purified preparations for the enzymes.

The simultaneous determination of two or more components based on measurements related to differences in kinetic behavior date at least to 1935 when Hass and Weber [1] reported selective determination of the monochlorides of n-pentane and isopentanes based on differences in rates of reaction with potassium iodide to produce the monoiodides. Since that time there have been numerous other applications [2, 3], most of which have utilized graphical or relatively simple computational methods to resolve the kinetic data. More recently, several papers [4—7] have described computerized, multipoint curve-fitting methods to resolve the data. Most of the kinetic-based simultaneous determinations reported to date have been based on parallel first-order processes. While there have been some applications based on parallel zero-order processes, they have generally required measurements made under two or more different sets of conditions [8].

This paper describes the extension of regression methods developed earlier for parallel first-order reactions [4—7] to parallel zero-order and first-order reactions. While the extended data-processing methods should be applicable

[a]Present address: Dow Chemical Co., Midland, MI 48640, U.S.A.

0003—2670/81/0000—0000/$02.50

to a variety of chemical and physical kinetic processes, they were evaluated in this work for simultaneous determinations of the so-called heart (H) and muscle (M) subunits [9] of lactate dehydrogenase (LD). The determination is based on different rates of inhibition of LD catalytic acitivity by pyruvate; the inhibition processes for the H and M subunits are resolved from absorbance vs. time data that reflect combined first-order decreases in the zero-order catalytic reaction velocities. In other words, the change in zero-order reaction velocity with time is used to monitor and resolve the first-order inhibition processes. Results are reported for single- and two-component synthetic samples.

GENERAL CONSIDERATIONS

Reactions

Catalysis by lactate dehydrogenase of the reaction

$$\text{Pyruvate} + \text{NADH} \overset{\text{LD}}{\rightleftharpoons} \text{NAD} + \text{Lactate} \tag{1}$$

is inhibited by high concentration of pyruvate, and it has been postulated [10] that inhibition results from the formation of a ternary complex as follows

$$\text{P} + \text{LD}\cdot\text{NAD} \underset{k_r}{\overset{k_f}{\rightleftharpoons}} \text{P}\cdot\text{LD}\cdot\text{NAD} \tag{2}$$

where P represents pyruvate. It is known from earlier work [10, 11] that the extents of inhibition in eqn. (2) are different for the H and M subunits of lactate dehydrogenase.

These reaction models are used to develop equations for four different data-processing options. The four options are conveniently grouped under the two general headings of "derivative methods" and "integral methods". In each case, absorbance vs. time data were acquired on-line with a digital computer. In the derivative method, the first derivative of each A vs. t data set was computed by a numerical method, and the resulting rate data were used in two fitting procedures. In the integral method, A vs. t data were used directly in two fitting procedures. For each of these two general approaches, one fitting model identified as an "initial velocity" version used the initial velocity for the subunits present as a fitting parameter and another model identified as a "discrete parameter" model used rate constants and absorbance values to be described later as the fitting parameters. In the initial velocity version, velocity data are generated directly; in the discrete parameter version, velocity data are computed from other parameters that are generated.

In the mathematical development, it will be convenient to develop equations for single components initially, and then to modify these for two-component samples.

Single-component equations

Primary equations. For sufficiently large concentrations of pyruvate and NADH and small concentrations of NAD, lactate, and enzyme, the rate of reaction (1) can be represented by

$$-\mathrm{d[NADH]}/\mathrm{d}t = k_0\,[\mathrm{LD}]_t \tag{3}$$

where k_0 is a pseudo-zero-order rate constant and $[\mathrm{LD}]_t$ is the instantaneous concentration of the catalytically active form of either enzyme subunit. Starting with eqn. (2) and assuming that virtually all of the active form of the enzyme is present as the binary complex ($[\mathrm{LD}]_t \simeq [\mathrm{LD{\cdot}NADH}]_t$) and that pyruvate concentration is much larger than the binary complex concentration ($[\mathrm{P}] \gg [\mathrm{LD{\cdot}NADH}]_t$), it can be shown that the time-dependent concentration of the active form of either enzyme subunit is

$$[\mathrm{LD}]_t = [\mathrm{LD}]_0\,[(k_r/k_1)\exp(-k_1 t)] \tag{4}$$

where $[\mathrm{LD}]_0$ is the initial concentration of the active form of either enzyme subunit and $k_1 = k_f' + k_r$ where $k_f' = k_f[\mathrm{P}]$. When eqn. (4) is substituted into eqn. (3), the reaction velocity for either enzyme subunit is given by

$$-\mathrm{d[NADH]}/\mathrm{d}t = k_0\,[\mathrm{LD}]_0\,[(k_r/k_1) + (1 - k_r/k_1)\ \exp(-k_1 t)] \tag{5}$$

which, after integration and rearrangement, yields

$$[\mathrm{NADH}]_t = [\mathrm{NADH}]_0 - k_0\,[\mathrm{LD}]_0\,\{(k_r t/k_1) + [(1 - k_r/k_1)/k_1]\} \times$$

$$[1 - \exp(-k_1 t)] \tag{6}$$

where $[\mathrm{NADH}]_0$ and $[\mathrm{NADH}]_t$ are the initial and time-dependent concentrations of the cofactor.

In this work, changes in NADH concentration were monitored by absorbance changes. Equation (5) can be rewritten as

$$-\mathrm{d}A/\mathrm{d}t = \epsilon b k_0\,[\mathrm{LD}]_0\,[(k_r/k_1) + (1 - k_r/k_1)\exp(-k_1 t)] \tag{7}$$

and eqn. (6) can be rewritten as

$$A_t = A_0 - \epsilon b k_0\,[\mathrm{LD}]_0\,\{(k_r t/k_1) + [(1 - k_r/k_1)/k_1]\}[1 - \exp(-k_1 t)] \tag{8}$$

where A is the absorbance and ϵ and b are the molar absorptivity of NADH and path-length, respectively. Equations (7) and (8) were used to compute the data in Fig. 1A and B which will be useful to illustrate several important features of the reaction system and the resulting equations.

Velocity components. It is apparent from Fig. 1A and B that the slope of the A vs. t plot starts at an initial high value at $t = 0$, and gradually decreases to a smaller constant value at longer times. Substituting the limits $t = 0$ and $t \to \infty$, into eqn. (7) yields

$$-\mathrm{d}A/\mathrm{d}t_{t=0} = \epsilon b k_0\,[\mathrm{LD}]_0 \equiv V_i \tag{9a}$$

and

$$-\mathrm{d}A/\mathrm{d}t_{t\to\infty} = (k_r/k_1)\,\epsilon b k_0\,[\mathrm{LD}]_0 \equiv fV_i \equiv V_{ss} \tag{9b}$$

where V_i and V_{ss} are the initial and steady-state velocities, respectively, expressed in absorbance change per unit of time (ΔA s^{-1}) and $f = k_r/k_1$. Thus, it is apparent that the steady-state velocity will be a fixed fraction of the initial velocity, where the fraction, f, is the portion of the enzyme present initially that remains uninhibited throughout the reaction and the complementary fraction, $1 - f$, is the portion of the enzyme that is eventually completely inhibited. Thus, eqn. (7) can be written in the forms

$$V_t = [f + (1-f)\exp(-k_1 t)]\,V_i \tag{10a}$$

or

$$V_t = V_{ss} + (1-f)V_i \exp(-k_1 t) \tag{10b}$$

where V_t is the instantaneous velocity. Equation (10a) is used later in what is identified as an "initial velocity" version of a "derivative model" to fit the kinetic data.

When the linear portion of the response curve in Fig. 1A is extrapolated to zero time, the portions of the response above and below the intersection at $t = 0$ represent absorbance changes resulting from the first-order and zero-order processes, respectively. The point of intersection at $t = 0$ is identified as A'_∞ to represent the final absorbance that would result if the portion of the enzyme that is completely inhibited were acting alone. It follows by analogy with other first-order processes that the initial velocity term associated with the exponential term in eqn. (10b) is equal to the product of the rate constant and the total absorbance change $(1 - f)\,V_i = k_1\,(A'_\infty - A_0)$, so that eqn. (10b) can be rewritten as

$$V_t = V_{ss} + k_1\,(A'_\infty - A_0)\exp(-k_1 t) \tag{11}$$

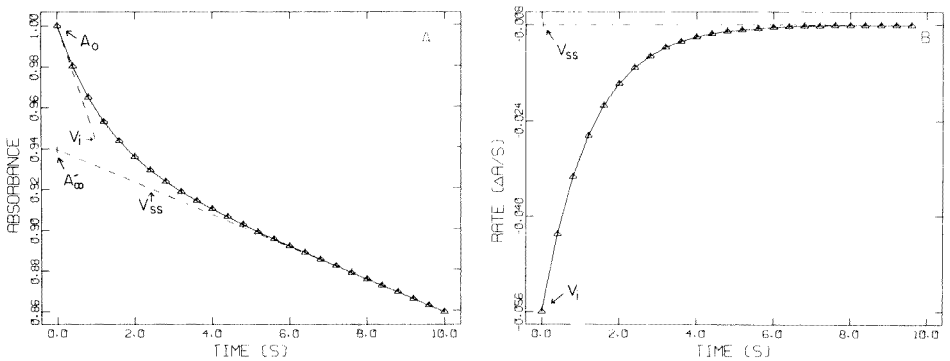

Fig. 1. Simulated responses for parallel zero-order and first-order processes. Simulation parameters: $A_0 = 1.00$; $k_1 = 0.80$ s^{-1}; $V_i = -0.056$ s^{-1}; $V_{ss} = -0.0080$ s^{-1}; ($A'_\infty = 0.94$). (A) Absorbance vs. time response; (B) first derivative of absorbance vs. time response.

where $V_{ss} = fV_i$ (eqn. 9b). Alternatively, eqn. (11) can be proven rigorously by integrating eqn. (10) (with $V \equiv dA/dt$), setting $A_t = A_0$ at $t = 0$ and $A_t = A'_\infty$ at $t = \infty$, and then differentiating the resulting expression. Equation (11) is used in what is identified as a "discrete parameter" version of a "derivative model" to fit the kinetic data.

Absorbance components. It is apparent from eqns. (8) and (9) that the time-dependent absorbance can be written in terms of the initial velocity as follows

$$A_t = A_0 + \{ft + [(1-f)/k_1]\,[1 - \exp(-k_1 t)]\}\,V_i \tag{12}$$

where the velocity is a negative quantity ($V_i = -dA/dt$). This equation is used later in what is identified as an "initial velocity" version of an "integral model" to fit A vs. t data for the rate processes.

Equation (8) can also be written in the form

$$A_t = A_0 + V_{ss}t + (A'_\infty - A_0)(1 - \exp(-k_1 t)) \tag{13}$$

by substituting V_{ss} and V_i from eqns. (9a) and (9b) into eqn. (8), and noting from the development of eqn. (11) that $(1-f)V_i = k_1(A'_\infty - A_0)$. This equation is used later in what is identified as a "discrete parameter" version of an "integral model" to fit A vs. t data for the rate processes.

Two-component equations

If it is assumed that the H and M subunits of lactate dehydrogenase react independently, then the effects are expected to be additive and equations developed above are easily modified to account for the presence of both components. However, because two-component samples were processed only by the initial rate version of the integral model, that is the only equation presented here. The two-component equation for the initial rate version of the integral model is

$$A_t = A_0 + \{[(1-f_H)/k_H]\,[1 - \exp(-k_H t)] + f_H t\}\,V_{i,H} + \{[(1-f_M)/k_M]\,[1 - \exp(-k_M t)] + f_M t\}V_{i,M} \tag{14}$$

where subscripts H and M refer to the heart and muscle subunits.

Curve-fitting approach

A multiple linear regression method similar to that described earlier [7] was used to fit absorbance or velocity and time data to each equation chosen for use. Briefly, the procedure consists of writing each equation in terms of the sum of products of the partial derivative with respect to each parameter times an incremental value of the parameter, and then using an iterative procedure to minimize the change in the ratio of the sum of the residuals squared and the variance (SD^2) of absorbance measurements. As an example, eqn. (13) would be represented as

$$\hat{A}_t = A_t^0 + \frac{\partial A_t^0}{\partial A_0}\delta A_0 + \frac{\partial A_t^0}{\partial A_\infty'}\delta A_\infty' + \frac{\partial A_t^0}{\partial k_1}\delta k_1 + \frac{\partial A_t^0}{\delta V_{ss}}\delta V_{ss} \quad (15)$$

where $\hat{A}_t$ is the estimated value for the absorbance at each point in time for each iteration, A_t^0 is an initial estimate of A_t expressed in terms of the several parameters via eqn. (13), and the partial derivatives are evaluated from eqn. (13), e.g., $\partial A_t/\partial A_0 = \exp(-k_1 t)$. This equation would be used in an iterative procedure to compute $\hat{A}_t$ values for different incremental values of the parameters until some preselected minimum change in the function

$$\chi^2 = \sum [(A_t - \hat{A}_t)^2/(\mathrm{SD})^2] \quad (16)$$

is obtained, where SD is the standard deviation of absorbance values. When the fitting procedure is complete, then appropriate parameters are used to compute enzyme activity. In this example for a single-component sample, the initial velocity would be computed as $\hat{V}_i = \hat{k}_1 (\hat{A}_\infty' - \hat{A}_0) + \hat{V}_{ss}$ (see eqn. 11 with $t = 0$).

Other equations are treated in analogous fashion. More complete details of procedures, including derivatives for all functions, are presented elsewhere [12].

EXPERIMENTAL

Instrumentation

The instrumental system used in this study was that described earlier [13], with some modifications [12] to improve noise characteristics at 340 nm where all absorbance measurements were made. The effective path length of the absorption cell was evaluated to be 0.9 mm.

Reagents

All reagents were prepared in water that was distilled in quartz after passing through a mixed cation-anion resin bed. Stock buffer was stirred vigorously under reduced pressure to reduce amounts of dissolved gases that could produce bubbles in the stopped-flow mixing system. All glassware was soaked in detergent, rinsed with dilute nitric acid followed by distilled water, and permitted to dry in air before use.

Buffer. Phosphate buffer was prepared from Na_2HPO_4 and KH_2PO_4 and ionic strength was adjusted with NaCl when necessary.

Lactate dehydrogenase. Purified LD isoenzyme fractions isolated from porcine heart and muscle were obtained at 5 mg ml^{-1} in 3.2 mol l^{-1} ammonium sulfate (Boehringer Mannheim Biochemicals, Indianapolis, IN 46250) and diluted (10^3 to 5×10^4 dilutions) in phosphate buffer. Enzyme concentrations were estimated assuming a stock protein value of 5 mg ml^{-1} and a molecular weight of 1.4×10^5 and reported in terms of molarity of active sites (four active sites/LD molecule). Actual protein concentrations were occasionally verified using a molar absorptivity of 2×10^5 l mol^{-1} cm^{-1} at

280 nm [14]. Because both sample and the above reagent were prepared in the same buffer, ionic strength was considered identical. Electrophoresis of a 10 000-fold dilution of H_4 or M_4 isoenzyme in buffer (0.5 μg ml^{-1}) with albumin added (6 mg ml^{-1}) was used to confirm the absence of other LD isoenzymes in the commercial preparations.

NADH·3H₂O. Reduced nicotinamide adenine dinucleotide, disodium salt of ChromatoPure grade (P-L Biochemicals, Milwaukee, WI 53205) was dissolved in buffer to give a concentration range of 2×10^{-4} to 4×10^{-4} mol l^{-1}.

Pyruvic acid. Sodium pyruvate was dissolved in buffer to yield concentrations 8×10^{-5}—2×10^{-1} mol l^{-1}.

Combined reagent. Amounts of pyruvate and NADH solutions to give desired concentrations were mixed to provide a single reagent.

Procedures

Preliminary data were collected at 340 nm and ca. 25°C using a procedure similar to that suggested by Tietz [15] but modified to allow variation of pyruvate concentration.

Stopped-flow methods. Initial runs were designed so that final concentrations in the flow cell were equal to those in the cuvette in the procedure described above. The reaction was initiated by mixing equal amounts of the enzyme sample and reagent at 25.0 ± 0.01°C. The transmittance at 340 nm was recorded on-line with a digital computer at variable data rates selected with a software programmable clock. Transmittance data were converted to absorbance and used by regression programs described above to extract pertinent kinetic parameters.

All velocities are reported as rates of change in absorbance per second (s^{-1}). Because NADH is the only chromophore affecting the absorbance at 340 nm, these rates can be converted to reaction rates ($-d[NADH]/dt$, mol l^{-1} s^{-1}) by use of the molar absorptivity ($\epsilon_{NADH} = 6.22 \times 10^3$ l mol^{-1} cm^{-1}) and path-length (0.90 cm).

Data analysis. Software written in Fortran IV is implemented on a HP 2100A laboratory computer (Hewlett-Packard, Palo Alto, CA 94304) with 32K of core memory and a custom-built dual-sided dual-drive floppy disk. Derivatives of A vs. t data were computed with the methods of Savitzky and Golay [16].

RESULTS AND DISCUSSION

Reaction parameter dependencies, instrumental characteristics, and reaction model validity were evaluated with single-component samples of the purified H and M subunits. Results of these studies were then used to establish conditions for simultaneous determinations of the two subunits in synthetic mixtures. Unless noted otherwise, all uncertainties are reported at the one standard deviation unit level (±1 SD). Individual regression residuals are normalized to the standard deviation of the data set and plotted as multiples of the standard deviation.

Response curves

Figure 2A and B show response curves obtained for purified samples of the H_4 and M_4 subunits, respectively. It is observed that each curve decelerates gradually toward a constant velocity, with the M_4 enzyme approaching the steady-state velocity more rapidly than the H_4 enzyme, and with the ratio of steady-state velocity to the initial velocity being substantially less for the H_4 sample than for the M_4 sample. One of the first questions that had to be answered was whether the parallel zero-order and first-order model proposed above would satisfy these data. Both the derivative and integral models were tested, and data are presented below for the H_4 enzyme; similar results were obtained for the M_4 sample.

Integral data. Figure 2C shows a response curve for the H_4 enzyme with a superimposed curve based on a fit with the initial velocity version of the integral model (eqn. 12). The horizontal plot represents residuals for the fit. It is observed that the shapes of the experimental and computed responses are very similar. Virtually identical results were obtained when the discrete parameter version of the integral model (eqn. 13) was used to fit these data.

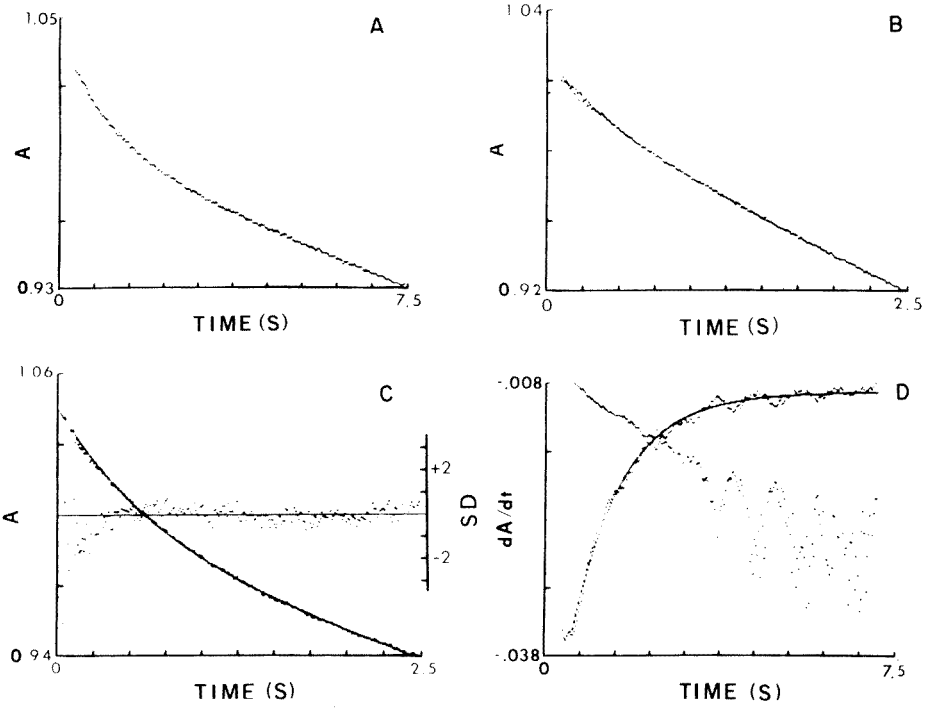

Fig. 2. Experimental and computed responses for H_4 and M_4 enzymes. (A) Average of three responses for H_4 enzyme (40 nmol l^{-1}); (B) average of three responses for M_4 enzyme (40 nmol l^{-1}); (C) response curve for H_4 enzyme (80 nmol l^{-1}) with fitted curve superimposed; (D) ascending plot shows first derivative data for H_4 enzyme (40 nmol l^{-1}) with fitted curve superimposed; descending plot shows $\ln(V_{ss} - V_t)$ vs. time. All frames: pyruvate, 20 mmol l^{-1}; NADH, 0.17 mmol l^{-1}; pH 7.5; T = 25.0°C.

Derivative model. Figure 2D shows the first derivative [16] of the H_4 response curve in Fig. 2A along with superimposed plot based on a first-order model. The computed response is based on an apparent first-order rate constant obtained from the slope of the descending plot which is a plot of $\ln(V_{ss} - V_t)$ vs. time; the rationale for this procedure is easily justified by rearrangement of eqn. (10b). The first derivative should effectively eliminate the zero-order component and leave only the response related to the first-order component of the process. It is observed that the shapes of the experimental and computed first-order responses are virtually identical.

The large noise component associated with the descending $\ln(V_{ss} - V_t)$ vs. t plot at longer times is analogous to that observed with $\ln(A_\infty - A_t)$ vs. t plots as $t \to \infty$ for uncomplicated first-order processes; it results from differences between similar large quantities, and the effect is amplified for derivative data.

Both the integral and derivative models offer strong support for the chemical model and mathematical descriptions when applied to the H_4 enzyme alone; similar data illustrate comparable agreement for the M_4 enzyme. The validity of the model having been demonstrated, it was used to evaluate dependencies upon reaction conditions, and results are summarized in the next section.

Dependencies on reaction conditions

In the following discussion, the reaction variables not being studied had fixed values; the values were pH 7.5 in 0.1 mol l^{-1} phosphate buffer (ionic strength 0.27), 20 mmol l^{-1} pyruvate, 0.166 mmol l^{-1} NADH, and either 40 or 80 nmol l^{-1} enzyme.

Pyruvate dependence. Figure 3 shows the effects of pyruvate concentration on initial and steady-state rates determined with the initial velocity version of the derivative model. Solid curves in Fig. 3 are predicted with the equation

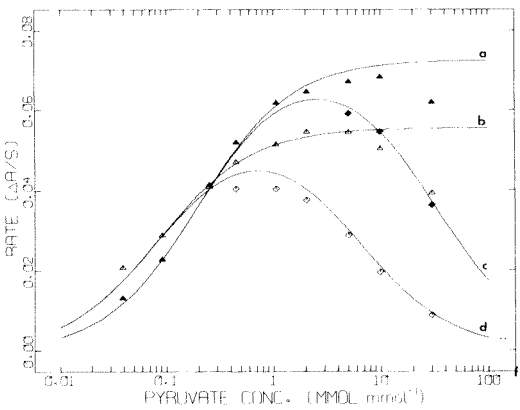

Fig. 3. Effects of pyruvate concentration on initial and steady-state velocities for purified enzymes. (△, ▲) Initial rates; (◇, ◆) steady-state rates; (△, ◇) H_4; (▲, ◆) M_4.

$$V_{max} = V_{ss} [1 + (K_M/[P]) + ([P]/K_I)] \quad (17)$$

with the Michaelis constant (K_M) and the inhibition constant (K_I) being determined by standard procedures. It is observed that both enzymes follow the pattern expected for uncomplicated uncompetitive substrate inhibition up to about 10 mmol l^{-1} pyruvate, but that above that level, the initial rate deviates from that pattern. Potential reasons for this behavior have been discussed [12]. The principal influence of the departure from expected behavior on the analytical procedures is to affect the values of the initial velocity; the behavior does not influence the validity of the mathematical description of the system. The single-component studies were performed at 20 mmol l^{-1} pyruvate; two-component studies reported below were performed at 7 mmol l^{-1} pyruvate to take advantage of the higher initial rates expected at that concentration.

Ionic strength and pH. Effects of ionic strength and pH on selected parameters are summarized in Table 1. Because all parameters listed change in an approximately linear fashion with pH and ionic strength between the limits studied, these data can be used to estimate values of each parameter at any point within those limits.

Effects of NADH concentration were not studied independently of the other variables; a somewhat arbitrary decision was made to restrict measurements to a range such that the NADH concentration did not decrease by more than 10% of the initial value (0.166 mmol l^{-1}).

Instrumental noise

It was noted above (eqn. 16) that the convergence criterion for the iterative regression procedure involves the standard deviation of instrumental measurements. During the early part of this work it was assumed that the SD term in eqn. (16) was the same for all absorbance measurements during an experiment with a typical value of SD = 0.0005 being used. However, as the work progressed, it became apparent that this was not a completely satisfactory assumption; the instrumental noise was substantially larger than the 0.0005 value near $t = 0$ and decayed toward that value as time progressed.

TABLE 1

Effects of pH and ionic strength on kinetic parameters for lactate dehydrogenase[a]

Variable		Heart subunit				Muscle subunit			
		k_1	V_i	V_{ss}	f	k_1	V_i	V_{ss}	f
pH	6.5	0.66	0.068	0.0087	0.13	1.5	0.12	0.014	0.12
	7.5	0.96	0.104	0.019	0.18	1.8	0.144	0.061	0.42
Ionic	0.27	—	0.097	0.017	0.18	—	0.15	0.073	0.49
strength	1.0	—	0.094	0.028	0.30	—	0.127	0.080	0.63

[a]Pyruvate, 20 mmol l^{-1}; NADH, 0.17 mmol l^{-1}; T = 25.0°C.

Subsequent more detailed study showed that the noise decay approximated a first-order pattern, and that the standard deviation as a function of time could be approximated by

$$SD_t \simeq SD_\infty + (SD_0 - SD_\infty) \exp(-k_d t) \quad (18a)$$

where SD_0. SD_∞, and SD_t are the standard deviations of absorbance measurements at $t = 0$, ∞, and t, respectively, and k_d is the decay rate constant. Because actual values of SD_∞ and SD_0 depend upon experimental conditions (amplifier gain, wavelength, etc.), and because it is difficult to measure SD_0 accurately, an empirical procedure was used to estimate SD_t for each set of experiments. The procedure was to use fixed absorbance samples, and to estimate SD from thirty measurements at $t = 0.1$ s and $t = 10$ s after mixing, where the 10 s measurement is a good estimate of SD_∞ ($k_d \simeq 14$ s^{-1} and $t_{1/2} = 0.05$ s). It is easily shown that eqn. (18a) can be rewritten in the form

$$SD_t \simeq SD_{10} + [(SD_{0.1} - SD_{10})/\exp(-0.1\, k_d)] \exp(-k_d t) \quad (18b)$$

This function was used in subsequent experiments to estimate SD_t values used in eqn. (16) above.

The data in Fig. 2C were fitted using a fixed value of SD = 0.0005; the same data are shown in Fig. 4 fitted with SD_t estimated from eqn. (18b) with $SD_{0.1} = 0.002$, $SD_{10} = 0.0005$, and $k_d = 14$ s^{-1}. The only observable difference from these Figs. is that the normalized residuals tend to be grouped tightly within ±0.5 SD in Fig. 2C, while they cover the range approaching ±2 SD in Fig. 4. The distribution in Fig. 4 is closer to that expected for random noise than is that in Fig. 2C.

Numerical data in Table 2 illustrate more complete details of differences that result from these two fitting approaches, as well as a third one in which SD is fixed at 0.0001, a value substantially smaller than the expected value. The principal difference between results for two fixed values of SD is that the χ^2 value is much smaller (12.7 vs. 317) for the more realistic estimate of absorbance uncertainty (SD = 0.0005); this difference is not surprising

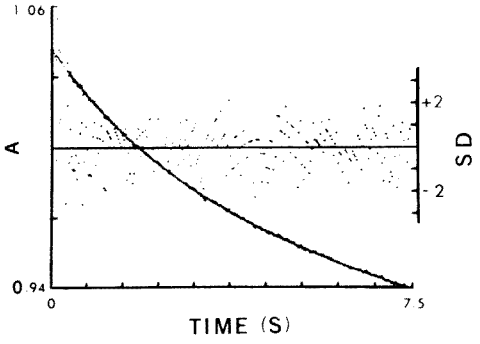

Fig. 4. Response curve for H_4 enzyme with fitted curve superimposed. Conditions as in Fig. 2C except SD_t computed with eqn. (18b).

TABLE 2

Comparison of regression results for pure H_4 enzyme data processed by integral model[a]

Parameter	SD = 0.0001[b]	SD = 0.0005[b]	$SD_{0.1}$ = 0.002[c]; SD_∞ = 0.0005[c]
Discrete parameter version			
A_0	1.05148 ± 0.00003	1.05148 ± 0.00016	1.04775 ± 0.00031
A'_∞	0.93932 ± 0.00019	0.98935 ± 0.00090	0.97090 ± 0.00220
V_{ss} (s^{-1})	−0.02122 ± 0.00007	−0.02123 ± 0.00034	−0.01530 ± 0.00084
k_1 (s^{-1})	1.4448 ± 0.0053	1.4455 ± 0.0254	1.0295 ± 0.0310
SE[e]	0.0018	0.0018	0.019
χ^2	317	12.7	1.02
Initial rate version			
A_0	1.05148 ± 0.00003	1.05148 ± 0.00016	1.04775 ± 0.00032
V_i (s^{-1})	−0.11104 ± 0.00018	−0.11105 ± 0.00086	−0.09441 ± 0.00120
f	0.19117 ± 0.00045	0.19120 ± 0.00218	0.16201 ± 0.00627
k_1 (s^{-1})	1.4450 ± 0.0053	1.4455 ± 0.0254	1.0295 ± 0.0341
SE[e]	0.018	0.018	0.0019
χ^2	317	12.7	1.02

[a]Pyruvate, 20 mmol l^{-1}; NADH, 0.17 mmol l^{-1}; pH 7.5; T = 25.0°C. [b]Value of SD used in eqn. (16). [c]Values used in eqn. (16) via eqn. (18b). [d]Standard error of residuals.

considering that χ^2 is a ratio with the estimate of SD in the denominator. There are more substantial differences between these two data sets and that in which the time dependence of absorbance uncertainty is taken into account. The most significant observation is that the χ^2 value of 1.02 for the case when SD_t is used approaches the ideal value of 1.00 very closely. There are also substantial differences between individual parameters (V_{ss}, k_1, A_0, etc.) obtained with the different estimates of SD; because there are no independent measures of these parameters, simulated experiments were used to evaluate the SD_t approach. Equation (18b) with $SD_{0.1}$ = 0.002, SD_{10} = 0.0005, and k_d = 14 s^{-1} was used to superimpose a time-dependent noise component on A vs. t data with known initial and steady-state noise components. A typical fit of these data yielded initial and steady-state velocities of 0.0503 s^{-1} and 0.00797 s^{-1} compared with input values of 0.050 s^{-1} and 0.0080 s^{-1}. The time-dependent noise component, SD_t, was used in the convergence criterion in the remainder of this study.

Linearity studies

Linearity studies were performed for single-component samples of the heart and muscle subunits of LD (20—100 nmol l^{-1}) using the initial rate versions of the derivative (eqn. 10a) and integral (eqn. 12) models. Similar studies were performed for two-component samples (0—20 nmol l^{-1}) with the initial velocity version of the integral model.

TABLE 3

Linearity data for single-component samples of purified H_4 and M_4 enzymes[a]

Parameter	Slope ($\Delta A\ l\ \mu mol^{-1}\ s^{-1}$)	Intercept ($\Delta A\ s^{-1} \times 10^3$)	SE ($\Delta A\ s^{-1} \times 10^3$)	r
Initial velocity version of derivative model				
$V_{i,H}$	1.096 ± 0.036	−1.5 ± 2.4	2.3	0.998
$V_{ss,H}$	0.177 ± 0.031	−1.1 ± 2.1	2.0	0.955
$V_{i,M}$	1.612 ± 0.016	−5.6 ± 1.1	1.0	0.999
$V_{ss,M}$	0.641 ± 0.007	−1.8 ± 0.5	4.6	0.999
Initial velocity version of integral model				
$V_{i,H}$	1.087 ± 0.024	−0.9 ± 1.6	1.5	0.999
$V_{ss,H}$	0.169 ± 0.012	−0.5 ± 0.8	0.7	0.992
$V_{i,M}$	1.591 ± 0.039	−4.1 ± 2.6	2.5	0.999
$V_{ss,M}$	0.633 ± 0.005	−1.4 ± 0.3	0.3	0.999

[a]Pyruvate, 20 mmol l^{-1}; NADH, 0.17 mmol l^{-1}; pH 7.5; T = 25.0°C. Results are based on 9—12 experiments processed as averages in groups of three.

Single-component samples. Results for one single-component data set are presented in Table 3 as the slopes and intercepts with appropriate statistics. The data confirm good linearity for both initial rate and steady-state rate data for the H subunit data processed by the derivative method. It is also observed that there is reasonable agreement between slopes and intercepts of data processed by the two models. Clearly, the multipoint regression methods coupled with the rapid mixing capability of the stopped-flow system permit both initial and steady-state rates to be related to enzyme concentration.

Two-component samples. The two-component sample experiments were performed with somewhat lower pyruvate concentration (7 mmol l^{-1}) than that used (20 mmol l^{-1}) for the single-component studies. Under these conditions, the initial velocities are somewhat higher (see Fig. 3), but the fractions of both enzymes inhibited are smaller. For these conditions, the rate constants were $k_{1,H} = 0.66\ s^{-1}$ and $k_{1,M} = 1.43\ s^{-1}$ and the fractions of each enzyme that remained active were $f_H = 0.48$ and $f_M = 0.83$. Calibration equations established with 0—80 nmol l^{-1} of each enzyme for these conditions were

$$V_{i,H} = (1.27 \pm 0.03)\ C_H^\circ + (0.61 \pm 1.4)\ s^{-1} \quad (SE = 1.1 \times 10^{-3}\ s^{-1};\ r = 0.9998)$$

and

$$V_{i,M} = (1.67 \pm 0.04)\ C_M^\circ - (0.70 \pm 2)\ s^{-1} \quad (SE = 1.6 \times 10^{-3}\ s^{-1};\ r = 0.9998)$$

where the concentrations, C_H° and C_M°, are expressed in nmol l^{-1} and where SE is the standard error of regression and r is the correlation coefficient. These equations were used to compute individual subunit concentrations from initial rates obtained with eqn. (14) applied to A vs. t data for mixtures.

Results for 4—7 determinations at each of six concentrations between 0 and 20 nmol l^{-1} for each enzyme are summarized as least-squares equations of amounts determined (y) vs. amounts added (x). The equations with appropriate statistics are

$$y_H = (0.97 \pm 0.02)\, x_H + (0.21 \pm 0.22)\ \text{nmol}\ l^{-1} \quad (SE = 0.741\ \text{nmol}\ l^{-1}; r = 0.994)$$

and

$$y_M = (0.98 \pm 0.01)\, x_M + (0.01 \pm 0.14)\ \text{nmol}\ l^{-1} \quad (SE = 0.46\ \text{nmol}\ l^{-1}; r = 0.997)$$

Neither slopes nor intercepts are significantly different from expected values of unity and zero at the 95% confidence level. The scatter about the regression lines is reflected in the standard error values (SE), and approaches 1.5 and 1 nmol l^{-1} at the 95% confidence level for the H and M subunits, respectively.

When results obtained for individual subunits were summed together and totals (y_T) were compared with total amounts of enzyme added (x_T), the resulting least-squares equation was

$$y_T = (1.01 \pm 0.01)\, x_T - (0.66 \pm 0.24)\ \text{nmol}\ l^{-1} \quad (SE = 0.44\ \text{nmol}\ l^{-1}; r = 0.998)$$

While the slope is not significantly different from zero at the 95% confidence level, the 95% confidence interval for the intercept does not include zero. The scatter about the least-squares line as reflected by the standard error is somewhat less than that for the muscle subunit determined alone. It should be noted that the range of total enzyme concentration in these studies was between 18 and 40 nmol l^{-1}.

DISCUSSION

It is believed that the data presented above provide strong support for the validity of the multipoint regression method used to resolve data for parallel zero-order and first-order processes. As expected, a single first-order process is resolved more reliably than two first-order processes with a zero-order process. However, in judging results obtained for the latter situation, it should be noted that the example chosen for illustration was far from ideal. The two first-order rate constants differ by a factor of only two ($k_{1,M} = 1.43$, $k_{1,H} = 0.66$), and the total absorbance change was seldom larger than 0.10 with a noise component ranging from greater than 0.002 near $t = 0$ to a minimum value of 0.0005 at longer times. Situations offering larger differences in rate constants and better signal-to-noise ratios should result in substantially improved results.

Before the data processing approach developed and evaluated above could be used to resolve the H and M subunits of lactate dehydrogenase in complex samples, it would be necessary to demonstrate that rate constants were not influenced by matrix components. Also, it would be highly desirable to use a detection system with better signal-to-noise characteristics. The principal

problem in the present case was that the initial absorbance was high (near 1.0) and that measured changes were kept small (<0.10) to avoid kinetic complications resulting from changes in NADH concentration greater than 10%. It is possible that fluorescence monitoring of NADH would yield better signal-to-noise characteristics. In addition to offering the possibility of differentiating between the two subunits of LD, the procedure developed here offers the possibility of obtaining a better measure of activity before substrate inhibition. While substantial effort has been devoted to so-called optimization studies intended to yield maximum values of activity, most of this effort has involved steady-state measurements, and data in Table 3 (and other data in the text) show that such measurements yield only a fraction, f, of the initial activity. The principal advantages of the present approach for LD with regard to traditional approaches that do not include a separation step are that it permits estimation of the true initial rate before substrate inhibition, and it permits differentiation between the H and M subunits. The principal advantage relative to methods that include a separation step is that it provides a measure of the in situ activities of the H and M subunits. The principal disadvantage relative to procedures that include a separation step is that the present method does not differentiate between the five different isoenzymes.

In addition to their potential use for quantitative determinations based on chemical reactions, the methods described above could also be useful for physical kinetic processes. As an example, recently developed flow-injection methods with a gradient chamber [17] include simultaneous zero-order and first-order processes when reactant is included in the reagent stream [18]. The methods should also be useful for fundamental kinetic studies of processes such as the lactate dehydrogenase example used herein. These and other applications are being continued in this laboratory.

This investigation was supported by Research Grant No. GM 13326-13 from the NIH, USPHS.

REFERENCES

1 H. B. Hass and P. Weber, Ind. Eng. Chem. Anal. Ed., 7 (1935) 231.
2 H. B. Mark and G. A. Rechnitz, Kinetics in Analytical Chemistry, Interscience, New York, 1968.
3 H. A. Laitinen and W. E. Harris, Chemical Analysis, McGraw-Hill, New York, 1975, p. 389.
4 B. G. Willis, J. A. Bittikofer, H. L. Pardue and D. W. Margerum, Anal. Chem., 43 (1970) 1340.
5 G. M. Ridder and D. W. Margerum, Anal. Chem., 49 (1977) 2098.
6 J. B. Landis and H. L. Pardue, Clin. Chem., 24 (1978) 1700.
7 G. E. Mieling and H. L. Pardue, Anal. Chem., 50 (1978) 1611.
8 P. A. Rodriguez and H. L. Pardue, Anal. Chem., 41 (1969) 1376.
9 R. D. Cahn, N. O. Kaplan, L. Levine and E. Zwilling, Science, 136 (1952) 962.
10 N. O. Kaplan, J. Evense and J. Admiraal, Ann. N.Y. Acad. Sci., 151 (1968) 400.
11 J. Evense, R. M. Reich, N. O. Kaplan and W. D. Finn, Clin. Chem., 21 (1975) 1277.

12 R. S. Harner, Differential Rate Evaluation of Parallel First and Zero Order Reactions and its Application to Lactate Dehydrogenase Determination, Ph.D. Thesis, Purdue University, 1980.
13 G. E. Mieling, R. W. Taylor, L. G. Hargis, J. English and H. L. Pardue, Anal. Chem., 48 (1976) 1686.
14 A. Pesce, T. P. Fondy, F. Stolzenbach, F. Castillo and N. O. Kaplan, J. Biol. Chem., 242 (1967) 2151.
15 N. W. Tietz, Fundamentals of Clinical Chemistry, W. B. Saunders, Philadelphia, 1976, p. 657.
16 A. Savitzky and M. J. E. Golay, Anal. Chem., 36 (1964) 1627.
17 J. Růžička, E. H. Hansen and H. Mosbaek, Anal. Chim. Acta, 92 (1977) 235.
18 H. L. Pardue and B. Fields, Anal. Chim. Acta, 124 (1981) 65.

Analytica Chimica Acta, 127 (1981) 39—46
Elsevier Scientific Publishing Company, Amsterdam — Printed in The Netherlands

FLOW INJECTION (CLOSED-LOOP CONFIGURATION) CATALYTIC DETERMINATION OF COPPER IN HUMAN BLOOD SERUM

S. M. RAMASAMY and HORACIO A. MOTTOLA*
Department of Chemistry, Oklahoma State University, Stillwater, OK 74078 (U.S.A.)
(Received 12th December 1980)

SUMMARY

Copper(II) ions catalyze the iron(III)—thiosulfate indicator reaction. This chemical system has been successfully used in a closed-loop apparatus with unsegmented continuous flow for the determination of copper in human blood serum. The sought-for species (the catalyst) is removed from the recirculating reagent by controlled-potential electrolysis after detection has taken place. Such electrolysis is also employed for in situ regeneration of the main reagent, iron(III). The reported method (a fixed-time, variable-signal kinetic determination) has a limit of detection for copper(II) of 0.25 μg ml^{-1} and permits 325 determinations per hour with a relative standard deviation of 2%.

The normal copper content in human blood serum is reported as 0.7—1.40 mg l^{-1} (ppm) in male subjects and 0.85 to 1.55 mg l^{-1} in female subjects [1]. The total serum copper content decreases in cases of Wilson's disease and hypoproteinemias, while elevated copper values are associated with leukemia, cirrhosis, hemochromatosis and various infections [2]. In the spectrophotometric determination of copper in blood serum, use is made of sensitive chromogenic reagents such as 1,5-diphenylcarbohydrazide, biscyclohexanone oxalyldihydrazone (cuprizone), and oxalyldihydrazide [2]. These methods, as proposed, require more than 1 ml of sample per determination and about 15—30 min for color development. Determinations based on neutron activation [3], atomic absorption [4, 5], flame emission [6], and x-ray fluorescence [7] have been reported, but they are not easily adapted to continuous flow determinations although the sample volume required is small. The literature also records a few air-segmented, continuous-flow-based determinations [8—10]. Analytical methods for copper, based on its catalytic role in a variety of chemical systems are numerous; indeed in the period 1978—1980 more catalytic applications and new reaction systems have been proposed for copper than any other element [11]. Few applications of these methods, however, can be identified in the literature for real biological samples and requiring small sample volumes [12—16]. These procedures (basically fixed-time, variable-signal determinations) are time-consuming; they offer, however, the good sensitivity and low limits of detection characteristic of catalytic determinations.

The present paper reports a method (fixed-time, variable-signal kinetic

determination) based on the catalytic effect of copper(II) ions in the oxidation of thiosulfate by iron(III) in acidic medium. This catalytic determination has been implemented in a closed-loop apparatus with unsegmented continuous flow and affords competitive limit of detection and sensitivity and high determination rate. Electrochemical removal of the catalyst permits the use of the closed-loop system [17]. Electrochemical removal of the catalyst is paralleled by reoxidation of iron(II) to iron(III) permitting maintenance of a constant level of the monitored species [the red $Fe(H_2O)_5\ SCN^{2+}$ complex]. The proposed method has been applied to the determination of copper in human blood serum samples and compared with independent determinations by atomic absorption.

EXPERIMENTAL

Apparatus

The spectrophotometric flow system was a custom-assembled unit illustrated in Fig. 1. Injection of the sample containing the sought-for species and the thiosulfate reactant was accomplished by means of Hamilton gas-tight syringes and a Hamilton PB600-1 repeating dispenser (Hamilton, Reno, NV) modified so as to drive two syringes simultaneously. In studies to extract rate proportionality constants, the strip-chart recorder readout was replaced by a Nicolet 1090A Explorer digital oscilloscope with 94A plug-in and model D amplifier (Nicolet Instrument, Madison, WI). For controlled potential electrolysis the anode potential was maintained at 0.60 V with respect to a saturated calomel electrode and with a MP-1026 potentiostat-regulated power supply operating in the potentiostat mode (Pacific Precision Instruments, Concord, CA). The cathode and anode were platinum gauze cylinders 3.2 cm

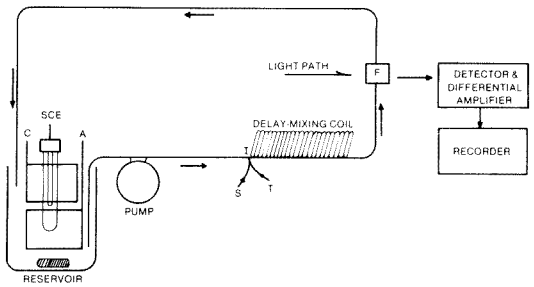

Fig. 1. Schematic diagram of closed-flow system for Cu(II) determinations. A, anode; C, cathode; SCE, saturated calomel electrode; pump, Masterflex with SCR model 7020 speed controller and 7014 pump head; I, injection port for the simultaneous injection of sample, S, and thiosulfate, T; delay-mixing coil (teflon), length 4.0 m, i.d. 1.32 mm; F, 80-μl, 10-mm flow cell (E-178-Q-10, Markson Science, Del Mar, CA). Detector, UDI silicone photodiode (United Detector Technology, Inc., Santa Monica, CA, USA); differential amplifier, Tektronix AM502 with Tektronix PS 501-1 power supply; Sargent SRL recorder. For details of the photometric system see [18].

in diameter and 3.1 cm tall. The photometric unit, detector, and readout have been described earlier [18]. Monitoring of the red complex of iron and thiocyanate was done at 480 nm. The delay-mixing coils were constructed from teflon tubing (i.d. 1.32 mm) of varying lengths.

Reagents and solutions

All reagents used were AR grade. The water used for solution preparation was deionized and double-distilled. Typical reservoir solutions (500 ml) contained 8.3×10^{-4} M iron(III) added as nitrate, 1.60×10^{-2} M thiocyanate added as potassium salt, and 0.20 M KNO_3, having the pH adjusted to 3.00 with perchloric acid. Typical size of the sample injected was 20.0 μl. The simultaneously injected 0.10 M thiosulfate reagent had also a volume of 20.0 μl.

RESULTS AND DISCUSSION

The overall uncatalyzed reaction between the reagents used in the proposed method is illustrated by

$$2\ Fe(III) + 2\ S_2O_3^{2-} = 2\ Fe(II) + S_4O_6^{2-} \quad (1)$$

This reaction is not sufficiently slow for the reactants to be mixed and circulated without baseline deterioration. To avoid this deleterious effect, one of the reactants (thiosulfate) is injected simultaneously with the sample. This results in a temporarily high concentration within the "plug" which is, however, reduced by dilution to considerably lower values upon reaching the reservoir; a deleterious rate of the uncatalyzed reaction is thus avoided. If the catalytic cycle is assumed to provide an "instantaneous" regeneration of the catalytic species, the concentrations of the main reactants are such that the rate of the overall catalyzed reaction may be considered to proceed via a pseudo-zero order process. The rate of reaction 1 in the absence of copper catalyst or in the presence of this catalyst is followed spectrophotometrically by the presence of thiocyanate in the reservoir solution with formation of the red $[Fe(H_2O)_5SCN]^{2+}$ complex. The iron(II) and iron(III) complexes with thiocyanate have formation constants that permit the successful anodic oxidation of iron(II) and regeneration of the monitored species [17]. Under the same electrochemical conditions, the catalyst is reduced to Cu(0) and the thiosulfate undergoes decomposition (to sulfur dioxide), which helps to diminish the rate of the uncatalyzed reaction.

Optimization of the system

In order to increase the extent of reaction and achieve maximum sensitivity and sample processing rate, the effect of increase of length of delay-mixing coils was studied. The corresponding experimental observations are summarized in Table 1. In selecting the optimum length for the mixing coil, a compromise must be reached so that the time for the "plug" to travel from

TABLE 1

Signal sensitivity and time for return to baseline as a function of mixing-coil length (average flow rate, 10 ml min^{-1} at 25°C)

Coil length (m)	1.0	2.0	3.0	4.0	5.0
Sensitivity (mV mg^{-1} l)	0.2	0.4	0.6	1.2	1.2
t_{bas} (s)	14.2	19.8	21.6	23.4	28.4

the injection point to the point of detection is long enough for a significant amount of chemical change but short enough to keep dispersion to a minimum. The increase of coil length increases the signal height up to a point but also increases the time, t_{bas}, needed for return to the baseline. With coil lengths at and above 5 m dispersion is so large as to cancel the usefulness of the corresponding increase in extent of reaction. A coil length of 4 m was adopted as the one providing maximum signal height without significant change in t_{bas} when compared with shorter coils.

Flow rate, by affecting the mean residence time of the plug in the transport system, influences signal height (sensitivity), S_{max}, as well as the time required to return to baseline. The same compromise indicated above on the length of mixing coil is needed in choosing the best flow rate. Signal development with time can be described by two first-order processes, one describing signal growth and the other describing signal disappearance [19]. The rate proportionality constants, k_1 and k_2, describing the processes can be extracted from the peak profile and used for method optimization [19]. Figure 2 shows the dependence of k_1 and k_2 on flow rate; both rate proportionality constants increase with increasing flow rate in such a fashion that the ratio k_1/k_2 remains practically constant and with it the signal height also, since its value depends on the ratio of the rate proportionality constants [19]. This trend is corroborated by the data of Fig. 3 in which the value of peak height is plotted vs. average flow rate. The increase in both constants indicates a continuous decrease in both the time to reach the peak height, t_{max}, and the time to return to baseline, t_{bas}. Such a trend is corroborated in the experimental results presented in Fig. 4. This peculiar parallel effect resulting in a proportional increase in both rate constants seems to indicate that the effect on signal parameters is mostly controlled by the mechanics (dynamics) of "plug" transport and that the rates of chemical changes have minimal impact on the signal height and time for return to baseline. Since the ratio k_1/k_2 remains constant over the range of flow rates studied, a rate of 20 ml min^{-1} is recommended with set-ups such as the one described in this paper. Higher flow rates should permit greater rate of sample injection but require tighter connections than those used here. In any event, at 20 ml min^{-1}, close to 325 injections per hour are possible, a rate that is higher than needed and competitive with that of other methods. In comparison, at 10 ml min^{-1}, the permissible sample rate is 150 per hour with about the same sensitivity. Obviously the main effect on determination

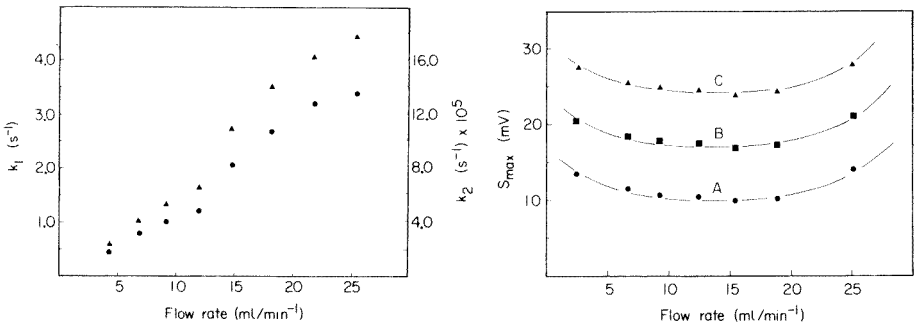

Fig. 2. Effect of flow rate on rate proportionality constants. Volume of sample injected, 20.0 μl; length of delay mixing coil, 4.0 m; temperature (reservoir), 40°C; amplification (differential), 100×; back-up potential, 30 mV. (▲)k_1; (●)k_2.

Fig. 3. Effect of flow rate on signal height: (A) uncatalyzed reaction; (B) 5 μg Cu(II) ml^{-1}; (C) 10 μg Cu(II) ml^{-1}. Other experimental conditions as in Fig. 2.

rate arises from decreases in dispersion and the time required to return to baseline with increase in flow rate.

Figure 5 shows typical working curves obtained at two different temperatures and with different concentrations of copper(II) in 20-μl aliquots as indicated earlier in this paper. Increases in temperature from 25 to 40°C improved not only the method sensitivity from 1.2 to 2.8 mV mg^{-1} l but decreased the limit of detection from 1 mg l^{-1} at 25°C to 0.25 mg l^{-1} at 40°C. The ratio of $S_{max}(40°C)/S_{max}(25°C)$ for both catalyzed and uncatalyzed reactions at various concentrations of copper(II) remains constant. This indicates that the temperature effect is largely or wholly due to an increase in the difference of rates of catalyzed and uncatalyzed reactions.

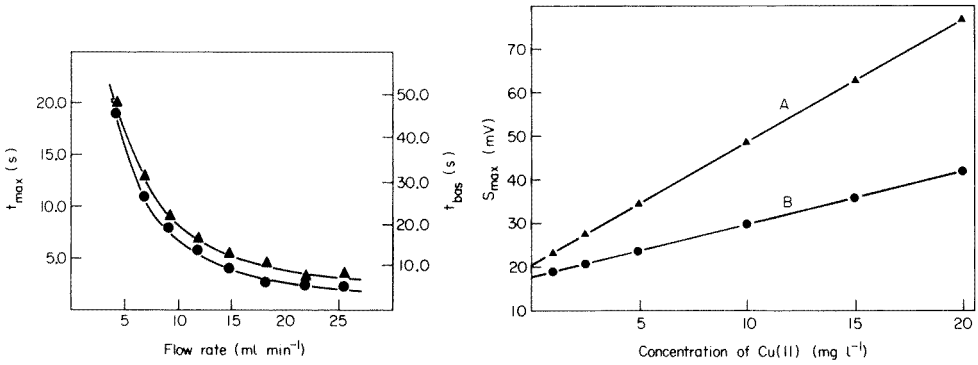

Fig. 4. Effect of flow rate on t_{max} and t_{bas}. Concentration of Cu(II) injected, 5 μg ml^{-1}. Other experimental conditions as in Fig. 2. (●) t_{max}; (▲) t_{bas}.

Fig. 5. Working curves for the determination of Cu(II) by the continuous-flow method proposed: (A) 40°C; (B) 25°C. [At 25°C: y = (1.20 ± 0.53)x + (7.7 ± 6.0), SE: 0.001; at 40°C: y = (2.8 ± 1.2)x + (10.4 ± 14.0), SE: 0.002].

Interferences and applications

Two types of interferences can be expected from other metal ion species: interferences with the catalytic effect of copper(II) on the reaction and interferences with the monitoring of $[Fe(H_2O)_5SCN]^{2+}$. Table 2 presents a summary of interference studies along with some cation levels in human blood serum (average normal values). Even though these levels in serum are too low to cause interference, direct injection of whole serum samples yielded distorted peaks (typical signals are illustrated in Fig. 6), probably because of complexation of either Cu(II) or Fe(III), or both, by ligands present in the proteins of the sample or pA gradient. Deproteinized serum gave well defined and reproducible peaks.

By use of the method of standard additions to minimize the matrix effect, copper in samples of human blood serum was estimated after first treating it with 2 M hydrochloric acid and trichloroacetic acid (20%) as recommended by Gubler et al. [20] for deproteinization. Results for determination of copper in 35 individual samples of human blood serum by the continuous-flow method proposed here were compared with those of independent determination by atomic absorption spectrometry (Perkin-Elmer 290B spectrophotometer). Figure 7 illustrates the correlation; the slope obtained by linear regression was 1.008 ± 0.18 with an intercept equal to 0.061 ± 0.029

TABLE 2

Effect of some metallic species (added as nitrate or chloride) and other foreign species in the repetitive determination of copper(II) by closed-loop flow injection[a]

Element	Normal level in serum (mg l^{-1})	Tolerance level (mg l^{-1})	Element	Normal level in serum (mg l^{-1})	Tolerance level (mg l^{-1})
Na	3200	—	Fe(II)[b]	0.8—1.6	100
K	120—214	—	Pb(II)	0.3—0.4	25
Ca	90—100	>1000	Al(III)	0.13—0.17	100
Mg	36—58	>1000	Cr(III)	0.03	50
Zn	1.2	50	Mn(II)	0.01—0.02	100
Cu	0.7—1.6	—	Cd(II)[c]	0.001—0.005	50

[a]Thiourea, cysteine, and dipyridyl, ligands which should stabilize Cu(I) formed in the catalytic cycle when added at levels of up to 10 mg l^{-1} (in the reservoir solution) failed to show activating or inhibiting effects. The pH of the injecting sample should be controlled between 2 and 4. At pH values lower than 2, distorted peaks are obtained because of the formation of colloidal sulfur and at pH higher than 4, the catalyzed reaction is very slow.
[b]A concentration of iron(III) in the injected sample of about 25 mg l^{-1} can be tolerated. A decrease in peak height is observed at higher concentrations. The formation of excess Fe(III)—thiocyanate complex may also result in the presence of a "negative" peak.
[c]Yatsimirskii [21] has determined Cd(II) using the inhibitory effect of this ion on the indicator reaction used here. No such effect was observed in these studies because the thiosulfate concentration is sufficiently high to cause reaction (1) even after complexation with Cd(II).

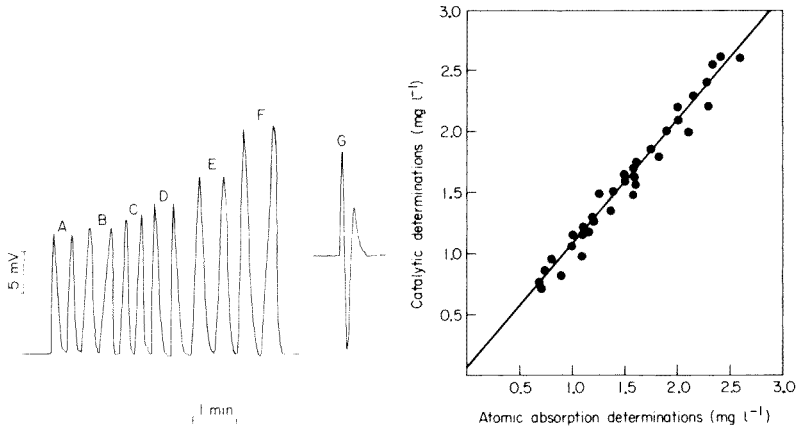

Fig. 6. Typical signal traces for Cu(II) determination. Cu(II) in mg l^{-1}: (A) 0.0; (B) 0.75; (C) 1.5; (D) 3.0; (E) 5.0; (F) 10.0. Curve G shows the split peak obtained when whole serum is injected. Average flow rate, 10 ml min^{-1}. Temp., 40°C.

Fig. 7. Comparison of results obtained by the catalytic method and atomic absorption determination. Regression line: $y = (0.061 \pm 0.29) + (1.008 \pm 0.18)x$; S.E. = 0.001.

(quite below the limit of detection of the continuous-flow method) with a standard error of 0.001 and Pearson's correlation coefficient of 0.983. The correlation can be considered as good and without bias toward either method of determination.

The authors are indebted to David Jackson (Oklahoma State University Student Hospital and Clinic) for samples of human blood serum. This work was supported by the National Science Foundation [Grant No. CHE-7923956].

REFERENCES

1 The Bio-Science Laboratories Handbook, 10th edn., Bio-Science Laboratories, Van Nuys, CA, 1973, p. 205.
2 N. W. Tietz (Ed), in Fundamentals of Clinical Chemistry, W. B. Saunders, Philadelphia, 1976, pp. 930–932.
3 A. P. Todd, M. E. Thorpe and V. M. Rosenoer, J. Clin. Pathol., 20 (1967) 276.
4 W. Oskar, Mikrochim. Acta, 2 (1979) 111.
5 H. Berndt and E. Jackwerth, At. Absorpt. Newsl., 15 (1976) 109.
6 M. R. McCullough and T. Vickers, Anal. Chem., 48 (1976) 1006.
7 J. Knoth, H. Schwenke, R. Marten and J. Glauer, J. Clin. Chem. Clin. Biochem., 15 (1977) 557.
8 H. Hirsh, H. Schenkel, I. Unger and D. Picinic, J. Clin. Chem. Clin. Biochem., 11 (1973) 465.
9 M. D. Barnett and B. Brozovic, Clin. Chim. Acta, 58 (1975) 295.
10 S.T. Ijpma, C. J. Jongkind and B. Liejnse, J. Clin. Chem. Clin. Biochem., 17 (1979) 331.

11 H. A. Mottola and H. B. Mark, Jr., Anal Chem., 52 (1980) 31R.
12 K. Khalifa, H. Doss and R. Awadallah, Analyst, 95 (1970) 207.
13 M. N. Orlova, Vopr. Med. Khim., 18 (1972) 16; Chem. Abstr., 76 (1972) 12388x.
14 A. A. Alexiev, P. R. Bontchev and V. Bardarov, Mikrochim. Acta, 1976 (II) 535.
15 M. Otto, H. Mueller and G. Werner, Talanta, 26 (1979) 781.
16 C. Fragale, P. Bruno and G. Fragale, Lab. (Milan), 4 (1977) 367.
17 S. M. Ramasamy, A. Iob and H. A. Mottola, Anal. Chem., 51 (1979) 1637.
18 E. W. Chlapowski and H. A. Mottola, Anal. Chim. Acta, 76 (1975) 319.
19 H. A. Mottola and A. Hanna, Anal. Chim. Acta, 100 (1978) 167.
20 C. J. Gubler, M. E. Lahey, H. Ashenbrucker, G. E. Cartwright and M. M. Wintrobe, J. Biol. Chem., 196 (1952) 209.
21 K. B. Yatsimirskii, Zh. Anal. Khim., 10 (1955) 339; Chem. Abstr., 50 (1956) 7647.

Analytica Chimica Acta, 127 (1981) 47—53
Elsevier Scientific Publishing Company, Amsterdam — Printed in The Netherlands

HIGH-PERFORMANCE LIQUID CHROMATOGRAPHIC DETERMINATION OF THE ANTITUMOR AGENT MITOMYCIN C IN HUMAN BLOOD PLASMA

J. DEN HARTIGH and W. J. VAN OORT*

Department of Analytical Pharmacy, Pharmaceutical Laboratory, State University of Utrecht, Catharijnesingel 60, 3511 GH Utrecht (The Netherlands)

M. C. Y. M. BOCKEN and H. M. PINEDO

Netherlands Cancer Institute and Department of Oncology, Academic Hospital of the Free University of Amsterdam, De Boelelaan 1117, 1007 MB Amsterdam (The Netherlands)

(Received 25th January 1981)

SUMMARY

A high-performance liquid chromatographic method for the determination of the antitumor drug mitomycin C in blood plasma samples of cancer patients is described. The drug is extracted from the plasma with chloroform—2-propanol (1 + 1, w/w) and chromatographed on a reversed-phase column with u.v. detection at 365 nm. The detection limit of the determination is 1 ng ml^{-1} for 0.2—1.0 ml plasma samples. Preliminary results of a pharmacokinetic study show that the sensitivity and selectivity of the assay are adequate for drug monitoring in clinical practice. The results obtained from multi-wavelength detection suggest the existence of metabolites.

Mitomycin C (MMC) is an antitumor antibiotic isolated from *Streptomyces caespitosus*. Initially, with daily administration of the drug, its clinical use was limited by severe bone marrow toxicity. The development of high-dose intermittent schedules, and combination with other antineoplastic agents in several regimens, has resulted in an increased therapeutic index, illustrating its effectiveness in tumor types such as breast cancer, adenocarcinoma of the lung, and cervical cancer. Clinical effectiveness and toxicity appear to depend on dose and schedule [1]. Little is known about the clinical pharmacokinetics of MMC because of the lack of a convenient selective assay, sensitive enough to determine MMC concentrations in biological samples. Most of the pharmacokinetic data have so far been obtained by a microbiological assay, with a detection limit of 100 ng ml^{-1} of serum, which could only be lowered to 2 ng per ml by the use of particularly sensitive micro-organisms [2].

Recently, a high-performance liquid chromatographic (h.p.l.c.) method has been described for the determination of MMC in serum [3]. Despite the potentially more sensitive detection, as shown by measurements of pure MMC samples, the described method does not permit the determination of MMC at concentrations below 40 ng ml^{-1} of serum; a reversed-phase chroma-

tographic system was applied with aqueous methanol as the mobile phase and u.v. detection at 365 nm. Kono et al. [3] showed a limited amount of data, obtained from analyzing blood samples of one patient and illustrated by a non-logarithmic serum concentration—time curve. However, a lower detection limit is needed for drug monitoring and pharmacokinetic studies. Biological half-lives which are shorter than one hour result in plasma disappearance curves that rapidly reach plasma levels of 1—5 ng ml^{-1}. These concentrations are still within the therapeutic range. Srivastava and Hornemann [4] described an h.p.l.c. method for separating mitomycin A, B, C and polar conversion products, using a normal phase chromatographic system and detection at 254 nm. This qualitative method is less suitable for the determination of MMC in plasma samples, because of the higher interference of plasma components and loss of sensitivity at the detection wavelength 254 nm, when compared to that at 365 nm. Edwards et al. [5] determined the stability of MMC and investigated qualitatively its decomposition in buffered aqueous media using various reversed-phase h.p.l.c. systems. A basic or acidic ion-pairing agent was added to the mobile phase in order to separate the charged decomposition products, and u.v. detection at 254 nm was used. Edwards et al. only described the kinetics of the decomposition in vitro, but their h.p.l.c. methods could possibly be applied in the analysis of biological samples containing metabolites and/or chemical decomposition products, with detection at 254 nm and at 365 nm.

The complex nature of the chemical behaviour of MMC limits the variation of procedural parameters, as the drug is rapidly decomposed in both acidic and basic aqueous solutions. In this paper, a new sample pretreatment procedure and a quantitative h.p.l.c. method for MMC in plasma and serum are reported. The method is sensitive enough for monitoring MMC concentrations down to 1 ng ml^{-1} of sample. Initial results of clinical pharmacokinetic investigations on MMC obtained by applying these techniques are presented.

EXPERIMENTAL

Chemicals and apparatus

The mitomycin C used was kindly supplied by Bristol Myers b.v. (Bussum, The Netherlands). Chromatographic solvents and other chemicals were of analytical-grade quality.

The chromatographic system consisted of a solvent delivery system type 6000A, a U6K septumless injection system (or an automatic sample injection device WISP Model 710) and a dual-cell u.v. absorbance detector 440 with fixed wavelength filters for detection at 254 nm and 365 nm (all from Waters Assoc., Milford, MA). A Waters Assoc. μBondapak C18 reversed-phase column (30 cm × 3.9 mm i.d., particle size 10 μm) was used. The mobile phase consisting of 0.01 M phosphate buffer pH 6.0—methanol (70 + 30, w/w), was filtered through a 0.2-μm filter and de-aerated ultrasonically before use. The flow rate was 1.0 ml min^{-1}. Retention times and

peak areas were measured with an SP4000 data system (Spectra Physics, Santa Clara, CA). The chromatographic analyses were done at ambient temperature.

Procedures

Plasma samples were collected from patients during 3—9 h after intravenous injection of MMC. Immediately after the blood had been sampled in heparin-containing tubes, the samples were centrifuged and the plasma was transferred to a glass tube and stored at −18°C. For the extraction of MMC, 0.2, 0.5 or 1.0 ml was mixed with respectively 2.0, 5.0 or 10.0 ml of chloroform—2-propanol (1 + 1, w/w). After shaking for 1 min and centrifuging for 5 min (2500 g), the clear supernatant liquid was transferred to a conical glass tube and evaporated to dryness at 30—40°C under nitrogen. The residue was dissolved in 100 μl of methanol. Aliquots of exactly 10 μl were injected into the chromatograph.

RESULTS AND DISCUSSION

Sample pretreatment

Following the extraction procedure with ethyl acetate, described by Kono et al. [3], the chromatograms obtained from blank serum showed no interfering peaks with k' factors similar to MMC. Chromatograms of MMC-spiked serum showed at least five peaks, three of which interfered seriously with the peak of MMC. This might be due to the addition of 0.1 ml of 0.5 M sodium dihydrogenphosphate (pH 4.2) in the extraction procedure, leading to the decomposition of MMC during mixing. Results obtained here on the kinetics of the decomposition of MMC and the nature of the products will be reported soon.

Table 1 lists the extraction solvents studied. Considering partition coefficient, boiling point, chromatograms of blank serum extracts, and stability during drying of the extract, a mixture of chloroform and 2-propanol (1 + 1,

TABLE 1

Extraction solvents tested

Solvent	Partition coefficient organic phase/aqueous phase	Boiling point (°C)
Ethyl acetate	0.51	77
$CHCl_3$	0.27	61
$CHCl_3$/2-propanol (90 + 10)	0.50	
$CHCl_3$/2-propanol (50 + 50)	1.52	
1-Pentanol	2.32	137.5
$CHCl_3$/1-pentanol (90 + 10)	1.12	
$CHCl_3$/1-pentanol (80 + 20)	1.85	
CH_2Cl_2/2-propanol (50 + 50)	1.04	

w/w) was selected for the extraction. This yielded recoveries of more than 90% with a phase volume ratio of serum/extractant of at least 1:8.

The danger of decomposition of MMC confines the evaporation temperature to 40°C; recovery at 40°C is 99%, at 60°C < 90%. The time needed for evaporation can be shortened by passing a stream of nitrogen over the solution. The residue was dissolved in methanol, because complete and reproducible dissolution of MMC in the mobile phase could not be achieved. Aliquots of 10 μl at the most could be injected without the chromatographic properties of the column becoming seriously affected.

Chromatography

The reversed-phase mode was selected for chromatographic separation of MMC, serum components and possible metabolites or decomposition products. For the selective determination of MMC, the optimal composition of the mobile phase was found to be 0.01 M phosphate buffer pH 6.0—methanol (70 + 30, w/w). Table 2 shows the variation of the k' factor for MMC with increase in the methanol content. At 30% (w/w) methanol there was no interference between serum and MMC peaks.

The wavelength of detection (365 nm) was chosen because of the u.v. spectrum of MMC (Fig. 1). As the specific absorption ($A^{1\%}_{1cm}$) at 365 nm in methanol is 680, sensitive detection may be expected. Detection at 254 nm will result in decreased sensitivity and, more seriously, an increased number of interfering peaks, close to the MMC peak. The use of an internal standard should allow a less rigid sample pretreatment. Structure-analogs are to be preferred, e.g. porfiromycin, in which the hydrogen atom at the aziridine ring is replaced by a methyl group. However, this compound is not generally available. Research is still in progress to find more easily available organic compounds, with sufficient u.v. absorption at 365 nm and which are stable enough during the evaporation step. Until now, none of a whole series of compounds studied meets these requirements.

In Fig. 2 the chromatograms of an MMC standard solution in methanol, of a blank serum extract, of a spiked serum extract and of a serum extract from a patient are presented. Calibration curves for MMC standard solutions in methanol were linear for injections of 0.5—1000 ng MMC in 10 μl of methanol and passed through the origin (r^2 = 0.9999). Calibration curves, obtained by analysis of spiked plasma from healthy volunteers, with the same sample pretreatment and chromatographic procedure as for the patient samples, were linear over the range studied from 1 ng ml^{-1} to 1500 ng ml^{-1}

TABLE 2

Variation of the k' value of MMC with the methanol fraction of the eluent

Mobile phase composition (% w/w methanol)	20	25	30	35	40	50
k' MMC	6.3	2.7	1.5	0.8	0.6	0.2

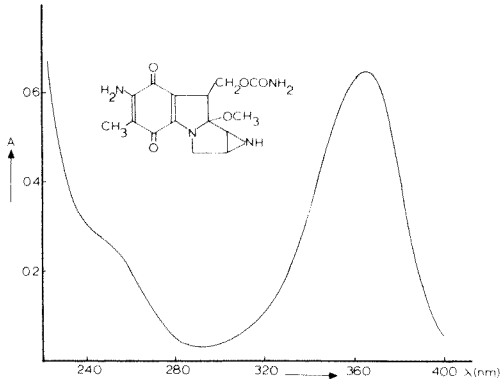

Fig. 1. U.v. spectrum of MMC in methanol (1 mg/100 ml).

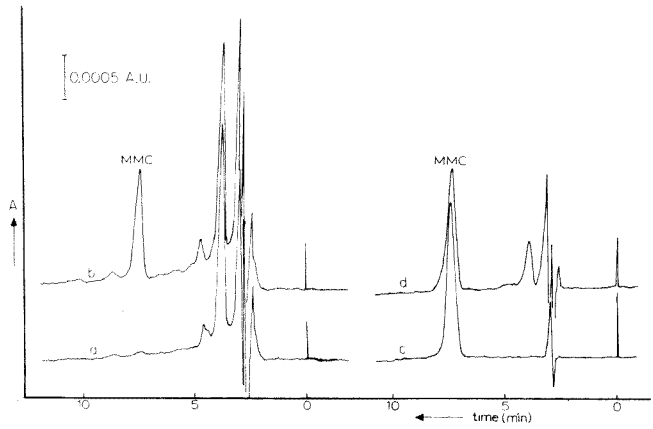

Fig. 2. Chromatograms obtained by analysis of serum and standards: (a) 1.0 ml of serum from a patient before administration of MMC; (b) 1.0 ml of serum from the patient, 3 h after intravenous administration of 35 mg MMC (MMC, 80 ng ml^{-1}); (c) a methanolic standard solution of MMC (1 μg ml^{-1}); (d) 0.2 ml of serum spiked with MMC to a concentration of 1 μg ml^{-1}. For conditions, see Experimental.

of serum, and again passed through the origin ($r^2 = 0.9998$). This calibration curve was used for calculating the MMC concentration in the samples from patients.

Preliminary clinical pharmacokinetic results

The method described was tested on blood samples from patients receiving MMC, either as a single agent or in combination with vincristin, bleomycin and cis-platinum. In Fig. 3, a typical logarithmic concentration/time curve is presented. Immediately after administration, the MMC level in plasma is about 1 μg ml^{-1}; the lower level could be established down to 1 ng ml^{-1} of plasma, 3—9 h after administration, depending on the dose and the rates of

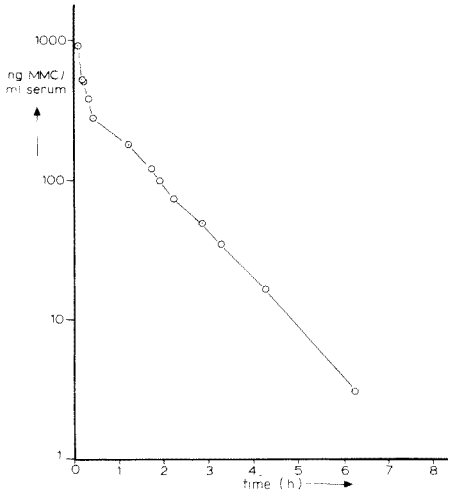

Fig. 3. Concentration of MMC as a function of time, obtained by analysis of serum samples from a patient, who had received 18 mg MMC intravenously (10 mg m^{-2}). For conditions, see Experimental.

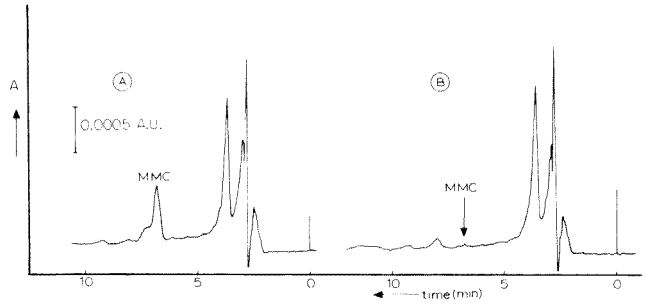

Fig. 4. Chromatograms obtained by analysis of 1.0 ml of serum from a patient: (A) 3 h after intravenous administration of 25 mg of MMC (MMC, 30 ng ml^{-1}); (B) before administration of MMC. For conditions, see Experimental.

distribution and elimination. Pharmacokinetic evaluation of such concentration/time curves for intravenously administered MMC in 7 patients (5—20 mg m^{-2}) fits a two-compartment model with half-lives of the elimination phase varying from 30 to 60 min. An extensive study on the clinical pharmacokinetics of MMC will be published.

Small differences were found between the MMC peak of spiked plasma extracts and plasma extracts from patients. One hour after administration a shoulder at the MMC peak appeared in the chromatogram, resulting in decreased accuracy of the integrated peak area used for calculation of the concentration (Fig. 4). Additional peaks became apparent in u.v. detection at lower wavelengths, even when the patients did not eat or receive any

co-medication during the period of therapy and monitoring of drug levels. The peaks, of which the heights increased and decreased with time, might possibly be ascribed to metabolites or decomposition products in vivo. Research is going on to investigate these phenomena, which may be important for the mechanism of action of MMC, as the drug itself is probably not active.

The help of Ms. Helen Gall (Academic Hospital, Free University, Amsterdam) in collecting the patient plasma samples is gratefully acknowledged.

REFERENCES

1 S. K. Carter and S. T. Crooke, Mitomycin C, Current Status and New Developments, Academic Press, New York, 1979, p. 3.
2 H. Fujita, Jpn. J. Clin. Oncol., 12 (1971) 151.
3 A. Kono, Y. Hara, S. Eguchi, M. Tanaka and Y. Matsushima, J. Chromatogr., 164 (1979) 404.
4 S. C. Srivastava and U. Hornemann, J. Chromatogr., 161 (1978) 393.
5 E. Edwards, A. B. Selkirk and R. B. Taylor, Int. J. Pharm., 4 (1979) 21.

Analytica Chimica Acta, 127 (1981) 55—61
Elsevier Scientific Publishing Company, Amsterdam — Printed in The Netherlands

A COMPARISON OF CAPILLARY CHROMATOGRAPHIC TECHNIQUES FOR THE SEPARATION OF VERY LARGE POLYCYCLIC AROMATIC MOLECULES

YUKIO HIRATA[a] and MILOS NOVOTNY*
Chemistry Department, Indiana University, Bloomington, IN 47405 (U.S.A.)
PAUL A. PEADEN and MILTON L. LEE
Chemistry Department, Brigham Young University, Provo, UT 84602 (U.S.A.)
(Received 24th September 1980)

SUMMARY

Current advances in the technology of capillary columns for gas chromatography permit extension of the range of polycyclic aromatic compounds which may be eluted. High-performance liquid chromatography (h.p.l.c.) in the non-aqueous, reversed-phase mode shows promise for separation of even larger molecules: an inquiry into the feasibility of capillary h.p.l.c. in this area has resulted in elution of polycyclic compounds containing up to eleven aromatic rings.

The detrimental health effects caused by polycyclic aromatic compounds (PAC) that are generated in various combustion processes are well-established. Certain of these substances are known to be mutagenic and carcinogenic. While various analytical procedures have been developed in numerous labortories for their determination, chromatographic separations play a prominent role in this field [1].

Mixtures of PAC isolated from various products of combustion (e.g., soot, coal tar, or smoke condensates) are frequently very complex, and the same is true for materials derived from petroleum or coal. When high-efficiency gas chromatographic columns are employed, it is not unusual to observe 100—200 compounds in such mixtures [2—4] in the range of 2-ring to 6-ring PAC structures.

Capillary gas chromatography (g.c.) and high-performance liquid chromatography (h.p.l.c.) have been developed over the years as successful methods for PAC separation. Both methods hold advantages and disadvantages of their own. As has been established in previous studies [2—4], relatively short thin-film glass capillary columns (yielding typically 30 000—80 000 theoretical plates for such separations) can elute PAC containing up to six rings within the usual temperature range of modern g.c. The typical

[a]Present address: School of Materials Science, Toyohashi University of Technology, Toyohashi, Japan.

upper temperature limits for these analyses lie between 240 and 260°C. Not only does capillary g.c. have the advantage of superior resolution (often necessary to distinguish various toxicologically important PAC isomers), but its combination with mass spectrometry provides a powerful identification tool. Very precise measurements of retention data [5, 6] are of additional benefit in structural assignments.

High-performance liquid chromatography, usually in the non-polar stationary phase mode, is a relatively easy separation technique for PAC from the operator's point of view. In conventional modern h.p.l.c., typical plate numbers are about an order of magnitude lower than in capillary g.c. Correspondingly, lower component resolution is obtained. This lack of resolution can often be overcome by the use of selective detectors [7—9], such as the variable-wavelength absorbance or spectrofluorimetric monitors. Thus, reliable quantitative measurements of selected PAC are feasible with h.p.l.c. methods in spite of the obvious complexity of certain mixtures. The compound range in typical determinations overlaps with that indicated for capillary g.c. above. The shortcomings of h.p.l.c. are seen primarily in the lack of ancillary techniques for "on-line" structure elucidation of PAC, as well as insufficiently standardized column technology [10] to measure retention data reliably.

Somewhat different considerations apply for PAC larger than 6-ring structures. Because of volatility constraints, liquid chromatography becomes preferable. Although recent advances in the preparation of more thermally stable capillary columns [11—14] can extend the range of separated compounds somewhat, the scope of this method for heavier PAC appears limited. This study examines the roles of both methods using the extracts of carbon black and coal tar as examples.

Temperature limitations of the state-of-the-art glass capillary columns, including those with advanced surface treatments [11] and chemically bonded polymers [12, 13], are demonstrated here. The recently developed capillary h.p.l.c. [15—17] is offered as an alternative for the separation of large PAC, although this method at present has limitations of its own. However, separations of up to 11-ring structures are shown to be feasible using non-aqueous, reversed-phase capillary h.p.l.c.

EXPERIMENTAL AND RESULTS

Sample preparation

The aromatic fraction of coal tar was obtained through a solvent partition scheme as previously described [18]. The carbon black sample used in this study was a gift from Cabot Corporation, Boston, MA. A Soxhlet extraction with methylene chloride was carried out as previously described by Lee and Hites [19]. Extract aliquots were concentrated through solvent evaporation to the volumes appropriate for chromatographic separations.

Capillary gas chromatography

All g.c. runs were obtained with a Perkin-Elmer Model 990 gas chromatograph with the injector and the flame ionization detector connections modified for the use of glass capillary columns.

A 15 m (0.27 mm i.d.) glass capillary was first leached with a dilute hydrochloric acid solution at 110°C [11], then silylated [20] and coated statically with SE-52 phenylmethylsilicone gum (Applied Science Laboratories, State College, PA) to have 0.25 μm average film thickness. The column was conditioned at 350°C for 100 h prior to its use in chromatography. The carbon black extract was injected at room temperature, and the column was subsequently programmed at 10°C min^{-1} from 40 to 110°C and at 2°C min^{-1} from 110 to 350°C. Figure 1 shows the chromatogram obtained, indicating only a slight elevation in baseline between 310 to 350°C. The structures of representative components were assigned, based on their mass spectra (Hewlett-Packard Model 5982A combined gas chromatograph/mass spectrometer) and retention of standard compounds. A complete identification of all sample components was not carried out. The last three structures on the chromatogram are only representative of the recorded "peak clusters"; the numbers placed below the structures represent the molecular weights.

A 40 m (0.3 mm i.d.) glass capillary column was prepared with 0.3-μm bonded film of a methylpolysiloxane according to the technology described by Blomberg and Wännman [12, 13] and washed extensively with a series of organic solvents. The column was subsequently conditioned at 330°C for several hours. Figure 2 shows a comparison of coal tar and carbon black extract samples chromatographed under identical conditions (programmed from 70 to 320°C at 2°C min^{-1}). Good baseline stability at high temperatures

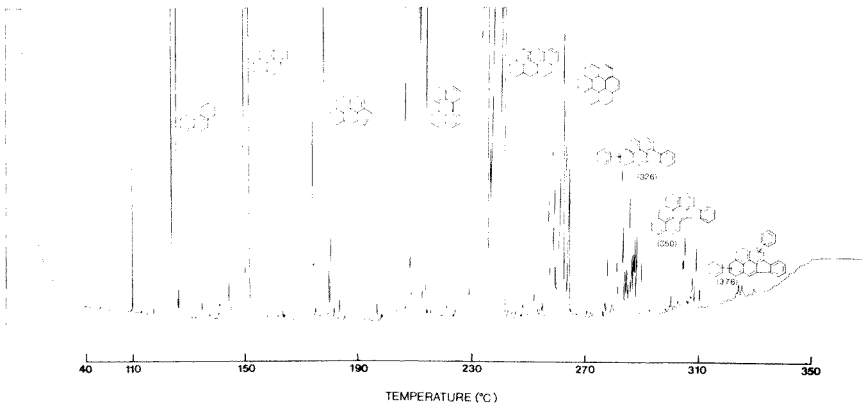

Fig. 1. High-temperature separation of the polycyclic aromatic components of carbon black obtained with 15 m (0.27 mm i.d.) glass capillary column coated with SE-52 silicone gum. Carrier gas, helium.

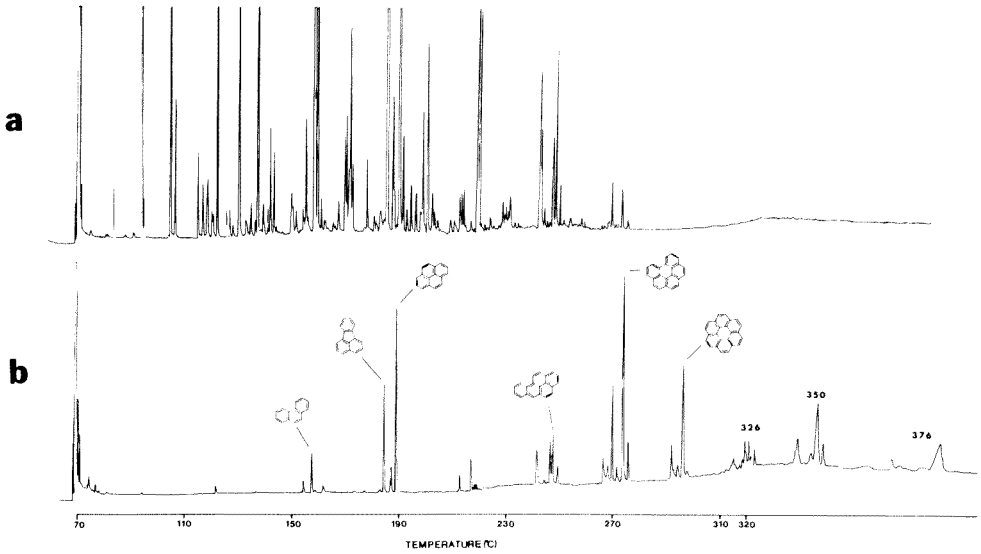

Fig. 2. Chromatrograms of (a) aromatic fraction of coal tar, and (b) carbon black extract, obtained with 40 m (0.3 mm i.d.) glass capillary column provided with a film of bonded polysiloxane phase. Carrier gas, helium.

is demonstrated. Again, a combined gas chromatograph/mass spectrometer was employed to ascertain the range of separation (see Fig. 2 b).

Capillary high-performance liquid chromatography

The equipment used for capillary h.p.l.c. was recently described [17]. The column used was a 100 m (70 μm i.d.) thick-walled glass micro-capillary packed with 30-μm alumina particles [15]. The stationary phase (an octadecylsilyl bonded phase) was generated inside the column via an in situ bonding technique [16]. The inlet pressure was set at 300 atm, while the flow rate was approximately 1 μl min^{-1}.

The stepwise gradient elution technique [17] was employed. The separated components were detected with a miniaturized spectrofluorimetric detector [17], with a cell volume of 0.1 μl. A full-scale recorder deflection corresponds to approximately 1-ng amounts.

Figure 3 shows the separation of the heavy components of the carbon black extract obtained during a 50-h run. Peaks from the selected parts of this chromatogram were trapped at the column exit and subjected to direct-probe mass spectrometry and spectrofluorimetric measurement as previously described [21]. Although most identifications are tentative because of the lack of suitable standards for the high molecular weights, the presence of at least 11-ring structures was suggested.

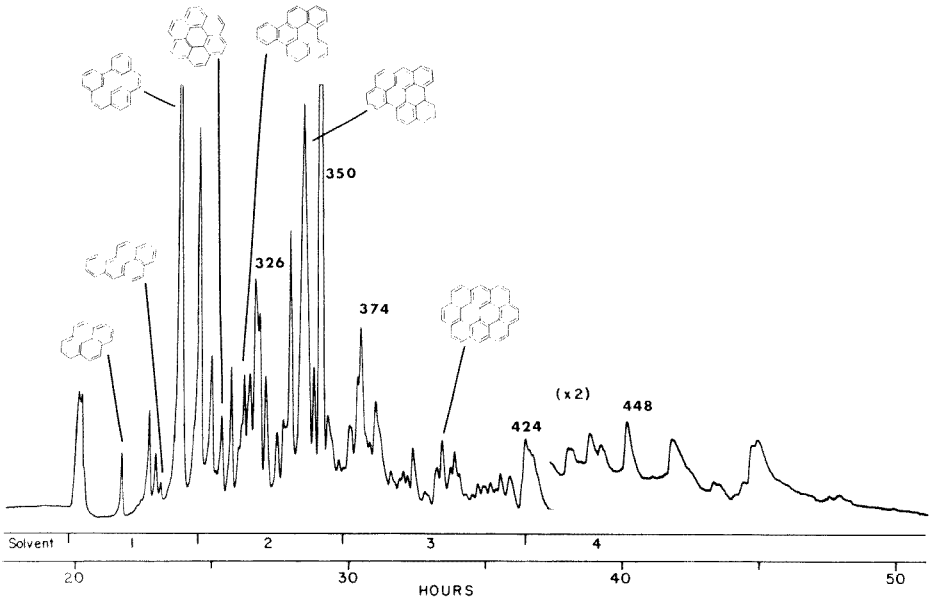

Fig. 3. Separation of the carbon black heavy aromatic components by h.p.l.c. obtained with 100 m (70 μm i.d.) glass capillary column containing 30 μm irregular alumina/C_{18}-bonded phase. Stepwise gradient: (1) 100% acetonitrile; (2) 80% acetonitrile—20% dichloroethane; (3) 50% acetonitrile—50% dichloroethane; (4) 100% dichloroethane.

DISCUSSION

The extraction of various PAC-containing materials with powerful organic solvents may result in an appreciable yield of extractables, but frequently only a small percentage of this material can be separated by g.c. For example, about 73% of solvent-refined coal (SRC) was found extractable [4] into methylene chloride, of which amount 18% and 21% correspond, respectively, to the aliphatic and the polyaromatic fractions. However, gas chromatography could cover only some 26% of the polyaromatic fraction and 11% injected aliphatic fraction, corresponding to 1 and 0.3%, respectively, of the original SRC sample. At present, the remaining non-volatile compounds can neither be separated effectively nor identified in this and similar materials.

Evidence exists for some very large PAC in numerous mixtures (e.g., certain petroleum fractions [22]), but again an effective methodology for their complete separation and identification has not been developed yet. The toxicological and chemical significance of most PAC above 6-ring structures is unknown because of the unavailability of standard compounds and the lack of structural characterization.

Recent advances in the technology of glass [11—13] and fused-silica [14] capillary columns make it feasible to extend the temperature limits of capillary g.c. As shown by Figs. 1 and 2, these improvements extend the

range for PAC up to eight rings. However, temperatures in excess of 350°C are judged to be the present technological limit of this method.

Recently developed polysiloxane bonded phases [12, 13] seem to offer an interesting approach to the preparation of stable columns for high-temperature g.c. work. As this technology develops further, columns with different selectivities may become available. Figure 2 also exemplifies how different combustion products may vary in terms of their PAC composition: coal tar (a by-product of the coking processes) has only a few major components at the high-molecular-weight end of the chromatogram, while the carbon black extract primarily consists of much larger molecules. The peak asymmetry of the late-eluting components can be attributed to their limited solubility in the methylpolysiloxane stationary phase.

Given the temperature limitations of g.c., liquid-chromatographic techniques become the only viable chromatographic alternative for sample components with more than seven or eight condensed aromatic rings. However, the problem of sample complexity becomes enormous (as occurrence of isomers increases with molecular weight) so that conventional h.p.l.c. resolution is insufficient. While capillary h.p.l.c. has the potential [15, 23] for improved resolution, Fig. 3 demonstrates that much improvement is needed. Apart from the current instrumental limitations [15, 17] of small-volume technology, long separation times are a major difficulty.

Identification of the separated PAC components is a major task at present. Although their mass and fluorescence spectra may provide useful information, practically no reference compounds are available for this compound range. Once the techniques of combined liquid chromatography—mass spectrometry are adequately developed, capillary h.p.l.c. will have a distinct advantage with its very low flow rates (typically, 1 μl min^{-1}) for "on-line" investigations of the separated PAC. Meanwhile, repeated trapping of capillary fractions is tedious at best.

Because of the limited solubility of large polycyclic molecules, the selection of the column phase system used in this work deserves further mention. The non-aqueous reversed-phase system is generally compatible with both solubility and retention of the large PAC molecules. It should be noted that the polarity of the octadecyl packing appears less than that of any of the solvents used. Severe tailing of the later components in Fig. 3 could be caused by solubility problems, insufficient column deactivation, or a combination of both.

This work was supported by Grant No. 24349 from the National Institute of General Medical Sciences, U.S. Public Health Service.

REFERENCES

1 M. L. Lee, M. Novotny and K. D. Bartle, Analytical Chemistry of Polycyclic Aromatic Compounds, Academic Press, New York, 1981 (in press).
2 M. L. Lee, M. Novotny and K. D. Bartle, Anal. Chem., 48 (1976) 405.

3 M. L. Lee, M. Novotny and K. D. Bartle, Anal. Chem., 48 (1976) 1566.
4 R. V. Schultz, J. W. Jorgenson, M. P. Maskarinec, M. Novotny and L. J. Todd, Fuel, 58 (1979) 783.
5 M. L. Lee, D. L. Vassilaros, C. M. White and M. Novotny, Anal. Chem., 52 (1979) 768.
6 M. Novotny, R. Kump, F. Merli and L. J. Todd, Anal. Chem., 52 (1980) 401.
7 H. Boden, J. Chromatogr. Sci., 14 (1976) 391.
8 D. C. Hunt, P. J. Wild and N. T. Crosby, J. Chromatogr., 130 (1977) 320.
9 K. Ogan, E. Katz and W. Slavin, Anal. Chem., 51 (1979) 1315.
10 K. Ogan and E. Katz, J. Chromatogr., 188 (1980) 115.
11 M. L. Lee, D. L. Vassilaros, L. V. Phillips, D. M. Hercules, H. Azumaya, J. W. Jorgenson, M. P. Maskarinec and M. Novotny, Anal. Lett., 12(A2) (1979) 191.
12 L. Blomberg and T. Wännman, J. Chromatogr., 168 (1979) 81.
13 L. Blomberg and T. Wännman, J. Chromatogr., 186 (1979) 159.
14 R. Dandeneau, P. Bente, T. Rooney and R. Hiskes, Am. Lab., 11 (9) (1979) 61. 61.
15 T. Tsuda and M. Novotny, Anal. Chem., 50 (1978) 271.
16 Y. Hirata, M. Novotny, T. Tsuda and D. Ishii, Anal. Chem., 51 (1979) 1807.
17 Y. Hirata and M. Novotny, J. Chromatogr., 186 (1979) 521.
18 M. Novotny, M. L. Lee and K. D. Bartle, J. Chromatogr. Sci., 12 (1974) 606.
19 M. L. Lee and R. Hites, Anal. Chem., 48 (1976) 1890.
20 M. Novotny and K. Tesarik, Chromatographia, 1 (1968) 332.
21 P. A. Peaden, M. L. Lee, Y. Hirata and M. Novotny, Anal. Chem., 52 (1980) 2268.
22 K. H. Altgelt nad T. H. Gouw, Adv. Chromatogr., 13 (1975) 71.
23 J. H. Knox and M. T. Gilbert, J. Chromatogr., 186 (1979) 405.

Analytica Chimica Acta, 127 (1981) 63—70
Elsevier Scientific Publishing Company, Amsterdam — Printed in The Netherlands

QUANTITATIVE SEPARATION OF CALCIUM FROM MAGNESIUM, ALUMINIUM, IRON(III) AND MANY OTHER ELEMENTS BY CATION-EXCHANGE CHROMATOGRAPHY IN METHANOLIC HYDROCHLORIC ACID ON A MACROPOROUS RESIN

F. W. E. STRELOW

National Chemical Research Laboratory, P.O. Box 395, Pretoria 0001 (Republic of South Africa)

(Received 21st January 1981)

SUMMARY

Calcium can be separated from Mg, Al, Cu(II), Fe(III), Ga, Zn, Mn(II), Co(II), U(VI) and Ti(IV) by cation-exchange chromatography on a column of AG MP-50 macroporous resin. Sr, Ba, Sc, Y, the lanthanides, Zr, Hf and Th are retained together with calcium. The separation factor for the Ca—Mg pair in 3 M HCl containing 50% methanol is about 20, which is considerably larger than those obtained by other ion-exchange procedures. Separations with the cation-exchange resin are sharp and quantitative. A column containing only 2 g (5.4 ml) of resin is sufficient to separate up to 0.2 mmol of calcium from 2 mmol of magnesium and larger amounts of Fe(III), Cu(II) and Zn. On a 10-g column, up to 2.5 mmol of calcium can be separated easily from similar and larger amounts of other elements. Distribution coefficients for calcium and magnesium with variation of cross-linkage and variation of methanol concentration are presented, together with relevant elution curves and results for synthetic mixtures.

From a practical point of view, probably the best and most selective ion-exchange method for the quantitative separation of calcium from other elements is that based on a cation-exchange resin and 3 M hydrochloric acid in 60% ethanol (or another water-soluble organic solvent) as eluant [1]. The separation factor, $\alpha_{Mg}^{Ca} = 5.6$, is considerably larger than the factor in aqueous hydrochloric acid ($\alpha_{Mg}^{Ca} = 2.0$) [2] and is comparable to the separation factors obtained in organic complexing agents [3, 4], while the inconvenient destruction of the organic complexing agent, which can interfere in the final determination, is avoided.

It has been pointed out that distribution coefficients of calcium show an increase with increasing cross-linkage from 2 to 16% divinylbenzene, whereas elements such as magnesium and aluminium show an increase only up to 12% cross-linkage and then decrease again [5]. With a 12% cross-linked resin the separation factor between calcium and magnesium, $\alpha_{Mg}^{Ca} = 8$, is appreciably larger than with a 8% cross-linked resin [1]. Unfortunately, the exchange rates also become considerably slower. This either leads to considerable peak broadening and larger elution volumes for magnesium or enforces slower elution rates. For this reason the 8% cross-linked resin has been preferred [1].

The macroreticular or macroporous resins, which have a wide open but rigid pore structure and a very high cross-linkage (20—25%) in the exchange region were introduced by Kunin et al. [6]. It seemed probable that such resins could provide satisfactory exchange rates even at very high cross-linkages because of their porosity. Macroreticular anion-exchange resins have been used for the separation of calcium from magnesium [7, 8] and from strontium [9] and barium [10] in nitric acid—organic solvent mixtures, and a specially prepared, partially sulphonated cation-exchange resin has been employed for the separation of traces of magnesium and calcium [11] by high-performance liquid chromatography. Very fast separations can also be obtained by using pellicular resins [12, 13] which have only a thin layer of exchange material at the surface. Unfortunately these resins have a very limited capacity and are unsuitable for the separation of large or widely differing amounts of elements. Apparently, no attempt has been described to use a commercial macroporous cation-exchange resin for the selective separation of larger amounts of calcium from many other elements over a wide concentration range. This paper describes such a separation.

EXPERIMENTAL

Reagents and apparatus

The chemicals used were of analytical-reagent grade. Water was distilled and passed through an Elgastat deionizer. The resin was the AG MP-50 macroporous cation exchanger on a polystyrene base (Bio-Rad Laboratories, Richmond, CA). Resin of 100—200 and 200—400 mesh particle size was used in the hydrogen form. Furthermore, AG50 microporous cation-exchange resins of various cross-linkages (100—200 mesh; Bio-Rad Laboratories) were used for distribution experiments.

Borosilicate glass columns (16 mm i.d., 40 cm long), fitted with a B19 ground glass joint at the top and a glass sinter plate (no. 2 porosity) and a tap at the bottom were used. For small amounts of calcium, the glass columns used (11 mm i.d., 15 cm long) had a wider part (20 mm i.d., 10 cm long) at the top. Glassware to be used for the separation of small amounts of calcium or other elements was heated in about 7 M nitric acid and rinsed with deionized water.

Atomic absorption measurements were done with a Varian-Techtron AA-5 instrument and a Zeiss PMQII spectrophotometer was used for molecular absorption measurements. Conditions are listed in Table 1.

Distribution coefficients

Effect of cross-linkage. Solutions (250 ml) of 1.00 M hydrochloric acid containing 2.5 mmol of calcium or magnesium were equilibrated with 2.5 g of dry AG-50 resin of the indicated cross-linkage by shaking for 24 h in a mechanical shaker at 20 ± 1°C. The resin had been dried at 60°C in a vacuum pistol over magnesium perchlorate. After equilibration, the resin was sepa-

TABLE 1

Analytical methods used

Element	Method
Ca, Mn(II)	Titration with DCTA in ammoniacal solution, methylthymol blue indicator, hydroxylammonium chloride for Mn(II). Small amounts of Ca by a.a.s. (422.7-nm line, N_2O-acetylene flame, K ionization suppressor).
Mg	Titration with EDTA at pH 10, eriochrome blueblack B indicator. Small amounts by a.a.s. (285.2-nm line, air—acetylene flame).
Al, Cu(II), Fe(III), Ga	Titration with DCTA, back-titration with $ZnSO_4$ at pH 5.5, xylenol orange indicator. Small amounts of Cu by a.a.s. (324.8-nm line, air—acetylene flame).
Zn	Titration with EDTA, pH 5.5, xylenol orange indicator.
Co(II)	Titration with EDTA, pH 6 (pyridine) naphthyl azoxine S indicator.
U(VI)	Gravimetrically as U_3O_8.
Ti(IV)	Spectrophotometric H_2O_2 method.

rated by filtration and the amounts of the elements in the aqueous and resin phases (after ashing) were determined by compleximetric titration. The distribution coefficients

$$D = \frac{\text{amount of element in resin phase}}{\text{amount of element in aqueous phase}} \times \frac{\text{g dry resin}}{\text{ml aqueous phase}}$$

were calculated from the results and are presented in Fig. 1.

Effect of methanol concentration. Appropriate amounts of 10 M hydrochloric acid, water containing 1 mmol of calcium or magnesium, and methanol were mixed and equilibrated with 2.5 g of dry AG MP-50 resin by shaking for 24 h at 20 ± 1°C. Volume changes caused by mixing were disregarded. The phases were separated, the elements determined, and the distribution coefficients calculated as indicated above. The results are presented in Fig. 2.

Elution curves. A column was filled with 27 ml (10 g dry weight) of AG MP-50 resin (100—200 mesh). The resulting resin bed was 13 cm long and 1.62 cm in diameter. It was cleaned from calcium by passing 5 M nitric acid until no calcium above background was observed by atomic absorption. The nitric acid was removed from the column with water and a solution containing 1 mmol of both calcium and magnesium in about 20 ml of 0.1 M hydrochloric acid was passed onto the resin. The ions were washed into the resin with 0.1 M hydrochloric acid. Magnesium then was eluted with 3.0 M hydrochloric acid containing 50% methanol at a flow rate of 2.2 ± 0.3 ml min^{-1}. The elution was continued until 500 ml had been passed. The calcium was eluted with 400 ml of 5.0 M nitric acid at a flow rate of 2.2 ± 0.3 ml min^{-1}. Fractions (25 ml) were taken from the beginning of the magnesium elution step and the amounts of calcium and magnesium in the fractions were determined by compleximetric titration (Table 1) or atomic absorption spectrometry (small amounts) after the excess of acid

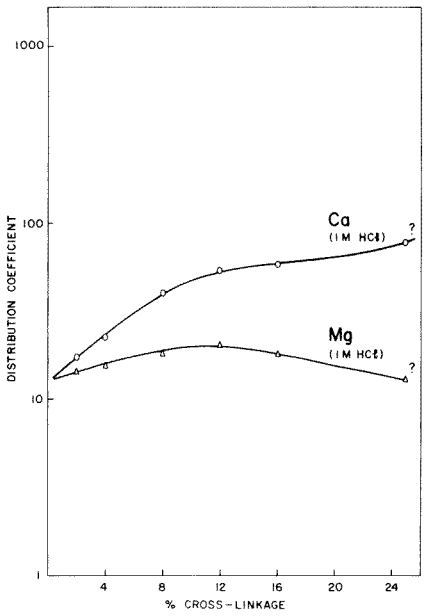

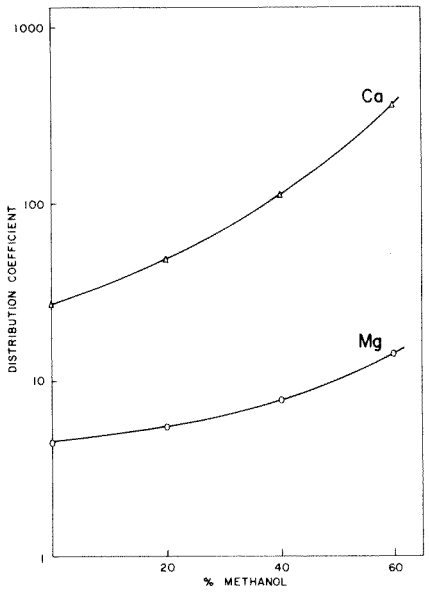

Fig. 1. Distribution coefficients of calcium and magnesium in 1 M HCl with AG 50W cation-exchange resins of various cross-linkages.

Fig. 2. Distribution coefficients of calcium and magnesium with AG MP-50 macroporous cation-exchange resin in 3 M HCl with various amounts of methanol.

had been removed by evaporation. The experimental elution curve is shown in Fig. 3, which also shows an elution curve for the Al—Ca pair on the same column, but with the flow rate for the elution of calcium increased to 3.5 ± 0.5 ml min^{-1}.

Figure 4 shows corresponding elution curves for the separation of 0.1 mmol of calcium from 1 mmol of magnesium or aluminium on a column containing only 2 g of AG MP-50 resin. The resulting resin bed was 5.4 cm long and 1.12 cm in diameter. Slower flow rates were used in these cases.

Quantitative separations

Columns with 10 g of resin. Appropriate volumes of standard solutions of calcium and one other element in dilute hydrochloric acid were measured out in triplicate and mixed. Triplicate standards for comparison were measured out at the same time and kept. The mixed solutions were passed onto columns containing 27 ml of AG MP-50 resin as described above and the ions were washed into the resin with 0.1 M hydrochloric acid. Magnesium, aluminium and other elements then were eluted with 300 ml of 3.0 M hydrochloric acid containing 50% methanol at a flow rate of 2.2 ± 0.3 ml min^{-1}, the elements being first washed into the column with two 10-ml portions. Finally calcium was eluted with 350 ml of 5.0 M nitric acid at a flow rate

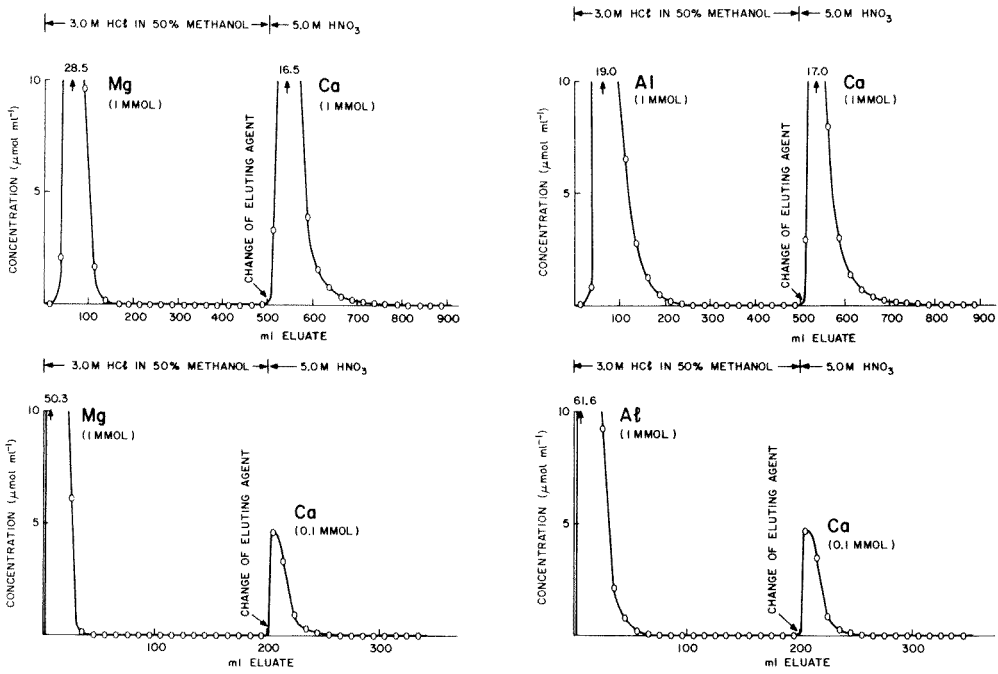

Fig. 3. Elution curves for Mg—Ca and for Al—Ca mixtures; 27 ml (10 g) of AG MP-50 resin (100—200 mesh); flow rates were 2.2 ± 0.3 ml min^{-1} for Mg and Ca in the Mg—Ca separation, but 2.2 ± 0.3 ml min^{-1} for Al and 3.5 ± 0.3 ml min^{-1} for Ca in the Al—Ca separation.

Fig. 4. Elution curves for Mg—Ca and for Al—Ca on small columns; 5.4 ml (2 g) of AG MP-50 resin (100—200 mesh); flow rates were 1.5 ± 0.2 ml min^{-1} for Mg or Al and 2.0 ± 0.3 ml min^{-1} for Ca.

of 3.0 ± 0.5 ml min^{-1}. Duplicate blank runs were carried out simultaneously. The eluates were received in clean 400-ml beakers and evaporated to dryness, and the elements in the fractions were determined (see Table 1). Corrections for the blank runs were applied. The results are presented in Table 2.

Columns with 2 g of resin. Because the calcium found in the blank runs was rather high (about 70 ± 10 μg) and the large columns therefore were unfavourable for the separation and determination of trace amounts of calcium, some separations were examined with smaller columns (5.4 ml, 2 g of resin; resin bed 5.4 cm long, 1.12 cm diameter). Magnesium and the other elements were adsorbed from 15 ml of 0.1 M hydrochloric acid and magnesium and others were eluted with a total volume of 80 ml of 3.0 M hydrochloric acid containing 50% methanol at a flow rate of 1.5 ± 0.3 ml min^{-1}. Calcium was then eluted with 80 ml of 5.0 M nitric acid at a flow rate of 2.0 ± 0.3 ml min^{-1}. Triplicate blank runs were carried out simultaneously. Large amounts of some elements with tendencies to chloride complex formation such as Fe(III), Cu(II) and Zn were adsorbed from

TABLE 2

Results of quantitative separations on 10-g resin columns

Taken			Found[a]	
Ca (mg)	Other element	Amount (mg)	Ca (mg)	Other element (mg)
39.61	Mg	24.40	39.60 ± 0.03	24.41 ± 0.02
99.03	Mg	0.610	99.05 ± 0.07	0.608 ± 0.007
1.98	Mg	61.00	1.98 ± 0.01	61.02 ± 0.06
39.61	Al	27.14	39.61 ± 0.04	27.13 ± 0.02
99.03	Al	2.71	99.04 ± 0.06	2.72 ± 0.01
1.98	Al	67.85	1.97 ± 0.01	67.84 ± 0.05
39.61	Cu(II)	63.90	39.62 ± 0.04	63.89 ± 0.03
99.03	Cu(II)	0.128	99.02 ± 0.07	0.128 ± 0.001
39.61	Fe(III)	59.21	39.60 ± 0.04	59.19 ± 0.04
39.61	Ga	69.52	39.60 ± 0.03	69.53 ± 0.05
39.61	Zn	65.96	39.61 ± 0.03	65.95 ± 0.04
39.61	Mn(II)	55.46	39.62 ± 0.03	55.46 ± 0.05
39.61	Co(II)	58.11	39.61 ± 0.04	58.09 ± 0.05
39.61	U(VI)	238.8	39.62 ± 0.04	238.9 ± 0.2
39.61	Ti(IV)[b]	47.14	39.63 ± 0.04	47.16 ± 0.06

[a]Averages of at least triplicate runs. [b]0.1% H_2O_2 present.

TABLE 3

Results of quantitative separations on 2-g resin columns

Taken			Found[a]	
Ca (mg)	Other element	Amount (mg)	Ca (mg)	Other element (mg)
6.665	Mg	24.40	6.663 ± 0.007	24.39 ± 0.02
0.167	Mg	48.80	0.168 ± 0.003	48.82 ± 0.04
Nil	Mg	24.40	0.019 ± 0.003 (blank)	24.40 ± 0.02
0.167	Al	27.14	0.169 ± 0.004	27.15 ± 0.02
0.167	Fe(III)[b]	592	0.167 ± 0.003	Not determined
0.167	Cu(II)[b]	639	0.168 ± 0.003	Not determined
0.167	Zn[b]	660	0.166 ± 0.004	Not determined

[a]Averages of quadruplicate runs. [b]Adsorbed from 0.5 M HCl in 90% acetone.

100 ml of 0.5 M hydrochloric acid containing 80% acetone. The results are presented in Table 3.

DISCUSSION

The methods described provide a useful means for the separation of calcium from Mg, Al, Fe(III), Ga, Cu(II), Zn, Mn(II), Co(II) U(VI) and Ti(IV).

Elements such as Ni(II), Cd, In, Bi(III), Be, Li, Na, Sn(IV), Pb(II), Hg(II) Au(III) and the platinum metals, though not investigated in detail, should also be separated without problems because they are considerably less strongly adsorbed from hydrochloric acid solutions than aluminium. Separations are sharp and quantitative for amounts ranging from trace quantities up to several millimoles. Titanium(IV) requires the presence of hydrogen peroxide in the adsorption and the elution steps because serious tailing occurs otherwise. Calcium and aluminium also show some tailing, but its extent is much less and recoveries are quantitative within the given elution volumes.

As is demonstrated by Fig. 1 the separation factor for the Ca—Mg pair in 1 M hydrochloric acid increases from a value of about 2 for the 8% cross-linked microporous resin to a value of about 6 for the macroporous resin (for which a cross-linkage of 25% was assumed). When the selective action of the organic solvent on the hydration shell of calcium is added, the separation factor increases to a value of about 20 in 3 M hydrochloric acid containing 50% methanol (Fig. 2). This is considerably larger than the separation factors obtainable with organic complexing agents [3], except for ammonium acetylacetonate, which provides a still larger separation factor [3]. The exchange kinetics are also reasonably good and the elution peaks for Mg, Al and Ti(IV) (H_2O_2 present) are similar, or slightly superior, to those obtained with the 8% cross-linked resin and 3 M hydrochloric acid containing 60% ethanol as eluting agent [1]. The peak for calcium is extremely wide when elution is continued with 3 M hydrochloric acid containing 50% methanol. At the 1-mmol level, calcium appears at a volume of about 900 ml in the eluate when a 10-g resin column is used. But the elution of the first traces of calcium is considerably less influenced by flow rate or resin particle size than in the case of a 8% cross-linked microporous resin. Quantitative elution of calcium in a reasonable time requires 5 M nitric acid; tailing is then fairly small. A 5 M hydrochloric acid eluent is somewhat less effective.

Some elements such as Sr, Ba, Sc, Y, the lanthanides, Zr, Hf and Th are also very strongly retained by the macroporous resin. They accompany calcium and some of them cannot be recovered easily by elution. The extremely strong adsorption of these elements seems to be the major disadvantage of the macroporous cation-exchange resin.

It also was observed that the resin itself contained an appreciable amount of calcium. It had to be cleaned very thoroughly by elution and by standing in 5 M nitric acid before blank runs for calcium became sufficiently low and reproducible. To obtain blank values acceptable for the determination of trace amounts of calcium was a major problem. Even with utmost care (clean glassware and conditions), triplicate blank runs with the small columns gave values of about 20 ± 4 μg of calcium. With the large columns, blank runs gave results of about 70 ± 10 μg of calcium. The relatively large scattering could have been due to atmospheric contamination, probably by way of the air filtering system which showed signs of chemical corrosion.

The separation factor of about 20 for the Ca—Mg pair obtained with the macroporous cation-exchange resin is also considerably larger than the separation factor of 8—9 obtained for the same separation on Amberlyst XN-1002 macroporous anion-exchange resin with nitric acid containing ethanol or 2-propanol as eluting agent [7]. The elution peak for magnesium appears to be considerably sharper with the cation-exchange resin, even when faster flow rates are used. Furthermore, with the anion-exchange resin, some other elements such as Cd, Cu(II) and Co(II) have considerably smaller separation factors for the separation from calcium than has magnesium and their separation is thus considerably less favourable. Their separation from calcium with the cation-exchange resin is even better than that of magnesium. Even aluminium, which is the most difficult of the elements separated, is still separated quite satisfactorily and quantitatively (Figs. 2 and 3, Tables 2 and 3). Many elements which tend to form anionic chloride complexes, such as Fe(III), Cu(II) and Zn, can be passed onto the column in 0.5 M hydrochloric acid in 90% acetone. They are not or only slightly adsorbed under these conditions and residual amounts can be eluted as described. Thus several hundred milligrams or even several grams of these elements can be separated from small amounts of calcium on a 2-g resin column.

REFERENCES

1 F. W. E. Strelow and C. R. van Zyl, Anal. Chim. Acta, 41 (1968) 529.
2 F. W. E. Strelow, Anal. Chem., 32 (1960) 1185.
3 F. W. E. Strelow and C. H. S. W. Weinert, Talanta, 17 (1970) 1.
4 F. W. E. Strelow, C. R. van Zyl and C. R. Nolte, Anal. Chim. Acta, 40 (1968) 145.
5 F. W. E. Strelow, D.Sc. Thesis, University of Pretoria, 1960, p. 23.
6 R. Kunin, E. Meitzner, J. Oline, S. Fischer and N. Frisch, Ind. Eng. Chem., Prod. Res. Develop., 1 (1962) 140.
7 J. S. Fritz and H. Waki, Anal. Chem., 35 (1963) 1079.
8 K. Kurokawa, J. Chem. Soc. Jpn., Pure Chem. Sect., 88 (1967) 188.
9 J. S. Fritz, H. Waki and B. B. Garralda, Anal. Chem., 36 (1969) 900.
10 K. Kurokawa, J. Chem. Soc. Jpn., Pure Chem. Sect., 88 (1967) 1171.
11 M. D. Arguello and J. S. Fritz, Anal. Chem., 49 (1977) 1595.
12 Y. Takata and G. Muto, Anal. Chem., 45 (1973) 1864.
13 D. J. Freed, Anal. Chem., 47 (1975) 186.

Analytica Chimica Acta, 127 (1981) 71—85
Elsevier Scientific Publishing Company, Amsterdam — Printed in The Netherlands

LASER-MICROPROBE ELEMENTAL DETERMINATIONS WITH AN OPTICAL MULTICHANNEL DETECTION SYSTEM

YAIR TALMI*
Scientific Consultant, 20-03 Fox Run, Plainsboro, NJ 08536 (U.S.A.)
H. P. SIEPER and L. MOENKE-BANKENBURG
Jenoptik, Jena (German Democratic Republic)
(Received 10th March 1980)

SUMMARY

The results obtained when a laser microprobe is adapted to imaging detectors for multi-wavelength detection are described. Detectors evaluated are a silicon-intensified target vidicon and a second-generation photodiode array. Data are presented to illustrate how the combined system can be used to monitor both surface and depth profiles of elemental content of a variety of sample types including a ruby rod and ceramic material with blemishes, electrical capacitors, integrated circuits, and surface-coated electrical conductors. It is also shown how the gating capability of the intensified vidicon can be used to monitor time-dependent changes in the several nanosecond range during the laser microprobe excitation process. Detection limits obtained with both detectors are in the range 2—500 ppm depending on the element, the wavelength used, the matrix, and other variables. The uncertainty associated with the measurement step can be improved by a factor of 2—3 by using ratios of spectral lines. Principal limitations of the laser microprobe method are the nonlinear response of intensity vs. concentration and the resulting need for reference materials with matrices similar to samples for calibration purposes.

The laser microprobe was one of the first analytical instrumentation concepts to follow the invention of the laser. It was introduced commercially in the early sixties as a new means for thermal evaporation and atomic excitation of microscope-selected microsamples [1—7]. However, its wide acceptance for surface studies has been slowed by the development of other microprobe techniques and perhaps even more by the time-consuming procedures required for spectral data processing from photographic plates that greatly offset its inherent advantages of easy operability and rapid sampling.

In the last five years there has been a steadily increasing awareness and recognition of the utility of optoelectronic image devices as multichannel spectrometric detectors. These devices are capable of simultaneously detecting an entire spectral region [8—19]. It is the intent of this paper to discuss the revitalization of the laser microprobe system via the incorporation of a multichannel spectrometric detection system, and to indicate application areas for which this combined system is most apt. The instrumentation used in this study was chosen based on performance and availability considerations.

INSTRUMENTATION

Laser microprobe

The intense energy burst from a ruby laser (694 nm) is focused through a specially designed optical microscope onto the surface of a sample. The optical path of the laser beam coincides with that of the visual optical path, thus allowing visual selection of the precise area of the sample, 10—250 μm in diameter, to be probed. A small fraction of the sample, $\leqslant 1$ μg, is thus evaporated and the microplasma formed is further heated by the laser energy to temperatures well above 5000 K. An intense emission spectrum, characteristic of the solid sample, is produced and detected spectrometrically by either a photographic or an optoelectronic image device. Additional excitation to enhance detectability and reduce self-reversal interferences can be accomplished by an auxiliary spark-gap device, positioned above the surface of the sample, which is available with the LMA-10 analyzer used (see Table 1).

Optical multichannel analyzer

The optical multichannel analyzer OMA-2 (EG&G Princeton Applied Research) is a detection system based on the use of a multichannel spectrometric detector [20], typically comprising 500 or 1024 individual light sensors. Two detectors were used in this study; a silicon-intensified target vidicon (SIT) and a silicon linear self-scanned photodiode array. Detailed descriptions of the OMA-2 system and its various array detectors have been given elsewhere [21].

The basic components of the laser microprobe/optical multichannel analyzer system and some of the relevant specifications are given in Table 1.

RESULTS AND DISCUSSION

Some performance characteristics were investigated experimentally and others were assumed on the basis of known (theoretically and experimentally established) performance characteristics of the individual system components.

Qualitative features

Contrary to most other spectrochemical methods, this system does not require sample preparation such as polishing, cutting, pulverising, etc. Samples need not be confined to a certain size or form. Components can be monitored in any sample that can be placed under the objective of the microscope. Moreover, unlike most microprobe systems, the laser microprobe does not require time-consuming evacuation of the sample chamber. Thus, determinations can be performed rapidly, an essential feature for many decision-making quality control processes. Well formed spectra were obtained for a variety of sample types including a small gold wire (0.2 mm

TABLE 1

Instrumental components

Laser Microspectral Analyzer	LMA-10 microscope/laser head unit with a power supply/control unit (Jenoptik, Jena, G.D.R.)
Solid-state ruby laser	694-nm output energy at maximum input: 0.6—1.2 J
Capacitor bank	900 μF or 1200 μF (for xenon flashlamp)
Flashlamp voltage	Variable to 1 kV.
Pulse repetition rate	4 pulses/min
Cross-excitation voltage	0—6 kV.
Inductances	30, 125, 500 μH
Triggering mode	External triggering of spark delayed with respect to laser shot, or variable, or synchronous.
Microscope head	Bright field, polarization, incident light, transmitted light, autocollimation, electrode projection (vertical alignment relative to entrance slit), photomicrography possible.
Objectives	Mirror lens (catadioptric) 40 × /0.5. Plane-field achromat 16 × /0.20. Plane-field achromat 4 × /0.08.
Specimen stage	Circular, centering rotation (360°, floating in 2 coordinates).
Polychromator	McPherson Model 218, 0.3 m
Gratings	1200 grooves/mm blazed at 300 nm and 2400 grooves/mm blazed at 240 nm.
Reciprocal linear dispersions	2.16 and 1.08 nm mm^{-1} or 0.054 and 0.027 nm/diode (25 μm wide).
Experimental triggering	EG&G-PARC Model 1301 optical trigger for reproducible initiation of target readout after each laser burst (eliminates errors from dark current variations).
Optical Multichannel Analyzer	EG&G-PARC Model 1215, computer console.
Detector controllers	Models 1216, 1218
Silicon-intensified vidicon (SIT)	Model 1254
Silicon photodiode array	Model 1412
Spectral coverage	SIT: 27 and 13.5 nm with the 1200 and 2400 grooves/mm gratings respectively. Photodiode array: 55.3 and 27.6 nm.
No. of channels	SIT: 500. Photodiode array: 1024.

diameter, 0.3 mm long), a dissected ruby rod, a razor blade, a capacitor, a photodiode array, and an aluminum alloy. Some of the more interesting features of the system capabilities are illustrated by data presented below.

Microprobe features. Visual selection of the sample region, i.e., the location and dimensions to be sampled, is achieved with a microscope with a total magnification of up to × 500. The focused laser pulse can then "hit" this region with a spatial accuracy of 1 μm. The spatial resolution of the microprobe and therefore the smallest microsample that can be individually sampled as determined from the dimensions of the crater produced by the

laser energy is approximately 10 μm. The dimensions of the crater, both its diameter and depth, are controlled accurately by an elaborate set of instrumental parameters.

The optical-pump, xenon flash lamp energy can be adjusted. The laser can operate either in a Q-switched or a non-Q-switched mode. In the latter, the laser burst, a pulse-train of a total duration of approximately 100 μs, consists of many small spikes with a typical duration of approximately 1 μs and an energy of approximately 10 mJ, each. For passive Q-switching of the laser resonator, a rotating six-compartment (discrete) cuvet with a dye solution with gradually increasing absorbance is used. The Q-switched operation provides excellent control over the number of pulses in each burst. The duration and associated energy of pulses typically range from 3 MW for a single giant pulse with a 30-ns duration time to a few somewhat smaller pulses a few tens of nanoseconds apart (up to 100 ns).

There are several choices of microscope objective, namely two plane-field achromats, a 4 × /0.05 for survey sampling, a 16 × /0.20, and one catadioptric lens, 40 × /0.5.

The microscope arm houses an optical matching unit (positioned between the objective lens and the laser-head) to ensure an accurate "hit" by the laser burst. Diaphragm stops (beam-diameter limiting apertures) can be inserted in this unit, in a plane aligned in parallel with the specimen plane. Three diaphragms are available to limit the laser beam diameter at the sample surface to 5, 20, and 40 μm. Each diaphragm can be centered individually by its own alignment mechanism, and is easily replaceable.

Defocusing of the beam can reduce the laser beam energy incident on the sample and therefore the depth of crater, but this is done at the expense of increasing the diameter of the crater. Alternatively, neutral density filters can be inserted between the objective lens and the sample to reduce the crater depth without increasing its diameter.

The dimensions and nature (round or irregularly shaped) of the crater are strongly dependent on the interaction between the ruby laser energy and the surface, i.e., the thermal and optical absorption and reflection properties of the material. Proper selection of instrumental parameters has been thoroughly investigated over the years; information is available from the manufacturer.

Lateral cross-section microprobe sampling. Figure 1 shows the emission spectrum of chromium obtained from two regions of an electrically nonconductive dissected ruby rod. The intensity differences between the two spectra correspond to local variations in chromium concentrations. Spectra in Fig. 1 illustrate differences in chromium content at just two points on the surface; by moving the sample, it was possible to obtain a spatial profile of the chromium content over any desired portion of the surface. Figure 2 is a similar presentation of the emission spectra obtained by lateral "probing" across a dark blemish found on a white ceramic tube. The high intensity emission lines causing a partial saturation of the analog-to-digital converter

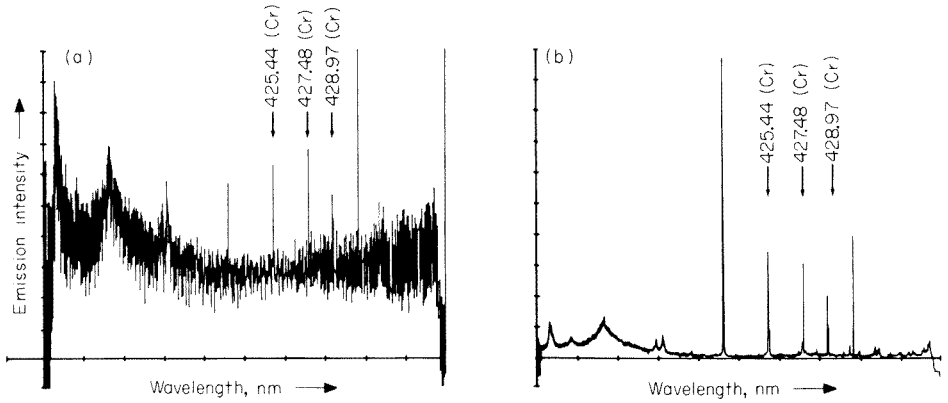

Fig. 1. Variation of chromium emission intensities from different regions of a dissected ruby rod. (a) Light pink (bulk) region; (b) dark pink (blemish) region. Intensified vidicon detector.

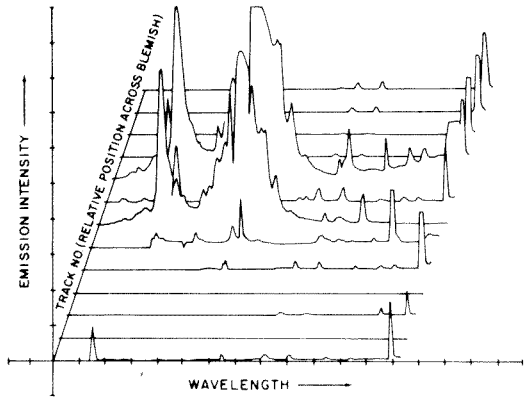

Fig. 2. A lateral spectral profile across a blemish (~0.2 mm diameter) on a ceramic tube. Intensified vidicon. Each trace represents 0.5 mm lateral translation. Conditions: xenon flashlamp, 950 V; capacitor bank, 1200 μF; objective 40 X/0.5; aperture, 20 μm.

have been identified as those of molybdenum, probably from contamination introduced during the fabrication process. By plotting the data in Fig. 2 with 180° rotation, it was possible to show that there were no lines hidden behind the broad molybdenum bands. Clearly, the system provides the means to obtain rapidly chemical composition of lateral profiles of solid surfaces, for either qualitative or quantitative determinations.

Depth microprobe sampling. Figure 3 is a pseudo depth profile, i.e., emission spectral characteristics vs. probing depth, of an electrical conductor with a silver-conducting layer. Each spectrum is the result of a single laser shot. Through focusing/defocusing manipulations, and aperture, objective, and Q-switch stage selection, the diameter of the laser beam was gradually reduced from approximately 140 μm to approximately 15 μm

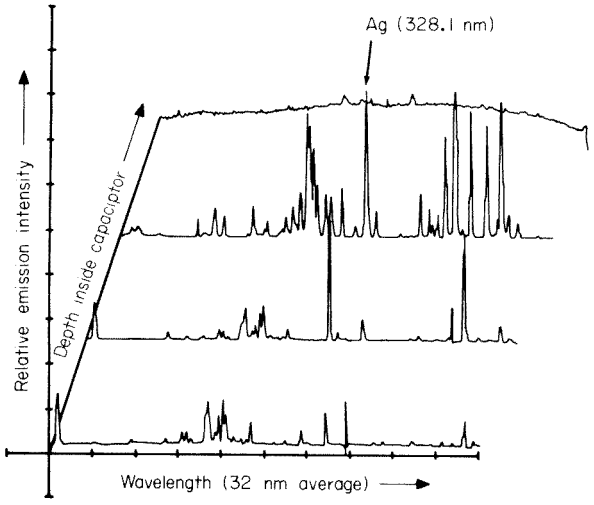

Fig. 3. A depth spectral profile of an electrical capacitor. Scans (bottom-to-top): surface, × 10 scale expansion; silver layer, × 5 scale expansion; through silver layer, × 1 scale expansion; below silver layer, × 100 scale expansion. Conditions: Intensified vidicon; xenon flashlamp voltage, 920 V; objective, 40 × /0.5; limiting aperture 5—40 μm; diameters of craters were reduced with increasing depth.

so that different depths of the capacitor were sampled. The depth of the first crater was only 12 μm. Cone-shaped (multisampled) craters are necessary to minimize chemical cross-contamination, primarily from sputtered material. The distinct spectral differences at different depths correspond to differences in the chemical composition of the various layers comprising the capacitor.

Figure 4 illustrates the nature of the craters formed by the defocusing process applied to a razor blade (Gillette "Platinum Plus") examined for traces of platinum with the 306.5-nm Pt line. Because the Cr_3Pt overcoat layer on the cutting edge is only 30 nm thick, its positive identification, in the presence of the iron matrix required a significant defocusing of the laser beam. The estimated total amount of platinum evaporated by the laser, was 4×10^{-11} g ($\approx 10^{11}$ atoms). Differences between emission from the bulk and the edge of the razor blade are illustrated in Fig. 5 where the arrow identifies the expected position of the 306.5-nm Pt line.

Figure 6 shows the emission spectra obtained from a very thin deposition of gold on palladium on titanium of a multilayer integrated circuit bonding on a ceramic substrate. By gradually defocusing the beam, it was possible to evaporate and detect the thin gold overlayer exclusively ($\approx$ 1 μm thick). Unfortunately, defocusing also caused expansion of the laser beam diameter, thus resulting in co-emission of aluminum from the ceramic substrate. By gradually refocusing the beam it was possible to evaporate the Ti (0.05—0.1 μm thick) and Pd ($\approx$ 0.2 μm thick) layers, but it was not possible exclus-

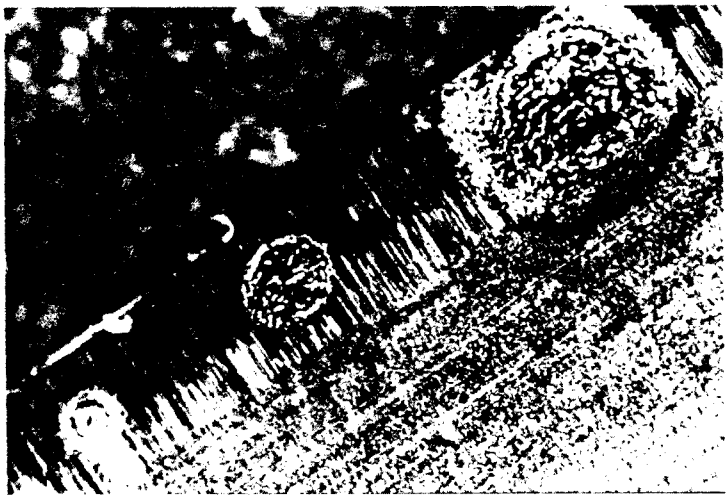

Fig. 4. Photograph of craters formed along the edge of a razor blade as the laser beam is gradually defocused. Magnification, × 20.

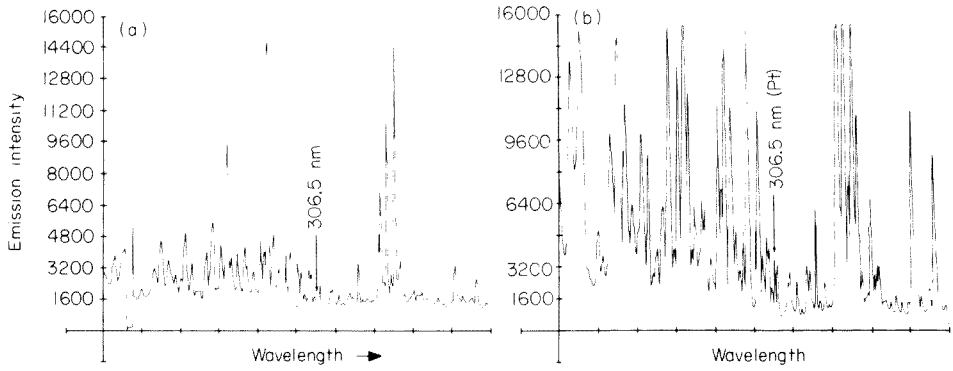

Fig. 5. Emission spectra from two regions of a razor blade. (a) Off the edge; (b) on the edge. Conditions: Gillette "Platinum Plus" blade; probing depth < 1 μm; photodiode array; xenon flashlamp voltage, 940 V; objective, 16 × /0.2; limiting aperture, 20 μm; defocusing, 1 mm; wavelength range, 291.23 to 318.95 nm.

ively to evaporate the Pd layer. Beam attenuation with neutral-density filters should provide a better means for studies of that nature.

The combined system can be useful in surface-contamination studies. Figure 7(a) is the spectrum of the surface of a defective silicon photodiode array that was sampled and shown to contain traces of sodium. Figure 7(b) shows the emission spectrum obtained from the same surface region after it had been contaminated with sodium by a fingerprint. Comparison of the figures confirms sodium contamination on the surface of the photodiode

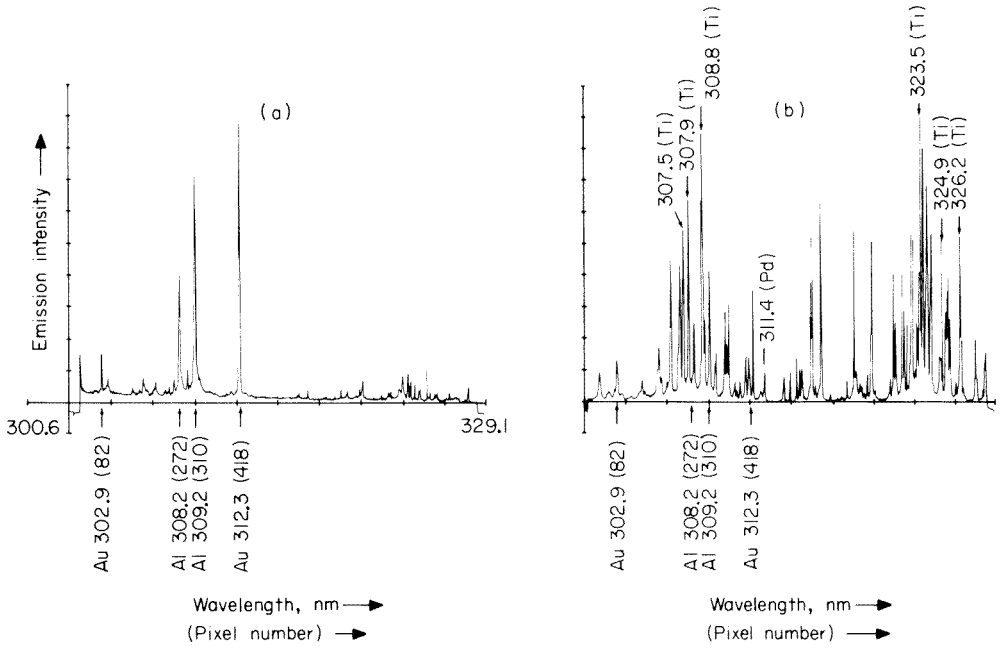

Fig. 6. Emission spectrum of a Au/Pd/Ti triple-layer thin electrical coating on a ceramic coupler. (a) Upper Au layer only, 500 μm defocusing, depth $\approx$ 0.3 μm; (b) all three layers, 120 μm defocusing. Conditions: photodiode array; xenon flashlamp voltage, 930 V; capacitance, 900 μF; Q-switch-cuvet no. 6; limiting aperture, 20 μm.

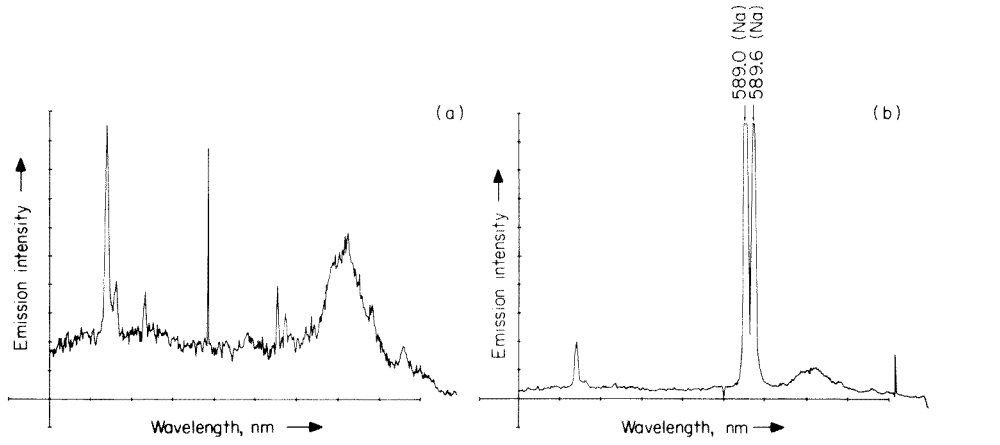

Fig. 7. Emission spectrum from the target surface of a photodiode array. (a) Clean surface; (b) fingerprint-contaminated surface. Conditions: photodiode array; xenon flashlamp voltage, 980 V; capacitance, 900 μF; Q-switch-cuvet no. 6; limiting aperture, 40 μm; crater dimensions, 160 μm diameter by 2 μm depth; wavelength range, 572.8 to 600.5 nm.

array. The origin of the sodium contamination has not yet been established, but contamination of the crystal itself, or more likely, a fabrication-contamination cannot be ruled out.

Quantitative characteristics

Detection limits. Table 2 summarizes some of the detection limits obtained with the silicon-intensified target vidicon and the silicon photodiode array. Clearly, the detection limits of the detectors are not significantly different, even though their optical sensitivities are very different; the SIT has produced signals approximately 100 times higher than those of the photodiode array, but with little improvement in signal-to-noise ratio.

The sensitivity study led to the conclusion that inadequate spectral resolution (which is due to usage of grating polychromators with insufficient linear dispersion) is the primary limiting factor for detection limits in samples with complex matrices. This limitation can be greatly ameliorated by using higher-resolution polychromators, particularly when the higher gain SIT is used, because, low-optical speed (high *f*/number) is less of a problem. Unfortunately, higher dispersion also means a smaller range of wavelengths covered by the detector.

TABLE 2

Detection limits for several elements in different matrices with the laser microprobe adapted to imaging detectors

Element	Matrix	Spectral line (nm)	Detection limits (ppm)[a]	
			Intensified vidicon	Photodiode array
Ag	Copper alloy	328.3	<15	
Ag	Gold wire	328.3	<15	
Cr	Copper alloy	429.0	2	5
Cr	Aluminum alloy	429.0		<5
Cr	Steel	429.0	<100[b,c]	<100
Ga	Aluminum alloy	417.2		<10
Cu	Steel	324.7	<20	
Cu	Gold wire	324.7		<10
Mn	Copper alloy	279.5	<10	<20
Sn	Copper alloy	284.0	<500[b]	
Pb	Copper alloy	280.1	<500[b]	
Pd	Gold wire	324.2		<50

[a]In the absence of reference materials with sufficiently low concomitant concentration levels, some of the detection limits were obtained by extrapolation to $S/N=2$ from concentration levels 2 to 20 times above the estimated detection limits. [b]The spectral resolution, 0.054 nm/channel, was inadequate for these measurements; the detection limits were limited by spectral interference. [c]The lowest-concentration steel sample available contained ≈ 100 ppm Cr.

The system as a whole seems to be limited by flicker noise and background noise, rather than photon shot-noise. Therefore, for most applications, the photodiode array with its wider spectral coverage and better geometric accuracy may be the detector of choice.

Nevertheless, the intensified vidicon, because of its higher sensitivity, has another potential advantage over the photodiode array; it provides more flexibility in selecting the plasma region where less interferences from background are present. In these regions where the emission intensity is lower, the photodiode array may not have adequate sensitivity.

Imaging detectors are effectively and easily amenable to compensation techniques for source fluctuations. Source intensity fluctuations affect the entire spectrum equally. Because the entire spectral window is simultaneously monitored by the imaging detector, it is possible to compensate for these fluctuations by deriving a normalization factor from a reference detector that monitors the source output. With source compensation, effects of laser shot-to-shot variations should become small enough to render the system photon shot-noise-limited. Under such circumstances the higher sensitivity of the intensified vidicon should translate into higher analytical sensitivity.

Finally, the detection limits of the intensified vidicon for Fe, Ni, and Mn were 1×10^{-11}, 5×10^{-12}, and 2×10^{-12} g, respectively, compared with values of 2×10^{-10}, 1×10^{-11} and 5×10^{-11} for a typical photographic plate (ASA value of approximately 100). These typical results are even more significant considering the fact that no auxiliary cross-excitation was used with the vidicon. However, the photographic detector was interfaced to a $f/28$ spectrograph compared with the $f/6$ polychromator used with the vidicon. Nevertheless, because the detectability of the vidicon has been limited by spectral interferences rather than by the photon shot noise, the use of $f/28$ polychromator with its associated greater linear dispersion should have further improved it, particularly for samples of a complex nature. In fact, the light sensitivity of the SIT, estimated at ASA values greater than 80 000, was so high that neutral density filters with absorbance values of 0.5—2.0 were placed in front of the entrance slit to avoid detector saturation. The diode array, in contrast, although substantially less light-sensitive than the intensified vidicon, has a great advantage over photographic detectors in that its spectral response is superior in the ultra-violet and near-infrared.

Reproducibility. The reproducibility of measurements of the laser microprobe—optical imaging system was determined for a few metallurgical samples including brass, aluminum, and copper alloys and steels and some nonmetallic samples including a ruby rod, a dissected pearl, and salt crystals. Relative standard deviations with average size craters were 10—14%. Generally, peak heights produced better results than peak areas, primarily because near line-wing spectral interferences reduced the accuracy of peak-area measurements based upon near line-wing channel interpolation. The use of reference lines internal standards improved the reproducibility considerably, as shown

in Table 3. Significantly worse results were obtained with small-size craters when absolute line intensities were used. Again, normalization with internal standards significantly improved the results.

Single shot dynamic range. The single shot dynamic range is defined as the ratio of the largest signal the detector can acquire from a single laser shot divided by the associated readout noise from both the excitation source and the detector itself. Both the diode array and the vidicon have linear transfer characteristics over a range of 16 284:1, corresponding to the limitation set by the 14-bit analog-to-digital converter. However, the single shot dynamic range of the vidicon can be lower than that value if a small number of diodes per channel is used. (The number of diodes per channel can be varied under computer control over a range of 2 to 512 diodes because channel saturation level is determined by the number of diodes used.) In contrast, the photodiode array is a linear diode array, i.e. each optical channel comprises a single diode (2.5 mm × 0.025 mm) with a saturation level of approximately 8×10^7 electrons. Also, the photodiode array does not suffer from discharge lag typical of vidicon detectors and therefore, its effective dynamic range is practically equal to that of the analog-to-digital converter.

The vidicon has another disadvantage relative to the photodiode array; it is more susceptible to "veiling glare", a stray light phenomenon originating from light reflections inside the detector enclosure [21].

Calibration curves. The linearity and dynamic range of working curves obtained with the laser microprobe are greatly affected by the instrumental parameters and have been investigated in the past. Calibration curves for chromium in steel obtained with a photodiode array using the 425.4-nm

TABLE 3

Imprecision of data with and without intensity ratios computed

Spectral line (nm)	Reference line (nm)	Detector response				Ratio	Rel. std. dev. (%)
		Spectral line		Reference line			
		Peak counts (Ave.)	Rel. std. dev. (%)	Peak counts (Ave.)	Rel. std. dev. (%)		
Cu, 327.4	Ti, 336.1	4377[a]	13.3	1665	15.8	2.604	5.2
		8244[a]	11.2	1633	19.8	5.126	8.3
Cr, 313.2	Fe, 322.6	6974[b]	11.3	12607	8.2	1.81	3.5
Cr, 313.2	Fe, 322.6		36.3[c]		28.3[c]		10.2[c]

[a]Sample was an aluminum alloy with 0.115% Cu and 0.055% Ti; xenon flashtube voltage, 970 V; capacitor, 900 μF; crater dimensions, 360 μm diameter and 160 μm depth. [b]Sample was steel with 2.85% Cr; flashtube voltage, 900 V; capacitor, 900 μF; crater dimensions, 120 μm diameter and 76 μm depth. [c]2.85% Cr; flashtube voltage, 850 V; capacitor, 900 μF; crater dimensions, 50 μm diameter and 14 μm depth.

Cr resonance line were nonlinear with slopes of log—log plots approaching 0.8 (γ = 0.8) between 0.01 and 0.1% and approaching 0.4 (γ = 0.4) above 0.17%. The nonlinearity is mostly due to self-reversal. When a non-resonance Cr line (313.2 nm) was selected, the deviation from linearity was mild (γ = 0.94) and became severe only at concentrations above 1%. Yet, non-linearity cannot be solely attributed to self-reversal interferences. For instance, determination of copper in steel with the 327.4-nm Cu resonance line produced a non-linear working curve (γ = 0.44) in the 0.01—0.65% range, while determination of copper in aluminum alloys, using the same Cu line, produced a virtually linear working curve in the 0.095—0.4% range. These non-linear responses require the use of reference standards, as indicated by the LMA manufacturer.

For bulk determinations, the spectra derived from a few consecutive laser shots, either from the same location but gradually deeper inside the crater, or from a few locations, can be averaged in memory in order to cancel out spatial concentration variations.

In the absence of reference materials with an adequately wide concentration range, it was impossible to demonstrate a ppm-to-percent dynamic range. Nevertheless, the few working curves studied (e.g. chromium in steel, 100 ppm to 2.85%) clearly demonstrated the potential dynamic range of the system. Experiments with a steel sample containing 100 ppm chromium demonstrated adequate sensitivity to allow extension of the working curve to at least 10 ppm Cr with the photodiode array detector. In cases where the signal intensity is too high, as often happens with the intensified vidicon, neutral density filters can be used to attenuate the light level accurately.

Spectral resolutions and range

The simultaneous spectral coverage of an imaging detector is equal to the reciprocal linear dispersion of the polychromator times the detector length. Because the length of the photodiode array (25.4 mm, 1024 diodes) is approximately twice that of the intensified vidicon, so is its spectral range for the same optics. It is important, however, to realize that the spectral resolution of an imaging detector is always worse than its channel bandwidth because of interchannel cross-talk. The resolution of the SIT vidicon is worse than that of the photodiode array because of the characteristic pin-cushion distortion (2—5%) of the former. In either case, spectral coverage and spectral resolution are trade-off parameters.

Proper selection of spectral windows provides reasonable multi-elemental analytical capabilities, and the wavelength setting of the polychromator can be altered in intervals to project different spectral windows sequentially across the multichannel detector. As examples, the spectral range from 280 to 290 nm includes useful lines that can be adequately resolved for Bi, Cr, Cu, Ga, In, Mg, Mn, Sb, Si, Sn, and Pb, and the range from 320 to 335 nm includes useful lines for Ag, Au, Cu, Ge, In, Pd, Sb, Sn, and Ti. In one set of experiments, the spectrum of manganese between 200 and 545 nm

was obtained in a series of twelve spectral windows with about one minute being required for each window.

Wavelength calibration

Wavelength calibration is easily achieved with the photodiode array because it has precise diode number-to-diode position relationship. Positive identification of two spectral lines anywhere across the 1024 available diodes is sufficient to produce a wavelength-to-diode number calibration, accurate to within a single diode or 0.027 nm with the 2400 mm grating. The SIT vidicon, because of its inherent pin-cushion distortion, requires a polynomial fit calibration which is available in standard software with the OMA-2. The OMA-2, basically a curve-processor, greatly facilitates wavelength calibration and line identification procedures. Any two stored spectra (up to 100 spectra can be stored on a single floppy disk) can be recalled and simultaneously displayed on a cathode ray tube screen. The two spectra can be shifted vertically and expanded horizontally. Any channels of interest can be visually intensified and compared. Thus the OMA-2 serves as a flexible digital spectrum comparator.

Time-resolved spectroscopy

The temporal behavior of microplasmas generated by a laser microprobe system was discussed elsewhere [22]. Significant temporal differences in the spectral emission characteristics such as rise-time, decay-time, and overall pulse width were found between the ions and the free atoms. For example, the emission pulse width at half-height of the Pb I line was 400 ns while that of the Pb II line was 130 ns. Also, the background continuum emission, most severe up to 0.4 mm above the sample surface, was found to be the first produced and could have been resolved temporally from the neutral species.

Because the intensified vidicon is a gatable detector, its ability to time-resolve the background continuum of line emission (free atoms), was tested. Figure 8 shows two emission spectra obtained from the 1-mm region above an aluminum alloy sample where there was high background continuum emission. Longer time delays (up to 3100 ns) showed the evolutionary stages of the excitation processes.

Measurements of this nature may be useful in assessments of methodology optimization procedures necessary for different types of samples.

Emission profile studies

The intensified vidicon is a two-dimensional imaging detector, and as such can be vertically subdivided by the electron readout beam into many tracks, each of which contains 500 individual optical channels. The vidicon is therefore very useful for emission spectral profile measurements of excitation sources. If the microplasma is focused along the entrance slit of a polychromator, then a three-dimensional spectral profile of wavelength vs.

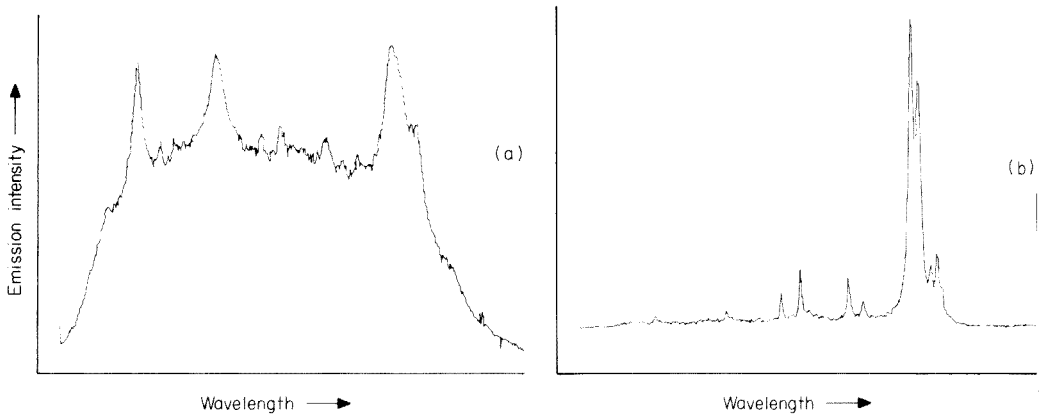

Fig. 8. Time-dependent spectra obtained from an aluminum alloy. (a) Gate pulse 60 ns, delay 100 ns; (b) gate pulse 60 ns, delay 600 ns. Conditions: intensified vidicon, wavelength range, 355.2 to 292.1 nm; xenon flashlamp voltage, 940 V; capacitance, 900 μF; Q-switch-cuvet no. 6; objective 16 X /0.2; no limiting aperture; gating controlled with EG&G—PARC pulse generator (Model 1211), polychromator, 0.3 m with 600 grooves/mm grating.

intensity vs. position can be instantly and simultaneously recorded on the target, with a resultant spatial resolution determined by the number of tracks selected. The data are then sequentially read off the tracks, digitized, and stored in memory.

Conclusions

The laser microprobe—optical multichannel analyzer system provides microprobe as well as bulk capabilities, at a fraction of the cost of most other microprobe systems. Because sample preparation and chamber evacuation are not necessary, and because the spectral record is instantly digitized and stored, very rapid qualitative and semi-quantitative determinations can be performed. The entire procedure, including positioning of a sample on the microscope stage, focusing on an area of interest, laser sampling, excitation, and display, can be performed in less than 30 s. Quantitative determinations are possible, but are subject to the availability of standard materials. Computer control greatly facilitates wavelength calibration, line identification, signal measurement, calculations, and compensation for shot-to-shot variations.

The intensified vidicon and photodiode array detectors are or can be made responsive in the vacuum—u.v. region and therefore, in conjunction with Jenoptik's newly designed vacuum chamber, could extend the applicability of the system to the detection of non-metals, such as carbon, phosphorus or sulfur. However, no quantitative data in this spectral region are yet available.

At the present time, the limited spectral window is the greatest disadvantage of the detection system, but computer-manipulated polychromator "window"

scan, could greatly alleviate this shortcoming. In future, two-dimensional format spectrometers [17] could be used to expand the spectral window.

The authors acknowledge Dr. T. H. Briggs of Western Electric Allentown Works, for supplying a few of the samples and assisting in data interpretation.

REFERENCES

1 F. Brech and L. Cross, Appl. Spectrosc., 16 (1962) 59.
2 K. G. Snetsinger and K. Keil, Am. Mineral., 52 (1967) 1842.
3 S. D. Rasberry, B. F. Scribner and M. Margoshes, Appl. Opt., 6 (1967) 81, 87.
4 E. S. Beatrice, J. Harding-Barlow and D. Glick, Appl. Spectrosc., 23 (1969) 257, and following paper.
5 L. Moenke-Blankenburg, Fortschr. Mineral., 44 (2) (review).
6 N. A. Peppers et al., Anal. Chem., 40 (1968) 1178.
7 S. D. Rasberry, B. F. Scribner and M. Margoshes, Colloq. Spectrosc. Int. XII, (1965) 336.
8 J. W. Busch, N. G. Howell and G. H. Morrison, Anal. Chem., 46 (1974) 1231, 2074.
9 D. O. Knapp, N. Omenetto, L. P. Hart, F. W. Plankey and J. D. Winefordner, Anal. Chim. Acta, 69 (1974) 455.
10 F. L. Fricke, O. Rhodes and J. Caruso, Anal. Chem., 47 (1975) 2018.
11 H. Haraguchi, F. O. Fowler, J. D. Johnson and J. D. Winefordner, Spectrochim. Acta, 32A (1976) 1539.
12 Y. Talmi, D. C. Baker, J. R. Jadamec and W. A. Saner, Anal. Chem., 50 (1978) 936A.
13 W. H. Woodruff and G. H. Atkinson, Anal. Chem., 48 (1976) 186.
14 A. Danielsson, P. Lindblom and E. Soderman, Chem. Scripta, 6, 5 (1974).
15 G. Horlick, Appl. Spectrosc., 30 (1976) 113.
16 M. J. Milano, H. L. Pardue, T. E. Cook, R. E. Santini, D. W. Margerum and J. M. T. Raycheba, Anal. Chem., 46 (1974) 374.
17 H. L. Felkel, Jr. and H. L. Pardue, Anal. Chem., 49 (1978) 602.
18 H. L. Felkel, Jr. and H. L. Pardue, in Y. Talmi (Ed.), Multichannel Image Detectors, ACS Symposium Series No. 102, p. 59.
19 K. W. Busch, B. Malloy and Y. Talmi, Anal. Chem., 51 (1979) 670.
20 Y. Talmi, Anal. Chem., 47 (1975) 658A.
21 Y. Talmi and R. Simpson, Appl. Opt., 19 (1980) 1401.
22 C. D. Allemand., Spectrochim. Acta, 27B (1972) 185.

Analytica Chimica Acta, 127 (1981) 87—92
Elsevier Scientific Publishing Company, Amsterdam — Printed in The Netherlands

BESTIMMUNG UND ABTRENNUNG VON SAUERSTOFFVERUNREINIGUNGEN IN REINST-SELEN

B. VOIGT* und G. DRESLER
Sektion Chemie der Friedrich-Schiller-Universität, Jena, 6900 Jena (D.D.R.)
(Eingegangen den 3. Dezember 1980)

SUMMARY

(The determination and separation of oxygen impurities in high-purity selenium)

By distillation in high vacuum, high-purity selenium is almost completely freed from impurities caused by metallic elements, oxides and water. If bulk vitreous selenium has a suitable thermal history, the oxygen content may be determined from the intensity of the oxide absorption band at 932 cm^{-1} in the i.r. spectrum of the glass. In distilled selenium this content is $< 1 \times 10^{-4}$ wt. %.

ZUSAMMENFASSUNG

Reinst-Selen wird durch Destillation im Hochvakuum weitgehend von Verunreinigungen durch metallische Elemente, Oxide und Wasser befreit. Bei geeigneter thermischer Vergangenheit des kompakten, glasartigen Selens kann der Sauerstoffgehalt aus der Intensität der Oxidadsorptionsbande bie 932 cm^{-1} in den IR-Spektren der Gläser bestimmt werden. In destilliertem Selen ist dieser Gehalt kleiner als $1 \cdot 10^{-4}$ Gew.%.

Handelsübliches, halbleiterreines Selen ist unabhängig von der ausgewiesenen Reinheitsangabe stets durch Sauerstoffspuren verunreinigt. Diese Oxidverunreinigungen können die Eigenschaften der unter Verwendung solchen Selens hergestellten Materialien, z.B. IR-transparenter optischer Chalkogenidgläser, negativ beeinflussen und müssen deshalb gegebenenfalls vorher möglichst quantitativ abgetrennt werden. Die meisten der in der Literatur beschriebenen Methoden zur Entfernung von Sauerstoffspuren aus Reinst-Selen nutzen den im Vergleich zum Selen viel höheren Dampfdruck des Selendioxides. So konnten z.B. Savage et al. [1, 2] oder Ležal und Srb [3] durch 0,5 bis 3-stündiges Erhitzen des Ausgangsmaterials im Vakuum auf 300—350°C den Oxidgehalt wesentlich reduzieren. Zur quantitativen Beurteilung des Reinigungsverfahrens ist eine einfache Analysenmethode zur Bestimmung von Sauerstoff in Selen wünschenswert. Dazu erscheint die IR-Spektroskopie geeignet, denn Oxidverunreinigungen rufen in den IR-Spektren des glasartigen Selens relativ starke Absorptionsbanden hervor.

Frühere Arbeiten von Vaško [4] sowie Abdullaev et al. [5] zeigen qualitativ einen Zusammenhang zwischen der Intensität der Oxidabsorptionsbanden

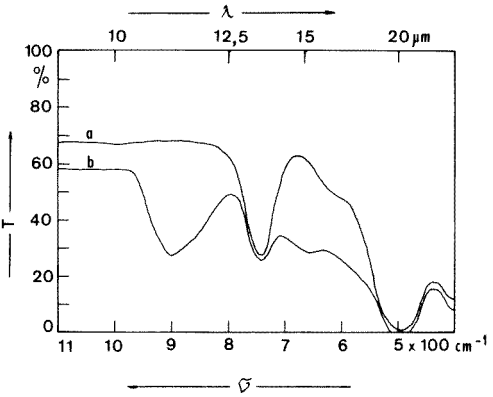

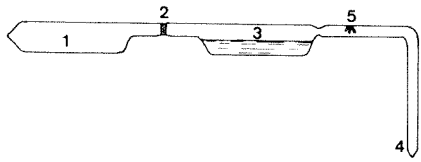

Abb. 1. IR-Transmissionsspektren kompakter, glasartiger Selenproben, die durch Einschmelzen handelsüblicher Reinst-Selengranalien gewonnen wurden. (a) 99,9999% Se (Dicke der Probe d = 11,1 mm); (b) 99,995% Se (d = 10,7 mm).

Abb. 2. Destillationsapparatur.

und dem Sauerstoffgehalt des Glases. Versuche von Burley [6], diese Beziehung für eine quantitative Bestimmung auszunutzen, scheiterten an der schlechten Reproduzierbarkeit der mit Selendioxid dotierten Eichproben. Ursachen dafür waren Oxidverluste bei der Herstellung dieser Gläser, Veränderungen der analytischen Banden mit der Zeit und der unterschiedliche Charakter der IR-Spektren von Ansatz zu Ansatz.

EXPERIMENTELLES UND ERGEBNISSE

Desoxydation von Selen

Abbildung 1a zeigt einen Teil des Transmissionsspektrums einer etwa 11 mm dicken Scheibe einer Probe, die durch 2-stündiges Schmelzen von Selengranalien hoher Reinheit (99,9999%) in einer evakuierten, abgeschmolzenen Rasothermglasampulle bei 300°C und anschließendes Kühlen an der Luft gewonnen wurde. Die Absorptionsbanden bei 490 und 744 cm^{-1} werden von Srb und Vaško [7, 8] als Kombinationsschwingungen der Fundamentalabsorptionsstellen des amorphen Selens bei 119, 253 und 269 cm^{-1} interpretiert. In den Spektren dickerer Proben tritt eine weitere, schwache Absorptionsbande des reinen amorphen Selens bei 995 cm^{-1} auf. Obwohl die eingesetzten Selengranalien nicht frei von Sauerstoffspuren waren, ist im Spektrum der so hergestellten Proben keine durch Sauerstoff hervorgerufene Bande zu erkennen.

Abbildung 1b zeigt das Spektrum einer weiteren, unter gleichen Bedingungen hergestellten Selenprobe von vergleichbarer Dicke. Das Ausgangsmaterial war jedoch in diesem Falle Granalien mit einem ausgewiesenen Gehalt von nur 99,995% Selen. Die wesentlichsten Verunreinigungen sind Alkali- und Erdalkalielemente, Silber, Kupfer und Silizium. Außerdem

fanden wir in diesen Granalien $4 \cdot 10^{-2}$ Gew.% Wasser. Abgesehen von der durch Inhomogenitäten generell geringeren Transparenz der Probe enthält das Spektrum bei 897 und 652 cm^{-1} relativ starke, durch Oxidverunreinigungen hervorgerufene, zusätzliche Absorptionsbanden. Während im ersten Beispiel das Austreiben des hochflüchtigen Selendioxides aus der Schmelze in den Gasraum selbst in geschlossenen, evakuierten Ampullen völlig unproblematisch ist, bleibt die Desoxydation von Selenschmelzen, die noch Spuren metallischer Verunreinigungen in der Großenordnung von 10^{-3} Gew.% enthalten, auch bei Erhitzen im offenen Vakuum unvollständig. Eine möglichst weitgehende Abtrennung der Sauerstoffspuren durch Austreiben als Selendioxid erfordert deshalb zunächst eine wesentliche Reduzierung des Gehaltes an metallischen Elementen.

Die kombinierte Abtrennung metallischer Verunreinigungen, des Wassers und Selendioxides aus Selen (99,995%) erfolgt in der in Abb. 2 dargestellten, auf etwa 10^{-3} Pa evakuierten, abgeschmolzenen Destillationsapparatur aus Rasothermglas. Etwa 200 g Selen werden bei 500°C aus dem Teil 1 der Apparatur durch eine Fritte (2) innerhalb von ca. 5 Stunden in die Vorlage 3 destilliert. Die schwerflüchtigen Verbindungen der metallischen Verunreinigungen verbleiden dabai als grau-weißer Belag im Rückstand. Wasser und geringe Mengen Selenwasserstoff kondensieren bei —196°C im Kühlfinger 4, während sich Selendioxid in dem auf Raumtemperatur befindlichen Teil des Kühlfingers bei 5 in Form langer, weißer Nadeln abscheidet. Das in der Vorlage befindliche Reinst-Selen wird während der Destillation auf einer Temperatur von etwa 250°C gehalten und anschließend durch Abkühlen an der Luft in den glasartigen Zustand überführt. In den IR-Spektren des so gereinigten Selens sind bei Proben mit einer Dicke von 22 mm keine Oxidabsorptionsbanden zu erkennen.

In einer Variante kann dem Selen vor der Destillation etwa 1 g durch Glühen von Magnesiumkarbonat bei 800°C frisch hergestelltes Magnesiumoxid zugesetzt werden. In diesem Falle scheidet sich das Selendioxid nicht bei 5 ab, sondern verbleibt, offensichtlich als Magnesiumselenit gebunden, im Rückstand. Durch chemische Analyse des Rückstandes wurde an einer Stichprobe ermittelt, daß an das Magnesiumoxid bezogen auf die eingesetzte Selenmenge $5{,}5 \cdot 10^{-3}$ Gew.% Selendioxid gebunden waren. Auf das Absorptionsverhalten des Selens im untersuchten Spektralbereich und bei den angewendeten Schichtdicken der Proben (max. 22 mm) hat diese Variante keinen Einfluß. Feltz und Aust [9] fanden jedoch, daß so hergestelltes glasartiges Selen eine deutlich niedrigere elektrische Leitfähigkeit hat als solches, was ohne Zusatz von Magnesiumoxid destilliert wurde. Möglicherweise wirkt sich die Behandlung mit Magnesiumoxid auf das IR-Transmissionsspektrum erst bei wesentlich höheren Schichtdicken aus; es ist jedoch auch denkbar, daß die Senkung der Leitfähigkeit nach der Destillation über Magnesiumoxid nicht auf eine weitere Erniedrigung des Oxidgehaltes, sondern der Konzentration anderer Spurenkomponenten zurückzuführen ist.

Sauerstoffbestimmung

Die sauerstoffhaltigen Standardselengläser wurden wie folgt hergestellt: jeweils etwa 30 g durch Destillation über Magnesiumoxid von Sauerstoffspuren gereinigtes Selen wurden in einer Rasothermglasampulle mit definierten Mengen Selendioxid versetzt. Die Einwaage der verhältnismäßig kleinen Mengen Selendioxid erfolgte auf einer Mikroanalysenwaage. Die Ampullen wurden nach dem Evakuieren auf etwa 10^{-3} Pa abgeschmolzen und für 2 Stunden auf 300°C erhitzt. Die Schmelzen wurden durch kontinuierliches axiales Drehen der Ampullen homogenisiert. Das Kühlen erfolgte bei senkrechter Stellung der Ampullen an der Luft. Dabei erstarrten die Schmelzen zu homogenen, spannungsfreien Glaszylindern.

In jedem Falle verdampfte ein Teil des Selendioxides aus der Schmelze und kondensierte beim Abkühlen an den freien Wänden der Ampulle. Dieses Oxid wurde nach dem Öffnen der Ampullen in Wasser gelöst und die genaue Menge durch Atomabsorptionsspektrometrie ermittelt. Die wirklich im Selen gelöste Menge Selendioxid ergibt sich aus der Differenz der ursprünglich zugesetzten und der im freien Volumen kondensierten Menge. In Tabelle 1 ist der so ermittelte Sauerstoffgehalt der Selenproben angegeben. Aus den oxidhaltigen Selenglaszylindern wurden Scheiben von 7 bis 15 mm Dicke geschnitten, beiderseits poliert und mit dem Zeiß-Spektrometer Specord 72 IR im Bereich zwischen 1100 und 400 cm^{-1} die Absorptionsspektren aufgenommen (Abb. 3). Durch den Einbau von Selendioxid in glasartiges Selen wird eine Absorptionsbande bei 932 cm^{-1} hervorgerufen. Die maximalen Abweichungen der Bandenlage von dem angegebenen Wert betragen bei den unterschiedlichen Proben ±6 cm^{-1}. Eine zweite Bande bei etwa 620 cm^{-1} verursacht bei niedrigen Oxidkonzentrationen nur eine Schulter an der starken Absorptionsbande des reinen Selens. Erst bei höheren Konzentrationen prägt sich ein Maximum aus, das sich bei weiterer Steigerung des Sauerstoffgehaltes von 625 cm^{-1} bei $11{,}3 \cdot 10^{-4}$ Gew.% Sauerstoff auf 643 cm^{-1} bei $70{,}3 \cdot 10^{-4}$ Gew.% Sauerstoff zu höheren Wellenzahlen verschiebt. Im Gegensatz zu den Ergebnissen von Burley [6] sind sich die Spektren in ihrer Struktur alle ähnlich und bei Wiederholungsmessungen nach mehreren Wochen mit den Erstmessungen identisch.

Da die Oxidabsorptionsbande bei 932 cm^{-1} durch Banden des reinen Selens praktisch nicht beeinflußt wird, erscheint sie als Indikator zur quantitativen Bestimmung des Sauerstoffgehaltes geeignet. Die von Ramsey [10] geforderte Bedingung, daß das Verhältnis von spektraler Spaltbreite des Spektrometers zur Halbwertsbreite der Bande bei der Bestimmung des Absorptionskoeffizienten α im Bandenbereich kleiner als 0,2 sein soll, war erfüllt. Deshalb konnte α im Maximum der Bande unter Verwendung der Gleichung $\alpha = 1/d \ \ln(T_0/T)$ ermittelt werden. T ist die gemessene Transparenz am Maximum der Absorptionsbande und d die Dicke der Probe in cm. T_0 ist die Transparenz unter der Annahme eines Absorptionskoeffizienten von Null und berechnet sich aus dem Brechwert n zu $T_0 = 2n/(n^2 + 1)$. Da der Brechwert des glasartigen Selens in diesem Spektralbereich 2,42 beträgt, ergibt sich für T_0 0,706.

TABELLE 1

Sauerstoffgehalt verschiedener Selenproben und Absorptionskoeffizient α im Maximum der Oxidabsorptionsbande bei 932 cm^{-1}

Nr.	Sauerstoffgehalt ($\times 10^{-4}$ Gew.%)	α ($\times 10^{-2}$ cm^{-1})
1	—	1,7 ± 0,7
2	5,3 ± 0,0	9,7 ± 0,6
3	7,4 ± 0,1	16,0 ± 1,2
4	11,3 ± 0,3	25,2 ± 1,5
5	27,6 ± 0,6	64,4 ± 2,0
6	70,3 ± 1,4	121,0 ± 4,7

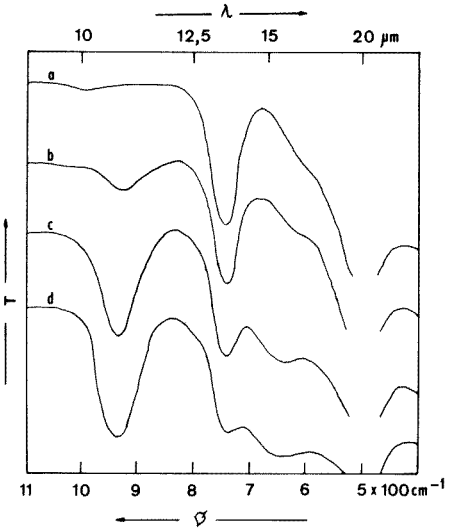

Abb. 3. Transmissionsspektren von reinem und sauerstoffdotiertem, glasartigem Selen: (a) reines Selen, d = 15,5 mm; (b) Se + 7,4·10^{-4} Gew.% O, d = 15,5 mm; (c) Se + 11,3·10^{-4} Gew.% O, d = 13,5 mm; (d) Se + 70,3·10^{-4} Gew.% O, d = 13,6 mm.

Die so ermittelten Absorptionskoeffizienten sind in Tabelle 1 enthalten. Die angegebenen Fehler wurden auf der Grundlage einer Meßunsicherheit von ±0,01 und Anwendung des Fehlerfortpflanzungsgesetzes auf die erste Gleichung berechnet. Der wahre Volumenabsorptionskoeffizient sollte bei allen Proben etwas niedriger sein als der angegebene Wert, da erfahrungsgemäß Transmissionsverluste bis zu 0,02 durch Streuung an den Oberflächen bzw. Abweichung von der idealen Probengeometrie in Erwägung gezogen werden müssen. Tabelle 1 zeigt, daß zwischen dem Sauerstoffgehalt des glasartigen Selens und dem Absorptionskoeffizienten im Maximum der Oxidbande bei 932 cm^{-1} zumindest in den niedrigen Konzentrationsbereichen (bis zu 27,6·10^{-4} Gew.% O) eine lineare Beziehung besteht und daß eine quantitative Bestimmung der Sauerstoffspuren im Selen auf diesem Wege prinzipiell möglich ist.

DISKUSSION

Sauerstoffspuren rufen in den IR-Transmissionsspektren reinen, glasartigen Selens Absorptionsbanden bei 932 und etwa 630 cm^{-1} hervor. Aus der Literatur, z.B. aus einem Übersichtsartikel von Paetzold [11] geht hervor, daß die erste Bande in dem für die Valenzschwingung einer SeO-Bindung mit partieller Doppelbindung charakteristischen Frequenzbereich liegt.

Vaško [4] und Burley [6] fanden in den Spektren sauerstoffdotierter Selengläser Absorptionsbanden, die mit denen des kristallinen Selendioxides identisch sind. Diese Beobachtungen konnten durch die vorliegenden Untersuchungen nicht bestätigt werden. Die Ursache dafür liegt offensichtlich in der unterschiedlichen thermischen Vergangenheit der Gläser. Burley erhielt seine Proben durch rasches Abschrecken der Schmelzen in einer gekühlten Metallform. Es ist denkbar, daß dabei das Selendioxid nicht die gleiche Einbindung in das Netzwerk des Glases erreichen kann, wie bei langsamer Abkühlung der Schmelze, und mikrodispers im Glas vorliegt.

Die Abtrennung von Sauerstoffspuren aus Selen mit ansonsten hoher Reinheit gelingt durch Erhitzen der Schmelze im Vakuum praktisch quantitativ. Sind aber zusätzlich Elemente geringerer Elektronegativität im Selen enthalten, können die Sauerstoffspuren nicht mehr restlos als flüchtiges Selendioxid ausgetrieben werden. Die Wechselwirkungen zwischen diesen Spurenverunreinigungen, Sauerstoff und Selen führen offensichtlich zur Bildung selenitähnlicher Struktureinheiten. Damit ist auch die Verschiebung der SeO-Schwingungsfrequenz von 932 cm^{-1} in hochreinen, sauerstoffdotierten Selengläsern zu 897 cm^{-1} in Übereinstimmung, denn die Bildung derartiger Strukturen muß zu einer Erniedrigung des Doppelbindungsanteiles der SeO-Bindung und damit der Kraftkonstanten führen. Mit der vorgeschlagenen Methode ist eine gleichzeitige Abtrennung von metallischen Verunreinigungen, Wasser und Sauerstoff möglich. Die Ergebnisse zeigen, daß der Sauerstoffgehalt des so gereinigten Selens unter $1 \cdot 10^{-4}$ Gew.% liegt.

LITERATUR

1 J. A. Savage, P. J. Webber und A. N. Pitt, J. Mater. Sci., 13 (1978) 859.
2 J. A. Savage, P. J. Webber und A. N. Pitt, Appl. Opt., 16 (1977) 2938.
3 D. Ležal und I. Srb, Collect. Czech. Chem. Commun., 36 (1971) 2091.
4 A. Vaško, Phys. Stat. Sol., 8 (1965) K 41.
5 G. B. Abdullaev, S. I. Mekhtieva, G. M. Aliev, D. S. Abdinov und T. G. Kerimova, Phys. Stat. Sol., 16 (1966) K 31.
6 R. A. Burley, Phys. Stat. Sol., 29 (1968) 551.
7 I. Srb und A. Vaško, Czech. J. Phys., B 11 (1961) 664.
8 I. Srb und A. Vaško, Czech. J. Phys., B 13 (1963) 827.
9 A. Feltz und H. Aust, J. Non-Cryst. Solids, in Vorbereitung.
10 D. A. Ramsey, J. Am. Chem. Soc., 74 (1952) 72.
11 R. Paetzold, Z. Chem., 4 (1964) 321.

Analytica Chimica Acta, 127 (1981) 93—101
Elsevier Scientific Publishing Company, Amsterdam — Printed in The Netherlands

DETERMINATION OF ng ml^{-1} LEVELS OF PHOSPHORUS IN WATERS BY DIISOBUTYL KETONE EXTRACTION AND INDUCTIVELY COUPLED PLASMA ATOMIC EMISSION SPECTROMETRY

AKIRA MIYAZAKI*, AKIRA KIMURA and YOSHIMI UMEZAKI
National Research Institute for Pollution and Resources, Yatabe, Ibaraki, 305 (Japan)
(Received 19th January 1981)

SUMMARY

Reduced molybdoantimonylphosphoric acid is extracted into diisobutyl ketone (DIBK) and phosphorus in the extract determined by i.c.p. emission spectrometry at the P I 214.91-nm line. The Mo II 213.61 nm line interfered with the P I 213.62-nm line. The method is applied to 0.2—200 μg of phosphorus in 500 ml of river or sea water. Arsenic(III), Si, Ge, Fe(III) and most anions do not interfere, but As(V) (>10 × P) causes positive errors. The detection limit is 0.37 ng P ml^{-1}, and the relative standard deviation for 5 μg of phosphorus is 2.1%.

Determination of traces of phosphorus in water is important, especially in environmental analysis in relation to the eutrophication problem. A spectrophotometric method based on the reduction of a molybdenum heteropoly acid has been mainly used for this purpose [1]. Determinations near the ng ml^{-1} level require preconcentration because of the comparatively poor detection limit. Liquid—liquid extraction of the reduced heteropoly acid has been most widely used, although some other concentration procedures such as ion-exchange [2] and a combination of coprecipitation and extraction [3] have been reported. Indirect determination of phosphorus by atomic absorption spectrometric measurement of the molybdenum concentration in the extract has also been used to increase the sensitivity [4].

These methods, however, have a common disadvantage in that arsenic, silicon and germanium cause positive errors because these elements also form reduced heteropoly acids. Direct measurement of phosphorus in the extract by atomic spectrometry would therefore be advantageous.

Recently, inductively coupled plasma atomic emission spectrometry (i.c.p.—a.e.s.) has been recognized as an effective analytical technique for a wide variety of samples. Several reports have been published on the determination of phosphorus by i.c.p.—a.e.s. [5—8]; these deal with the direct nebulization of samples into the plasma without any pretreatment. Winge et al. [9] reported a detection limit of 0.076 ppm for the phosphorus 213.62-nm and 214.91-nm emission lines. Thus, a preconcentration factor of 100 would allow the determination of ng ml^{-1} of phosphorus by i.c.p.—a.e.s. with sufficient reproducibility and accuracy.

TABLE 1

Instrumental operating conditions

I.c.p. source	Shimadzu ICPS-2H	
Operating frequency	27 MHz	
Load coil	2-turn copper tubing with teflon coating	
Nebulizer	concentric	
Spectrometer	Shimadzu GEW 170, 1.7-m Ebert	
Grating	2160 line mm^{-1}	
Entrance slitwidth	30 μm	
Exit slitwidth	50 μm	
Reciprocal linear dispersion	0.26 nm mm^{-1} (1st order)	
Recording console	Shimadzu RE-7	
Preintegration time	5 s	
Integration time	20 s	
Attenuation for photomultiplier high voltage	33 divisions	
	DIBK extract	*Aqueous solution*
Operating power	1.6 kW	1.2 kW
Argon flow rates		
coolant	13 l min^{-1}	12 l min^{-1}
plasma	1.1 l min^{-1}	0.9 l min^{-1}
carrier	0.7 l min^{-1}	0.8 l min^{-1}
Observation height above load coil	14 mm	16 mm
Sample uptake rate	1.8 ml min^{-1}	1.9 ml min^{-1}

In liquid—liquid extraction, minimal solubility of organic solvent in water is important for obtaining a high concentration factor. Eisenreich and Going [10] suggested that butyl acetate and acetophenone were the best extractants for reduced molybdoantimonylphosphoric acid. Diisobutyl ketone (DIBK), however, has an aqueous solubility an order of magnitude less than these solvents, and should give a higher concentration factor. This paper demonstrates the effectiveness of DIBK extraction of reduced molybdoantimonylphosphoric acid combined with i.c.p.—a.e.s. in the determination of ng ml^{-1} levels of phosphorus, using a conventional pneumatic nebulizer.

EXPERIMENTAL

Apparatus

The i.c.p.—a.e.s. instrument and its operating conditions are described in Table 1. The spectrometer was equipped with 14 fixed slits and a moving slit. It was also capable of selecting different wavelengths by changing the angle of the grating. The wavelength profile of the analytical line was obtained by moving the entrance slit over a small distance.

Reagents

Phosphorus stock solution (1000 μgP ml^{-1}) was prepared by dissolving potassium dihydrogenphosphate in water. This solution was diluted with water to prepare the working standards just before use.

The molybdate—antimony reagent was prepared by dissolving 15 g of ammonium heptamolybdate and 0.19 g of antimony potassium tartrate in water, adding 180 ml of concentrated sulfuric acid and diluting to exactly 1 l with water.

Ascorbic acid solution (10%) was used as reductant. Ammonia solution used to neutralize the acidic samples was super-special grade (Wako Chemicals, S.S.G.). All other chemicals were of analytical grade. Artificial seawater was prepared as described in the literature [11]. Phosphate-free washing reagent (Merck, Extran MA 03) was used for the cleaning of glassware. Distilled, deionized water was used throughout.

Extraction procedure

The extraction procedure was similar to that described previously [1] except for the particular organic solvent used. Transfer 500 ml of sample containing not more than 20 μg of phosphorus to a separatory funnel. Add 60 ml of the molybdate—antimony reagent and mix well. Allow the contents of the funnel to stand for 15 min. Add 2 ml of ascorbic acid solution and leave for 30 min for complete reduction. Extract the reduced molybdoantimonylphosphoric acid with exactly 5 ml of DIBK by shaking for 5 min. After phase separation, discard the aqueous phase.

For samples containing higher concentrations of phosphorus, use 100 ml of sample, 12 ml of the molybdate—antimony reagent, 2 ml of ascorbic acid solution and 10 ml of DIBK.

Determination of phosphorus by i.c.p.—a.e.s.

Introduction of organic solvent into the plasma, the matching network of which has been tuned to water, increases the reflected power and makes the plasma unstable. This difficulty was overcome by using the following tuning procedure for organic solvents suggested by Omori and Masuda [12] and Ito et al. [13]. Ignite the plasma and introduce water. Tune the matching network so that the reflected power is a minimum. Increase the reflected power up to about 100 W and introduce DIBK. Tune the matching network again. (The minimum reflected power for DIBK was below 5 W, which was less than that for methyl isobutyl ketone (MIBK, 12 W). Although MIBK caused carbon to deposit on the wall of the torch, DIBK did not. These features indicate that DIBK is better than MIBK for application with i.c.p.—a.e.s.) Allow the plasma system to stabilize for 30 min and measure the P I 214.91-nm emission line intensity while spraying the extract.

Spectrophotometric determination of phosphorus

The absorption spectrum of the reduced heteropoly acid in DIBK has maxima at 638 and 716 nm. Eisenreich and Going [10] reported that a MIBK solution had two maxima at 687 nm and 800 nm. The maxima for DIBK were similar to those for acetate esters (around 640 nm and 720 nm) reported by Eisenreich and Going. Since the absorbance at 638 nm was larger than that at 716 nm, spectrophotometric measurements were made

at 638 nm, using 500-ml water samples extracted with 5 ml of DIBK as described above, and measured in a 1-cm cell, to verify the results obtained by i.c.p.—a.e.s.

RESULTS AND DISCUSSION

Choice of analytical line

Kirkbright et al. [5] compared the intensities of phosphorus emission lines in i.c.p.—a.e.s. between 177.50 nm and 255.49 nm. They reported that the P I 213.62-nm line was the most intense and gave the best limit of detection. Winge et al. [9] reported a detection limit of 0.076 ppm for this line and the P I 214.91-nm line. The profiles of these lines for an aqueous phosphorus solution and molybdoantimonylphosphoric acid in DIBK are shown in Fig. 1. Nebulization of DIBK shifted the background slightly upwards

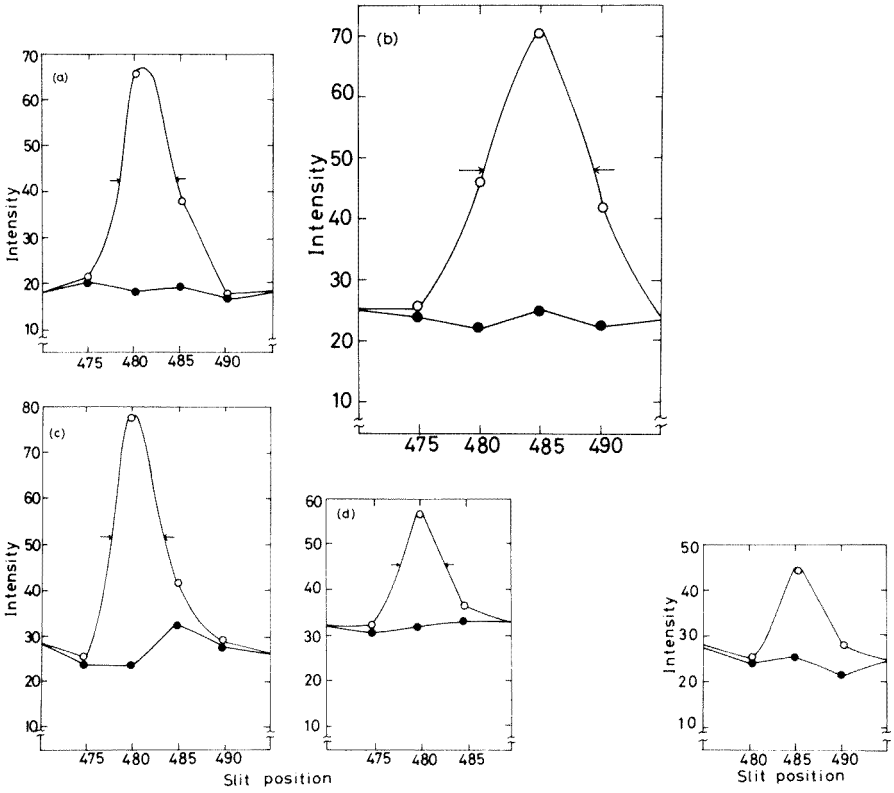

Fig. 1. Profiles of the P I 213.62-nm emission line: (a) aqueous solution; (b) DIBK extract. Profiles of the P I 214.91-nm emission line; (c) aqueous solution; (d) DIBK extract. (○) Signal; (●) background.

Fig. 2. Profile of the Mo II 213.61-nm emission line from aqueous solution; (○) signal; (●) background.

compared to the aqueous solution. The profile of the P I 213.62-nm line from the extract (Fig. 1b) had a larger half-width and its peak was at a shorter wavelength by five divisions of the slit dial than that for aqueous solution. These characteristics suggested that some spectral interference existed at this line in the extract. Figure 2 shows the wavelength profile of the Mo II 213.61-nm emission line for an aqueous solution. The peak position is the same as that in Fig. 1(b) and indicates that the Mo II 213.61-nm line in the reduced heteropoly acid interferes with the P I 213.62-nm line. The profile of the P I 214.91-nm line from the extract was identical with that from aqueous solution. Since the spectrometer had a reciprocal linear dispersion of 0.26 nm mm^{-1}, no spectral interference from the Mo II 214.98-line [14] was observed. The phosphorus 214-91-nm line, therefore, was selected for use in all subsequent measurements.

Optimization of instrumental and extraction parameters

Five parameters (forward power to the coil, observation height and the three gas flow rates) were optimized by using a univariate search method based on signal intensity to background ratio (I/B) measurements. Four parameters were held constant, and the I/B ratio was measured as the fifth parameter was varied. The effects of these parameters are shown in Fig. 3. For DIBK extracts, the I/B ratio depended strongly on the coolant and carrier gas flow rates and forward power to the coil. The plasma gas flow rate and observation height had smaller effects. For an aqueous solution, the effects of forward power and coolant gas were smaller than those for DIBK extracts. The optimized conditions for the DIBK extract and aqueous solution are compared in Table 1.

The amounts of the molybdate—antimony reagent and ascorbic acid were varied. The results, given in Table 2, show that 60 ml of the molybdate reagent and 1 ml of ascorbic solution gave the greatest signal intensity. However, for samples containing a large amount of iron, more ascorbic acid (2 ml) was necessary to depress the interference in the reduction of the heteropoly acid.

Calibration, precision and interferences

The effects of other ions are summarized in Table 3. No interference from silicon and germanium (which cause positive errors in the spectrophotometric method) was observed even at 1000-fold excesses. Arsenic(V) was permissible up to 10 times the weight of phosphorus. Above this amount, a slight upward background shift was observed which caused a positive error of >5%. However, natural water containing arsenic(V) in amounts more than 10 times that of phosphorus is rare. Most of the other anions did not show any interference, and that of nitrite was decreased by addition of sulfamic acid. There was no interference from peroxodisulfate, indicating that pretreatment with peroxodisulfate as used for the determination of total phosphorus in water is also applicable to this method.

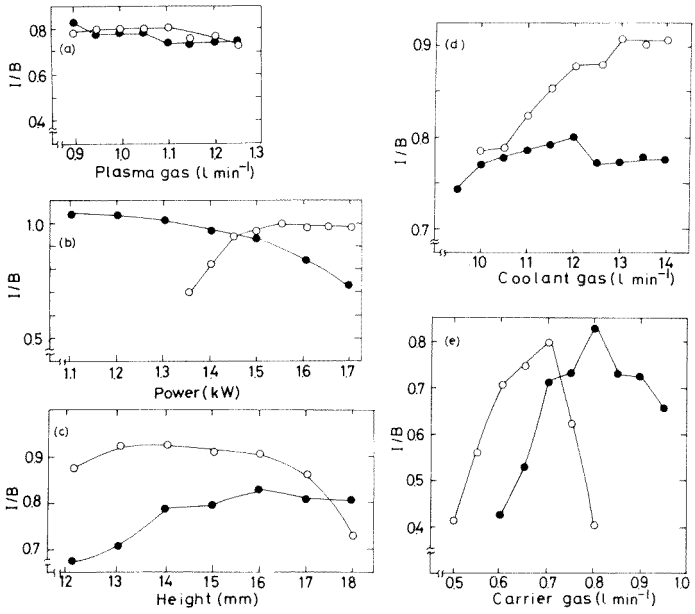

Fig.3. Effects on the emission intensity of the P I 214.91-nm line of: (a) plasma gas flow; (b) power; (c) observation height; (d) coolant gas flow; (e) carrier gas flow. (○) DIBK extract; (●) aqueous solution.

The calibration graph obtained by the proposed extraction method was linear for at least three orders of magnitude of concentration above the detection limit. The detection limit, defined as the concentration of phosphorus equivalent to three times the standard deviation of the background signal (3σ), was 37 ng P ml^{-1} in the 5 ml of extract, which is slightly better than that in aqueous solution (53 ng P ml^{-1}). Hence, the detection limit for the original samples (500 ml) was 0.37 ng P ml^{-1}.

Ten measurements of 5 μg of phosphorus, extracted from 500-ml portions of aqueous solution, were made using the recommended procedure. The relative standard deviation was 2.1%. This value reflects not only the repro-

TABLE 2

Optimization of extraction conditions

Ascorbic acid soln. (ml)	Emission Intensity (arbitrary units)			
	Molybdate reagent (ml)			
	30	40	50	60
1.0	0.87	1.03	1.12	1.13
2.0	0.92	1.00	1.01	1.04
3.0	0.94	1.02	1.04	1.01

TABLE 3

Effect of other ions on phosphorus results (sample, 100 ml; DIBK, 5 ml; P, 10 μg)

Other ion	Amount added	Recovery (%)	Other ion	Amount added	Recovery (%)
None	—	100	Fe(III)	1 mg	101
As(V)	10 μg	100	Cl^-	2 g	101
	50 μg	102	I^-	10 mg	102
	100 μg	105	Br^-	10 mg	99
As(III)	1 mg	104	NO_2^-	10 mg	91
Si	10 mg	102		10 mg	104[a]
Ge	10 mg	101	$S_2O_8^{2-}$	1 g	103

[a]20 mg of sulfamic acid added.

TABLE 4

Recovery of phosphorus added to artificial sea water (500-ml samples, 5 ml of DIBK)

P added (μg)	P found (μg)[a]	Recovery (%)	P added (μg)	P found (μg)[a]	Recovery (%)
1.0	0.97	97	10.0	10.1	101
2.0	1.9	95	12.0	11.8	98
4.0	3.9	98	16.0	15.8	99
6.0	5.9	98			

[a]Average of two measurements.

ducibility of the instrumental response but also that of the extraction procedure. The relative standard deviation of the background signal was 0.3%.

Analytical applications

Table 4 shows the results of recovery tests for various amounts of phosphorus added to artificial sea water. Recoveries of more than 95% were obtained for all the samples tested.

The values obtained by the proposed method for river and sea water samples are compared with those obtained by the spectrophotometric method in Table 5. They are in good agreement with each other. The precision of the values obtained by i.c.p.—a.e.s. is better than that achieved spectrophotometrically, especially at low phosphorus concentrations (samples A and G), where the absorbance is less than 0.05.

It is known that the concentration of phosphorus in sea water decreases continuously to several ng ml^{-1} at decreasing depths, although the average concentration of phosphorus in sea water is significantly higher [15]. All the sea-water samples in Table 5 were from the surface. Samples L and M were polluted with industrial waste-water or municipal sewage. For samples A to F, hydrochloric acid had been added so that the acidity was 0.1 M to prevent

TABLE 5

Phosphorus determination in river and sea water samples (500-ml samples, 5 ml of DIBK)

Sample	Phosphorus concentration (ng ml^{-1})			
	I.c.p.—a.e.s.		Spectrophotometry	
	Range[a]	Average	Range[a]	Average
River water				
A	0.3—0.4	0.4	0.2—0.4	0.3
B	5.1—5.3	5.2	5.0—5.3	5.2
C	4.3—4.5	4.4	4.5—4.8	4.7
D	21.2—22.2	21.9	20.4—22.6	21.5
E	7.4—8.1	7.7	7.8—8.5	8.3
F	22.2—23.8	23.1	23.0—26.2	25.0
Seawater				
G	1.0—1.0	1.0	0.8—1.3	1.1
H	8.8—9.9	9.3	8.8—10.7	9.8
I	3.0—3.2	3.1	3.0—3.1	3.0
J	4.0—4.6	4.2	3.7—4.8	4.2
K	10.5, 10.2	10.4	10.6, 10.0	10.3
L	30.5, 32.4	31.5	27.9, 29.5	28.7
M[b]	282, 280	281	255, 264	260

[a]Range of 4 measurements except for samples K, L and M. [b]100 ml of sample; 10 ml of DIBK.

loss of metals. These samples were neutralized with ammonia solution before the molybdate reagent was added. The blank was below the value equivalent to 40 ng of phosphorus. Potassium hydroxide could not be used because of the high blank value from its phosphorus content.

Although the color of the extract was stable for at least several hours, it faded after a day, but the phosphorus emission intensity in the extracts had not changed, even after 3 days. This means that the extracts can be stored at least for 3 days before measurements by i.c.p.—a.e.s.

In conclusion, DIBK extraction combined with i.c.p.—a.e.s. provides an effective method for the determination of phosphorus at the ng ml^{-1} level. The proposed method is simple and rapid. The total time required for the extraction and the measurement of phosphorus was less than 2 h. The indirect determination of phosphorus by measurement of molybdenum or antimony in the extract by i.c.p.—a.e.s. is also possible. It is more sensitive than the proposed method, and will be reported in a subsequent paper.

REFERENCES

1 APHA, AWWA, WPCF, Standard Methods for the Examination of Water and Wastewater, 14th edn., Washington, DC, 1976, p. 481.
2 A. D. Westland and I. Boisclair, Water Res., 8 (1974) 467.

3 K. Hiiro, A. Kawahara and T. Tanaka, Bull. Gov. Ind. Res. Inst., Osaka, Jpn., 28 (1977) 234.
4 G. F. Kirkbright and M. Marshall, Anal. Chem., 45 (1973) 1610.
5 G. F. Kirkbright, A. F. Ward and T. S. West, Anal. Chim. Acta, 62 (1972) 241.
6 A. M. Gunn, G. F. Kirkbright and L. N. Opheim, Anal. Chem., 49 (1977) 1492.
7 H. Kawaguchi, T. Ito and A. Mizuike, Bunseki Kagaku, 27 (1978) 53.
8 A. Sugimae, Bunseki Kagaku, 29 (1980) 502.
9 R. K. Winge, V. J. Peterson and V. A. Fassel, Appl. Spectrosc., 33 (1979) 206.
10 S. J. Eisenreich and J. E. Going, Anal. Chim. Acta, 71 (1974) 393.
11 The Oceanographical Society of Japan, Kaiyo Kansoku Shishin, 1970, p. 145.
12 Y. Omori and T. Masuda, Shimadzu Kagakukiki News, 20 (1979) 11.
13 T. Ito, H. Kawaguchi and A. Mizuike, Bunseki Kagaku, 28 (1979) 648.
14 Massachusetts Institute of Technology Wavelength Tables, MIT Press, Cambridge, MA, 1969.
15 T. Koyama, N. Handa and Y. Sugimura, Kosui Kaisui no Bunseki, Kodansha, Tokyo, 1972, p. 256.

Analytica Chimica Acta, 127 (1981) 103—108
Elsevier Scientific Publishing Company, Amsterdam — Printed in The Netherlands

ELECTROTHERMAL ATOMIC ABSORPTION SPECTROMETRIC TECHNIQUES FOR THE DETERMINATION OF ZINC AND COPPER IN MICROLITER AND SUBMICROLITER VOLUMES OF AQUEOUS AND SERUM MATRICES

S. LEVI[a], RICHARD C. FORTIN and WILLIAM C. PURDY*

Department of Chemistry, McGill University, 801 Sherbrooke St. W., Montreal, Quebec H3A 2K6 (Canada)

(Received 25th August 1980)

SUMMARY

Two electrothermal atomic absorption techniques which provide linear working functions over wide concentration ranges, and are suitable for the determination of zinc and copper in aqueous and 10-fold diluted blood serum matrices are evaluated. The first technique is based on modification of the furnace tube to provide a significant decrease of the atomic absorption signal when microliter and larger volumes of sample are injected. The second technique involves a delivery system capable of dispensing micro- and submicroliter sample volumes to the furnace tube. The precision of the two techniques is about 98%.

Atomic absorption spectrometry (a.a.s.) has been widely used for the determination of trace elements in aqueous and biological matrices. When the essential requirements are high sensitivity, low solution volumes, or the direct determination of low concentrations in solid samples, non-flame atomization is superior to flame atomization. Large dilutions (i.e., 20-fold or higher) are often required for the flameless a.a.s. determination of serum samples. These high dilutions have resulted in poor reproducibility. Therefore Chool et al. [1] have recommended a 10-fold dilution of the serum sample. In this laboratory, non-linear calibration curves have been obtained for the determination of zinc in microliter volumes of 10-fold diluted serum samples. In fact, a 2-μl sample produced an absorption signal far beyond the linear range of the calibration curve.

If the use of flame atomization is not a viable option, other solutions to the problem must be sought. One of these would be to decrease the atomic absorption signal by modifying the furnace tube design so that the light beam from the hollow-cathode lamp encounters fewer atoms in the graphite tube [2]. Another would be to use a reliable technique for delivering volumes of 1 μl or less. In our experience, 1-μl pipets and microsyringes have failed to deliver these volumes to the furnace with adequate precision.

[a]Present address: Department of Pharmacological Sciences, School of Basic Health Sciences, Health Science Center, SUNY at Stony Brook, Long Island, NY 11794, U.S.A.

The present study was undertaken to determine whether furnace tube modification and/or a new delivery system could yield linear calibration curves for zinc in these samples. The two approaches were also applied to the determination of copper in 10-fold diluted serum.

EXPERIMENTAL

Reagents and materials

All reagents, diluents, and containers were regarded as potential sources of copper and zinc contamination. A principal source of error when dealing with concentrations in the $\mu g\ l^{-1}$ range is the adsorption and desorption of metal ions onto and from container walls [3]. The cleaning procedure used for bottles, flasks, teflon tubing, tips, etc. is described elsewhere [4].

Aqueous standards of copper and zinc (1000 mg l^{-1}) were obtained from BDH Chemicals (Montreal, Que.) and were prepared as described in the literature [5]. Stock solutions (1000 mg l^{-1} in each metal ion) were also prepared by dissolving copper and zinc metals (Baker Analyzed Reagent) in a minimum volume of nitric acid (Ultrex, J. T. Baker Chemical Co.) and hydrochloric acid (Ultrex), respectively and diluting with conductivity water (1.138×10^{-6} mhos-cm). Serial dilutions of the stock gave the secondary standards.

Blood serum controls

Six 4-ml aliquots of a serum pool were transferred to polyethylene containers. These containers were closed to minimize evaporation. To each of the six containers was added in turn 40 μl of, 1,2,3,4,5, and 6 mg l^{-1} (in each metal) solution to obtain serum controls containing added concentrations of 10,20,30,40,50, and 60 $\mu g\ l^{-1}$, respectively.

Collection and handling of specimens

Blood samples were drawn by 1-ml disposable polyethylene syringes attached to silicone-coated stainless-steel needles and were transferred carefully (to avoid hemolysis; platelets and red blood cells introduce high levels of zinc into the sample [6, 7]) to specially cleaned 0.5-ml polypropylene centrifuge microtubes (Fisher Scientific Co.). The samples were allowed to clot and were then centrifuged in a clinical centrifuge (International Equipment Co., Boston, MA) fitted with an aluminium adaptor plate (part no. 5-408, Fisher Scientific Co.) constructed to hold 0.5-ml microtubes. A 200-μl sample of serum from each centrifuge tube was delivered by Eppendorf pipet to screw-capped Oak Ridge tubes and the serum was frozen at $-20°C$ until the time of measurement.

Apparatus and analytical procedures

Modified tube technique. An S.G.E. syringe equipped with a 5-cm teflon tip and a gain to facilitate the reproducible dispensing of volumes was used

to deliver 4.5 μl and 20 μl of zinc and copper solutions, respectively. A commercial pyrolytic graphite tube suitable for use with a Perkin-Elmer HGA-2000 system was cut to a length which could be accommodated by the Model HGA-2200 atomizer. The Perkin-Elmer HGA-2200 and Model 603 atomic absorption spectrometer with deuterium background corrector formed the system used in this study. The final length of the graphite tube was measured and was 28 cm. In addition the optical aperture or cone was modified to accept this new tube [7]. This necessitated increasing the cone diameter from 9 to 13 cm.

Modified delivery technique. A 10-μl Hamilton microsyringe was tipped with 0.38-mm i.d. teflon tubing. The end of this tubing was sharpened to aid delivery of the sample. The tubing was marked to deliver volumes of 0.8 μl or larger in the following manner. The tubing wall was grooved with a razor blade, the grooves were filled with black ink and before drying the tubing was wiped clean, leaving very thin but clear black lines.

An aqueous or blood serum solution is drawn to some point (about 1 cm) above the desired black mark. To achieve complete delivery of the solution, the tubing is removed from the syringe needle and the syringe piston is withdrawn about 2 cm further. This operation increases the pressure for evacuating the solution. The needle is re-inserted in the tubing and the solution volume is adjusted to the desired black mark. After drops in excess have been wiped clean, the tubing is inserted into the center of the preconditioned pyrolytic graphite tube of the HGA-2200 furnace. The end of the tubing is gently pressed against the wall of the HGA tube and the solution is injected smoothly and completely. The program button of the HGA-2200 control unit is used to start and complete the sample atomization cycle. The instrument settings for the atomic absorption spectrometer are given in Table 1. The absorption signal is read from the electronic display and from a strip-chart recorder (Heath-Schlumberger, Model SR 204). Sample volumes of 0.8 and 10 μl were used in the measurement of zinc and copper, respectively.

Calibration. Calibration curves were prepared by constant injected volume and constant injected concentration procedures. Each point on each calibration curve was the average of four runs. After each set of four samples, a standard was run to check and compensate for the effect of furnace tube aging. Calibration curves were prepared and sample measurements for each metal were done on the same day.

RESULTS AND DISCUSSION

Initially, the instrumental settings given in the Perkin-Elmer instrument manual were used. These settings were then modified until appropriate conditions (listed in Table 1) were obtained for each element. However, even these settings produced a signal far beyond the linear range of the instrument when zinc was determined in 2 μl of 10-fold diluted serum. Furthermore, when dealing with 0.8 μl of the diluted zinc sample, the

TABLE 1

Instrument settings

Resonance lines:	Hollow-cathode lamps operated at 15 mA, Cu 324.7, Zn 213.9 nm.
Slit width:	4 (0.7 nm nominal spectral bandwidth).
Purge gas:	N_2, high purity grade, position: Normal 3, 40 (= gas flow is reduced to 40 ml min^{-1} for 3 s during the atomization stage).

HGA program:	Temperature (°C)		Time (s)		Ramp (s)	
	Cu	Zn	Cu	Zn	Cu	Zn
Modified tube technique						
Drying	120	120	40	40	0	0
Charring	600	450	50	50	20	20
Atomizing	2200	2000	8	8	0	0
Modified delivery technique						
Drying	120	130	60	20	20	10
Charring	600	450	30	30	20	10
Atomizing	2000	1900	10	10	0	0

shape and height of the signal peak was affected by matrix constituents. Hence background correction was used in the determination of both elements.

It was also found that higher temperatures and longer drying and charring times were required for the diluted serum than for aqueous solutions. Charring temperatures above 450°C led to considerable losses of zinc. The drying time of 50—60 s for the determination of copper in 10-μl serum samples may seem long. However, shorter drying times led to decreased reproducibility because of sample sputtering during the charring stage. The atomization temperatures and times given in Table 1 were the minimum consistent with complete volatilization of the element and were selected to permit the maximum possible number of firings per tube. Useful tube life depended greatly on the atomization temperature, a decrease in graphite tube sensitivity being linearly related to the number of tube firings [8]. After every set of four firings, a standard was run to correct for tube aging effects.

Calibration curves prepared by the constant injected volume procedure were compared to those prepared by the constant injected concentration procedure. The former resulted in a greater working range. In agreement with literature reports [7], the same result was observed when the electronic display on the instrument was used rather than the tracing on the strip-chart recorder.

Aqueous and serum calibrations were prepared for copper and zinc by the modified tube and modified delivery techniques. For the modified tube technique, the slopes of the aqueous and serum calibration curves were similar but the intercepts were different. This difference could be corrected by use of the background corrector or by use of standard additions. The slopes of the aqueous curves by the modified delivery technique were con-

siderably larger than those of the serum calibration curves indicating that aqueous calibration curves could not be used as standards for serum samples. Matrix matching was an alternative, but it was very difficult to obtain the zinc- or copper-free protein and lipid materials necessary to approximate successfully the matrix composition of serum. Therefore, working curves were prepared from serum controls. In using these controls, however, it was essential that the pooled serum gave a low atomic absorption signal to have a reasonable concentration range of standard additions for plotting the linear working curve.

The linear regression data for the serum control calibration curves are given in Table 2. The concentrations of copper and zinc in the pooled serum obtained from the modified tube and modified delivery calibration curves are 1221 ± 20 and 1285 ± 17 $\mu g\ l^{-1}$ and 1099 ± 60 and 909 ± 35 $\mu g\ l^{-1}$, respectively. The techniques provide linear calibration curves over the range 45—13500 and 8—100 pg, respectively for zinc and 200—6000,000 and 100—1200 pg, respectively for copper.

Recovery studies

The average recoveries obtained from the calibration curves by the modified delivery technique for zinc and copper (40 $\mu g\ l^{-1}$) added to 4 ml of serum were (mean ± r.s.d.) 98 ± 4% and 98.5 ± 1.5%, respectively. Average recoveries from the modified tube technique were 98.4 ± 1.6% and 98 ± 5.5%, respectively. These recoveries of added concentrations were calculated from the differences between the added concentrations and their values on the

TABLE 2

Linear regression of serum control calibration curves[a]

Element	$y = aC + b$	r	S.d. slope	S.d. intercept	S_{yx}	Added conc. range ($\mu g\ l^{-1}$)
	Modified tube technique					
Zn	$y = 0.175C + 0.392$	0.9948	6.01×10^{-3}	5.01×10^{-4}	0.23×10^{-3}	0—80
Cu	$y = 0.180C + 0.493$	0.9957	4.26×10^{-3}	3.16×10^{-3}	3.42×10^{-3}	0—80
	Modified delivery technique					
Zn	$y = 1.198C - 0.590$	0.9985	2.91×10^{-2}	1.05×10^{-2}	3.06×10^{-3}	0—60
Cu	$y = 1.336C + 1.929$	0.9986	3.21×10^{-2}	1.16×10^{-2}	2.18×10^{-3}	0—60

[a] y = absorbance × 10^3, C = $\mu g\ l^{-1}$, a = slope, b = intercept; r = correlation coefficient; s.d. slope = standard deviation of the slope; s.d. intercept = standard deviation of the intercept; S_{yx} = standard error of estimate = $[1/(n-2)\ \Sigma\ (y_i - a - bx_i)]^{1/2}$. Number of points was 6 for modified tube technique, and 7 for modified delivery technique, each point being the average of 5 determinations. The mean (n = 5) of the y values of serum samples with zero addition of metal ions (blank) was subtracted from the y values of the serum controls before regression parameters were computed.

regression lines. Precision was tested by determining the recovery of zinc and copper (40 $\mu g\ l^{-1}$) added to 4 ml of pooled serum. Twenty aliquots were examined and five atomic absorption measurements were performed on each aliquot. Recoveries calculated from the serum control calibration curves were found to be 97 ± 3.3% for zinc and 99.2 ± 1.4% for copper. The reproducibility of the measurements is reflected by the relative standard deviation calculated from 100 (5 × 20) atomic absorption readings; values were 3.5% for zinc and 1.3% for copper.

The authors are indebted to the Medical Research Council and the Natural Sciences and Engineering Research Council of Canada for financial support.

REFERENCES

1 M. K. Chool, J. K. Todd and N. D. Boyd, Clin. Chem., 21 (1975) 632.
2 R. W. Marrow and R. J. McElhaney, J. Appl. Spectrosc., 27 (1973) 387.
3 M. M. West, J. F. Molina, C. L. Yuan, D. G. Davis and J. V. Chauvin, Anal. Chem., 51 (1979) 2370.
4 S. Levi and W. C. Purdy, Anal. Chim. Acta, 116 (1980) 375.
5 J. Toffaletti and J. Savory, Anal. Chem., 47 (1975) 2091.
6 R. T. Lofberg and E. A. Levri, Anal. Lett., 7 (1974) 775.
7 F. D. Posma, H. C. Smit and A. F. Rooze, Anal. Chem., 47 (1975) 2087.
8 J. F. Chapman and L. S. Dale, Anal. Chim. Acta, 111 (1979) 137.

Analytica Chimica Acta, 127 (1981) 109—120
Elsevier Scientific Publishing Company, Amsterdam — Printed in The Netherlands

ELECTROTHERMAL ATOMIZATION FROM METALLIC SURFACES
Part 3. Some New Developments in Design and Performance of a Tungsten-Tube Atomizer†

P. PÜSCHEL and Z. FORMÁNEK

Research Institute for Brown Coal, 434 37 Most (Czechoslovakia)

R. HLAVÁČ, D. KOLIHOVÁ and V. SYCHRA*

Laboratory of Flame Spectrometry, Institute of Chemical Technology, 166 28 Prague 6 (Czechoslovakia)

(Received 19th January 1981)

SUMMARY

A new design of a work-head for a tungsten-tube atomizer as well as voltage- and temperature-feedback circuits added to the power supply of a Varian model CRA-63 atomizer are described. The importance of rapid, temperature-controlled heating of the atomizer is shown. The effect of heating rate (0.5—20 K ms^{-1}) on the analytical signal of many elements is investigated; experimental atomization and residence times and peak absorbance values are evaluated. The analytical performance of the tungsten-tube atomizer is tested for elements of different volatilities.

In Part I [1], the design and performance were described for a simple tungsten-tube electrothermal atomizer that can be accommodated in the work-head of a Varian carbon rod atomizer (CRA-63 or CRA-90) and operated as an alternative to the graphite tubes and cups. The atomizer itself was made from two profiled tungsten strips held in two copper supporting electrodes and forming a cylindrical cavity (5 mm long, 3.5 mm i.d.). A special silica chamber was placed on top of the chimney of the CRA-63 work-head to improve the efficiency of the inert gas sheath. A simple modification of a Varian CRA-63 power supply was made to heat the atomizer. Although this atomizer exhibited good analytical performance, further studies showed that its geometry (particularly the length) and heating characteristics did not allow the theoretically predicted sensitivity to be achieved.

With 5-mm tungsten tubes, experimental residence times were extremely short so that τ_1/τ_2 ratios (see below) were rarely less than 3. Moreover, samples had to be delivered into the atomizer cavity from either end (a delivery hole made in the center of the upper strip significantly reduced the lifetime of the tube); the use of automatic dispensers was thus excluded.

†Presented (in part) at the XXI C.S.I. and 8th I.C.A.S., July, 1979, Cambridge, U.K. and at the 3rd Czechoslovak Conference on a.a.s., October, 1979, Chlum u Třeboně, Czechoslovakia.

0003—2670/81/0000—0000/$02.50

The need for longer tungsten tubes was evident. Practical experience acquired with a tungsten-tube atomizer 10-mm long and operated in a modified CRA-63 work-head (in the same way as for 5-mm tubes) suggested a need for more sophisticated means of holding and uniform heating of the tungsten tube, and for its rapid and reproducible adjustment and replacement. Moreover, for a metal-based electrothermal atomizer, a fully enclosed system would by very advantageous. In this paper, a new work-head is described which is especially designed for metal-tube atomizers and which fulfils all the requirements mentioned above.

The advantages of temperature-feedback control of power supplies for electrothermal atomizers as well as the importance of rapid heating of the atomizer have been well documented [2—11]. Uncontrolled heating of our original tungsten-tube atomizer (by means of the simply modified CRA-63 power supply) resulted in a less stable voltage applied to the atomizer and therefore a less stable temperature, compared to the normal, unmodified mode of operation with graphite tubes. The maximum attainable heating rate was only about 6 K ms^{-1} and was dependent of the preset atomization temperature. This paper describes a voltage-feedback circuit (for controlling atomization) added to the Varian CRA-63 power supply.

EXPERIMENTAL

Apparatus

All measurements were carried out with a Varian AA6 single-beam atomic absorption spectrometer. A shorter response time was achieved by altering the time constant of the damping amplifier to 10 ms as described by Lundberg [12]. A Perkin-Elmer M-56 recorder with a 0.3-s full-scale response was used for recording transient signals. Absorbance—time and temperature—time profiles were measured with a six-channel storage oscilloscope (Tesla OPD 280U, Czechoslovakia). The voltage applied to the atomizer work-head was measured with a Keithley digital multimeter. The slit-widths, wavelengths and lamp currents recommended by the manufacturer were used throughout.

Atomizer

The atomizer consisted of two profiled tungsten strips (0.1 mm thick, 10 mm wide, and 26 mm long) fabricated in the laboratory from 10-mm tungsten strips (ultrapure tungsten, Metallwerk, Plansee, Austria) by means of a special bottom die. The strips formed a cylindrical tube (10 mm long, 3.5 mm i.d.). A sampling hole (2.3 mm) was drilled in the centre of the upper strip. A small circular depression made in the centre of the bottom strip (facing the sampling hole) served for accurate and reproducible location of the test solution. In the flat ends of both strips, 2-mm holes were made for placing the atomizer on locating pins on the work-head electrodes (see Fig. 1 and text below).

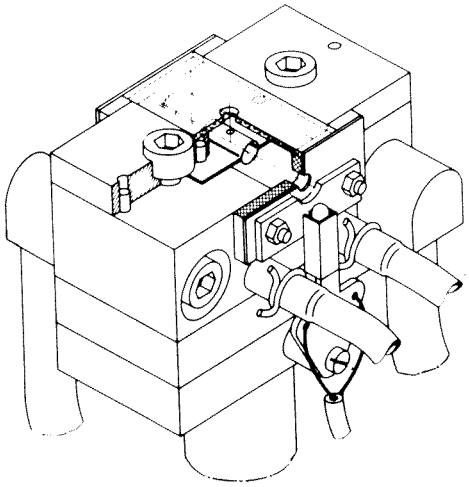

Fig. 1. Work-head designed for metal-tube operation.

Work-head

The work-head developed is shown schematically in Fig. 1. The basic design (dimensions, water cooling, inert gas inlet, position of the tube) was very similar to that of the original Varian CRA-63 (CRA-90) work-head but had the following additional features.

Both brass work-head electrodes were cut horizontally into two parts; the bottom part was provided with two locating pins, the upper part with two corresponding locating holes. The inner pins served also for simple and reproducible location of the metal tube. Both parts of the electrodes were mounted together with massive vertical clamping screws. This simple demountable system enabled rapid exchange and adjustment of the tungsten tube and ensured very good electrical contact between the tube and the electrodes. The power cables had conical brass connections provided with an inside thread. The connections fitted into conical holes in the bottom part of the work-head electrodes and were tightened with a massive horizontal screw. This arrangement ensured perfect contact between the power cables and the work-head. For good mass balance of the work-head (which should be located horizontally with respect to the optical axis of the instrument), the power cables were mounted on opposite sides of the bottom parts of the work-head electrodes.

The compartment containing the atomizer itself was almost entirely enclosed. This was achieved by two special teflon masks (fitted with 5.5-mm circular quartz windows) mounted to both sides of the work-head and by means of a 1-mm thick quartz plate cover. A 4-mm hole was drilled in the centre of the quartz plate which served for sampling as well as being an inert gas outlet. Very efficient and homogeneous gas shielding was achieved with this arrangement even when very small flow rates of argon were used.

A photodiode (in its housing) was attached to the work-head (from the right-hand side); it viewed the radiation emitted from a definite part of the inner surface of the tungsten tube via a light pipe (made from an optical glass filter) positioned in the teflon mask just below the quartz window.

Power supply

The 10-mm tungsten tubes were heated with a modified Varian CRA-63 power supply. Because the resistance of the metallic atomizer is generally lower than that of the carbon atomizer, it is advantageous to use a transformer of a lower secondary voltage and increased current-carrying capacity. Thus a transformer capable of delivering 4—6 V at 450 A was used, instead of the original 12 V—150 A version, located outside the box of the CRA-63 power supply. Because of the increased current on the primary side of the transformer, the current-carrying capacity of the triac, fuse and breaker-switch were also increased to handle the increased current. To increase the current-carrying capacity of the power cables, power cables with a cross-section of at least 200 mm^2 were used.

The CRA-63 does not have any feedback from the atomizer. To improve the stability of the voltage applied to the tungsten-tube atomizer in the drying and ashing steps, a voltage feedback was developed. It is shown schematically in Fig. 2. The voltage was led from the atomizer over a matching and insulating transformer and a rectifier to the control unit, where it was subtracted from the control voltage. The circuit was tested (by using a 6 V—60A) transformer from which a double-wave rectified voltage was led across 10 kΩ resistors to pins 12 and 14 of the PCB assembly of the CRA-63, from which resistors R59 and R60 were removed.

A metal-based electrothermal atomizer is generally capable of very rapid heating (because it is usually of small mass and low specific heat). In order fully to utilize this feature, a temperature-feedback circuit was added to the CRA-63 power supply which enabled very high heating rates to be achieved as well as very precise temperature control. The circuit (shown schematically in Fig. 3) incorporated a photodiode which accepted a small fraction of the

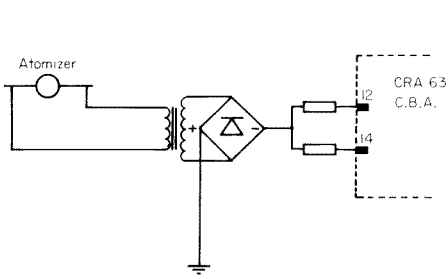

Fig. 2. Schematic diagram of the voltage-feedback circuit.

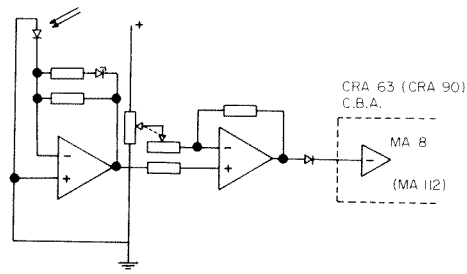

Fig. 3. Schematic diagram of the temperature-feedback circuit.

radiation emitted from inside the tungsten tube. The current of the photodiode was amplified by an operational amplifier with a non-linear feedback. The non-linear dependence of the photodiode current on the temperature of the atomizer and the non-linear amplification by the operational amplifier tended to compensate mutually, so that when a germanium photodiode was used (with maximum spectral response in the near-i.r. region), a nearly linear dependence of the output voltage on temperature (above 900 K) was attained. The output voltage was compared by means of a comparator with the voltage set by the control potentiometer. The output of the comparator was connected via a diode with input 2 of the integrated circuit MA8 (see the PCB assembly of the CRA-63 power supply). In this way, the current supplied to the atomizer was reduced if the output voltage of the amplifier (corresponding to the temperature of the atomizer) was higher than the preset voltage. To obtain as fast a heat-up rate as possible without danger of oscillations and temperature overshoot, the gain of the amplifier was trimmed by a non-linear feedback and the gain of the comparator was trimmed by a variable resistor mechanically coupled with the control potentiometer.

The circuit described featured a variable rate temperature ramping function (up to 25 K ms^{-1}) nearly independent of any preset temperature. The normal, unmodified mode of operation could be selected if desired.

Measurement of the atomizer temperature

The surface temperatures of the tungsten tube were measured with a sensitive germanium photodiode (Tesla 12PP70, Czechoslovakia) used in the temperature-feedback circuit. The signal from the amplifier was led directly to one channel of the storage oscilloscope and was calibrated by means of an optical pyrometer and with Pt/Pt—Rh and Ir/W miniature thermocouples. All temperatures measured with the optical pyrometer were corrected, taking into account differences between tungsten radiation and black-body radiation.

Sampling

Aliquots (5-μl) of the sample were placed in the center of the lower metal strip either manually with an adjustable 5-μl syringe (Scientific Glass Engineering Pty. Ltd., Melbourne, Australia) or by means of an automatic sample dispenser (Varian ASD-53). The relative standard deviation of sampling was less than 1% or 3% when ASD-53 or manual sampling was used, respectively.

Reagents

Specpure metals (Johnson-Matthey Ltd., U.K.) were used for preparation of the stock solutions of metal ions (1000 μg ml^{-1}). Solutions of Al, Ba, Cd, Li and Ni were prepared as nitrates; V, Cr, Ti and Be were prepared as sulphates, and phosphorus as diammonium hydrogen phosphate. A germanium

stock solution was prepared by dissolving germanium dioxide in the minimum of sodium hydroxide solution, acidifying with hydrochloric acid and diluting with deionized water. An arsenic solution was prepared by dissolving arsenic(III) oxide in sodium hydroxide. All working solutions were prepared immediately before use by dilution with twice-distilled deionized water and were acidified with the appropriate acid to a final concentration of 1% (v/v). The solutions were stored in plastic bottles.

RESULTS AND DISCUSSION

The effect of heating rate

The heating rate of an electrothermal atomizer is one of the critical factors which determine the kinetics of atomization and nearly all the processes by which an analyte is removed from the atomizer, such as inert gas expansion, matrix gas expansion, inert gas convection, diffusion, recombination in the gas phase, etc. The heating rate thus affects the shape of the transient absorption pulse and the value of the maximum absorbance. The dependence of peak absorbance on the heating rate is known to be generally affected by analyte volatility, atomizer geometry, atomization mechanism and the response of the electronic measurement system used (usually defined by the time constant of its damping amplifier) [10].

Transient absorption signals generated in the tungsten-tube were investigated for a number of elements over a wide range of heating rates. Oscilloscopic traces were used to evaluate the effect of heating rate on the experimental atomization time (τ_1), the experimental residence time (τ_2) and the peak absorbance. Typical examples are given in Table 1 and Fig. 4.

Table 1 gives a picture of τ_1, τ_2, and peak absorbance values for elements with significantly different volatilities when they are atomized at different heating rates. For all three elements, τ_1 decreases rapidly (nearly exponen-

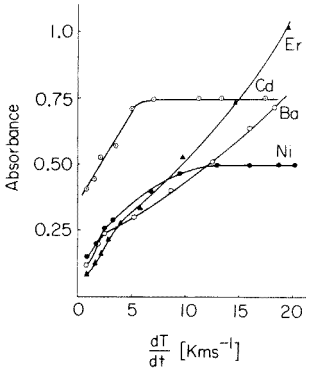

Fig. 4. Effect of heating rate (dT/dt) of the tungsten-tube atomizer on the maximum absorbance A of some elements.

TABLE 1

Effect of heating rate on experimental atomization time (τ_1), experimental residence time (τ_2) and peak absorbance (A) for erbium, barium and cadmium

Heating rate (K ms^{-1})	Erbium[a,b]			Barium[a,c]			Cadmium[a,d]		
	τ_1 (ms)	τ_2 (ms)	A	τ_1 (ms)	τ_2 (ms)	A	τ_1 (ms)	τ_2 (ms)	A
0.75	1050	830	0.080	530	280	0.115	340	170	0.405
1.5	530	440	0.130	400	205	0.145	245	115	0.440
3.0	340	190	0.220	175	85	0.255	150	80	0.570
4.0	260	160	0.276	145	65	0.275	120	60	0.630
6.0	155	130	0.355	120	50	0.315	90	40	0.740
7.5	140	90	0.410	100	45	0.355	70	30	0.745
10.0	110	55	0.515	90	35	0.430	55	25	0.745
15.0	85	40	0.755	80	30	0.590	—	—	0.745
20.0	65	40	1.080	70	25	0.785	—	—	0.745

[a]In an atmosphere of 2.1 l Ar min^{-1} and 0.8 l H_2 min^{-1}. [b]2.5 ng (as chloride). [c]50 pg (as nitrate). [d]25 pg (as nitrate).

tially) with increasing heating rate; the most pronounced decrease is observed for the element with the lowest volatility (erbium). The experimental τ_2 values also decrease very rapidly with increasing heating rate but become nearly constant at very high heating rates. At any heating rate studied, the element with the highest volatility (cadmium) exhibits the shortest τ_2 value. The experimental residence times τ_2 obtained with the 10-mm long tube are still very short (resulting in $\tau_1:\tau_2 > 1$); however, they are nearly twice the τ_2 values obtained with the 5-mm tungsten tube. It was not possible to find any correlation between experimental τ_1/τ_2 ratios (calculated from the values in Table 1) and the peak absorbance values. At very high heating rates, this could be due to the relatively low precision of the measurement of very small values of τ_1 and of τ_2 because of the distortion of very fast transient signals caused by the still relatively slow instrumental response time.

Figure 4 shows the variation in the maximum (peak) absorbance as a function of the heating rate. As expected, a sharp increase in the maximum absorbance with heating rate was observed for elements of low volatility (Er, Ba), which vaporize when the temperature of the atomizer has nearly reached a steady state (see also Fig. 5); the loss of the analyte atomic vapour by expulsion and convection is thus mostly eliminated. High heating rates give much less enhancement in sensitivity for elements of medium volatility (Ni) or high volatility (Cd) which atomize at a time when the temperature of the atomizer is rising extremely rapidly, resulting in the expulsion of the analyte vapour with the rapidly expanding gases (i.e., giving very small τ_2 values). The greater the volatility of the analyte, the lower the heating rate at which the curves bend toward the abscissa (compare Cd and Ni in Fig. 4).

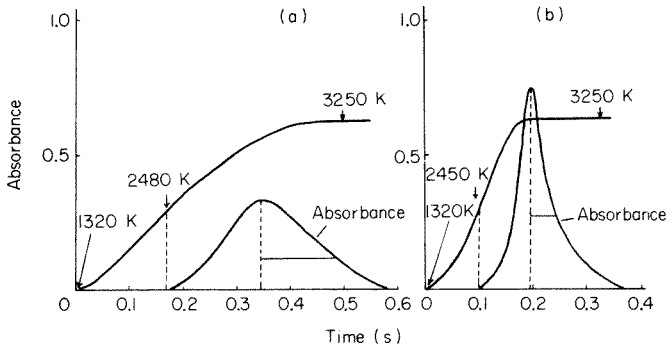

Fig. 5. Oscilloscopic absorbance—time and temperature—time traces for 0.25 ng of erbium atomized at (a) 5.7 K ms^{-1}; (b) 14.5 K ms^{-1}.

Because the transient signals for the highly volatile elements are too fast for the time constant (10 ms) of the amplifier in the instrument used, part of this bending at high heating rates is probably due to the slow response of the amplifier.

The results described above are in a good agreement with many of those published by Chakrabarti et al. [8, 10] for capacitive discharge heating of a graphite furnace. However, it was found [10] that high heating rates gave greater enhancement in sensitivity for those analytes which form atoms by solid-phase decomposition or reduction on the graphite surface (i.e. by contact with the atomizer wall) than for those which form atoms by vapour-phase dissociation. With the tungsten-tube atomizer, a dramatic increase in sensitivity with increasing heating rate was found for most of the elements studied including those which atomize (in the tungsten tube) via dissociation of the analyte monoxide in the vapour phase (e.g. lead, manganese [13] and some lanthanides).

This disagreement between the present results and those of Chakrabarti et al. [10] can be explained as follows. At the high rate of heating of the graphite tube by a capacitive discharge, the vapour-phase temperature is supposed to lag behind the surface temperature of the atomizer; the greater the heating rate, the greater the lag in the vapour-phase temperature. Thus, the analytes which have a vapour-phase dissociation mechanism of atomization should show less enhancement in their sensitivity because of the slower rate of increase in the vapour-phase temperature. The results obtained with the tungsten-tube atomizer would therefore indicate that in the rapidly heated small tungsten tube there is no significant lag in the vapour-phase temperature behind the surface temperature of the atomizer. Also, it seems reasonable to assume that at very high heating rates, the rate of vaporization of the analyte monoxide (even of low mass) will lag behind, and, for analytes for which it is thermodynamically and chemically possible, solid-phase atomization will also occur, thus enabling a greater sensitivity enhancement to be

achieved with increasing heating rate. Both explanations need direct experimental verification.

Figure 5 depicts both the absorbance—time and temperature—time transients observed for 0.25 ng of erbium atomized at two different heating rates. The appearance temperature in both instances is approximately the same (2480 and 2450 K), but the temperature experienced by erbium atoms leaving the tungsten surface later in the transient differs in the two cases. At the higher heating rate (14.5 K ms^{-1}), nearly the whole absorbance peak is observed when the tungsten tube has reached isothermal conditions. In general, the higher the heating rate, the more isothermal are the peaks that can be obtained. For analytes of low volatility, isothermal atomization is achieved easily. The importance of this result for matrix effect control is evident. Figure 6 shows that isothermal atomization can also be reached for analytes which exhibit appearance temperatures lower than 2000 K (Ba) when very high heating rates (20 K ms^{-1}) are applied.

For elements of high and medium volatility, conditions very close to isothermal atomization can be reached easily by means of the L'vov platform technique [9, 14]. A miniature, semicircular tungsten platform was used for this purpose. Atomization from a tungsten platform in the tungsten-tube atomizer will be the subject of a separate paper.

Conventional chart recorders (with a response time of 0.2—0.3 s) are not quick enough to follow very fast transient signals generated in rapidly heated electrothermal atomizers. The peak height absorbance signal is always diminished compared to the "true" value. This decrease depends on the magnitude of the absorbance measured, analyte volatility and the heating rate applied to the atomizer. When the heating rate does not exceed ca. 5 K ms^{-1}, the use of a strip-chart recorder is usually acceptable because the distortion of the recorded signals is not significant (except for highly volatile analytes). For higher heating rates, the use of a storage oscilloscope for

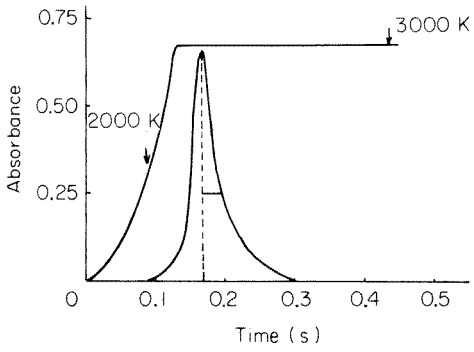

Fig. 6. Oscilloscopic absorbance—time and temperature—time traces for 50 pg of barium at 20 K ms^{-1}.

recording fast transient signals is advisable. A storage oscilloscope (16 × 24 cm screen) is now routinely used in this laboratory for evaluating absorbance peaks.

Analytical data

Table 2 lists the atomization temperatures and absolute characteristic concentrations (calculated from oscilloscope traces) for some elements in the tungsten-tube atomizer at optimized heating rates. Characteristic concentrations calculated from signals recorded with a Perkin-Elmer M-56 recorder were 1.5—3 times worse because of the relatively slow response of the recorder. The characteristic concentrations presented in Table 2 are much better (by factors of 5—25) than those published earlier [1] for a 5-mm tungsten tube and better than those for commercial graphite furnaces. A particularly significant improvement in sensitivity was attained for elements of low volatility.

Calibration graphs (based on peak absorbance signals taken from the oscilloscope) were often linear up to an absorbance of 1.0. The linearity depends on the heating rate, analyte volatility and instrument (and/or recorder) response. Calibration graphs for traces of beryllium are illustrated in Fig. 7. The relative standard deviation for 16 manual injections and determinations of 50 pg of beryllium was 1.4%.

TABLE 2

Characteristic concentrations for some elements in the tungsten-tube atomizer at optimized heating rates and oscilloscopic recording

Element	Wavelength (nm)	Atomization temperature[a] (K)	Heating rate (K ms^{-1})	Characteristic concentration (pg/1% absorption)
Al	309.3	2950	16.4	8
As	193.7	2150	10.0	14
Ba	553.6	3000	20.4	0.3
Be	234.9	2800	9.7	0.08
Cd	228.8	2400	7.0	0.15
Cr	357.9	2500	16.4	0.2
Er	400.8	3200	20.4	9
Ge	265.1	3250	20.4	500
Li	670.8	2500	7.0	0.1
Ni	232.0	2800	9.4	2.5
P	213.6	3300	2.7[b]	4500
Ti	364.3	3200	20.4	80
V	318.5	3000	20.4	14

[a]In 2.1 l Ar min^{-1}, 0.8 l H_2 min^{-1}. [b]With tungsten platform.

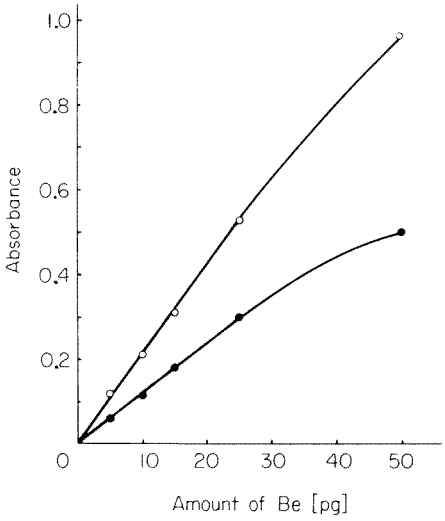

Fig. 7. Calibration graphs for beryllium: (•) Perkin-Elmer M-56 recorder; (○) storage oscilloscope. Heating rate 4.0 K ms^{-1}; atomization temp. 2800 K.

Conclusions

Based on this study, the following conclusions may be arrived at. The new design of the tungsten-tube furnace, work-head and power supply significantly improved the analytical performance and ease of manipulation of the system. A rapidly heated tungsten-tube atomizer with a temperature-feedback circuit represents an unusual system which enables very high heating rates (i.e., very high sensitivity) and nearly isothermal atomization conditions for most elements to be achieved by simpler means and at less cost than by capacitive discharge heating of anisotropic graphite tubes. Troubles encountered with atomization of analytes forming graphite—metal compounds of low volatility in graphite furnaces are readily overcome.

At present a new power supply designed specially for a metal-based atomizer is being tested in this laboratory. This power supply, with the work-head and tungsten tube described above will provide an electrothermal accessory (as an alternative to graphite-based furnaces) which can be used with any atomic absorption spectrometer designed for flame as well as for electrothermal operation.

REFERENCES

1 V. Sychra, D. Kolihová, Q. Vyskočilová, R. Hlaváč and P. Püschel, Anal. Chim. Acta, 105 (1979) 263.
2 G. Lundgren, L. Lundmark and G. Johansson, Anal. Chem., 46 (1974) 1028.
3 B. L'vov, Atomic Absorption Spectrochemical Analysis, Hilger, London, 1970.
4 E. Lundberg and W. Frech, Anal. Chim. Acta, 104 (1979) 75.
5 D. Siemer and H. Wei, Anal. Chem., 50 (1978) 147.

6 D. Siemer, Appl. Spectrosc., 33 (1979) 613.
7 F. D. Posma, H. C. Smit and A. F. Rooze, Anal. Chem., 47 (1975) 2087.
8 D. C. Gregoire, C. L. Chakrabarti and P. C. Bertels, Anal. Chem., 50 (1978) 1730.
9 B. V. L'vov, Spectrochim. Acta, B, 33 (1978) 153.
10 C. L. Chakrabarti, H. A. Hamed, C. C. Wan, W. C. Li, P. C. Bertels, D. C. Gregoire and S. Lee, Anal. Chem., 52 (1980) 167.
11 D. Siemer and J. M. Baldwin, Anal. Chem., 52 (1980) 295.
12 E. Lundberg, Chem. Instrum., 8 (1978) 197.
13 O. Vyskočilová, V. Sychra and D. Kolihová, Anal. Chim. Acta, 105 (1979) 271.
14 D. C. Gregoire and C. L. Chakrabarti, Anal. Chem., 49 (1977) 2018.

Analytica Chimica Acta, 127 (1981) 121—133
Elsevier Scientific Publishing Company, Amsterdam — Printed in The Netherlands

HIGH FLOW-RATE CELLS FOR CONTINUOUS MONITORING OF LOW CONCENTRATIONS OF ELECTROACTIVE SPECIES BY POLAROGRAPHY AND STRIPPING VOLTAMMETRY AT THE STATIC MERCURY DROP ELECTRODE

A. M. BOND*, H. A. HUDSON and P. A. VAN DEN BOSCH
Division of Chemical and Physical Sciences, Deakin University, Waurn Ponds 3217, Victoria (Australia)
(Received 29th December 1980)

SUMMARY

A high-capacity flow-through cell which can be used at a maximum flow rate of 300 ml min^{-1} has been developed for continuous monitoring of electroactive substances. The cell is compatible with the recently developed static mercury drop electrode. Comparative studies with a cell employing a conventional dropping mercury electrode are described. A wide range of polarographic techniques is applied, and it is demonstrated that the static mercury drop electrode improves the limits of detection, that laminar flow conditions are essential for low noise levels of operation, and that solution flow through a sulphite bed is a more effective method of oxygen removal than nitrogen bubbling. The combination of a microprocessor-controlled polarographic system, static mercury drop electrode and high-volume flow cell is very versatile for the determination of trace levels of electroactive species in flow streams. Preliminary results on anodic stripping voltammetry in flow streams are reported.

The determination and continuous monitoring of low concentrations of inorganic and organic species is required frequently in process control, quality control and environmental chemistry. Polarographic and related electrochemical methods of analysis are well recognised as being applicable to the determination of a broad spectrum of inorganic species, fungicides, pharmaceuticals, pesticides, surfactants, etc. [1—9]. In principle, this technique, being of such wide use, should be extremely suitable for continuous monitoring of low concentrations of many species of importance in environmental and industrial chemistry.

Matsuda et al. [10] have studied thoroughly the theoretical aspects of a variety of shapes and configurations of solid electrodes in hydrodynamic voltammetry. Flow-through cells of low capacity using solid electrodes have received considerable attention [11—14] particularly for use as electrochemical detectors interfaced with high-performance liquid chromatography [15, 16]. Fleet and Little [17] have discussed the difficulties associated with solid electrodes in flow cells. The major problems are linked with maintaining a constant active surface area; adsorption, film formation, etc., all contribute to this problem, and cleaning of the electrodes and their maintenance are often difficult.

0003—2670/81/0000—0000/$02.50

By contrast, the dropping mercury electrode (DME) with its constantly renewed surface avoids many surface-related problems, and in general the surface area is highly reproducible. The DME has, of course, the same restrictions in flow cells as in quiet solutions, i.e., the accessible potential range and interference from oxygen reduction waves, the latter problem becoming more difficult with faster flow rates and very low concentrations. In addition, vibration or turbulence in flow cells can easily produce unsatisfactory performance; the higher the flow rates, the more relevant becomes the hydrodynamics.

Early work [18] showed that quantitative polarography in flowing systems was possible but, in view of the above difficulties with the DME, little work has been reported at very low concentration levels. More recent publications have been concerned with column effluents, e.g., from liquid chromatography [19, 20], or ion exchange [21, 22]. Such studies are characterized by very low flow rates and small volumes; oxygen is removed by an inert gas and the associated problems of oxygen are minimised by the separation achieved by the column [19]. Generally the current at a constant d.c. potential has been measured.

In other and more general applications of flow cells (e.g. small-volume injection analysis for proteins [23] where the specific attributes of a column are not involved), detection limits and oxygen problems are those normally associated with the polarographic method (see, e.g., [24—27]).

The use of modern techniques in flow-through cells, e.g., square-wave voltammetry at the DME [28], gives considerably improved limits of detection compared to conventional d.c. polarography. However, there has been little endeavour to exploit the higher sensitivities available with these more sophisticated methods and to discover the problems associated with the use of flow cells at very low concentrations.

Recently, a new kind of dropping mercury electrode, the so-called static mercury drop electrode, has been developed [29] and has considerable advantages in analytical work [30, 31]. In principle, this new concept in renewable surface mercury electrodes should be extremely valuable in continuous monitoring of electroactive species at high flow rates.

In the present study, the techniques of d.c., a.c. and pulse polarography and voltammetry at a conventional DME and at the newly developed static mercury drop electrode (SMDE) are examined at concentrations below 10^{-3} M, with high-volume flow rates under rigidly controlled flow concentrations. Additionally, the possible use of stripping voltammetry with the SMDE has been investigated under similar conditions. Different designs of cells, use of microprocessor-controlled instruments, removal of oxygen by degassing the stream with nitrogen or by passing through a bed of a sulphite salt are described. These techniques were applied to an aqueous solution (0.2 M NaCl at pH2) and to liquors of practical importance to industry, e.g., a nickel production liquor, industrial effluent and zinc sulphate electrolyte.

In industrial process control, rapid continuous monitoring of species is essential if corrective action for variations has to be made very rapidly. Also for the determination of trace constituents by off-line techniques, it is well recognised that sampling and storage of solutions are the source of many errors from contamination and chemical changes with time [32]. By using a continuous enclosed sampling system with fast flow rates interfaced with a sensitive microprocessor-controlled analytical technique, the above difficulties would be overcome. Fast flow rate with a large volume throughput, as in this work, enables a response time of less than 15 s to be obtained routinely. The SMDE allows ready interchange between polarography and stripping voltammetry and a cell design incorporating this electrode should provide optimum flexibility in addition to other advantages.

EXPERIMENTAL

Chemicals

All chemicals used were of analytical-reagent grade. Nitrogen was purified of oxygen by bubbling the gas stream through a train of gas scrubbers containing the following solutions in this sequence: purified distilled water, vanadium(II) solution, sodium hydroxide solution and purified distilled water. All standard solutions were prepared with high-purity water.

Instrumentation

Two polarographic systems were used. An EG & G PAR Model 174 Polarographic Analyser with appropriate interfaces enabled all polarographic techniques to be undertaken in their various forms. This instrument was used with either cell A or cell B (see below) and with either a conventional DME or the EG & G PAR Model 303 Static Mercury Drop Electrode. The second system was an EG & G PAR Model 374 Microprocessor-controlled instrument, which was used only with cell B and the SMDE. All stripping voltammetric work and some pulse experiments were done with this instrumentation.

A G.E.C.-Elliott rotameter Model 1100 with tube 2-D-150 measured nitrogen flow rates. Solution flow rates were measured directly by monitoring the volume passed per unit time.

Equipment

A schematic layout of the analytical system is shown in Fig. 1. A 50-W nylon centrifugal pump was used to circulate all the solutions. All the tubing used was polyethylene of 0.90 mm i.d. The sample for analysis was collected from the circulating solution by using a probe which projected into the centre of the flow. After collection and prior to reaching the polarographic cell, the sample solution was deoxygenated either by bubbling with nitrogen or by passing it through the sulphite bed. The nitrogen was introduced through a sintered glass frit placed at the bottom of a 250-ml separating funnel so that immediate mixing occurred with the ascending sample solu-

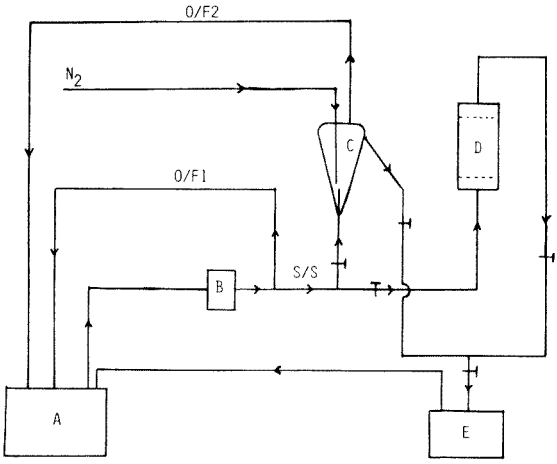

Fig. 1. Schematic diagram of the analytical system. The solution is stored in A. The pump B recycles this solution via an overflow pipe O/F1 from which a continuous sample stream S/S is withdrawn. By operating the appropriate valves, T, the sample can be deoxygenated either in vessel C by nitrogen gassing or directed through D, the sulphite bed. After oxygen removal, the sample is determined in E, the electrolytic cell, using whichever instrument and cell system is selected.

tion. The frit improved the contact area of nitrogen with the solution whereas the conical funnel increased the contact time.

The sulphite bed was prepared by compressing sodium sulphite in a cylinder (7 cm long, 2.5 cm i.d.). When necessary, the sulphite was purified by recrystallisation following electrolysis over a mercury pool to remove the metal ions being determined.

Finally, the deoxygenated stream entered either cell A or cell B for the measurement step. The flow rate of the stream to the polarographic cell was controlled by varying the fluid head above the cell entrance or more conveniently by using a teflon control valve. Ambient temperature (typically 16—20°C) was used throughout.

The type of fluid flow in the polarographic cells was examined visually by introducing a dye (methylene blue) just upstream of the entrance to the cell. Reynolds' numbers (Re) were calculated to verify the results of the observations.

Polarographic cells

Cell A. Figure 2 is a schematic diagram of cell A, which is basically a conventional cell with addition of an inlet and outlet placed so that a constant level of flowing solution is maintained. The inlet, outlet and DME are in the same vertical plane. The volume of solution in the cell during measurement is 30 ml. The reference electrode is Ag/AgCl (saturated KCl solution) and the auxiliary electrode was platinum wire. The flow through the cell must be laminar, to minimize any effects from turbulence.

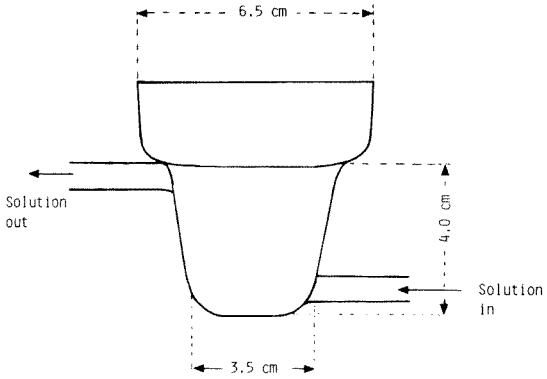

Fig. 2. Schematic diagram of continuous flow cell A.

This system was set up as a basis for comparison between the conventional DME and the SMDE. In contrast to the designs by Barnes and Metters [33] and Jura [34], it was shown that a sheath is unnecessary to protect the mercury drop in either of these new cell designs.

Cell B. Figure 3(a) is a photograph of this cell and Fig. 3(b) is a dimensioned schematic diagram. Cell B was designed to fit exactly the cell assembly of the Model 303 SMDE. A template for fabrication of this cell has been prepared and cells may be made available on request to the authors. The elliptical cell was specifically designed to ensure laminar flow at high flow rates and to prevent the development of a concentration profile. It is assumed that thorough mixing of the solution occurs upstream. On entry, the flow energy is dissipated by a baffle which also uniformly redirects the solution laterally, and then the solution passes through a narrow vertical slit to the electrode chamber. The slit assists in developing laminar flow conditions. The electrode cluster is situated at the widest section of the cell. The outlet is a mirror image of the inlet but the vertical slit is considerably wider in order to prevent any back-pressure, thus avoiding localised turbulence in the cell and ensuring the minimum time of residence of the solution in the cell. Cell capacity is 50 ml. Mercury is removed continuously from the cell floor via a small S bend.

POLAROGRAPHIC STUDIES

Flow rate characteristics under various polarographic conditions

From the point of view of calibration and simplicity of use, it is most convenient to achieve conditions where the limiting or peak currents in polarographic work are independent of flow rate. For example, Blaedel and Strohl [25] used a conventional DME with gravity-controlled drop time and the solution flowed through a very narrow bore tube. Under these circumstances the limiting current in d.c. polarography was a function of the flow

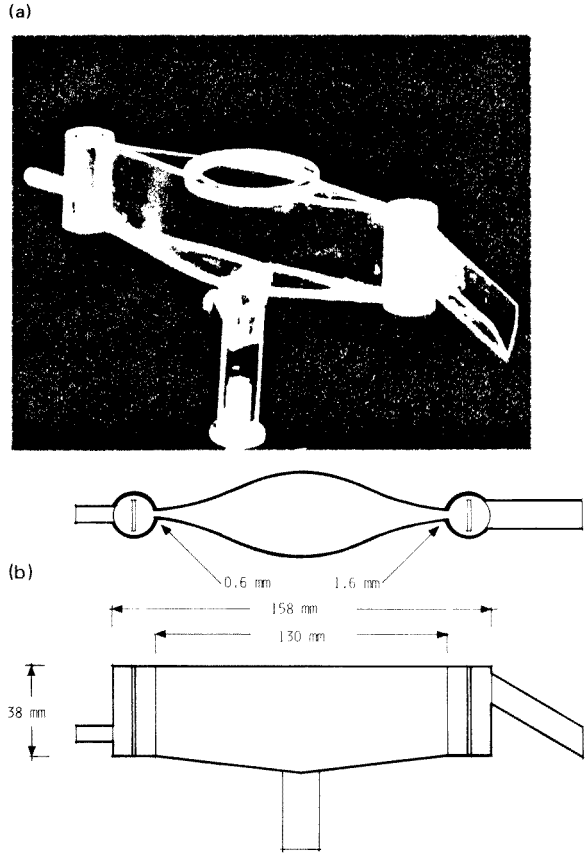

Fig. 3. (a) Photograph of continuous flow cell B; (b) schematic diagram of flow cell B.

rate and the internal diameter. In contrast, using a rapidly dropping mercury electrode and a considerably wider tube Tamamushi et al. [26] demonstrated an independence of the limiting current on flow rate at rates up to a linear velocity of 3 cm s^{-1} or an equivalent volume flow rate of 200 ml min^{-1}.

In view of the above results it appeared possible that, with the use of the DME with mechanically controlled drop time and a.c. and pulse techniques, it might be possible to provide results that are truly independent of flow rate over a wide range. The necessity that Blaedel and Strohl [24, 25] mention for precise control of flow rate if accurate results are required would thus be avoided. Table 1 presents data at various flow rates using a range of polarographic techniques for both cell A and cell B. Figure 4 shows some typical polarograms obtained with cell A and cell B.

With cell A, results are independent of flow rate up to 180 ml min^{-1}, i.e., results are the same as for the static sample solution for 10^{-4} M cadmium or lead concentration. With cell B, equivalence between the static and flowing

TABLE 1

Summary of results for cell A (DME) and cell B (SMDE) in 0.2 M NaCl (pH 2) with the PAR 174 instrument

Conc. (M)	Cell	Method[a]	Current at 0 ml min^{-1} (nA)	Current at max. flow (nA)	Flow range (ml min^{-1})	Average flow increment (ml min^{-1})	No. of runs	Mean current over flow range (nA)	
								$\bar{x}$	S.d.
Cadmium									
10^{-4}	A	D.c.	400	400	0—120	10	13	395	2.4
10^{-4}	A	D.p.p.	590	590	0—180	15	14	596	1.4
10^{-5}	A	S.d.c.	44	51	0—60	10	8	45	2.4
10^{-5}	A	D.p.p.	55	59	0—125	10	18	59	0.3
10^{-4}	B	S.d.c.	106	105	0—120	20	8	102	1.3
10^{-4}	B	D.p.p.	1540	1590	0—300	10	26	1580	7.4
10^{-5}	B	D.p.p.	159	161	0—260	10	22	159	0.4
Lead									
10^{-4}	B	D.p.p.	1490	1510	0—190	10	16	1510	3.4
10^{-5}	B	D.p.p.	154	157	0—180	15	13	155	0.6

[a]D.c., direct current polarography; s.d.c., sampled d.c. polarography; d.p.p., differential pulse polarography.

conditions was observed for flow rates up to 300 ml min^{-1} with respect to the faradaic current (peak height) in differential pulse polarography (d.p.p.). These results assume that the peak height in d.p.p. is obtained with reference to the more positive potential side of the peak. However, as can be seen in Fig. 5, the background current on the more negative side of the peak varies with flow rate, and the direction of variation differs with cells A and B. This distortion appears to have its origin in the d.c. terms which contribute to the more negative potentials in d.p.p. [29—31]. Distortion terms are known to be in opposite directions with the DME and SMDE [29—31]. Whether the origin of this distortion arises from electroactive impurities, charging current or combinations thereof is not clear. However, provided that the above-mentioned method of measurement is used, no difficulty arises with respect to flow rate in d.p.p.

The use of high flow rates (e.g., 330 ml min^{-1}) introduces considerable noise into the readout. Examination of the cell flow pattern using methylene blue demonstrated that the introduction of significant noise at the 10^{-4} M concentration level coincided with departure from laminar flow and onset of localised turbulence. Other cell designs (not reported here) showed departure from laminar flow at much lower flow rates with a concomitant increase in noise. The critical aspect of cell design with respect to noise characteristics is therefore associated with maintenance of laminar flow.

In view of the ability to achieve the same result with the flow cell as with

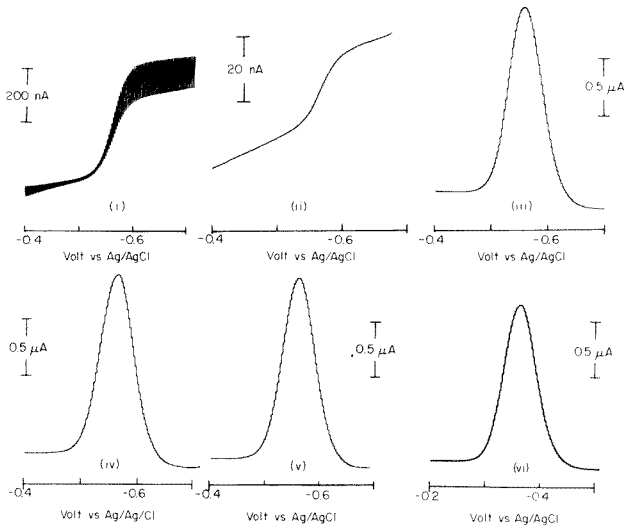

Fig. 4. Typical polarograms obtained with cell A and cell B.
Technique: (i) d.c.; (ii) s.d.c.; (iii)—(vi) d.p.p.
Cell: (i), (ii) cell A; (iii)—(vi) cell B.
Flow rate (ml min^{-1}): (i) 60; (ii) 55; (iii) 100; (iv) 200; (v) 300; (vi) 115.
Concentration: (i), (iii)—(v) 10^{-4} M Cd; (ii) 10^{-5} M Cd; (vi) 10^{-4} M Pb.
Drop time (s): (i), (iii)—(vi), 0.5; (ii) 1.
Scan rate (mV s^{-1}): (ii) 2; (i), (iii)—(vi), 5.
Modulation amplitude (mV): (iii)—(vi), 50.
Abbreviations as for Table 1.

the static situation, limits of detection and performance of the polarographic methods should in principle be identical to those normally associated with the various polarographic techniques. Therefore, not surprisingly, it was found that the limits of detection are lower with the SMDE than the conventional DME because of the more favourable faradaic to charging current ratio [29, 30]. For each of lead, cadmium and zinc in 0.2 M NaCl solution, approximately 10^{-7} M detection limits can be obtained with d.c., a.c., differential pulse and pulse polarographic and fast sweep methods at the SMDE in cell B. At the conventional DME with cell A this same limit of detection could be achieved with the differential pulse mode, but not other techniques; clearly cell B is to be preferred and all future discussion applies only to the cell B system.

Removal of oxygen

All the above results are contingent upon removal of oxygen. With concentrations of species below 10^{-5} M, the presence of oxygen can be critical in determining performance. Deoxygenating by nitrogen bubbling is imperfect at fast flow rates, particularly in determinations of species like zinc in which the peak position becomes confused by an oxygen reduction wave (see Fig. 6).

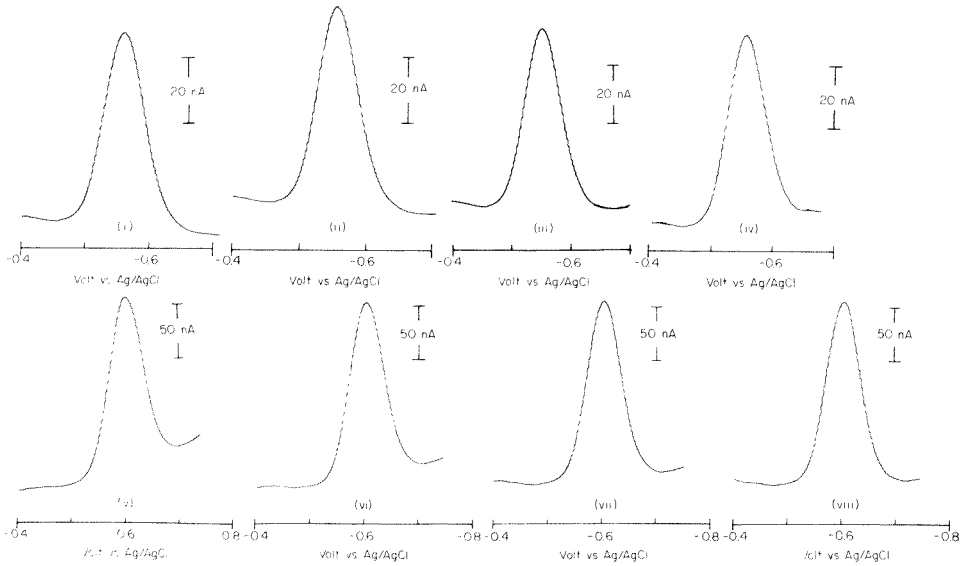

Fig. 5. Changes in background current with flow rate: d.p.p. at the conventional DME in cell A at flow rates of (i) 0, (ii) 55, (iii) 80, and (iv) 100 ml min^{-1}; and at the SMDE in cell B at flow rates of (v) 0, (vi) 30, (vii) 70, and (viii) 140 ml min^{-1}. Solution was 10^{-5} M Cd in 0.2 M NaCl (pH 2). Other experimental conditions in d.p.p. as for Fig. 4.

A similar situation occurs with copper although for cadmium the problem is not so significant.

With concentrations below 10^{-5} M, to the limit of detection, the use of a compressed sulphite bed proved to be a superior approach to the problem of oxygen removal. Dissolution of the sulphite bed occurred slowly and the sulphite and sulphate ions introduced into the solutions caused slight negative shifts of the wave positions (E_p or $E_{1/2}$). Figure 6(b) shows the improvement offered with the sulphite method. The sulphite bed has to be replaced periodically but this needs to be compared with the replacement of a nitrogen cylinder. The only disadvantage of using the sulphite bed is the possibility of introducing contamination. Problems with the removal of oxygen for trace polarographic analysis have been discussed [35], while Hanekamp et al. [36] have designed an electrochemical scrubber to remove oxygen. Historically, sulphite is a long-recognised scavenger of oxygen, and was one of the earliest methods used to remove oxygen in polarography [37]. The sulphite bed method does not appear to have been used previously in flow cells, but has proved very useful here for the efficient and rapid removal of oxygen.

Cell response

One aspect of the cell response is governed by the length of the path from the sampling probe to the polarographic cell. For example, with a flow rate of 200 ml min^{-1}, there was a 15-s delay time between concentration changes

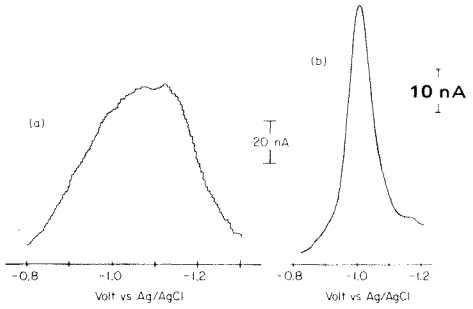

Fig. 6. Determination of zinc in the presence and absence of oxygen: (a) oxygen reduction masking zinc wave; (b) zinc wave with a sulphite bed to remove oxygen. 10^{-5} M Zn; flow rate 100 ml min^{-1} in cell B; instrument and other conditions as for d.p.p. in Fig. 4.

in the stream and polarographic detection. Obviously the time lag would be decreased by shortening the flow path.

With the wide variety of detection methods available, many kinds of response can be obtained. For example, monitoring of the d.c.p. limiting current as a function of time with the SMDE has restricted use in the sense that it will rarely be specific for a particular species, while measuring the current at a peak potential as in a.c. or d.p.p. methods may permit highly selective detection of a given species. Alternatively, the use of repetitive rapid scanning provides the required information as, for example, in the square-wave technique described by Wang et al. [28].

Reproducibility and calibration

Table 2 provides data to show the excellent reproducibility of results obtained with the flow-through cells under various conditions. Because of the close correlation between results obtained in the flowing system and the standard procedure, calibration using cells A and B can be undertaken in the static mode.

TABLE 2

Reproducibility at different concentrations and flow rates with d.p.p.[a]

Ion	Conc. (M)	Cell	Flow rate (ml min^{-1})	No. of runs	Mean current (nA)	
					$\bar{x}$	S.d.
Cd	10^{-5}	A	30	21	58	0.1
	10^{-5}	A	80	10	60	0.3
	10^{-4}	B	80	16	1590	7.8
	10^{-4}	B	200	19	1590	5.8
	10^{-5}	B	110	14	159	0.6
Pb	10^{-4}	B	160	12	1520	2.6

[a]System and abbreviations as in Table 1.

When the microprocessor-controlled system is used, the sample flow can be stopped at a given time and the analytical result at that point stored in memory. Standard additions can be made and manipulation of the results produces a calibration curve which can be used for subsequent determinations. Any of the accepted methods of calibration can be used with cell B.

STRIPPING VOLTAMMETRY

The application of anodic stripping voltammetry (a.s.v.) to a flowing electrolyte involves consideration of the dependence of peak height on flow rate and of the fact that the concentration found is an average taken over the deposition time.

Because of the dependence of the a.s.v. response on flow rate (Table 3), the system has to be calibrated under conditions equivalent to the sample solutions. This is readily achieved by connecting the outlet of the cell through a small pump to the inlet of the cell, and spiking the solution in the known volume of this closed-circuit flow system. A suitable rotameter can be included in the circuit to monitor the flow rate and ensure constancy of flow. Experiments with dyes can be used to determine the time taken to produce uniform conditions. The spiking is easily carried out via the port provided in the Model 303 SMDE unit. Lead, cadmium or zinc in a 0.2 M NaCl solution could be determined to the 10^{-9} M level by d.p.a.s.v. in the flowing system.

INDUSTRIAL APPLICATIONS

The flow cell (B) performed very well for the determination of Cd, Cu, Pb and Zn in industrial liquors. The electrolytic production of zinc requires that the concentrations of trace elements be continuously monitored. Elements reduced at more positive potentials than zinc decrease the current efficiency of the electrolytic cells, even very low concentrations causing significant cost problems [38]. Flow cell B in the microprocessor-controlled format was

TABLE 3

Variation of d.p.a.s.v. peak position and current with flow rate measured with the PAR 374 system, SMDE and cell B[a]

	Flow rate (ml min^{-1})	Peak position (V)	Peak current (nA)
10^{-7} M Cd	0	−0.608	230
	90	−0.610	450
	100	−0.610	530
	120	−0.610	560

[a]Deposition time 120 s; deposition potential −0.9 V; modulation amplitude 50 mV; duration between pulses 1 s. Solution was 0.2 M NaCl, pH 2.

used successfully with a zinc plant electrolyte. Studies with a synthetic nickel plant electrolyte which included a very fine pulp were equally successful, particularly as deposition of the suspension did not occur at a flow rate of 100 ml min^{-1} and the particulate matter did not interfere with the determination of copper and lead.

CONCLUSIONS

A wide range of cell designs and polarographic techniques were examined for the DME and SMDE, and two methods for the removal of oxygen were tested. It was confirmed that the use of the SMDE provides considerably improved limits of detection. Laminar flow conditions are an important feature of cell design for low-noise operation. The sulphite bed method for the removal of oxygen is more efficient than the commonly used nitrogen bubbling. The use of d.c., a.c. and pulse polarographic methods offer their well known advantages under the operating conditions described here because static and flow results proved to be essentially identical. With the SMDE, stripping voltammetry for the determination of very low concentrations of species can be used.

The value of flow cell B is that continuous monitoring should be possible for many electrochemically active species present in trace quantities in solution. The cell should have distinct advantages in the determination of significant species in natural waters and in on-line analysis for industries using electrolytes.

The financial contribution of the Australian Research Grants Commission in support of this work is gratefully acknowledged.

REFERENCES

1 T. M. Florence, J. Electroanal. Chem., 35 (1972) 237.
2 A. M. Bond, Modern Polarographic Techniques in Analytical Chemistry, M. Dekker, New York, 1980.
3 M. R. Smyth and J. G. Osteryoung, Anal. Chem., 50 (1978) 1632.
4 J. P. Hart, W. F. Smyth and B. J. Birch, Proc. Anal. Div. Chem. Soc., Nov. (1976) 336.
5 G. Gillain, G. Duyckaerts and A. Disteche, Anal. Chim. Acta, 106 (1979) 23.
6 W. Lund and R. Eriksen, Anal. Chim. Acta, 107 (1979) 37.
7 M. A. Brooks, J. A. F. de Silva and M. R. Hackman, Anal. Chim. Acta, 64 (1973) 165.
8 J. B. Flato, Anal. Chem., 44 (1972) 75A.
9 W. Purdy, Chemtech., 8 (1978) 436.
10 K. Tokuda and H. Matsuda, J. Electroanal. Chem., 79 (1977) 237, and references therein.
11 O. H. Müller, J. Am. Chem. Soc., 69 (1947) 2992.
12 W. J. Blaedel and S. L. Boyer, Anal. Chem., 43 (1971) 1538, and references therein.
13 W. J. Blaedel and J. Wang, Anal. Chem., 51 (1979) 1724, and references therein.
14 A. N. Strohl and D. J. Curran, Anal. Chem., 51 (1979) 1050.
15 P. T. Kissinger, C. Refshauge, R. Dreiling and R. N. Adams, Anal. Lett., 6 (1973) 465.
16 A. MacDonald and P. D. Duke, J. Chromatogr., 83 (1973) 331.

17 B. Fleet and C. J. Little, J. Chromatogr. Sci., 12 (1974) 747.
18 L. D. Wilson and R. J. Smith, Anal. Chem., 25 (1953) 218.
19 J. G. Koen, J. F. K. Huber, H. Poppe and G. den Boef, J. Chromatogr. Sci., 8 (1970) 192.
20 W. J. Blaedel and J. W. Todd, Anal. Chem., 30 (1958) 1821.
21 R. L. Rebertus, R. J. Cappell and G. W. Bond, Anal. Chem., 30 (1958) 1825.
22 C. K. Mann, Anal. Chem., 29 (1957) 1385.
23. P. W. Alexander and M. H. Shah, Talanta, 26 (1979) 97.
24 W. J. Blaedel and J. H. Strohl, Anal. Chem., 33 (1961) 1631.
25 W. J. Blaedel and J. H. Strohl, Anal. Chem., 36 (1964) 445.
26 R. Tamamushi, S. Momiyama and N. Tanaka, Anal. Chim. Acta, 23 (1960) 585.
27 H. W. Bertram, M. W. Lerner, G. J. Petretic, E. S. Roszkowski and C. J. Rodden, Anal. Chem., 30 (1958) 354.
28 J. Wang, E. Ouziel, Ch. Yarnitzky and M. Ariel, Anal. Chim. Acta, 102 (1978) 99.
29 W. M. Peterson, Am. Lab., 11, Dec. (1979) 69.
30 A. M. Bond and R. D. Jones, Anal. Chim. Acta, 121 (1980) 1.
31 J. E. Anderson, A. M. Bond and R. D. Jones, Anal. Chem., submitted for publication.
32 See, e.g., G. E. Batley and D. Gardner, Water Res., 11 (1977) 745.
33 D. Barnes and C. H. Metters, U.S. Patent 4,138,322 (1979).
34 W. H. Jura, Anal. Chem., 26 (1954) 1121.
35 A. M. Bond and B. S. Grabaric, Anal. Chem., 51 (1979) 337.
36 H. B. Hanekamp, W. H. Voogt, P. Bos and R. W. Frei, Anal. Chim. Acta, 118 (1980) 81.
37 J. Heyrovsky and J. Kuta, Principles of Polarography, Academic Press, New York, 1966.
38 E. S. Pilkington, C. Weeks and A. M. Bond, Anal. Chem., 48 (1976) 1665.

Analytica Chimica Acta, 127 (1981) 135—145
Elsevier Scientific Publishing Company, Amsterdam — Printed in The Netherlands

REMOVAL OF INTERFERENCE IN THE DIFFERENTIAL PULSE POLAROGRAPHIC DETERMINATION OF PROGESTOGENS IN SOME COMBINED LOW-DOSAGE ORAL CONTRACEPTIVES

A. M. BOND* and I. D. HERITAGE

Division of Chemical and Physical Sciences, Deakin University, Waurn Ponds 3217, Victoria (Australia)

M. H. BRIGGS

Division of Biological and Health Sciences, Deakin University, Waurn Ponds 3217, Victoria (Australia)

(Received 10th December 1980)

SUMMARY

Previously published differential pulse methods for the determination of certain progestogens (laevonorgestrel and norethisterone) are not applicable to combined low-dosage oral contraceptives because interference from excipients in the tablets completely eliminates the polarographic response. An ultrafiltration device allows rapid prior extraction of the interfering substances before the polarographic determination in 50% (v/v) methanol—phosphate buffer (pH 6.0). Recoveries of 100 ± 1% were obtained by the recommended method, and data for a range of formulations are in excellent agreement with expected values. Electrode characteristics of the progestogens and interfering substances are reported, based on studies employing cyclic voltammetry at a hanging mercury drop electrode, a.c. polarography and normal pulse polarography. Competitive adsorption processes seem to occur when the progestogen and excipients are simultaneously present.

Oral contraceptives are widely prescribed and consequently, considerable interest has been displayed in their determination [1]. The combined form of low-dosage oral contraceptives, whose prescription is currently most popular, has as its active constituents two different classes of synthetic steroid hormones, namely a progestogen, norethisterone (I; 17α-ethynyl-17-hydroxy-4-oestren-3-one) or laevonorgestrel (II;d-17α-ethynyl-17β-hydroxy-13-ethyl-4-gonen-3-one), and an oestrogen, ethynyl oestradiol (III; 17α-ethynyl-1,3,5(10)-oestratriene-3,17β-diol).

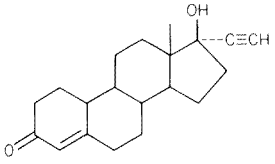

(I)

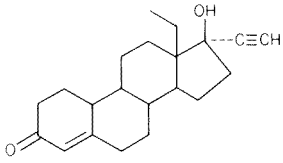

(II)

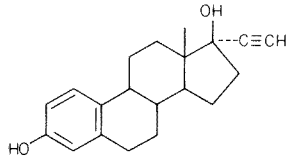

(III)

The most frequently used methods of analysis for contraceptive steroids in

pharmaceutical formulations are based on absorption in the u.v.-visible spectrum of both natural and derivatized steroids [1].

Polarographic determinations of certain steroids are possible because of the electroreducible conjugated carbonyl group contained in the "A" ring of steroids, such as laevonorgestrel. Brezina and Zuman [2] studied the behaviour of deoxycorticosterone and related compounds. Kabaskalian et al. [3] demonstrated the applicability of polarography for the determination of mixtures of two corticosteroids, prednisone and cortisone. Cohen [4] studied the polarographic reduction of a number of Δ^4-3-ketosteroids and characterized their polarographic behaviour according to structure. In an extensive survey, De Boer et al. [5—8] have examined the electroanalytical properties of a wide range of corticosteroids and then determined them in pharmaceutical preparations. Other polarographic data are available on the determination of steroids [9—11]. All authors [2—11] have reported an analytically useful polarographic response for steroids containing a conjugated carbonyl group at the carbon-3 position of the A ring.

Chatten et al. [10] developed a polarographic method for the determination of certain progestogens in various oral contraceptives. They used differential pulse polarography to determine the progestogenic component of the various formulations in (buffered) ethanol or dimethylformamide solutions. The progestogenic content in these formulations ranged from 0.5 mg to 25 mg per tablet and the results reported were the average of 20 tablets. Opheim [9] described the determination of norethisterone in oral contraceptive pills at the mg per tablet level. Interference from the excipients was noted, and unless the standard sample method was used results were suspect; the method of standard additions was not in agreement with the standard sample method. Clearly, the determination of progestogens in oral contraceptives even at relatively high levels can be prone to subtle forms of interference.

The use of oral contraceptives has been associated with a number of adverse side effects including hypertension and thrombo-embolic disorders, which appear to be dosage related. Low-dosage oral contraceptives, of the combined and single-component types, have been developed in response to the normal pharmaceutical rationale that the lowest effective dose is advisable. The development of combined low-dosage oral contraceptives (CLDOC) and the dosage relationship to side effects has seen the widespread use of CLDOC. The typical progestogen content in such tablets marketed at this time is 150 μg per tablet, which is substantially less than that used when Chatten et al. [10] examined the use of the polarographic technique. Problems encountered in determining low concentrations may render methods developed for high concentrations invalid, and this occurs in this instance. Indeed, no polarographic response is observed and interferences occurring with the existing method for high-dosage tablets are catastrophic when applied to CLDOC. In view of the above, the development of an interference-free quantitative polarographic method for the determination of the progestogen content of CLDOC was considered desirable. During the course of this study,

various techniques such as direct current, differential pulse, normal pulse and alternating current polarography as well as cyclic voltammetry were used in an attempt to characterize the electroreduction of the progestogens considered. The techniques were also used to elucidate the action of the interference observed in extracts of the CLDOC tablets.

EXPERIMENTAL

Reagents and standard solutions

All chemicals used were of analytical grade unless otherwise stated. Standard solutions of each steroid were prepared by dissolving appropriate amounts of steroid in methanol. Pure steroids used in preparation of the standard solutions were obtained from the sources cited in the acknowledgements. Their purity was confirmed by reverse-phase liquid chromatography employing u.v. detection. Phosphate buffer (pH 6.0, 0.2 M) was prepared in distilled water [12].

Instrumentation

Polarographic determinations were performed with a Princeton Applied Research (PAR) Model 174 Polarographic Analyzer. The three-electrode system comprised a dropping mercury electrode (d.m.e.) of flow rate 0.9 mg s^{-1}, a Ag/AgCl (saturated NaCl) reference electrode and a platinum wire auxiliary electrode. Controlled drop times, below those available with the PAR Model 174 instrument, were achieved with the use of a digital drop time [13].

Cyclic voltammograms, at a hanging mercury drop electrode, were performed by interfacing the PAR Model 174 with a PAR Model 175 Universal Programmer. For potential scan rates above 500 mV s^{-1}, the voltammograms were recorded with a storage oscilloscope, otherwise an x-y recorder was used. Variable pulse width experiments, in the normal pulse mode, were obtained using a microprocessor-based wave form generator [14]. Data were collected with a microprocessor-based acquisition system [15] and subsequently displayed on an x-y recorder using the transient recorder features of the microprocessor system. Alternating current polarography was performed at the d.m.e. using the system described elsewhere [16]. Test solutions were maintained at 25 ± 0.5°C by using a water-jacketed, 10-ml polarographic cell. Sequential extraction was performed in a Millipore (type XX42 013 10) ultrafiltration vessel, with a Millipore FH filter (0.5 μm pore size).

Procedure for progestogens

Extraction. A single tablet was placed in the Millipore ultrafiltration vessel and 2 ml of distilled water was added. The tablet disintegrated on stirring and the slurry was filtered under pressure. The tablet residue was washed and subsequently filtered with a further 1 ml of distilled water and both filtrates were discarded.

To the residue from this extraction was added 3 ml of methanol, and the solution was stirred for 30 min, during which period, the contents of the cell were warmed to about 55°C. The methanol was then filtered from the cell and collected. A further 2 ml of methanol was added, in 1-ml lots, to the cell. These solutions were stirred for 5 min each, filtered and pooled with the other filtrate, which was then made up to a total volume of 5 ml with methanol.

Polarography. To the 5 ml of methanol extract was added 5 ml of 0.2 M phosphate buffer (pH 6.0). The resulting solution was transferred to the polarographic cell and purged with high-purity nitrogen for 15 min. During the measurements, the surface of this test solution was blanketed with the nitrogen. Differential pulse polarography was applied with a scan rate of 2 mV s^{-1}, a drop time of 1 s and a pulse modulation amplitude of −50 mV.

Standard addition curves were obtained by measuring the peak height of the test solution and then plotting the peak heights obtained after standard additions to the same solution. Standard addition volumes were typically 50 μl delivered with a 50-μl Hamilton piston microburette.

RESULTS AND DISCUSSION

Determination of components of oral contraceptives

After extensive investigation of various combinations of buffer and solvent with pure steroids, the medium chosen for the polarographic study of the CLDOC was 0.1 M phosphate buffer pH 6.0—0.50% (v/v) methanol. Linear peak height vs. concentration plots were obtained by differential pulse polarography (d.p.p) for these steroids in the range 10^{-6}—10^{-3} M. Figure 1 shows a typical d.p.p. response of laevonorgestrel in this medium. Other polarographic techniques such as d.c., a.c., normal pulse and linear sweep were inferior to d.p.p. D.p.p. was therefore used exclusively in all quantitative work.

The extraction procedure described by Chatten et al. [10] was used in initial experiments for the single tablet determination of the CLDOC Microgynon 30, which according to the manufacturer contained 150 μg of laevonorgestrel per tablet; these tests produced disconcerting results. Attempted application of d.p.p. to this solution yielded no measurable response at either the expected potential or the current sensitivity values obtained from tests on standard solutions, or at any other accessible potential and current sensitivity. Furthermore, repeated standard additions of laevonorgestrel up to an amount in 10-fold excess of the expected value gave no measurable response. Identical results were obtained in the analytical medium finally chosen in this work as well as in a wide range of other buffer—solvent combinations.

These experiments indicated the presence of interfering compound(s) extracted from tablets that overwhelming interfered with the d.p.p. response. This is a catastrophic form of the interference noted by Opheim [9]. How-

ever, with no response, obviously neither the method of standard additions nor a standard sample can be applied and Opheim's method is inapplicable to CLDOC. Similar results were obtained for all the CLDOC studied. A precise description of the non-contraceptive components of the CLDOC tablets was unavailable. The interference could therefore not be identified directly and hence remedial action had to be essentially empirical in nature.

In the sequential extraction procedure developed in this work (see Experimental), the extraction of the interference was maximized whilst the loss of steroid was minimized. The criteria for this procedure were, first that both laevonorgestrel and norethisterone are virtually insoluble in distilled water at room temperature, and secondly that the response, after extraction, yielded quantitative results based on recoveries of pure steroids.

In view of this inherent matrix problem of unknown origin, the method of standard additions was employed for the determination of the steroids as an alternative to a calibration curve. Consistently low results were obtained when calibration curves were used. A notable feature of the standard addition d.p.p. data was the change in background current caused by subsequent additions of the steroid. This background change has significant analytical implications for measurement of the peak current. Peak current of an electroactive species is usually measured after subtraction of the current

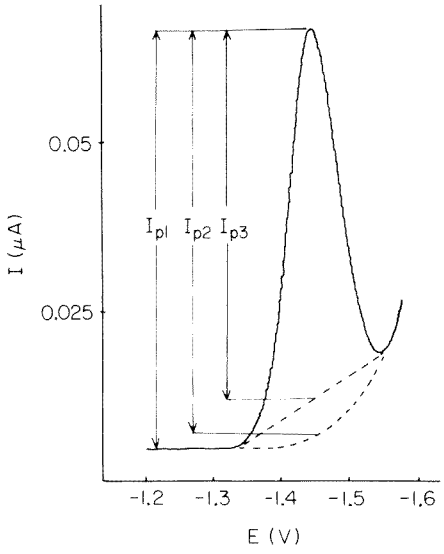

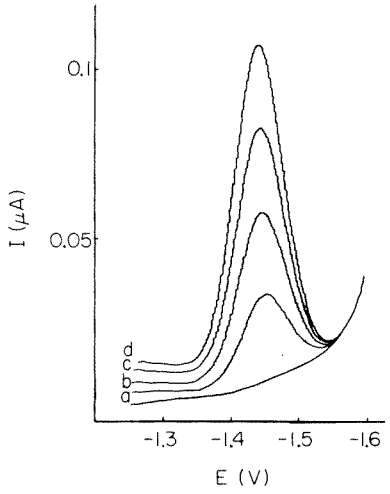

Fig. 1. D.p.p. of a 2×10^{-5} M solution of laevonorgestrel in 50% (v/v) methanol—0.1 M phosphate buffer (pH 6.0). Drop time 1 s; pulse amplitude —50 mV; temperature 25 ±0.5°C; scan rate 2 mV s^{-1}. Methods of peak (I_p) measurement are shown: (I_{p1}) measured from foot of wave; (I_{p2}) measured from background "fitting" technique; (I_{p3}) measured from straight-line approximation of background.

Fig. 2. Background change casued by additions of standard 50-μg amounts of laevonorgestrel: (a) 50 μg; (b) 100 μg; (c) 250 μg; (d) 200 μg. Experimental conditions as for Fig. 1.

arising from any overlapping electrochemical response. In the case in point, the reduction of both laevonorgestrel and norethisterone occurs in close proximity to the reduction of the supporting electrolyte medium (see Fig. 1). The contribution to the peak current of the steroids by this response is normally determined by (i) measuring the background current from the supporting electrolyte and subtracting (manually or electronically [17]) this response from each separately measured steroid response, or (ii) drawing a straight line from the foot of the wave to the inflection point so that the background current is approximated at the peak potential.

Figure 1 displays both methods applied to a typical response from a 2×10^{-5} M solution of laevonorgestrel. It is obvious that the first method of background subtraction is inherently more accurate for responses that are incompletely resolved from the background. The method of background fitting is, however, not applicable to the determination of laevonorgestrel (or norethisterone) because of the change in background observed on standard additions of these compounds (Fig. 2). A background curve could therefore not be fitted accurately to the subsequent polarogram of a steroid. The peak current was therefore measured from the foot of the reduction wave for both laevonorgestrel and norethisterone rather than by the usual approaches.

Ethynyl oestradiol (III), the other steroid component of the CLDOC was found to produce no measurable changes in either progestogen response. Five-fold quantities of this steroid still did not produce measurable changes in the responses and therefore correction for this steroid was unnecessary.

The procedure described was applied to a number of CLDOC formulations currently marketed. The results (Table 1) for laevonorgestrel- and norethisterone-containing tablets show reasonable agreement with the manufacturers' content descriptions and imply that this method is applicable to a range of progestogen content and types. The standard deviations quoted,

TABLE 1

Results for the progestogen content of various oral contraceptives

Brand name	Progestogen content stated (μg)	Mean result (μg)[a]	S.d. (μg)	R.s.d. (%)
Microgynon 30[b]	150[c]	146.0	1.5	1.0
Biphasil[d]	125[c]	121.4	2.7	2.2
Trinordiol[d]	125[c]	120.4	2.7	2.2
Trinordiol[d]	75[c]	74.5	2.1	2.8
Biphasil[d]	50[c]	49.0	3.4	6.9
Trinordiol[d]	50[c]	52.0	2.2	4.2
Brevinor-1[e]	1000[f]	985	15	1.5
Brevinor[e]	500[f]	480	12	2.5

[a]Average of 5 determinations. [b]Schering. [c]Laevonorgestrel. [d]Wyeth. [e]Syntex. [f]Norethisterone.

reflect not only instrumental and chemical parameters, but also the content uniformity since the analyses were done on single tablets.

The efficiency of the extraction procedure was determined by the following method. Ten tablets were finely pulverized and a sample, representative of 1 tablet, was taken and determined as before. Three similar samples were spiked with known amounts of laevonorgestrel (added volumetrically in methanol, followed by evaporation of methanol) and then subjected to the same measurement procedure. A standard addition plot was constructed and the extraction efficiency was determined to be 100 ± 1%. The use of a representative sample rather than one tablet is necessary to minimize any error caused by non-uniformity of the tablets.

Explanation of interference

In view of the considerable matrix problem encountered in this work and possibly generally present in steroid determinations [7—10, 18], an understanding of some of the features of the electrode process is essential as an aid to using the method systematically rather than empirically. In the present instance, a study was needed on the reduction process of both laevonorgestrel and norethisterone in the methanol/buffer medium used. From d.c. polarograms, the slopes of the linear plots of E vs. $\log i/(i_d - i)$ for laevonorgestrel and norethisterone were 61 and 56, respectively. These values together with the independence of $E_{1/2}$ on drop time for both steroids imply a Nernstian one-electron reversible charge transfer process.

The pH vs. $E_{1/2}$ dependence for both steroids was studied in 50% (v/v) methanolic buffer solutions. From the slope of the plots (approximately 65 mV) values of Z of approximately 1 were obtained for each steroid calculated from the equation $d(E_{1/2})/d(pH) = -(0.0592/n)Z$ where n is the number of electrons and Z the number of protons involved in the electrode process (apparent pH values were used for buffered methanol solutions). This result is in agreement with some earlier work on corticosteroids [2, 5] but not with other work [18].

Cyclic voltammograms were recorded at a hanging mercury drop with slow and fast scan rates (Fig. 3). Oxidation processes were not observed on reverse scans at scan rates less than 500 mV s^{-1}; this indicates that the reversible charge-transfer step is followed by an irreversible process such as dimerization [5, 19]. The single cycle scan at fast scan rates (Fig. 3, curve d) is indicative of adsorption of the reactant; the reduction peak is sharp and the oxidation on reverse scan is broad [17, 20]. The steady-state experiment (Fig. 3, curve e) shows a second wave on the cathodic scan; the implication is that two oxidation products from the anodic scan are reduced. In addition to indicating the presence of adsorption, the results for fast scan rates may suggest the existence of a chemically reversible couple with the product of the reaction decomposing rapidly in a very complicated manner.

Jacobsen and Korvald [18] showed that hydrocortisone was strongly adsorbed on the d.m.e. at the reduction potential of the steroid. The cyclic

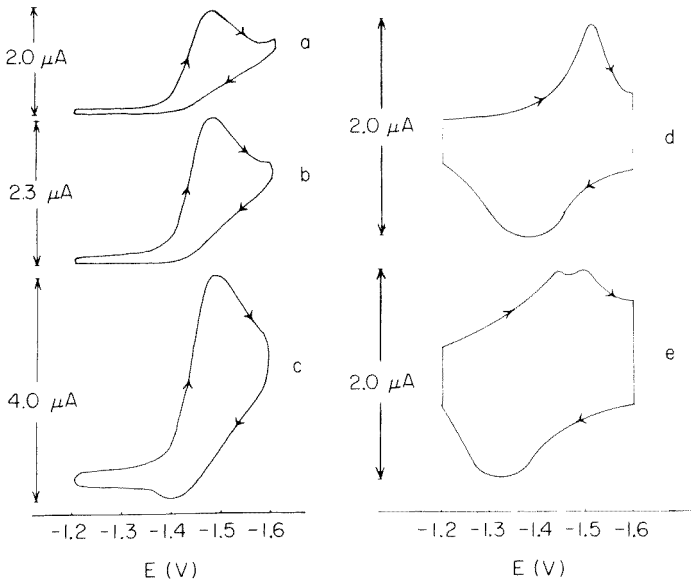

Fig. 3. Cyclic voltammograms at a hanging mercury drop electrode for a solution of laevonorgestrel in 50% (v/v) methanol—0.1 M phosphate buffer (pH 6.0) at 25 ± 0.5°C. Scan rates: (a) 100 mV s^{-1}; (b) 200 mV s^{-1}; (c) 500 mV s^{-1}; (d) 10 V s^{-1} (single cycle); (e) 10 V s^{-1} (steady state). Concentrations: a, b, c = 10^{-4} M; d, e = 10^{-5} M.

voltammetric experiments described here also indicate this feature. A.c. polarographic experiments were undertaken to confirm that adsorption of the progestogens occurred at the d.m.e. Figure 4 shows the a.c. polarograms for the supporting electrolyte and for laevonorgestrel. The presence of laevonorgestrel markedly lowers the background current which is definitive of strong reactant adsorption at the d.m.e. [21]. Similar results were obtained for norethisterone.

Normal pulse experiments were used as described by Flanagan et al. [22]. The normal pulse polarograms (Fig. 5) displayed maxima at pulse widths less than 40 ms. For reversible (Nernstian) reactions coupled with adsorption, the rate of reduction of adsorbed reactant at potentials in the vicinity of the standard potential is limited by the rate at which the reaction product can diffuse away from the electrode surface. As a result, an additional current, corresponding to reduction of the adsorbed reactant, appears. However, the size of the maxima on the normal pulse polarogram is enhanced as the sampling time decreases, as was observed by Flanagan et al. [22]. This enhancement was observed only at pulse widths below 40 ms; therefore the polarograms used analytically would not be expected to be subject to this problem, as the sampling time for the pulse component of the d.p.p. waveform generated by the PAR Model 174 is considerably longer than 40 ms. It is stressed, however, that whilst reactant adsorption of the steroids at the d.m.e. is evident from the results obtained by cyclic voltammetry,

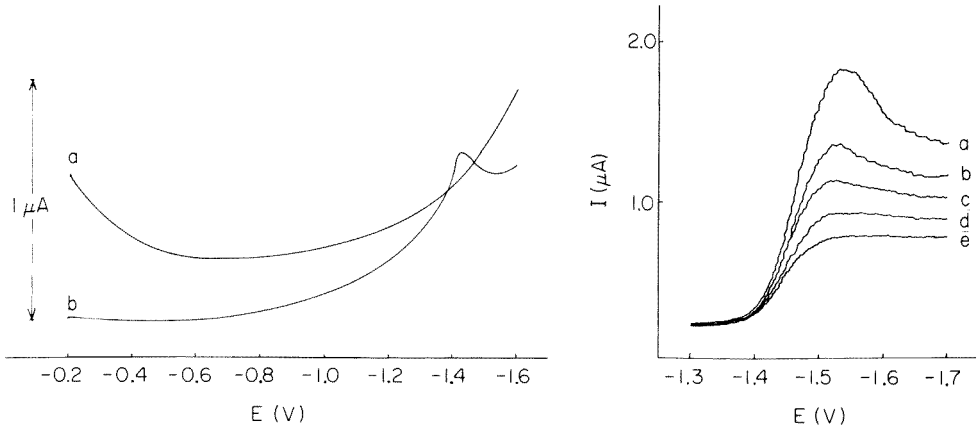

Fig. 4. Alternating current polarograms of: (a) supporting electrolyte (50% v/v methanol—0.1 M phosphate buffer pH 6.0); (b) laevonorgestrel (10 μg ml^{-1}) in supporting electrolyte. Conditions: 10 mV peak-peak at 200 Hz; drop time 1 s, 25 ± 0.5°C.

Fig. 5. Normal pulse polarograms of a 5 × 10^{-5} M solution of laevonorgestrel (50% v/v methanol—0.1 M phosphate buffer pH 6.0) at 25 ± 0.5°C. Scan rate 2 mV s^{-1}, drop time 1 s. Pulse width; (a) 10 ms; (b) 15 ms; (c) 20 ms; (d) 30 ms; (e) 40 ms.

a.c. polarography and normal pulse polarography, the peak current in d.p.p. is linearly proportional to concentration in the concentration range studied.

The above results clearly show that a very complex reaction mechanism occurs in the medium used analytically. The use of a range of techniques displays features observed in other media as previously described (5, 18—19). The one-electron, one-proton reduction mechanism involves the equilibria $S + e \rightleftharpoons S^{\cdot-}$ and $S^{\cdot-} + H^+ \rightleftharpoons S^{\cdot}H$, giving the overall reaction $S + H^+ + e \rightleftharpoons S^{\cdot}H$. This, however, is complicated by adsorption processes and instability of the product, all of which need to be accounted for in a definitive mechanism. Qualitatively, the electrode characteristics of analytical significance are available from the above data and enable the interference to be rationalized.

A small quantity (15% by volume of the distilled water extract) of the CLDOC Microgynon was found to reduce the d.p.p. response of a 10^{-5} M solution of laevonorgestrel under the standard analytical conditions employed. Addition of the complete extract eliminated the wave completely and the decrease in peak height was proportional to the quantity of extract added. The drop time under these conditions was 1 s, but when the drop time was decreased (Fig. 6) the laevonorgestrel response improved dramatically in contrast to normal expectation where the smaller electrode area would be expected to produce decreased currents. Alternating current polarograms of the supporting electrolyte containing the distilled water extract show a significant decrease in the background current after addition of the extract (Fig. 7). The reduction in background current occurred over the entire accessible potential range. These data indicate strong adsorption of an unknown substance on the d.m.e.

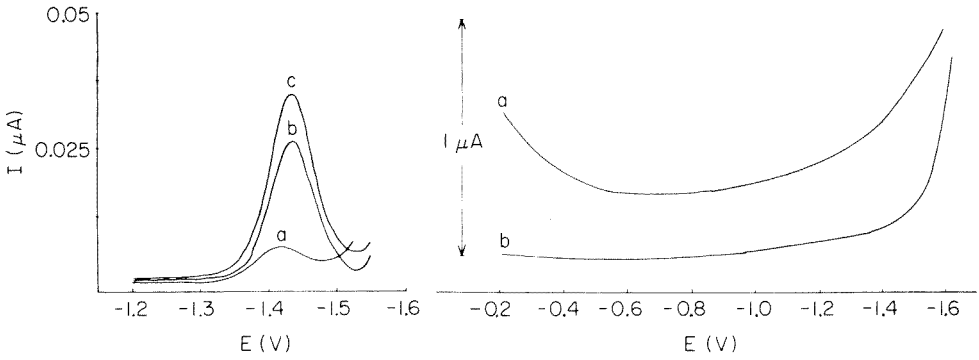

Fig. 6. Differential pulse polarographic response of a 10^{-5} M solution of laevonorgestrel in 50% v/v methanol—phosphate buffer pH 6.0 with 15% by volume of distilled water extract of CLDOC tablet. Scan rate 2 mV s^{-1}; pulse amplitude —50 mV. Drop time: (a) 1; (b) 0.5 s; (c) 0.3 s.

Fig. 7. Alternating current polarograms of: (a) 50% (v/v) methanol—0.1 M phosphate buffer pH 6.0; (b) this solution +15% by volume of distilled water extract from CLDOC tablet. Experimental conditions as for Fig. 4.

The results described above indicate that the interference arises from surface adsorption of a surfactant onto the d.m.e. which interferes with the required electrode process. As the steroid being determined is also adsorbed, a competitive interaction must occur. Kinetics of adsorption of the unknown interferent are presumably important because at short drop times the effect is minimized. Hydrocortisone cannot be determined in the presence of the surfactant, polyethyleneglycol [18]. The determination of steroids via calibration curves on solutions of unknown matrix therefore seems fraught with danger, and in general the method of standard additions is strongly recommended in all analytical work.

The authors gratefully acknowledge the assistance of J. E. Anderson and R. D. Jones in some of the experimental work. Discussion with T. G. Watson in the early stages of the work is also appreciated. Samples of pure steroids were generously donated by Schering and Wyeth International. Financial assistance was provided by the Australian Research Grants Committee, Schering and Wyeth International.

REFERENCES

1 S. Gorog and G. Szasz, Analysis of Steroid Hormone Drugs, Akademia Kiado, Budapest, 1978.
2 M. Brezina and P. Zuman, Polarography in Medicine, Biochemistry and Pharmacy, Interscience, New York, 1958; and references cited therein.
3 P. Kabaskalian, S. DeLorenzo and J. McGlotten, Anal. Chem., 28 (1956) 1669.
4 A. I. Cohen, Anal. Chem., 35 (1963) 128.
5 H. S. de Boer, J. den Hartigh, H. Ploegmakers and W. van Oort, Anal. Chim. Acta, 102 (1978) 141.

6 H. S. de Boer, P. H. Lansaat and W. J. van Oort, Anal. Chim. Acta, 108 (1979) 389.
7 H. S. de Boer, P. H. Lansaat, K. R. Kooistra and W. J. van Oort, Anal. Chim. Acta, 111 (1979) 275.
8 H. S. de Boer, P. H. Lansaat and W. J. van Oort, Anal. Chim. Acta, 116 (1980) 69.
9 L. N. Opheim, Anal. Chim. Acta, 89 (1977) 225.
10 L. Chatten, N. Y. Ram, S. Binnington and R. Moskalyk, Analyst, 102 (1977) 323.
11 B. Z. Chowdhry, in W. Franklin Smyth (Ed.), Polarography of Molecules of Biological Significance, Academic Press, London, 1979, pp. 173—175.
12 S. P. L. Sørensen, Biochem. Z., 21 (1909) 131.
13 A. M. Bond and R. J. O'Halloran, J. Electroanal. Chem., 68 (1976) 257.
14 A. M. Bond and A. Norris, Anal. Chem., 52 (1980) 367.
15 J. E. Anderson, R. N. Bagchi, A. M. Bond, H. G. Greenhill, T. L. Henderson and F. L. Walter, Int. Lab., Nov. (1980) 35.
16 A. M. Bond and R. J. O'Halloran, Anal. Chem., 47 (1975) 1906.
17 A. M. Bond, Modern Polarographic Methods in Analytical Chemistry, M. Dekker, New York, 1980.
18 E. Jacobsen and B. Korvald, Anal. Chim. Acta, 99 (1978) 255.
19 P. Kabaskalian and J. McGlotten, J. Am. Chem. Soc., 78 (1956) 5032.
20 R. H. Wopschall and I. Shain, Anal. Chem., 39 (1967) 1514.
21 B. Breyer and H. Bauer, Chemical Analysis, Vol. 13. Alternating Current Polarography and Tensammetry, Interscience, New York, 1963.
22 J. Flanagan, K. Takahashi and F. Anson, J. Electroanal. Chem., 85 (1977) 257.

Analytica Chimica Acta, 127 (1981) 147—156
Elsevier Scientific Publishing Company, Amsterdam — Printed in The Netherlands

COMPUTERIZED POTENTIOMETRIC STRIPPING ANALYSIS FOR THE DETERMINATION OF CADMIUM, LEAD, COPPER AND ZINC IN BIOLOGICAL MATERIALS

LARS-GÖRAN DANIELSSON, DANIEL JAGNER*, MATS JOSEFSON and STIG WESTERLUND

Department of Analytical and Marine Chemistry, Chalmers University of Technology and University of Göteborg, S-412 96 Göteborg (Sweden)

(Received 10th February 1981)

SUMMARY

Two different types of tinned mussels and a bovine liver reference sample have been analyzed for Zn, Cd, Pb and Cu by means of computerized potentiometric stripping analysis and atomic absorption spectrometry. The samples were digested by two different procedures, one employing nitric acid only and the other employing nitric and perchloric acids. It is shown that computerized stripping analysis can be used in samples containing high concentrations of electroactive organic nitro compounds, without sample deoxygenation.

Potentiometric stripping analysis [1—4] is an electroanalytical technique in which the trace metal analytes are pre-concentrated by potentiostatic deposition on a glassy carbon electrode coated with a mercury film, according to $M^{n+} + ne^- \rightarrow M(Hg)$. After this pre-concentration, the potentiostatic circuitry is disconnected and the amalgamated elements are re-oxidized: $M(Hg) \xrightarrow{\text{oxidant}} M^{n+}$; the oxidant is transported at constant rate to the electrode surface by means of constant rate stirring and diffusion control. During re-oxidation (stripping), the potential of the glassy carbon/mercury film electrode is monitored on a strip-chart recorder. The potential vs. time curve thus recorded has the form of a redox titration curve superimposed on a background curve. The sample may contain an oxidant, or oxidants, which vary in nature from one kind of sample to another. Those oxidants most frequently exploited hitherto are mercury(II) ions [1, 2] and dissolved oxygen [3]. The presence of very high concentrations of oxidants in the sample will, however, cause the $M(Hg) \rightarrow M^{n+}$ reaction to take place very rapidly, which makes it difficult to register the stripping curve on a normal speed strip-chart recorder. The microcomputer [5] system used in connection with a conventional potentiometric stripping analyzer in this work overcomes this difficulty. The main task of the microcomputer system is to register the rapid oxidation curve, store it in random access memories, and then display it at a reduced rate on the strip-chart recorder. Prior to this

0003—2670/81/0000—0000/$02.50

display, however, the microcomputer also registers the background curve which is digitally subtracted from the combined analytical/background curve [5]. This background correction increases the signal-to-noise ratio by approximately one order of magnitude.

Electroanalytical determinations of trace elements in biological materials by means of anodic stripping voltammetry has been attempted many times [6—10]. In anodic stripping voltammetry it is, however, necessary to destroy all organic matter completely because the presence of even trace concentrations of electroactive organic matter gives rise to stripping peaks which obscure the metal stripping peaks. Furthermore, the samples must be deoxygenated prior to analysis. Since no current is drawn through the working electrode during potentiometric stripping, electroactive organic matter, even if present in very high concentrations, will not interfere with the trace metal determination. The electroactive material will, however, increase the rate of the re-oxidation reaction. The purpose of this paper is to illustrate how computerized potentiometric stripping analysis can be exploited for the determination of trace metals in biological material after a simple pretreatment of the sample.

EXPERIMENTAL

Instrumentation, electrodes and electrochemical cell

The potentiometric stripping analyzer (Radiometer, ISS 820) was supplemented with a laboratory-built microcomputer system based on an Intel 8085 microprocessor. The real-time data acquisition rate was 30.7 kHz [5].

A glassy carbon electrode with a total surface area of 8 mm^2 (Radiometer F3500) was used as working electrode. A saturated calomel electrode was used as reference and a platinum wire as counter electrode (Radiometer K4040 and P1312, respectively). The electrode vessel was made of glass and had a total volume of 35 ml. Stirring was achieved mechanically with a three-edged teflon stirrer (Radiometer, TTA 80).

The flame atomic absorption measurements were done with a Perkin-Elmer 370 equipped with a standard single-slot burner head, and the graphite furnace measurements were made with a Perkin-Elmer 403 and a heated graphite atomizer, HGA 2100.

Chemicals

Stock solutions (1 mg l^{-1}) of copper(II), cadmium(II), lead(II) and zinc(II) were prepared by diluting commercial standards (Merck, Titrisol) with 0.14 M nitric acid. From these stock solutions, working standards of suitable concentration were prepared by dilution with doubly-distilled water. All chemicals used except perchloric acid (Merck, Suprapur) were of analytical grade.

All glassware used was rinsed first with 7 M nitric acid and then with doubly-distilled water prior to use.

Samples

Two different types of tinned mussels were investigated, one type originating from the Limfjord in Denmark and the other from Korea. The bovine liver reference sample, obtained from the U.S. National Bureau of Standards (NBS) was freeze-dried and homogenized.

Digestion methods

Two different digestion procedures were used, one using nitric acid only and one using both nitric and perchloric acids.

The nitric acid procedure. Approximately 5 g of wet mussel or 2 g of freeze-dried bovine liver was transferred to the reaction vessel which was a 50-ml thick-walled pyrex bottle with a polypropylene screw-cap. Concentrated nitric acid (10 ml) and 10 ml of doubly-distilled water were added and the bottle was heated gently on a hot plate for about 2 min, without its screw-cap. When foaming started, 0.5 ml of octanol was added and heating was continued until the initial vigorous reaction stopped, which normally took about 4 min. The bottle was then closed with the screw-cap and transferred to a pressure boiler where it was heated for about 1 h. The sample was then diluted to a total volume of 50 ml with doubly-distilled water. This procedure yielded a yellow solution with some drops of fatty acid residues floating on the surface. Reagent blanks were obtained according to the same procedure.

The nitric acid—perchloric acid procedure. Approximately 5 g of wet mussel was transferred to a 100-ml double-necked round-bottomed flask and 20 ml of concentrated nitric acid was added. The sample was heated gently on a hot plate and, at the first sign of foaming, 1.0 ml of octanol was added. Heating was continued and the nitric acid was slowly sucked off through a sodium hydroxide trap during a period of about 2 h. Perchloric acid (10 ml) was then added and heating was continued until, after approximately 1.5 h, the formation of white fumes commenced. If the solution was colourless, the digestion was regarded as complete, otherwise the perchloric acid treatment was repeated. The sample was diluted to a final volume of 50 ml. This procedure gave a slight mineral residue, probably the skeletons of siliceous algae which form part of the mussel diet.

Analytical procedures for the nitric acid digest

Potentiometric stripping analysis for cadmium and lead. An aliquot (1 ml) acid digest was diluted to 20 ml in the electrochemical cell, using a solution containing 0.06 M hydrochloric acid and mercury(II) nitrate (25 mg Hg l^{-1}). After 4 min of potentiostatic pre-electrolysis at −1.05 V vs. SCE, the stripping curve was measured by the computer system. If the glassy carbon electrode had not been coated with mercury in a previous sample, the first 4 min of the pre-electrolysis/stripping cycle was repeated prior to the addition of the standard addition aliquots. Once coated with mercury, the working electrode could be used for several samples provided that it was not

left in the sample for any significant period of time without an applied potential. In this case, the nitro compounds present in the sample slowly oxidized the mercury film. All the electrodes were rinsed with distilled water between samples. The mercury-coated electrode could be stored for several days in distilled water provided that it had been rinsed carefully before immersion in distilled water.

The concentrations of Cd(II) and Pb(II) in the sample were evaluated by means of the standard addition technique, the 4-min pre-electrolysis/stripping cycle being repeated after each addition. In most experiments, two standard additions were used and the concentration of the standard addition solution was chosen so that the first addition approximately doubled the concentration of the analyte.

Potentiometric stripping analysis for copper. The acid digest was diluted as for cadmium and lead above. After 2 min of pre-electrolysis at −1.0 V vs. SCE, the stripping curve was measured, a standard aliquot of copper(II) was added as quickly as possible, and a new cycle was started. If pre-electrolysis was not started within 10 s, the mercury film was affected and the precision of the copper(II) determination decreased. Consequently in most copper determinations the mercury film was wiped off after each pre-electrolysis/stripping cycle. A new mercury film was then formed during the first few seconds of the next pre-electrolysis.

Potentiometric stripping analysis for zinc. An aliquot (0.5 ml) of acid digest was diluted to 20 ml with a solution containing 0.06 M hydrochloric acid, 0.18 M acetic acid, gallium(III) nitrate (25 mg Ga l^{-1}) and mercury(II) nitrate (25 mg Hg l^{-1}). After pre-electrolysis for 1 min at −1.45 V vs. SCE, the stripping curve was measured. If the working electrode had not been coated with mercury in a previous sample, the first pre-electrolysis/stripping cycle was repeated before the standard addition aliquots were added. This mercury film could then be used for at least ten samples. Since the purpose of the gallium(III) is to form a Ga—Cu intermetallic compound in the mercury film, thus preventing the formation of a Zn—Cu compound [11], gallium must be in excess of copper in the film. If this is the case, a gallium stripping signal appears on the potential stripping curve, thus indicating complete masking of copper. If no gallium signal appears, the concentration of gallium must be increased. In the bovine liver digests which had very high copper concentration, 50 mg Ga l^{-1} was used.

TABLE 1

Experimental parameters used for the heated graphite furnace

Element	Sample volume (μl)	Gas interrupt	Drying		Ashing		Atomizing	
			Time (s)	°C	Time (s)	°C	Time (s)	°C
Cd	20	No	25	100	15	250	11	2200
Pb	20	Yes	25	100	15	200	11	2400

Atomic absorption determination of lead and cadmium. These elements were determined with the heated graphite atomizer using a deuterium background corrector. The instrumental parameters used are listed in Table 1. Prior to analysis, the acid digests were diluted 20 times with a solution of lanthanum(III) nitrate (200 mg La l^{-1}) in order to avoid chloride interference [12]. Lead and cadmium were determined by a standard addition procedure. The sensitivity for cadmium in the diluted acid digest was the same as in an acidified aqueous solution. The sensitivity for lead in the acid digest was approximately 50% of the sensitivity in an acidified standard solution.

Atomic absorption determination of copper and zinc. Those elements were determined after dilution by means of flame atomic absorption spectrometry, using calibration curves prepared from acidified aqueous solutions. The deuterium background correction was not necessary.

Analytical procedures for the nitric—perchloric acid digest

Potentiometric stripping analysis for cadmium and lead. An aliquot (4 ml) of the acid digest was diluted to 20 ml with a solution containing 0.06 M HCl and mercury(II) nitrate (25 mg Hg l^{-1}). After pre-electrolysis for 1 min at −1.0 V vs. SCE, the stripping curve was measured. If the working electrode had not been mercury-plated in a previous sample, the pre-electrolysis/stripping cycle was repeated prior to the addition of the standard addition aliquots. This mercury film could be used for a large number of samples, provided that the electrode was stored in distilled water.

Potentiometric stripping analysis for copper. An aliquot (1 ml) of digest was diluted to 20 ml with a solution containing 0.03 M HCl and mercury(II) nitrate (5 mg Hg l^{-1}). After pre-electrolysis for 1 min, the stripping curve was measured, the first pre-electrolysis/stripping cycle being used for mercury pre-plating of the glassy carbon electrode. The same mercury film could be used for several samples, provided that the working electrode was not left in the sample without an applied potential.

Potentiometric stripping analysis for zinc. The analytical procedure was the same as for the nitric acid digest.

Atomic absorption determination of lead, cadmium, copper and zinc. The analytical procedures were the same as for the nitric acid digests.

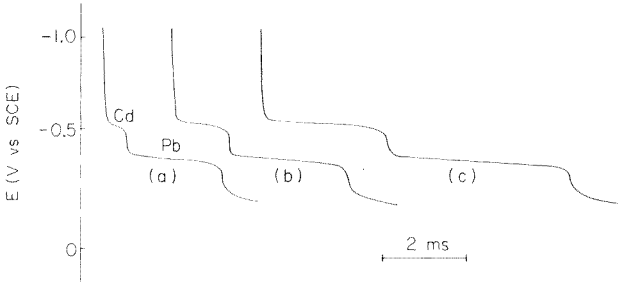

Fig. 1. Potentiometric stripping analysis for lead and cadmium in a diluted nitric acid digest (curve a). Pre-electrolysis for 4 min and 6 $\mu g\ l^{-1}$ (curve b) and 4 and 12 $\mu g\ l^{-1}$ (curve c) for cadmium and lead, respectively.

RESULTS

Determination of cadmium and lead

Potentiometric stripping curves for cadmium and lead in a diluted nitric acid digest are shown in Fig. 1. Because of the high amounts of organic nitro compounds the stripping was extremely rapid. In the nitric—perchloric acid digests, the concentrations of nitro compounds were much lower and the sensitivity in these digests was approximately one order of magnitude higher than that shown in Fig. 1. For these samples a pre-electrolysis time of 1 min was sufficient.

The correlations between the results obtained by potentiometric stripping analysis and atomic absorption spectrometry are shown in Fig. 2A for cadmium and in Fig. 2B for lead. Considering the relative precision of the two techniques, there was no significant difference between the results obtained for the nitric acid digests or for the mixed acids digests. The results obtained for the cadmium and lead content of mussels are in good agreement with previous determinations [13].

The precision of the two analytical techniques was determined by analyzing the same acid digest five times. The mean values and the standard deviations are summarized in Table 2. The difference between mussel sample I and mussel sample II might depend on differences from one mussel to another in the same tin.

Determination of copper and zinc

The copper signal by potentiometric stripping analysis after pre-electrolysis for 2 min in a diluted nitric acid digest is shown in Fig. 3. The signal ob-

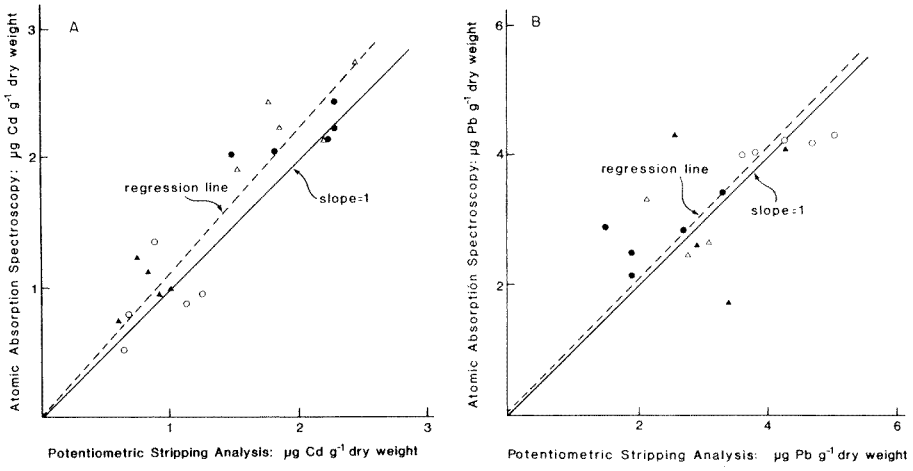

Fig. 2. Comparison between the results obtained by potentiometric stripping analysis and by atomic absorption spectrometry for (A) the cadmium content and (B) the lead content of two different kinds of mussels, using two different digestion procedures. (○) HNO_3, sample 1; (●) HNO_3, sample 2; (△) HNO_3—$HClO_4$, sample 1; (▲) HNO_3—$HClO_4$, sample 2.

TABLE 2

Results obtained by atomic absorption spectrometry (a.a.s.) and potentiometric stripping analysis (p.s.a.) for Zn, Pb, Cd and Cu in mussels
(Each digest was measured five times by both techniques)[a]

Sample	Digestion method	μg Cd g^{-1}		μg Pb g^{-1}		μg Cu g^{-1}		μg Zn g^{-1}	
		P.s.a.	A.a.s.	P.s.a.	A.a.s.	P.s.a.	A.a.s.	P.s.a.	A.a.s.
Danish mussel I	HNO_3	2.3 ± 0.8	2.1 ± 0.3	2.3 ± 0.8	2.4 ± 0.4	6.5 ± 2.1	7.6 ± 1.9	132 ± 32	136 ± 36
Danish mussel II	HNO_3—$HClO_4$	2.0 ± 0.4	2.3 ± 0.3	2.4 ± 0.5	2.6 ± 0.5	8.0 ± 0.9	7.9 ± 1.0	156 ± 32	252 ± 48
Korean mussel I	HNO_3	0.92 ± 0.28	0.92 ± 0.32	4.3 ± 0.6	4.2 ± 0.1	12.1 ± 2.3	11.8 ± 3.0	176 ± 40	184 ± 32
Korean mussel II	HNO_3—$HClO_4$	0.84 ± 0.16	1.00 ± 0.20	3.5 ± 0.8	3.3 ± 1.1	7.8 ± 2.3	9.2 ± 3.0	180 ± 20	188 ± 8

[a]All results refer to dry weight of sample; the standard deviations quoted refer to 5 measurements.

tained for zinc in dilute nitric acid after pre-electrolysis for 1 min is shown in Fig. 4. The correlations between the results obtained for copper and zinc by atomic absorption spectrometry and by potentiometric stripping analysis are illustrated in Fig. 5 and the precision of the two techniques is given in Table 2. As can be seen from these results, there were no significant differences between the two analytical techniques or between the two different digestion procedures.

Analysis of the NBS bovine liver reference sample

The bovine liver samples were digested and analyzed in the same way as the mussel samples. In Table 3 the results obtained by potentiometric stripping analysis and by atomic absorption spectrometry are compared with the values certified by the National Bureau of Standards. All values, with the exception of one copper determination, are within the range specified by the Bureau. If the relative precision (cf. Table 2) of the techniques is taken into account, all values given in Table 3 are well within the certified range.

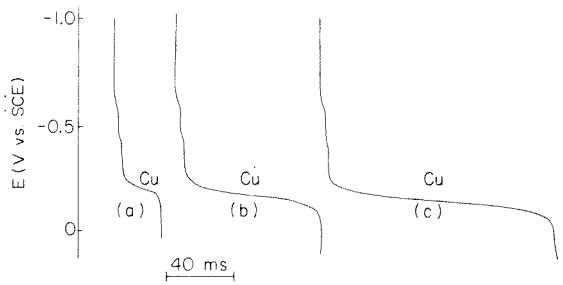

Fig. 3. Potentiometric stripping analysis for copper in a diluted nitric acid digest (curve a). Pre-electrolysis for 2 min at −1.0 V vs. SCE. Two copper(II) standard additions of 20 μg l^{-1} (curve b) and 40 μg l^{-1} (curve c).

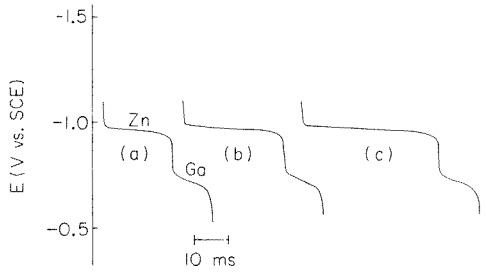

Fig. 4. Potentiometric stripping analysis for zinc in a diluted nitric acid digest (curve a). Pre-electrolysis for 1 min at 1.45 vs. SCE. Two zinc standard additions of 80 $\mu g\ l^{-1}$ (curve b) and 160 $\mu g\ l^{-1}$ (curve c).

Blank values

For the nitric acid digestion method, the blank value for all elements could be neglected. For the nitric—perchloric acid digestion method, the blank value for lead was approximately 20% of the bovine liver value. The lead result given in Table 3 has been corrected for this background value.

DISCUSSION

The accuracy of potentiometric stripping analysis for determinations of cadmium, lead, copper and zinc in mussels and bovine liver has been demonstrated. Since these two kinds of biological samples differ greatly with

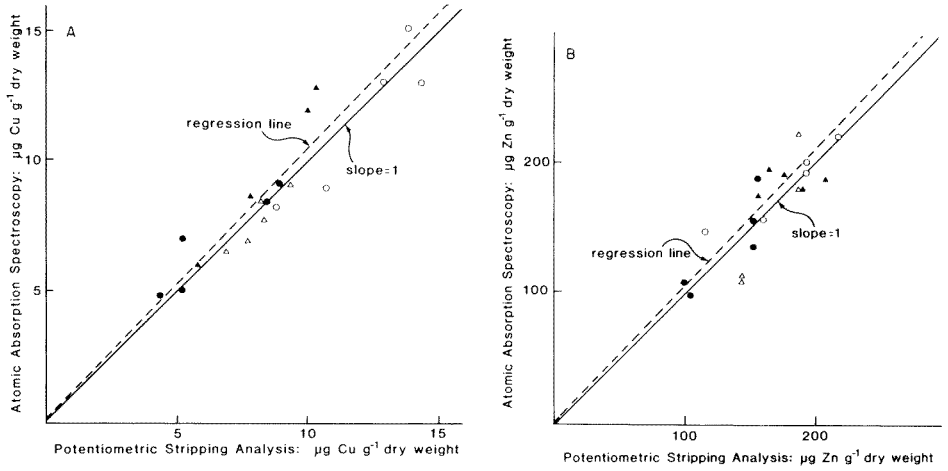

Fig. 5. Comparison between the results obtained by potentiometric stripping analysis and atomic absorption spectrometry for (A) the copper content and (B) the zinc content of two different kinds of mussels, using two different digestion procedures. (○) HNO_3 digest, sample 1; (●) HNO_3 digest, sample 2; (△) HNO_3—$HClO_4$ digest, sample 1; (▲) HNO_3—$HClO_4$ digest, sample 2.

TABLE 3

Results obtained for NBS bovine liver reference sample by p.s.a. and a.a.s., using two different digestion techniques

Element	Digestion method	Trace element concentration ($\mu g\ g^{-1}$)		Certified value
		P.s.a.	A.a.s.	
Cd	HNO_3	0.29	0.31	0.27 ± 0.04
Cd	HNO_3—$HClO_4$	0.26	0.32	
Pb	HNO_3	0.39	0.36	0.34 ± 0.08
Pb	HNO_3—$HClO_4$	0.39	0.34	
Cu	HNO_3	216	191	193 ± 10
Cu	HNO_3—$HClO_4$	207	193	
Zn	HNO_3	133	127	130 ± 13
Zn	HNO_3—$HClO_4$	118	122	

respect to protein and lipid content, it can be concluded that the potentiometric stripping technique could be used for a great variety of biological samples and food-stuffs.

The relative precision of the potentiometric stripping analysis for trace elements in biological materials is of the order of 20%, as can be estimated from Table 2. This is very close to the precision obtained by atomic absorption spectrometry (cf. Table 2) and quite satisfactory in the concentration range under consideration. Preliminary investigations using a rotated glassy carbon electrode, instead of mechanically stirring the sample, indicate that the precision in computerized potentiometric stripping analysis can be increased considerably.

As can be seen from Table 2, there are no significant differences between the results obtained by the nitric acid digestion procedure and those obtained by the nitric—perchloric acid procedure. Since, however, the nitric acid digest contains considerably higher concentrations of electroactive nitro compounds, which cause very rapid stripping, it is necessary to increase the time for pre-electrolysis by a few minutes in the nitric acid digests compared to the mixed acids digests. Even so, the nitric acid digestion method is preferable because it is quicker and simpler and, furthermore, the use of perchloric acid is avoided.

Only the nitric—perchloric acid digests can be analyzed by non-computerized potentiometric stripping analysis. Furthermore, it is necessary to deoxygenate the samples prior to measurement, by means of bubbling inert gas for 15 min. By this procedure, cadmium and lead could be determined after 16 or 32 min of pre-electrolysis and copper after 4—8 min. Zinc was not attempted.

A significant advantage of the computerized system is that it can be applied to samples containing high concentrations of organic nitro compounds. This is not possible with anodic stripping voltammetry or differential pulse anodic stripping voltammetry.

REFERENCES

1 D. Jagner and K. Årén, Anal. Chim. Acta, 100 (1978) 375.
2 D. Jagner, Anal. Chem., 50 (1978) 1924.
3 D. Jagner, Anal. Chem., 51 (1979) 342.
4 D. Jagner and K. Årén, Anal. Chim. Acta, 105 (1979) 33.
5 A. Granéli, D. Jagner and M. Josefson, Anal. Chem., 52 (1980) 2220.
6 M. Oehme, W. Lund and J. Jonsen, Anal. Chim. Acta, 100 (1978) 389.
7 W. Lund and P. Sagberg, Anal. Chim. Acta. 115 (1980) 337.
8 G. Chittleborough and B. J. Steel, Anal. Chim. Acta, 119 (1980) 235.
9 W. Holak, J. Assoc. Off. Anal. Chem., 58 (1975) 777.
10 J. T. Kinard, Anal. Lett., 10 (1977) 1147.
11 T. R. Copeland, R. A. Osteryoung and R. K. Skogerboe, Anal. Chem., 46 (1974) 2093.
12 M. Bengtsson, L.-G. Danielsson and B. Magnusson, Anal. Lett., 12 (1979) 1367.
13 B. L. Bayne (Ed.), Marine Mussels, Cambridge University Press, Cambridge, 1974.

Analytica Chimica Acta, 127 (1981) 157—164
Elsevier Scientific Publishing Company, Amsterdam — Printed in The Netherlands

THEORETICAL TREATMENT OF INTERMEDIATE ELECTROLYSIS ELECTROCHEMICAL DETECTORS

JOSEPH WANG

Department of Chemistry, New Mexico State University, Las Cruces, NM 88003 (U.S.A.)

(Received 15th September 1980)

SUMMARY

A simple approach for deriving expressions for the limiting steady-state response of the open tubular electrode, under conditions of intermediate electrolytic yields, is described. This approach couples the principles of laminar fluid dynamics with the theory of the porous electrode reactor. The dependence of the limiting current, I_l, on flow rate, V_f, has the form of $I_l \propto V_f^m$, with $m \geqslant 1/3$, depending upon the electrolytic yield. The effects of electroactive species depletion upon the detector response are discussed. Experimental results are incorporated to support the theoretical conclusions. For a tubular electrode (4-cm long) the degree of conversion decreases from 0.21 to 0.03 and m decreases from 0.42 to 0.32 as the flow rate increases from 0.15 to 3.5 ml min^{-1}.

Increasing attention and effort are being directed toward continuous measurements on flowing solutions with solid electrodes. Application of hydrodynamic theory in the manner of Levich [1] is used to understand the behavior of these detectors and to optimize their performance. The limiting current response, I_l, of a flow-through electrode is described by the general equation

$$I_l = nFAK_1C_bV_f^{\alpha} \quad (1)$$

where n is the number of electrons in the reaction, F is the value of Faraday, A is the electrode area (cm^2), K_1 is the limiting, specific, mass-transfer coefficient ($cm^{1-3\alpha}s^{\alpha-1}$), C_b is the bulk concentration of the electroactive species (mol cm^{-3}), V_f is the fluid flow rate (cm^3 s^{-1}) and α is a constant dependent on the flow regime and the electrode geometry.

Many designs have been reported for electrodes to be used for detection in flowing solutions. Generally, flow-through electrodes can be divided into two categories: those which electrolyze only a negligible fraction (often 0.1—5%) of the electroactive species passing through the detector (amperometric detectors), and those for which the electrolytic efficiency is 100% (coulometric detectors). For coulometric detectors, α and the product AK_1 are unity and the limiting current is given by Faraday's law: $I_l = nFC_bV_f$.

Recently an increased number of sensitive and reliable detectors, operating in the intermediate range of electrolytic efficiency (mainly 10—30%) have been described [e.g., 2, 3]. Increased electrolytic yield is also obtained when

electrochemical detectors are coupled with microcapillary liquid chromatography, because of the very low flow rates (typically 0.5—5 μl min^{-1}) involved with this approach. Intermediate electrolysis detectors seem to be very promising for analytical purposes because they combine a much larger response compared to the low-yield amperometric detectors with elimination of the complexity necessary to achieve complete conversion.

Equations for the steady-state limiting current, solved rigorously for various low-yield amperometric detectors, are not applicable to intermediate electrolysis detectors; depletion of electroactive species along the electrode axis tends to invalidate these expressions which are based on the assumption of uniform concentration. At present, no simple approach exists to derive an expression for the limiting current at the various flow cell geometries operating under conditions of intermediate electrolysis [4]. This is due to the mathematical complexity involved with boundary conditions describing change in the electroactive species along the detector axis. In this paper, a simple approach for deriving such expressions, which does not involve such boundary conditions, is described. This method of derivation is based on combining the principles of fluid hydrodynamics [1] with the theory of the porous electrode reactor [5, 6]. For demonstrating the utility of this approach, an expression for the response of intermediate electrolysis in open tubular electrodes is derived. The tubular electrode is chosen because this geometry has become very popular and the equation of mass transport under laminar fluid flow and negligible electrolysis has been solved rigorously [1, 7]. The dependences of the limiting degree of conversion and the limiting current upon the tubular electrode parameters are discussed.

THEORY

Consider a tubular electrode of length L (along the X-axis) and radius r with a laminar flow regime. The total limiting current under partial electrolytic conditions is given [5] by

$$I_l = nFC_0V_fR \tag{2}$$

where C_0 is the initial concentration of the electroactive species before entering the detector and R is the limiting degree of conversion. The parameter, R, is described by $R = 1 - C_L/C_0$, where C_L is the outlet concentration of the electroactive species at the end of the tubular electrode.

The theory of the porous electrode reactor is applicable for describing the distribution of a steady-state electroactive species in other "plug flow" intermediate electrolysis detectors (operating under limiting current conditions). The outlet concentration of the electroactive species is given [5] by

$$C_L = C_0\exp(-jsq^{\alpha-1}L) \tag{3}$$

where j is a mass transfer constant, s the specific internal surface, and q is the specific flow mass. By analogy with the theory of Levich [1], the limiting

current, i_l, at an element of the area of the electrode can be expressed as $i_l = jnFCq^{\alpha}$, where C is the local concentration. According to the Nernst theory [8], i_l can be expressed also as $i_l = nFCD\delta^{-1}$, where D is the diffusion coefficient and δ is the thickness of the diffusion boundary layer. By comparison of these two equations for i_l, we obtain $j = D/\delta q^{\alpha}$.

For tubular electrodes under conditions of laminar fluid dynamics, δ is given [9] by

$$\delta = 1.142\, D^{1/3} X^{1/3} r V_f^{-1/3} \tag{4}$$

Based on their definitions, q^{α} and s for the tubular electrode geometry are described by $q^{\alpha} = V_f^{1/3}(\pi r^2)^{-1/3}$ and $s = 2r^{-1}$.

Combination of the equations for j and q^{α} with eqn. (4) yields

$$j = 1.2825\, D^{2/3} X^{-1/3} r^{-1/3} \tag{5}$$

Substitution of the equations for j, q^{α} and s into eqn. (3) yields

$$C_L = C_0 \exp(-5.502\, D^{2/3} L^{2/3} V_f^{-2/3}) \tag{6}$$

Combination of the equation $R = 1 - C_L/C_0$ with eqn. (6) leads to the following expression for the limiting degree of conversion for an open tubular electrode

$$R = 1 - \exp(-5.502\, D^{2/3} V_f^{-2/3} L^{2/3}) \tag{7}$$

Substituting eqn. (7) in eqn. (2) gives an expression for the total limiting current for an intermediate electrolysis tubular electrode

$$I_l = nFC_0V_f[1 - \exp(-5.502\, D^{2/3} V_f^{-2/3} L^{2/3})] \tag{8}$$

Following Sioda [10], eqn. (7) can be expressed in a simpler form, using the dimensionless parameter $J = 5.502\, D^{2/3} V_f^{-2/3} L^{2/3}$, and then $R = 1 - \exp(-J)$. For small values of J (e.g., high flow rates and/or short electrodes), $\exp(-J)$ can be approximated by $(1 - J)$. From eqn. (7), an approximate expression for R, for cases of short residence times, can then be obtained

$$R \cong 5.502\, D^{2/3} V_f^{-2/3} L^{2/3} \tag{9}$$

and according to eqns. (2) and (9),

$$I_l \cong 5.502\, nFD^{2/3} C_0 L^{2/3} V_f^{1/3} \tag{10}$$

This expression is similar to the following expression, derived for tubular electrodes under conditions of neglected electrolysis (assuming $C = C_0$) [1, 7]

$$I_l = 5.43\, nFD^{2/3} C_0 L^{2/3} V_f^{1/3} \tag{11}$$

The same approach can be applied to other detector geometries for which boundary value problems under negligible electrolysis have been solved (e.g., flow-through thin layer or annular electrodes). By combining the proper expression for δ, q^{α}, and s for these geometries with those describing the distribution of the electroactive species along the detector axis (eqn. 3),

similar expressions for the limiting current and the limiting degree of conversion are obtainable for intermediate electrolysis conditions.

EXPERIMENTAL

All solutions were prepared from deionized water and Baker Analyzed potassium chloride and potassium hexacyanoferrate(II). The sample was stored in a 250-ml Nalgene beaker. Solution flowed from the beaker by gravity via tygon tubing (1/16-in. i.d., 1/8-in. o.d.). The tubing working electrode was inserted into the system by press-fitting tygon tubular over its ends. Two platinum tubes used were: (a) 4.0-cm length, 0.10-cm diameter, and (b) 2.54-cm length, 0.05-cm diameter. The dead volumes of these electrodes were 32 and 5 μl, respectively. The inner surface of the electrode was polished with 0.1-μm alumina slurry which was applied on a thin wire drawn back and forth in the tubular channel. The alumina particles were removed from the channel with a stream of deionized water. Fingernail polish was used in the interface between the electrode and the tubing to help guard against contact from solution that might creep out of the inner channel. The other end of the electrode was connected through a 0.5-cm length tygon tubing to the vertical arm of an inverted glass T-tube (0.2-cm i.d., with each arm 0.8-cm length). The salt-bridge of the reference electrode (Ag/AgCl, KCl (sat.)) was introduced to the system through one of the horizontal arms of the T-tube. A tubular platinum counter electrode (1.0-cm length, 0.1-cm i.d.) was connected through a short (0.5-cm) section of tygon tubing to the second horizontal arm of the T-tube. The other end of the counter electrode was connected to tygon tubing through which the solution was discarded to waste. The flow rates were calibrated and checked volumetrically. The three electrodes were connected to a Sargent—Welch 3001 Polarograph. The electrodes were preconditioned at +0.9V, −0.9V, and +0.9V, for 1 min at each potential. After preconditioning, the desired working potential (+0.60V, in the plateau region for the oxidation of hexacyanoferrate(II)) was applied and transient currents were allowed to decay. All steady-state data were corrected for background. Stopped-flow measurements were performed by turning on and off a stopcock that was inserted between the beaker and the cell.

RESULTS AND DISCUSSION

Dependences of the current and of the degree of conversion on flow rate and electrode length

Table 1 shows the theoretical dependence of the limiting degree of conversion upon the volume flow rate for tubular electrodes 4, 5, and 7 cm long which, assuming 1 mm diameter, correspond to working volumes of 32, 40 and 55 μl, respectively. The R values are calculated with eqn. (7). Decreased flow rate (V_f) and increased electrode length (L) (i.e., increased

TABLE 1

Dependence of calculated values of limiting degree of conversion on volume flow rate

Volume flow rate (ml min^{-1})	Degree of conversion (R)		
	4 cm[a]	5 cm[a]	7 cm[a]
0.06	0.47	0.52	0.61
0.12	0.33	0.37	0.45
0.24	0.22	0.26	0.32
0.6	0.12	0.15	0.19
1.2	0.08	0.10	0.12
3.0	0.04	0.05	0.07
4.8	0.03	0.04	0.05
6.0	0.03	0.03	0.04

[a]Electrode length; diffusion coefficient, 1×10^{-5} cm^2 s^{-1}.

residence time of an element of solution in the electrode volume) provide a larger degree of conversion. The maximum conversion calculated is 61%, which would be increased for longer residence times.

The dependence of the detector response on the flow rate is of great analytical interest. This dependence has been subject to some controversy in the literature; different values of α have been found for the same detector geometry [e.g., 11, 12]. These deviations from the theoretical predictions were attributed to different electrode pretreatments, contribution by axial diffusion, improper applied potential, or incorrect statistical treatment of data. The effect of partial depletion upon the current—flow rate dependence, which has not been investigated yet, is the subject of the following section.

Figure 1 presents the theoretical logarithmic dependence of the limiting current upon volume flow rate for a 5-cm long tubular electrode, where I_l is calculated with eqn. (8). As the flow rate decreases from 6.0 to 0.06 ml min^{-1}, the slope of this plot increases from 0.345 to 0.607. The dotted line represents calculated values for a 5-cm tubular electrode under conditions of neglected electrolysis (eqn. 11).

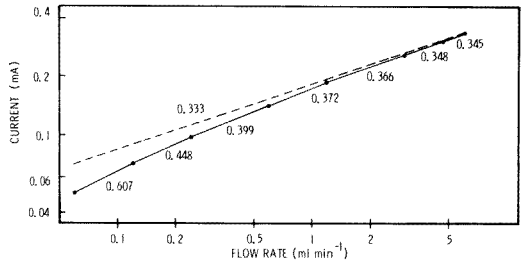

Fig. 1. The theoretical dependence of the total limiting current on volume flow rate. Values of I_l were calculated for electrode length, 5 cm; concentration, 10^{-3} mol cm^{-3}; diffusion coefficient 10^{-5} cm^2 s^{-1}. Number on each section represents the value of the slope.

For detectors in which electrolysis is negligible, the increasing value of the slope of the log I_l vs. log V_f is usually interpreted as an indication of change in the flow regime: from laminar flow through tubular electrodes at value of the slope of 1/3, to turbulent flow at higher values of slope. (For other detector geometries, laminar flow is characterized by different values of the slope up to 1/2.) However, for the data of Fig. 1, the slope increases for decreasing flow rate for which turbulent flow is not expected. This is due to the fact that for intermediate electrolysis detectors, the actual value of the slope of log I_l vs. log V_f plots is not α but a complex function of the degree of conversion and α, as will be discussed below.

Following the theory of the porous electrode reactor [10, 13], it would be convenient if the complex expression for the total limiting current (eqn. 8) could be described in the following simple form

$$I_l = fC_0V_f^m \tag{12}$$

where f and m are experimental parameters. By taking the logarithm of both sides of eqn. (8) and differentiating with respect to log V_f, the following relationship between m, R, and α is obtained

$$m = 1 + (1 - \alpha)[(1 - R)\ln(1 - R)]/R \tag{13}$$

where R for the tubular electrode is given by eqn. (7).

Equation (12), as well as eqn. (8) transform into the conventional equation $I_l = nFC_bV_f$ and eqn. (11) for the limiting cases of complete electrolysis and negligible electrolysis, respectively. In the intermediate range of conversion yields, both m and f change; as the conversion yield increases from 3% to 52%, m increases from 0.345 to 0.607 (Fig. 1 and Table 1). The parameter, m, approaches the theoretical value of α = 1/3 (dotted line in Fig. 1) for larger flow rate and/or shorter electrode. Even small electrolysis yields (as little as 3%) contribute to change in the exponent (0.345), indicating that whenever the actual value of the slope deviates from that predicted for laminar flow dynamics, electrolysis may be considered as the reason.

Figure 2 shows the experimental dependence of the limiting current and of the limiting degree of conversion upon the flow rate for the 4-cm long tubular electrode. The degree of conversion decreases from 0.21 to 0.03 as the flow rate increases from 0.15 to 3.5 ml min^{-1}. The dotted line in the degree of conversion plot represents calculated values according to eqn. (7). (A diffusion coefficient of 0.9×10^{-5} cm^2 s^{-1} [7] was used for this purpose.) Good agreement is observed between the theoretical predictions and the experimental results with deviations that may be the result of adsorbed material or local turbulence at the electrode surface and contribution of "end-diffusion" to the total flux. For these reasons, the actual response of a practical tubular electrode may vary significantly from the theoretical [12]. The log—log plot of current vs. flow rate (also shown in Fig. 2) results with increased value of the slope, from 0.32 to 0.42, as the flow rate decreases from 3.5 to 0.15 ml min^{-1}. Increased value of the slope from that character-

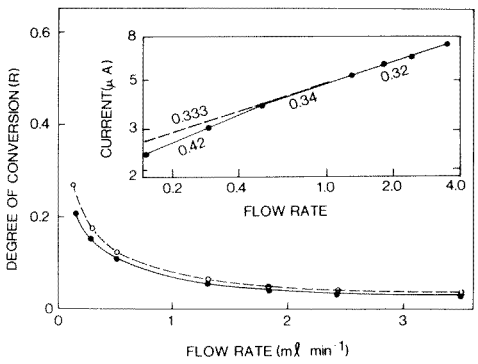

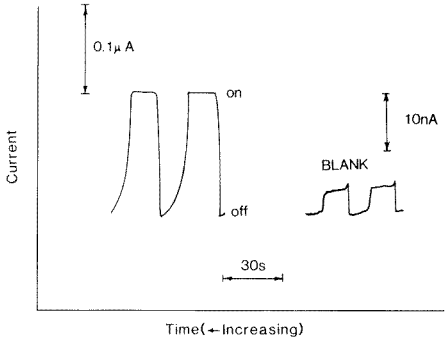

Fig. 2. Experimental dependences of the limiting current and of the limiting degree of conversion upon volume flow rate. $[K_4Fe(CN)_6]$ = 50 μM in 0.1 M KCl; electrode length, 4 cm; applied potential, +0.6 V; experimental data are represented by the solid lines; numbers on the log I_l—log V_f plot represent the value of the slope.

Fig. 3. Stopped-flow response for 3.4 μM $K_4Fe(CN)_6$. Electrode length, 2.54 cm; supporting electrolyte and applied potential, as in Fig. 2; flow rate, 2.5 ml min^{-1} (flow-on).

izing laminar flow with negligible electrolysis (1/3, shown by the dotted line) is observed at flow rates lower than 1 ml min^{-1}. Similar experiments with the 2.54-cm long electrode resulted in increased conversion yield from 0.02 to 0.11, and increased slope of the log I_l vs. log V_f plot from 0.31 to 0.36 for a decreased flow rate from 2.8 to 0.3 ml min^{-1}.

Hydrodynamic modulation voltammetry at intermediate electrolysis detectors

Hydrodynamic modulation techniques are acquiring increasing importance in the quantitative exploitation of solid electrodes because they permit discrimination against the major components of the background current. When applied to flowing streams, pulsed-flow voltammetry is the most useful approach [14]. In this approach, a difference current is measured between two flow rates, one high (H) and one low (L). This difference current, which is purely convective, is given by

$$\Delta I_l = nFAK_1C_b(V_{f,H}^{\alpha} - V_{f,L}^{\alpha}) \tag{14}$$

When this approach is incorporated with intermediate electrolysis detectors, the two steady-state currents would have different dependences on flow rate; based on eqns. (7) and (8), the current difference can be described by

$$\Delta I_l = nFC_0(V_{f,H}R_H - V_{f,L}R_L) \tag{15}$$

For both the negligible and intermediate electrolysis detectors, the experimental objective is to achieve a larger value for the expression in parentheses in eqn. (15). In the first case, a large value for the parenthetical term is achieved by employing a larger difference in flow rates (e.g., a 75% increase in the flow rate will cause a (75α)% change in the current). For the inter-

mediate electrolysis detectors, as the flow rate increases the degree of conversion decreases and thus a careful optimization is required to achieve a larger current difference.

The detection limit of the detector is demonstrated by the stopped-flow measurement of 3.4 μM hexacyanoferrate(II) (Fig. 3). The blank stopped-flow current (shown on the right) amounted to 5 nA, corresponding to a concentration around 0.12 μM. The noise level is only around 0.3 nA. Based on a signal-to-noise ratio of 2, the limit of detection for hexacyanoferrate(II) would be around 14 nM.

Work is in progress toward applying this approach to other configurations of intermediate electrolysis flow-through detectors, with electroactive species depletion along the detector axis.

The support of the Research Center of the College of Arts and Science (NMSU) through its Minigrant Program is gratefully acknowledged.

REFERENCES

1 V. G. Levich, Physico-Chemical Hydrodynamics, Prentice-Hall, Englewood Cliffs, NJ, 1962.
2 J. Lown, R. Koile and D. C. Johnson, Anal. Chim. Acta, 116 (1980) 41.
3 C. Bollet, P. Oliva and M. Caude, J. Chromatogr., 149 (1977) 625.
4 D. C. Johnson, Anal. Chem., 52 (1980) 131R.
5 R. E. Sioda, Electrochim. Acta, 15 (1970) 783.
6 S. Kihara, J. Electroanal. Chem., 45 (1973) 31.
7 W. J. Blaedel and L. N. Klatt, Anal. Chem., 35 (1963) 2100.
8 W. Nernst, Z. Phys. Chem. (Leipzig), 47 (1904) 52.
9 G. W. Schieffer and W. J. Blaedel, Anal. Chem., 49 (1977) 49.
10 R. E. Sioda, Anal. Chem., 46 (1974) 964.
11 B. Oosterhuis, K. Brunt, B. H. C. Westerink and D. A. Doornbos, Anal. Chem., 52 (1980) 203.
12 P. L. Meschi and D. C. Johnson, Anal. Chem., 52 (1980) 1304.
13 R. E. Sioda, J. Appl. Electrochem., 5 (1975) 221.
14 W. J. Blaedel and D. G. Iverson, Anal. Chem., 49 (1977) 1563.

Analytica Chimica Acta, 127 (1981) 165—172
Elsevier Scientific Publishing Company, Amsterdam — Printed in The Netherlands

COATED-WIRE ORGANIC ION-SELECTIVE ELECTRODES IN TITRATIONS BASED ON ION-PAIR FORMATION
Part 2. Determination of Ionic Surfactants†

K. VYTŘAS,* M. DAJKOVÁ[a] and V. MACH

Department of Analytical Chemistry, College of Chemical Technology, 532 10 Pardubice (Czechoslovakia)

(Received 10th November 1980)

SUMMARY

Both cationic and anionic surfactants can be determined titrimetrically using a coated-wire electrode with a PVC membrane plasticized with 2-nitrophenyl 2-ethylhexyl ether. Cationic surfactants and other organic compounds of cationic character are titrated with sodium tetraphenylborate; for the titration of anionic compounds, cetylpyridinium bromide or 1-(ethoxycarbonyl)pentadecyl-trimethylammonium bromide (Septonex) is recommended. Characteristics of titration curves together with statistical evaluation of results are described for determinations of 15 specimens, involving pure substances as well as technical samples.

Cationic as well as anionic surfactants have usually been determined by methods based on two-phase titration. The determinations involve precipitation with an oppositely charged reagent; the end-point is indicated visually with a suitable colour indicator which will form an extractable ion-pair with the titrant after the equivalence point has been reached. Possibilities for end-point indication have been extended simultaneously with the development of ion-selective electrodes. Gavach and Seta [2] were probably the first to apply such electrodes for the titration of long-chain alkyltrimethylammonium salts with sodium tetraphenylborate. Cetyltrimethylammonium and cetylpyridinium bromides have been used as titrants for the determination of anionic substances [3].

More recently, several other papers have dealt with applications of ion-selective electrodes in titrimetric analysis for surfactants [4—18]; both home-made and commercial electrodes have been applied (Table 1). Besides conventionally constructed electrodes, the coated-wire type of electrode has become attractive because of their simple fabrication and manipulation [19]. Such electrodes can be applied advantageously in titrations based on ion-pair formation [20], the determination of ionic surfactants representing a typical

†For Part 1, see ref. [1].

[a]Present address: Regional Agricultural Laboratory, Agrochemical Corporation, 738 01 Frýdek-Místek, Czechoslovakia.

0003—2670/81/0000—0000/$02.50

TABLE 1

Titrimetric determinations of ionic surfactants with ion-selective indicator electrodes

Substances determined	Titrant	Indicator electrode	Ref.
Cationic surfactants			
Long-chain alkyl trimethylammonium and tetrabutylammonium salts	$NaBPh_4$	Liquid membrane, long-chain alkyltrimethylammonium picrate or BPh_4^- in $PhNO_2$ or $PhNO_2$ + benzene	2
Cetylpyridinium and butyltriphenylphosphonium sulphates	$NaClO_4$, $AgClO_4$	Membrane of phenol, formaldehyde, ammonia, and $Ni(NO_3)$ or $Ni(ClO_4)_2$ by polycondensation	4
Quaternary ammonium and other organic cations	$NaBPh_4$	Crytur 19—15 (PVC, valinomycin, dipentylphthalate)	5
Zephiramine[a] and other "onium" salts	$NaBPh_4$	Liquid membrane, tri-n-octylmethylammonium tetraphenylborate in $PhNO_2$	6
Quaternary ammonium	$NaBPh_4$	K^+-selective electrode, porous membrane	7
Zephiramine, cetylpyridinium bromide, benzylcetyldimethylammonium bromide	$K_3Fe(CN)_6$	Pt, with $K_4Fe(CN)_6$ medium	8
Trioctylmethylammonium bisulphate	Picric acid	Picrate-selective membrane (with crystal violet in $PhNO_2$)	9
Amine bases and quaternary ammonium	Picric acid	Picrate-selective, two-phase titration	10
Long-chain amines	Na laurylsulphate	Trioctylamine—laurylsulphate in $PhNO_2$, liquid membrane, two-phase titration	11
Anionic surfactants			
Na dodecylsulphate and other anions	CTAB[b], CPB[c]	Silicone-rubber membrane, cetyltrimethylammonium dodecylsulphate	3
Linear alkylbenzenesulphonate	Hyamine[d]	Orion 92-20 Ca^{2+}-selective	12
Dodecylbenzenesulphonate anion	Zephiramine[a]	Pt or Ag/AgCl, zephiramine-dodecylbenzenesulphonate in $PhNO_2$ and naphthalene	13
Soaps alone and with anionic surfactants	CDBAC[e]	Co(III)-bis(dimethylglyoxime)-1,10-phenanthroline dodecylsulphate in *o*-dichlorobenzene and n-decanol	14
Na long-chain alkylsulphates	CDBAC	Liquid membrane, similar to [14]	15
Benzenesulphonates	CTAB, CPC	Various (Orion)	16
Long-chain sulphates and sulphonates, soaps	CTAB, CPC, Hyamine	Various (Orion)	17
Surfactants, soaps	CPC	Various	18

[a]Tetradecyldimethylbenzylammonium chloride. [b]Cetyltrimethylammonium bromide. [c]Cetylpyridinium bromide. [d]Diisobutylphenoxyethoxyethyl(dimethyl)benzylammonium chloride. [e]Cetyldimethylbenzylammonium chloride.

example. The results of a recent study carried out in this laboratory are described below.

EXPERIMENTAL

Solutions

Sodium tetraphenylborate stock solution ($NaBPh_4$, 2.5%) was prepared as described previously [1] and was kept in a polyethylene bottle. A 0.25% $NaBPh_4$ titrant solution was prepared either by diluting this stock solution or by direct dissolution of the salt without addition of an adsorbent. Solutions of both concentrations were standardized potentiometrically against recrystallized thallium(I) nitrate [21, 22].

Cetylpyridinium bromide solution (10^{-3} M) was prepared by dissolving a weighed amount of the substance (purum, Lachema) in nearly the required volume of warm water; after cooling to laboratory temperature the solution was diluted to volume. Such a solution is practically saturated. The other cationic reagent, 1-(ethoxycarbonyl)pentadecyl-trimethylammonium bromide (Septonex, purum, Slovakofarma) was used at the same concentration (10^{-3} M), but more concentrated solutions could also be prepared. These solutions of cationic reagents were standardized potentiometrically against the above $NaBPh_4$ solution by using a 878C electrode (see below).

Stock solutions of the substances titrated were prepared from accessible specimens at the molar concentrations given in parentheses. These solutions were sodium lauryl sulphate (0.01 M), cetyltrimethylammonium bromide (5×10^{-4} M), phenyltrimethylammonium iodide (0.1 M), triphenyltetrazolium chloride (0.01 M), and tetraphenylphosphonium chloride (0.01 M). The following technical samples were also analysed (the chemical compositions and the concentrations of the solutions prepared are given in parentheses): Katexol 298 (1-[2-[(1-oxododecyl)-amino]ethyl]-pyridinium chloride; ca. 5×10^{-3} M), Orthosan MB (alkyldimethylbenzylammonium chloride, with an alkyl chain containing 12—14 carbon atoms; 5×10^{-3} M), Dextrosil KA (2-hydroxy-3-chloroethyltrimethylammonium chloride; 5×10^{-3} M) [all from Spolek pro chemickou a hutní výrobu, Ústí n.L.], Retacel (2-chloroethyltrimethylammonium chloride; VCHZ Kolín; ca. 0.01 M), Syntapon LA (long-chain alkyl sulphate; 10^{-3} M), Tensaryl, and Dubacid (long-chain alkyl arenesulphonates; 10^{-3} M) [all from VÚTP, Rakovník].

Instrumentation and procedure

Potentiometric measurements were done with OP-205 and OP-208 pH meters (Radelkis, Budapest). The potentiometric cell consisted of the appropriate ion-selective electrode with a saturated calomel electrode (SCE) and a 0.01 M $NaNO_3$ salt bridge. Titrations were made as usual in unbuffered medium: ca. 50 ml of the solution was titrated in a 100-ml beaker, the titrant being added from a 10-ml automatic burette.

Ion-selective electrodes

Coated-wire ion-selective electrodes were prepared by using an aluminium conductor as described previously [1] from tetrahydrofuran solutions of plastic and plasticizer. Different plasticizers were used for poly(vinyl chloride) (PVC) and poly(vinyl butyral) (PVB) membranes (the first number in parentheses is the electrode code number for PVC membranes, and the second for PVB membranes): dioctylphthalate (878A, 279E), 2-nitrophenyl 2-ethylhexyl ether (878C, 279C), tricresylphosphate (878M, 279G), dioctylsebacate (878J, 279D), n-butylbenzenesulphonamide (479B, 279I), and 2-ethylhexyl 4-hydroxybenzoate (479A, 279H). Electrodes were prepared without additions of ion-exchangers and were pre-conditioned by the appropriate ion-pair titration [20].

RESULTS AND DISCUSSION

Choice of optimal indicator electrode

As indicated by Higuchi et al. [23], any organic plastic matrix of limited hydrophilicity could be used as the gelling component of the electrode membrane, the selection being guided primarily by its compatibility with the desired liquid plasticizer. In order to select an optimal combination of plastic matrix and plasticizer, several solvents were examined for two plastics, PVC and PVB. As is apparent from Fig. 1, better results were obtained with PVC membranes; the total potential jump of the titration curves was mostly higher with PVC membranes than with PVB membranes. The shapes of the potentiometric titration curves are governed primarily by the solubility product of the precipitate formed. The electrode selectivity towards organic ions is established by liquid—liquid distribution principles. The most advantageous plasticizer from this point of view was 2-nitrophenyl 2-ethylhexyl ether.

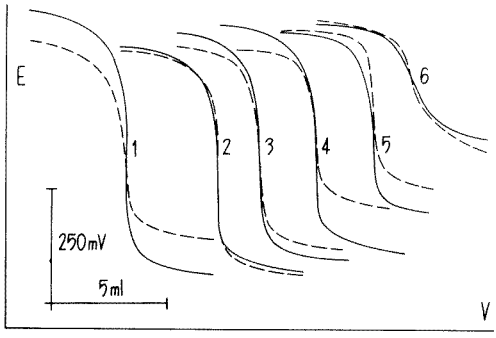

Fig. 1. Influence of plasticizer on the shape of potentiometric titration curves of cetylpyridinium bromide (5×10^{-4} M) with sodium tetraphenylborate (6.3×10^{-3} M) for coated-wire electrodes with poly(vinyl chloride) membranes (——) or poly(vinyl butyral) membranes (----). Plasticizer: (1) 2-nitrophenyl 2-ethylhexyl ether; (2) tricresylphosphate; (3) dioctylphthalate; (4) dioctylsebacate; (5) n-butylbenzenesulphonamide; and (6) 2-ethylhexyl 4-hydroxybenzoate.

TABLE 2

Titrimetric determinations with the recommended electrode system

Sample	Molecular mass	Conc.[a] (M)	Titrant	Titration curve		Percentage	
				Overall potential jump (mV)	Steepness (mV/0.1 ml)	Declared	Found[b]
Cationic surfactants							
Cetylpyridinium bromide	402.5	5×10^{-4}	0.25% $NaBPh_4$	540—590	200—250	purum	98.3 ± 2.9 (4)
Cetyltrimethylammonium bromide	364.5	5×10^{-4}	0.25% $NaBPh_4$	450—470	40—60	purum	93.5 ± 1.4 (3)
Septonex	421.5	5×10^{-4}	0.25% $NaBPh_4$	525—540	225—255	purum	97.5 ± 1.7 (5)
Orthosan MB	354	5×10^{-4}	0.25% $NaBPh_4$	550—590	40—50	50	52.4 ± 1.5 (3)
Katexol 298	355	5×10^{-4}	0.25% $NaBPh_4$	290—330	20—30	?	57.6 ± 3.6 (3)
Other cationic substances							
Triphenyltetrazolium chloride	334.8	8×10^{-4}	0.25% $NaBPh_4$	270—300	20—30	purum	79.9 ± 2.3 (8)
Tetraphenylphosphonium chloride	374.8	10^{-3}	0.25% $NaBPh_4$	520—540	140—150	?	81.4 ± 0.8 (5)
Phenyltrimethylammonium iodide	263.1	6×10^{-3}	2.5% $NaBPh_4$	250—300	60—85	p.a.	100.5 ± 1.7 (4)
Retacel	158.1	5×10^{-3}	2.5% $NaBPh_4$	180—210	22—40	55—60	55.3 ± 1.5 (5)
		7.5×10^{-4}	0.25% $NaBPh_4$	130—160	10—16		56.3 ± 1.7 (5)
Anionic surfactants							
Na laurylsulphate	288.5	10^{-4}	10^{-3} M CPB[c]	200—250	24—30	p.a.	97.8 ± 3.9 (5)
		10^{-4}	10^{-3} M Septonex	185—230	8—10		95.6 ± 4.7 (5)
Syntapon LA[d]	280—300	10^{-4}	10^{-3} M CPB	230—280	8—11	30—40?	28.9 ± 3.1 31.0 ± 3.3 (3)
Tensaryl	340—345	2×10^{-4}	10^{-3} M CPB	175—190	8—10	?	47.5 ± 2.7 48.2 ± 2.7 (4)
Dubacid, Na salt	340—345	10^{-4}	10^{-3} M CPB	170—190	16—18	40—50?	39.3 ± 1.8 39.9 ± 1.8 (3)
Dubacid, NH_4 salt	335—340	10^{-4}	10^{-3} M CPB	170—190	16—18	72.5?	71.9 ± 3.4 73.0 ± 3.5 (3)

[a]Approximate concentration in the solution titrated (50 ml). [b]The amount of substance found is expressed statistically as an interval for significance level 0.05 (95% probability); summation of errors (in standardization of titrant and in the titration) was applied. The number of titrations is given in parentheses. [c]Cetylpyridinium bromide. [d]Results for the technical products are given twice, for the lowest and highest molecular masses declared; the declared contents were very approximate.

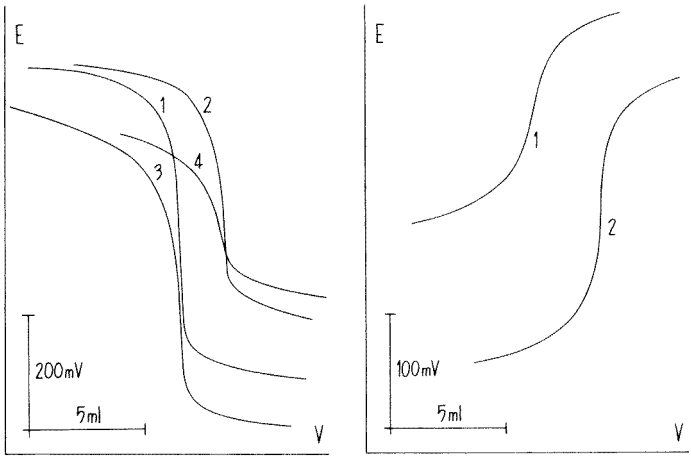

Fig. 2. Potentiometric titration curves of cationic surfactants (ca. 5×10^{-4} M solutions) using 6.3×10^{-3} M $NaBPh_4$ and the 878C coated-wire electrode: (1) cetylpyridinium bromide; (2) Septonex; (3) Orthosan MB; (4) Katexol 298.

Fig. 3. Titration of sodium lauryl sulphate (10^{-4} M) with different cationic agents (10^{-3} M) using the 878C electrode: (1) Septonex; (2) cetylpyridinium bromide.

A PVC membrane electrode plasticized with this solvent (878C) was therefore applied in further determinations.

Titrations of cationic surfactants

Although different titrants for cationic surfactants are listed in Table 1, sodium tetraphenylborate is preferred as the reagent for univalent cations [22]. The general applicability of this reagent was confirmed in this study when titration curves were compared with those recorded with other reagents such as Reinecke salt and sodium picrate. Titrations with $NaBPh_4$ gave the steepest and the largest potential breaks.

Pure samples of cationic surfactants were titrated without difficulties. With increasing mass of the cation, the solubility of the corresponding tetraphenylborate usually decreases and, consequently, both the steepness and the overall size of the potential shift increase. The symmetry of charge distribution and the presence of other groups play important roles [5]. This can be seen from Table 2 where titrations of triphenyltetrazolium and tetraphenylphosphonium salts are included for comparison. Samples of the technical products Orthosan MB and Katexol 298 had to be titrated slowly before the end-point. It should be noted that Retacel (which contains the smaller 2-chloroethyltrimethylammonium cation) was titrated successfully whereas useless titration curves were obtained in titrations of Dextrosil KA (2-hydroxy-3-chloroethyltrimethylammonium ion) because of the presence of the hydrophilic hydroxy group. Examples of some determinations of cationic surfactants are shown in Fig. 2.

Titrations of anionic surfactants

As $NaBPh_4$ has no equivalent among cationic agents, the choice of a suitable titrant for substances of anionic character is less unequivocal (see Table 1). The possibilities were limited by the number and purity of salts available here; therefore, five titrants (cetylpyridinium bromide, cetyltrimethylammonium bromide, phenyltrimethylammonium iodide, Septonex, and tetraphenylphosphonium chloride) were compared for titrations of sodium lauryl sulphate. Cetylpyridinium bromide gave the best titration curves, but Septonex can be recommended for titrations of more concentrated solutions because of its better solubility. As can be seen from the quantitative evaluation in Table 2, both these reagents yield accurate results; some titration curves are recorded in Fig. 3. It could be concluded that sodium lauryl sulphate is useful for the standardization of cationic titrants. Compared with standardization against $NaBPh_4$, however, the reproducibility is less satisfactory though it is adequate considering the nature of the technical products. Phenyltrimethylammonium and tetraphenylphosphonium salts did not give useful titration curves.

Cetylpyridinium bromide was then used in titrations of technical products based on long-chain alkyl sulphates and arenesulphonates. Results were reasonably reproducible. Since the declared percentage composition of these samples was only approximate, all results of the potentiometric titrations were compared with those obtained by a standard method (two-phase titration in alkaline medium using bromocresol green as an indicator [24]) and tested using Lord's u-test. Differences in the results obtained by the two methods were statistically insignificant.

Conclusions

Coated-wire electrodes can be prepared easily even in simply equipped laboratories and can be used advantageously in titrations of ionic surfactants, which are good representatives of determinations based on ion-pair formation. A further advantage of these electrodes is that, for titration purposes, they can be covered with "blank" membranes containing a plastic matrix and a plasticizer only. The organic solvent in the membrane is gradually saturated with the ion-pair formed in the titrated solution after each addition of titrant. Thus the concentration of the compound in the membrane plasticizer increases gradually to an optimal value, limited by distribution ratio of the ion-pair extracted. This is important because larger additions of ion-exchangers to the membranes would reduce the detection limit of the electrodes. Pre-conditioning the electrodes in this way (usually two titrations are sufficient) gives titration curves that are almost identical from the third titration. If the titrimetric system is changed, only one or two titrations are usually needed to re-establish an extraction equilibrium for a new ion-pair. This simplicity in constructing and handling the electrodes together with their low cost should help to widen their application in analytical practice.

REFERENCES

1 K. Vytřas, M. Remeš and H. Kubešová-Svobodová, Anal. Chim. Acta, 124 (1981) 91.
2 C. Gavach and P. Seta, Anal. Chim. Acta, 50 (1970) 407.
3 A. G. Fogg, A. S. Pathan and D. T. Burns, Anal. Chim. Acta, 69 (1974) 238.
4 J. Vošta and J. Havel, Scripta Fac. Sci. Nat., Univ. Purkynianae Brunensis, Chem., 3 (1973) 99.
5 K. Vytřas, Collect. Czech. Chem. Commun., 42 (1977) 3168.
6 M. Kataoka, M. Kudoh and T. Kambara, Denki Kagaku, 46 (1978) 548.
7 S. Pinzauti and E. La Porta, J. Pharm. Pharmacol., 31 (1979) 573.
8 M. Kataoka, H. Tanaka and T. Kambara, Denki Kagaku, 47 (1979) 21.
9 I. A. Borisova and I. A. Gurev, Zavod. Lab., 45 (1979) 309.
10 I. A. Gurev and T. S. Vyatchanina, Zh. Anal. Khim., 34 (1979) 976.
11 I. A. Gurev, G. M. Lizunova and N. S. Bulanova, Zh. Anal. Khim., 34 (1979) 1809.
12 R. A. Llenado, Anal. Chem., 47 (1975) 2243.
13 M. Kataoka and T. Kambara, Denki Kagaku, 43 (1975) 209.
14 D. F. Anghel, G. Popescu and N. Ciocan, Mikrochim. Acta, (1977/II) 639.
15 N. Ciocan and D. F. Anghel, Fresenius Z. Anal. Chem., 290 (1978) 237.
16 W. Selig, Mikrochim. Acta, (1979/II) 437.
17 W. Selig, Microchem. J., 25 (1980) 200.
18 W. Selig, Fresenius Z. Anal. Chem., 300 (1980) 183.
19 G. J. Moody and J. D. R. Thomas, Lab. Pract., 27 (1978) 285.
20 K. Vytřas, M. Ďajková and M. Remeš, Cesk. Farm., 30 (1981) 61.
21 K. Vytřas, V. Říha and S. Kotrlý, Sb. Ved. Pr., Vys. Sk. Chemickotechnol., Pardubice, 35 (1976) 41.
22 K. Vytřas, Am. Lab., 11 (1979) No. 2, 93; Internat. Lab., 9 (1979) No. 2, 35.
23 T. Higuchi, C. R. Illian and J. L. Tossounian, Anal. Chem., 42 (1970) 1674.
24 A. Blažej, P. Hodul, E. Markušovská, L. Novák, M. Paulovič and I. Vyskočil, Tenzidy, Alfa, Bratislava, 1977, pp. 300—345.

Analytica Chimica Acta, 127 (1981) 173—180
Elsevier Scientific Publishing Company, Amsterdam — Printed in The Netherlands

POTENTIOMETRIC DETERMINATION OF NICOTINE IN TOBACCO PRODUCTS WITH A NICOTINE-SENSITIVE LIQUID MEMBRANE ELECTRODE

C. E. EFSTATHIOU, E. P. DIAMANDIS and T. P. HADJIIOANNOU*
Laboratory of Analytical Chemistry, University of Athens, Athens (Greece)
(Received 12th December 1980)

SUMMARY

A simple potentiometric method with standard additions is described for the rapid determination of nicotine in tobacco products. A nicotine-sensitive electrode with a liquid membrane of nicotine hydrogen tetra(*m*-chlorophenyl)borate dissolved in *o*-nitrotoluene is used. The electrode exhibits near-Nernstian response to monoprotonated nicotine cation activity from 0.08 to 10^{-5} M, in the pH range 4—7. Nicotine down to 2 mg per g of sample can be determined with a standard deviation of about 0.5 mg of nicotine. Comparison with an official method gave satisfactory results.

Ion-selective electrodes are used extensively for the quality control of various products. Commercially available ion-selective electrodes have been successfully applied for determinations of traces of nitrate and ammonia in tobacco, and of hydrogen cyanide, hydrogen sulfide, nitrogen oxides and ammonia in tobacco smoke [1].

Nicotine is the most important alkaloid of tobacco, occurring in relatively large quantities (2—8%) as its malate or citrate salt in tobacco leaves [2]. Nicotine is determined routinely during quality control of tobacco and tobacco products. In all established methods, nicotine is separated from its natural matrix by steam distillation and subsequently determined spectrophotometrically by direct measurements at 259 nm [3].

Recently, several sensitive potentiometric sensors for some organic bases of pharmaceutical importance have been reported. Electrodes have been constructed that are sensitive to the following compounds: methacholine, neostigmine [4], ephedrine [5], novocaine [6], codeine, morphine, ethylmorphine [7], and strychnine [8]. These electrodes are generally sensitive but have a narrow spectrum of possible applications because of their nature and their limited selectivity. This drawback is partially counterbalanced by their relatively convenient and inexpensive construction, making their use acceptable in certain cases.

In this paper, a nicotine-sensitive liquid-membrane electrode is described. The liquid ion-exchanger consists of nicotine hydrogen tetra(*m*-chlorophenyl)borate, ($NicH^+$)($TCPB^-$), dissolved in *o*-nitrotoluene. This electrode

is sufficiently selective to be used for the determination of nicotine in tobacco products without any prior separation. With a standard addition technique, down to 2 mg of nicotine per g of sample can be determined potentiometrically with a standard deviation of about 0.5 mg of nicotine per g of sample.

EXPERIMENTAL

Apparatus

The nicotine-sensitive electrode was used with an Orion 90-01-00 Ag/AgCl single-junction reference electrode; its chamber was filled with Orion 90-00-01 equitransferent solution. E.m.f. values were measured with an Orion Ion-analyzer (Model 801 digital pH/pIon meter) and pH with a Metrohm pH meter (Model E350B). All solutions were measured at ambient temperature with constant magnetic stirring.

Reagents

All solutions were prepared with deionized distilled water from reagent-grade materials. Sodium tetra(*m*-chlorophenyl)borate, NaTCPB, was prepared as described by Jarzembowski et al. [9].

Standard 0.1000 M nicotine. Dissolve 4.056 g of nicotine (British Drug Houses) in 200 ml of water, adjust the pH to 6.0 ± 0.1 with 1 M HCl and dilute to exactly 250 ml with water (solution A). Store this solution in a refrigerator.

Nicotine electrode liquid ion-exchanger. Dissolve 0.096 g of NaTCPB (0.20 mmol) in 2 ml of water and mix the resulting solution with 2.00 ml of solution A. Extract the resulting heavy precipitate of ($NicH^+$)($TCPB^-$) into 10.00 ml of *o*-nitrotoluene. Filter the organic layer through a filter paper containing 1—2 g of anhydrous sodium sulfate. The filtrate should be clear and light yellow. This solution is approximately 0.020 M in ($NicH^+$) ($TCPB^-$) and is almost saturated.

Phosphate buffer (0.041 M, pH 6.3). Mix 0.20 M sodium hydroxide and 0.055 M phosphoric acid solutions, in a ratio of 1:3.

Procedures

Electrode preparation. An Orion liquid-membrane electrode barrel (Model 92) is used as the electrode assembly with a Millipore LCWPO-1300 teflon membrane. After assembly in the usual manner, the internal reference solution (solution A is suitable) and the liquid ion-exchanger are injected into the appropriate ports. When not in use, the electrode is kept in air. The electrode should be immersed in a dilute nicotine solution (10^{-3}—10^{-2} M, pH 6—7) for 10 min before each series of measurements.

Determination of calibration slope. Pipet 20.0 ml of phosphate buffer solution into the measurement cell (a 50-ml beaker), immerse the electrodes in the solution, start stirring at the maximum speed at which air bubbles

are not formed, and add 30 μl of solution A. Read the e.m.f. when it has stabilized to ±0.1 mV (0.5—2 min). Continue with four more increments of solution A (50, 100, 100, 100 μl) and read the meter after each addition. Calculate the slope, S, of the calibration curve, i.e., E (mV) vs. logarithm of analytical nicotine concentration. Repeat the measurements if the correlation coefficient is less than 0.999. In case of consistent curvature in the lower concentration range, refill the nicotine-sensitive electrode.

Determination of nicotine in tobacco products. Pulverize the tobacco sample (from cigarettes, cigars or pipe tobacco) with a mortar and pestle. Into 20-ml vials with well-fitting stoppers, weigh appropriate amounts of the pulverized samples containing 3—20 mg of nicotine. Pipet 10.00 ml of 0.20 M sodium hydroxide solution into each vial, stopper the vials tightly, shake and immerse them in a water bath, thermostatted at 70 ± 2°C, for 45 min with frequent shaking. Cool the vials and centrifuge at 3000 rpm for 5 min. Transfer to the measurement cell 5.00 ml of the supernatant brown extract and 15.00 ml of 0.055 M phosphoric acid solution, immerse the electrodes in the solution (immersing the electrodes in the alkaline extract before neutralization will cause erratic responses), start stirring, and record the corresponding potential, E_1. Add 100 μl of solution A and record the new potential, E_2.

Calculate the amount of nicotine from the equation: nicotine (mg/sample) $= 3.245\,[1.005 \cdot 10^{(E_2-E_1)/S_{-1}}]^{-1}$. Instead of this rather inconvenient equation, a nomogram (Fig. 1) can be used; if solution A is not 0.1000 M, appropriate corrections must be made.

RESULTS AND DISCUSSION

Membrane material

The nicotine (Nic) molecule forms mono- and di-protonated species:

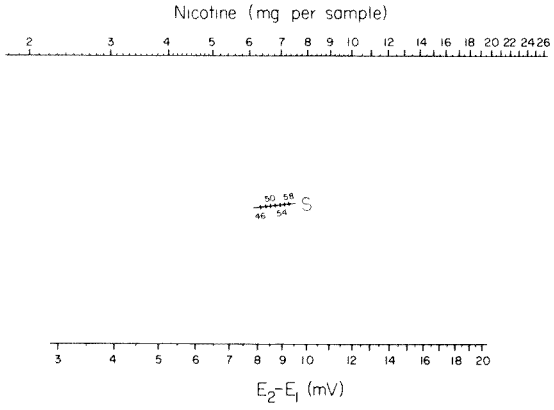

Fig. 1. Nomogram for the direct calculation of nicotine, in mg per sample, for given $E_2 - E_1$ and S values.

$$\text{Nic} \underset{OH^-}{\overset{H^+}{\rightleftharpoons}} \text{NicH}^+ \underset{OH^-}{\overset{H^+}{\rightleftharpoons}} \text{NicH}_2^{2+}$$

For $NicH_2^{2+}$, $pK_1 = 3.04$, $pK_2 = 7.84$, and so $NicH^+$ is the predominant species in the pH range 4—7. If equimolar amounts of nicotine and NaTCPB solutions are mixed in this pH range, $(NicH^+)(TCPB^-)$ precipitates; little of either reactant remains in the supernatant solution which indicates the 1:1 composition. This ion associate is the active ingredient of the liquid ion-exchanger used.

Sodium tetra(*m*-chlorophenyl)borate was chosen because it forms salts, which are generally sparingly soluble in water but soluble in oils, with several compounds containing basic nitrogen atoms and its aqueous solutions are more stable than those of sodium tetraphenylborate [9]. *o*-Nitrotoluene was chosen as the solvent because it gives faster and more complete extraction of $(NicH^+)(TCPB^-)$ than the other solvents tested (1-decanol, nitrobenzene, chlorobenzene, and *o*-dichlorobenzene).

Effect of pH

To check the pH-dependence of the potential of the nicotine electrode, potential—pH curves at various nicotine concentrations were constructed. The pH of the initial solution was altered by addition of very small volumes of hydrochloric acid. The plots (Fig. 2) show that the potential is little affected by pH in the range 4—7, in accordance with the fact that the electrode responds mainly to the monoprotonated nicotine species. At higher pH values there is a gradual decrease in potential because of the gradual increase in the concentration of unprotonated nicotine. Prolonged immersion of the electrode in alkaline solutions causes deterioration of its response, probably because of back-extraction of nicotine from the membrane to the aqueous phase. The movement of the electrode response below pH 4 is inconsistent for the three concentration levels tested. Probably, the electrode becomes progressively sensitive to $NicH_2^{2+}$, so that the slope factor decreases; this is indicated by the gradual decreasing difference in the potentials for the three concentrations.

Characteristics of the electrode

Linear response range. Typical calibration curves for the electrode under different experimental conditions are shown in Fig. 3. The response is linear in the range 0.08—10^{-5} M for pure nicotine solutions (curve A). In the presence of phosphate buffer (curves B and C), the linear range and limit of detection decrease because of electrode response to sodium ions. At pH 2.7 (curve D), there is practically no linear range and the slope is much smaller, indicating response to $NicH_2^{2+}$ species.

Selectivity coefficients. The interference of various ions was studied by the mixed solution method and the selectivity coefficients, $k^{pot}_{NicH^+,j}$, were calculated from

$$k^{pot}_{NicH^+,j} = [(10^{(E_2 - E_1)/S})\alpha_{NicH^+} - \alpha'_{NicH^+}]/\alpha_j^{1/z}$$

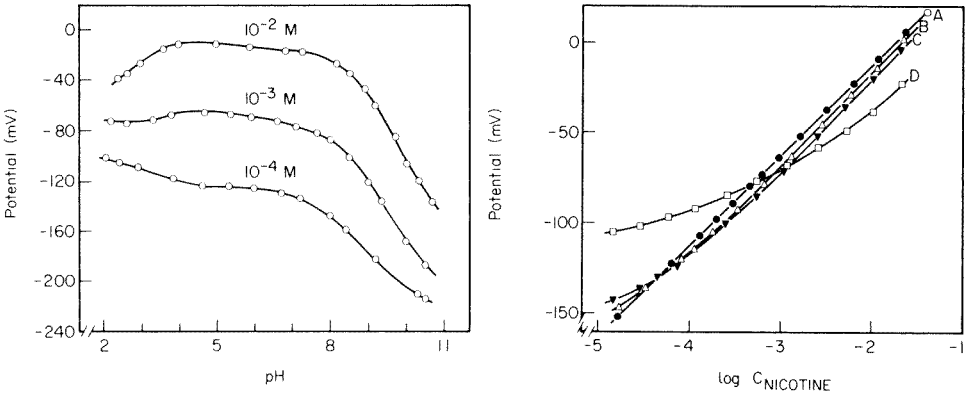

Fig. 2. Effect of pH on the potential of the nicotine-sensitive electrode.

Fig. 3. Calibration curves for the nicotine-sensitive electrode: (A) in pure nicotine solutions adjusted with HCl to pH 6—6.5; (B) in NaH_2PO_4—Na_2HPO_4 buffer, 0.059 M, pH 6.3; (C) as in B, but with a total phosphate concentration of 0.0083 M; (D) in sodium citrate—citric acid buffer, 0.059 M, pH 2.7.

where E_1 is the potential in a nicotine solution of activity α_{NicH^+}, E_2 is the potential in a solution containing nicotine and interfering cation j of activities α'_{NicH^+} and α_j, respectively, S is the electrode slope, and z is the valency of the cation j. The selectivity coefficients obtained are presented in Table 1.

Response times. The electrode provides stable potential readings (±0.1 mV) within 30 s to 2 min, depending on the actual nicotine concentration, presence of interferences, pH, etc. Generally, fast response (less than 1 min) is observed when the electrode is used in the proposed buffer solution.

Stability of response. The electrodes exhibited a day-to-day reproducibility within ±2 mV for nicotine concentrations in the range 2×10^{-4}—2×10^{-3} M,

TABLE 1

Potentiometric selectivity coefficients for the nicotine-sensitive electrode

Interference j	[j] (M)	[$NicH^+$] (M)	$k^{pot}_{NicH^+,j}$
Li^+	1.7×10^{-2}	4.2×10^{-4}	1.6×10^{-2}
Na^+	1.7×10^{-2}	4.2×10^{-4}	1.6×10^{-2}
K^+	1.7×10^{-2}	4.2×10^{-4}	1.4×10^{-2}
NH_4^+	1.7×10^{-2}	4.2×10^{-4}	1.1×10^{-2}
Ca^{2+}	1.7×10^{-2}	4.2×10^{-4}	4.0×10^{-3}
Mg^{2+}	1.7×10^{-2}	4.2×10^{-4}	3.5×10^{-3}
$(CH_3)_4N^+$	1.7×10^{-3}	4.2×10^{-3}	2.5
Pyridine H^+	1.7×10^{-3}	4.2×10^{-3}	1.0
Pyrrolidine H^+	1.7×10^{-3}	4.2×10^{-3}	0.18
Piperidine H^+	1.7×10^{-3}	4.2×10^{-3}	0.36

actually used in the analytical application, provided that the electrode was not used under unfavorable extreme conditions, i.e., in highly acidic or alkaline solutions or in the presence of strong interferences.

Electrode aging has no effect on the response time but has a marked effect on the slope S. The electrodes tested had an initial slope of about 58 mV/concentration decade but in one month of normal use, the slope decreased to about 48 mV/concentration decade. This not unusual disadvantage must be allowed for by determining the slope before each series of measurements because the slope must be accurately known for the standard addition method.

The electrode must be refilled when the liquid ion-exchanger has been exhausted or the supporting membrane has been damaged, and stable potentials are no longer obtainable.

Potentiometric titration of nicotine

The electrode can also be used as indicator electrode for the precipitation titration of nicotine with sodium tetraphenylborate. Such titrations can be used for the determination of the titer of relatively concentrated (ca. 0.01 M) nicotine solutions. In Fig. 4 two typical titration curves of nicotine with sodium tetraphenylborate are shown.

Treatment of samples and analytical results

Extraction of nicotine from tobacco products was incomplete with water or buffer at any temperature. Extraction with 0.2 M sodium hydroxide was incomplete at room temperature. The selected temperature and time of the alkaline extraction ensure complete separation of nicotine from its natural matrix provided that the sample is finely powdered. Erratic results were obtained when the electrodes were directly immersed in the tobacco suspension. Centrifugation was found to be the best way to remove the fine tobacco particles.

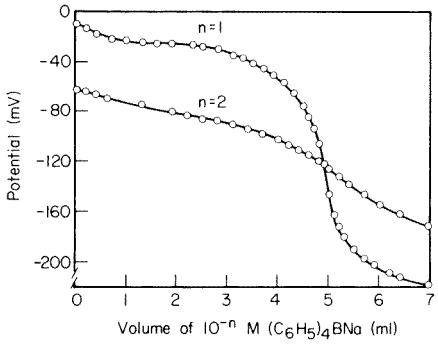

Fig. 4. Titration curves of 50.0 ml of $1.00 \times 10^{-(n+1)}$ M nicotine with 10^{-n} M sodium tetraphenylborate at pH 6.0.

TABLE 2

Potentiometric determination of nicotine in pure aqueous solutions with the nicotine-sensitive electrode
(Results are given as mg/20 ml)

Taken	0.65	0.97	1.61	2.26	2.58	3.21
Found[a]	0.69	0.96	1.63	2.30	2.63	3.32
Found[b]	0.69	0.97	1.56	2.20	2.55	3.07

[a]Based on the calibration curve obtained for the determination of S. [b]Based on the determined value of S and the difference of potential response after the addition of 100 μl of solution A (1.62 mg of nicotine).

For the determination of nicotine in aqueous solutions either the calibration curve method or the standard addition method can be used. Results for both methods are shown in Table 2.

The method was applied to the determination of nicotine in various brands of cigarettes, cigars and pipe tobacco. Nicotine was determined by both the proposed method and the official AOAC method [3]. Typical results are shown in Table 3. Results are generally in good agreement but the potentiometric method is less precise than the official method.

The accuracy of the proposed method was further checked by means of recovery experiments carried out on one representative tobacco sample. The results are shown in Table 4.

Conclusions

The potentiometric method for the determination of nicotine eliminates prior separation steps involving steam distillation techniques. Consequently a large number of samples may be processed simultaneously. The selectivity

TABLE 3

Comparison of potentiometric and AOAC methods for the determination of nicotine in tobacco products

Sample	Nicotine found (mg g^{-1})		Difference
	Present method[a]	AOAC method[b]	
1[c]	3.3 ± 0.2	2.7	0.6
2	10.0 ± 0.3	9.8	0.2
3	13.5 ± 0.3	12.9	0.6
4	14.8 ± 0.2	14.3	0.5
5	15.9 ± 0.6	16.6	−0.7
6	16.1 ± 0.5	15.8	0.3
7	16.7 ± 0.3	15.9	0.8
8	20.6 ± 0.9	19.9	0.7
9	20.8 ± 0.8	21.2	−0.4
			Av. 0.53

[a]Average and standard deviation of five measurements. [b]The standard deviation for the AOAC method was about 0.1 mg g^{-1}. [c]Cigarette tobacco partially extracted with ether.

TABLE 4

Recovery of nicotine added to tobacco samples

Amount of nicotine (mg per sample)			Recovery (%)
Initially present	Added	Found	
1.82	0.97	2.83	104.1
2.74	0.97	3.79	108.2
1.62	1.95	3.48	95.4
2.93	1.95	4.73	92.3
1.40	2.92	4.29	99.0
2.75	2.92	5.52	94.9
			Av. 98.9

and the sensitivity of the described nicotine-sensitive electrode are sufficient for the proposed application. This electrode may find a number of possible applications in the tobacco industry, such as in the quality control of tobacco products and in the process control by continuous monitoring of the nicotine content of various effluents and wastes.

The authors thank S. Michalakakis for the synthesis of NaTCPB and the Tobacco Institute of Greece for the results obtained by the standard method. This research was financially supported in part by the Greek National Institute of Research.

REFERENCES

1 G. P. Morie, Beitrage zur Tabakforschung, 9(1) (1977) 19.
2 Martindale, Extra Pharmacopeia, 25th edn., The Pharmaceutical Press, London, 1967, p. 840.
3 W. Horwitz (Ed.), Official methods of analysis of the Association of Official Analytical Chemists, 12th edn., Assoc. Off. Anal. Chem., Washington, DC, 1975, p. 54.
4 K. Kina, N. Maekawa and N. Ishibashi, Bull. Chem. Soc. Jpn., 46 (1973) 2772.
5 K. Fukumachi, R. Nakagawa, M. Morimoto and N. Ishibashi, Bunseki Kagaku, 24 (1975) 428.
6 E. Hopirtean and F. Kormos, Stud. Univ. Babes-Bolyai Ser. Chem., 22 (1977) 35.
7 T. Goina, S. Hobai and L. Rozenberg, Farmacia (Bucharest), 26(3) (1978) 141.
8 S. M. S. Hassan and M. B. Elsayes, Anal. Chem., 51 (1979) 1651.
9 F. Jarzembowski, F. Cassareto, H. Posvic and C. E. Moore, Anal. Chim. Acta, 73 (1974) 409.

Analytica Chimica Acta, 127 (1981) 181—193
Elsevier Scientific Publishing Company, Amsterdam — Printed in The Netherlands

LOSSES OF SILVER, ARSENIC, CADMIUM, SELENIUM AND ZINC TRACES FROM DISTILLED WATER AND ARTIFICIAL SEA-WATER BY SORPTION ON VARIOUS CONTAINER SURFACES

R. MASSEE and F. J. M. J. MAESSEN*

Laboratory for Analytical Chemistry, University of Amsterdam, Nieuwe Achtergracht 166, 1018 WV Amsterdam (The Netherlands)

J. J. M. DE GOEIJ

Interuniversity Reactor Institute, Mekelweg 15, 2629 JB Delft (The Netherlands)

(Received 2nd January 1981)

SUMMARY

Sorption losses were studied for Ag, As, Cd, Se, and Zn at a concentration level of 10^{-7} M from distilled water and artificial sea-water during storage in containers made of borosilicate glass, high-pressure polyethylene, or polytetrafluoroethylene. Apart from pH (1, 2, 4, and 8.5) and storage time (1 min to 28 days), special attention was paid to the effect of the ratio of inner container surface to sample volume. The results are compared with literature data. In addition, a survey is given of literature references on sorption of 41 elements from aqueous solutions under different experimental conditions.

Interest in the concentration of trace elements in water, ranging from drinking water to sea-water, has never been greater than at this time. Consequently, a very significant proportion of current research in analytical chemistry is directed towards improved methods of measuring trace concentrations. However, sampling, sample storage, and sample preparation may easily constitute a weak, or even the weakest, link in the total analytical chain. Serious losses of trace elements may occur by sorption on the materials to which the samples are exposed during storage and measurement, invalidating the final results.

Various studies have been published dealing with sorption phenomena in relation to matrix composition (e.g. salinity and organic constituents), concentration and chemical form of the analyte, nature of the container material, contact time, and addition of complexing agents or acids. Hitherto minor attention has been paid to the effect of the specific surface, i.e., the ratio of the inner container surface in contact with solution, to the volume of the solution. This ratio is denoted in the present study by R (cm^{-1}).

In analytical practice the numerical value of R varies notably with the container dimensions. The R values of commonly used sample bottles with volumes of 1 l and 0.1 l are about 0.5 and 1 cm^{-1}, respectively. For tubes of small diameter, such as are employed in automatic dilution apparatus, R may even reach a value of 50 cm^{-1}.

The study described here was undertaken in the frame of an assessment of the applicability of electrothermal atomic absorption spectrometry for direct determinations of Ag, As, Cd, Se, and Zn in sea-water. In this context, the sorption behaviour of these selected trace elements was examined in distilled water and artificial sea-water using polyethylene, polytetrafluoroethylene (PTFE; teflon), and borosilicate glass as typical container materials.

EXPERIMENTAL

Reagents and materials

Distilled water was prepared by distillation in quartz of demineralized water. For the preparation of artificial sea-water the following reagents (p.a., Merck) were dissolved in 10 l of distilled water: 69.9 g of $MgSO_4 \cdot 7H_2O$, 50.5 g of $MgCl_2 \cdot 6H_2O$, 14.8 g of $CaCl_2 \cdot 2H_2O$, 1.00 g of KCl, 1.77 g of Na_2CO_3, and 268 g of NaCl. Batches of distilled water and artificial sea-water were adjusted to pH 1, 2, 4 or 8.5 by suitable additions of nitric acid or sodium hydroxide.

The following radiotracers were used: ^{110}Ag (1.2 mCi mg^{-1}), ^{74}As (0.9 mCi mg^{-1}), ^{109}Cd (0.27 mCi mg^{-1}), ^{75}Se (3.8 mCi mg^{-1}), and ^{65}Zn (1.3 mCi mg^{-1}) (Radiochemical Centre, Amersham, England). From these radionuclides stock solutions were prepared at radioactive concentrations of 5—10 μCi ml^{-1} and a mass concentration of 10^{-4} M by adding amounts of the corresponding stable elements. The acidity of the stock solutions was adjusted to pH 2 by adding nitric acid.

The containers tested were 200-ml borosilicate glass bottles (Duran, Jena, Mainz, F.R.G.), 100-ml high-pressure polyethylene bottles (Kautex, Bonn-Holzlar, F.R.G.), and 100-ml polytetrafluoroethylene bottles (Gaflon, Plastic Omnium, Levallois-Perret, France). New bottles were used exclusively. The differences in R values were achieved by adding pieces of the material considered. To avoid the possibility of highly active sites for sorption arising from fresh fractures, the edges of the added pieces of borosilicate glass were sealed in a flame. Prior to the use of all materials, the surfaces were cleaned by shaking with 8 M nitric acid for at least 3 days and by washing five times with distilled water.

Procedures

Working solutions (1 l) which were 10^{-7} M in one of the elements to be studied were prepared by appropriate addition of the radioactive stock solutions to pH-adjusted distilled water and artificial sea-water. After the pH had been checked, 100-ml portions were transferred to the bottles to be tested. The filled bottles were shaken continuously and gently in an upright position, at room temperature and in the dark. At certain time intervals, ranging from 1 min to 28 days, 0.1-ml aliquots were taken. These aliquots were counted in a 3 × 3-in. NaI(Tl) well-type scintillation detector, coupled to a single-channel analyser with a window setting corresponding to the γ-rays to be measured.

The counting times were chosen in such a way that at least 15 000 pulses were counted. The sorption losses were calculated from the activities of the aliquots and the activity of the aliquot taken at time zero. Taking into account the various sources of errors, mainly counting statistics, the maximum imprecision is about 3%. Therefore, calculated sorption losses of 3% and lower are omitted from the listings as being not significant.

RESULTS AND DISCUSSION

Tables 1—3 show the percent loss as a function of time of, respectively, silver, cadmium, and zinc from distilled water and artificial sea-water stored in polyethylene, borosilicate glass, and PTFE at various pH and R values.

Silver

At pH 1 and 2 sorption from either distilled water or artificial sea-water was not observed for any of the types of container materials. However, from distilled water at pH 4 silver was substantially sorbed on polyethylene, borosilicate glass, and PTFE (Table 1). In polyethylene, silver was almost completely lost; in the case of larger R values the rate of loss increased. In borosilicate glass, inconsistent behaviour was observed which could not be explained, e.g., the percent sorption at pH 4 for R = 1.0 cm^{-1} and R = 4.2 cm^{-1} after 24 h (cf. Table 1, columns 6 and 7). After 28 days the loss of silver appeared to be independent of the R value considered. In PTFE, silver was stable in solution up to 24 h in distilled water. At the end of a 28-day storage period the loss of silver in the PTFE vessel with R = 5.5 cm^{-1} was almost 4 times higher than in the vessel with R = 1.0 cm^{-1}.

From artificial sea-water at pH 4, losses of silver were observed only in borosilicate glass containers. At pH 8.5, silver was sorbed from both distilled water and artificial sea-water regardless of the container material. The same anomaly as in distilled water was observed, though to a lesser extent.

In the literature, there have been several reports of losses of silver [1—8]. Streumpler [2] noticed no sorption from ca. 0.5×10^{-9} M silver solutions on borosilicate and polyethylene container surfaces at pH 2. However, when the test solutions were stored at pH 4, tests with both types of container material showed that approximately 50% of the silver was sorbed. Streumpler also noticed that after ageing for a few days some containers exhibited erratic sorption characteristics; this is confirmed by the present findings.

Schutz and Turekian [7] concluded that no significant sorption of silver occurred when sea-water was stored at its natural pH in pyrex glass bottles for a period up to 6 months. Robertson [8] reported insignificant sorption on pyrex glass and polyethylene surfaces if the sea-water was acidified with hydrochloric acid to pH 1.5. West et al. [3, 4] studied the sorption behaviour of silver under various conditions and reported losses of 20—30% on borosilicate glass from a 0.01 M NaCl solution at a pH of about 4.6 after contact times up to 248 h, whereas losses of 7—10% were observed from 0.1 M NaCl

TABLE 1

Sorption behaviour of silver

Matrix	Distilled water												Artificial sea-water											
Material	Polyethylene				Borosilicate glass				PTFE				Polyethylene				Borosilicate glass				PTFE			
pH	4		8.5		4		8.5		4		8.5		4		8.5		4		8.5		4		8.5	
R (cm^{-1})	1.4	3.4	1.4	3.4	1.0	4.2	1.0	4.2	1.0	5.5	1.0	5.5	1.4	3.4	1.4	3.4	1.0	4.2	1.0	4.2	1.0	5.5	1.0	5.5
Contact time	Sorption (%)												Sorption (%)											
1 min	—[a]	8	—	12	—	—	—	—	—	—	—	—	—	—	—	7	—	—	—	—	—	—	—	—
30 min	7	12	19	33	—	3	6	19	—	—	—	10	—	—	7	8	—	—	—	—	—	—	—	3
1 h	10	15	25	36	—	4	9	21	—	—	—	10	—	—	6	5	—	—	3	3	—	—	—	4
2 h	12	20	36	44	3	5	15	27	—	—	3	13	—	—	10	9	—	—	3	5	—	—	—	6
4 h	14	28	45	49	4	8	18	35	—	—	3	14	—	—	14	13	—	—	3	4	—	—	—	7
8 h	17	42	51	49	9	12	23	42	—	—	4	18	—	—	16	18	3	4	5	10	—	—	—	8
24 h	25	66	72	49	32	18	26	48	4	6	5	25	—	—	24	28	4	4	6	9	—	—	6	12
2 d	30	83	76	60	72	31	28	58	3	5	7	24	—	—	35	36	6	7	10	31	—	—	13	17
3 d	37	91	75	74	83	56	65	56	5	18	9	26	—	—	44	45	6	11	31	80	—	—	13	23
7 d	51	88	66	78	84	79	70	60	6	32	11	27	—	—	64	64	74	60	27	73	—	—	14	29
14 d	83	95	61	98	85	70	70	57	7	55	19	28	—	—	66	72	81	76	39	84	—	—	20	30
21 d	95	100	59	100	84	75	72	64	10	54	20	27	—	—	58	77	80	73	39	64	—	—	26	37
28 d	96	100	59	100	82	80	72	63	15	55	22	28	—	—	46	78	82	71	40	67	—	—	27	37

[a]—Denotes a loss smaller than 3%.

TABLE 2

Sorption behaviour of cadmium

Matrix	Distilled water												Artificial sea-water											
Material	Polyethylene				Borosilicate glass				PTFE				Polyethylene				Borosilicate glass				PTFE			
pH	4		8.5		4		8.5		4		8.5		4		8.5		4		8.5		4		8.5	
R (cm^{-1})	1.4	3.4	1.4	3.4	1.0	4.2	1.0	4.2	1.0	5.5	1.0	5.5	1.4	3.4	1.4	3.4	1.0	4.2	1.0	4.2	1.0	5.5	1.0	5.5
Contact time	Sorption (%)												Sorption (%)											
1 min	—[a]	—	—	—	—	—	—	—	—	—	—	—	—	—	—	—	—	—	—	—	—	—	—	—
30 min	—	—	5	32	—	—	5	25	—	—	8	36	—	—	—	—	—	—	—	—	—	—	—	—
1 h	—	—	7	69	—	—	6	26	—	—	7	38	—	—	—	—	—	—	—	—	—	—	—	—
2 h	—	—	—	70	—	—	8	26	—	—	5	53	—	—	—	—	—	—	—	—	—	—	—	—
4 h	—	—	—	70	—	—	8	26	—	—	5	58	—	—	—	—	—	—	—	—	—	—	—	—
8 h	—	—	—	59	—	—	8	29	—	—	6	57	—	—	—	—	—	—	—	—	—	—	—	—
24 h	—	—	—	47	—	—	10	32	—	—	10	48	—	—	—	—	—	—	—	—	—	—	—	—
2 d	—	—	—	30	—	—	10	32	—	—	8	45	—	—	—	—	—	—	—	—	—	—	—	—
3 d	—	—	—	29	—	—	11	30	—	—	12	43	—	—	—	—	5	—	—	—	—	—	—	—
7 d	—	—	—	31	—	—	9	31	—	—	13	46	—	—	—	—	14	40	—	—	—	—	—	—
14 d	—	—	—	30	—	—	—	—	—	—	14	44	—	—	—	—	13	43	—	—	—	—	—	—
21 d	—	—	—	30	—	—	—	—	—	—	15	45	—	—	—	—	15	41	—	—	—	—	—	—
28 d	—	—	—	31	—	—	—	—	—	—	15	46	—	—	—	—	14	36	—	—	—	—	—	—

[a]—Denotes a loss smaller than 3%.

TABLE 3

Sorption behaviour of zinc

Matrix	Distilled water												Artificial sea-water											
Material	Polyethylene				Borosilicate glass				PTFE				Polyethylene				Borosilicate glass				PTFE			
pH	4		8.5		4		8.5		4		8.5		4		8.5		4		8.5		4		8.5	
R (cm^{-1})	1.4	3.4	1.4	3.4	1.0	4.2	1.0	4.2	1.0	5.5	1.0	5.5	1.4	3.4	1.4	3.4	1.0	4.2	1.0	4.2	1.0	5.5	1.0	5.5
Contact time	Sorption (%)												Sorption (%)											
1 min	—[a]	—	—	—	—	—	21	20	—	—	—	—	—	—	—	—	—	—	—	—	—	—	—	—
30 min	—	—	—	66	—	—	24	21	—	—	5	12	—	—	—	—	—	—	12	31	—	—	—	—
1 h	—	—	—	65	—	—	23	22	—	—	3	16	—	—	—	—	—	—	9	31	—	—	—	—
2 h	—	—	3	64	—	—	24	21	—	—	5	22	—	—	—	—	—	—	10	29	5	—	—	—
4 h	—	—	3	60	—	—	25	21	—	—	4	28	—	—	—	—	—	—	9	30	4	—	—	—
8 h	—	—	5	58	—	—	25	23	—	—	3	33	—	—	—	—	—	—	9	28	5	—	—	—
24 h	—	—	8	56	—	—	26	22	—	—	5	27	—	—	—	—	—	—	5	26	4	—	—	—
2 d	—	—	9	52	—	—	25	20	—	—	3	25	—	—	—	—	—	—	4	21	4	—	—	—
3 d	—	—	6	53	—	—	20	22	—	—	3	19	—	—	—	—	—	—	4	18	5	—	—	—
7 d	—	—	11	57	—	—	—	—	—	—	4	20	—	—	—	—	10	4	3	9	4	—	—	—
14 d	—	—	11	57	—	—	—	—	—	—	5	20	—	—	—	—	27	19	—	10	5	—	—	—
21 d	—	—	10	55	—	—	—	—	—	—	4	20	—	—	—	—	25	17	3	9	5	—	—	—
28 d	—	—	12	56	—	—	—	—	—	—	6	20	—	—	—	—	20	19	4	9	5	—	—	—

[a]—Denotes a loss smaller than 3%.

under the same conditions. For distilled water rather erratic sorption characteristics of silver on borosilicate glass and polyethylene were again reported. West et al. also found that sorption of silver on both polyethylene and borosilicate was stronger at pH 4 than at pH 7, which is in contrast with the findings of Dyck [5] and with the results of the present study.

An explanation of the absence of sorption of silver in artificial sea-water at pH 4 and the weak sorption at pH 8.5 onto polyethylene and PTFE may be the formation of $AgCl_2^-$, because this is the predominant form present in sea-water [9]. This suggestion is supported by the findings of West et al. [3, 4] who found less sorption of silver from 0.1 M NaCl than from 0.01 M NaCl solutions.

Since silver is less sorbed on polyethylene and PTFE from a matrix with a high chloride concentration and/or a low pH, it is advisable to acidify samples for determinations of traces of silver with hydrochloric acid to pH $\leqslant 2$ and to store them in polyethylene or PTFE.

Cadmium

At pH 1 and 2, there was no significant sorption for any of the three container materials. At pH 4 sorption of cadmium was observed only from artificial sea-water stored in borosilicate glass. In distilled water at pH 8.5, cadmium was lost onto all three materials, whereas sorption of cadmium was not observed from artificial sea-water. In all cases, the amount of cadmium sorbed increased with increasing R value.

In general, the data from the literature indicate that no sorption of cadmium occurs below pH 4; this was confirmed by the present study. At pH 6, Streumpler [2] measured losses up to 20% from distilled water in 20 days for borosilicate glass containers. Smith [10] found a loss of 10% at pH 6.5 within 24 h in the same material. Shendrikar et al. [11] did not observe significant sorption below pH 7 in either polyethylene, borosilicate glass or flint glass. Gardiner [12] reported a 10% loss of cadmium from natural water, if stored in polyethylene at pH 7.5—8.0. The sorption appeared to be slightly stronger in pyrex than in polyethylene.

In general, the results of the present study indicate losses of cadmium lower than those reported in the literature. However, unambiguous conclusions cannot be drawn because of the lack of information on various parameters, especially about the specific surface. This parameter seems to be critical in considering the sorption phenomena of cadmium, as may be seen from Table 2. Although the pH seems to be the dominant factor in preventing sorption of cadmium, it should be noted that at pH 8.5 and in the case of the highest R value cadmium was substantially sorbed from distilled water, whereas sorption was not observed from artificial sea-water. The absence of sorption of cadmium from sea-water may be explained either by the formation of chloride complexes, analogously to silver, or by competition between cadmium and other bivalent ions (Mg, Ca) in occupying active sorption sites.

In general, it may be concluded that for the determination of trace con-

centrations of cadmium, the sample has to be acidified to pH $\leqslant 4$ and it is usually advantageous to use polyethylene or teflon containers.

Zinc

At pH 4 losses of about 20% of zinc were observed from artificial sea-water stored in borosilicate glass. There was no apparent relation between the R value and the size of the losses. At pH 8.5 zinc was lost from distilled water in all container materials. The rate of loss in polyethylene and PTFE increased with increasing R value. In the case of borosilicate glass, an immediate loss of 20% was observed, whereas after 7 days all the initially sorbed ^{65}Zn activity was found to be in solution again. At pH 8.5 artificial sea-water showed some loss of zinc in polyethylene after 28 days. In borosilicate glass similar effects were observed for sea-water and distilled water, i.e., a decrease of loss with increasing storage time.

Streumpler [2] aged a solution of ca. 10^{-9} M zinc ions in distilled water at pH 2 and 5 in borosilicate glass and polyethylene. After 60 days, a loss (20%) was detected only at pH 5 in borosilicate glass. Contamination by zinc proved to be a real problem, because a blank of 10^{-7} g Zn ml^{-1} was established by leaching zinc from borosilicate containers. Shendrikar et al. [11] studied the sorption behaviour of several elements in the pH range 0—7 stored in pyrex, in flint glass, and in polyethylene. For zinc, only slight adsorption (6.46%) was noticed in flint glass at pH 7. Smith [13] found no losses of zinc within 24 h from 0.5% NaCl stored at pH $\leqslant 5$ in borosilicate glass. At pH 6.5 and 8.0 the losses of zinc were 10% and 50%, respectively. Subramanian et al. [14] investigated the loss of eleven trace metals during storage from both synthetic water samples and natural water samples in pyrex, polyethylene and PTFE. For zinc, only PTFE containers could be used because of a continuous increase in the zinc concentration of the solutions stored in pyrex or polyethylene. No loss of zinc was observed in PTFE containers in the pH range 1.5—8.0.

No significant sorption of zinc from artificial or natural sea-water was noted by Schutz and Turekian [7] in pyrex, by Robertson [8] in polyethylene and pyrex, or by Dokiya et al. [15] in polyethylene, whereas Petrov [16] found appreciable sorption of zinc from sea-water on glass and on polyethylene at pH 7.5 within a period of 2 min. Petrov also noted that sorption decreased with increasing storage times, which is confirmed by the results of the present study.

Although zinc shows a behaviour similar to that of cadmium regarding sorption on polyethylene and PTFE, the results should be interpreted with caution because contamination may affect the equilibrium between the stable zinc and the radioactive zinc.

For the determination of traces of zinc, the sample should be acidified to pH $\leqslant 4$ and the use of PTFE containers is advisable, because of the absence of substantial contamination as reported by Subramanian et al. [14].

Arsenic and selenium

For arsenic (added as sodium arsenate) and selenium (added as sodium selenite), losses were insignificant in all the container materials considered, irrespective of matrix composition. For arsenic, literature data on sorption from aqueous matrices could not be found. For selenium, a few authors have mentioned small losses. Shendrikar and West [17] reported a loss of 4% of selenium within a 15-day period from distilled water at pH 7 in flint glass; losses of about 8% occurred in polyethylene. Acidification reduced the sorption. Recently, Cheam and Agemian [18] studied the stability of Se(IV) and Se(VI) in natural waters. They observed that sorption was dependent on the specific surface, and that Se(VI) was more stable than Se(IV) in aqueous solution. For longer storage times, i.e. over 6 weeks, the formation of algae became a serious source of losses. Schutz and Turekian [7] observed no loss of selenium from sea-water.

As the present study and literature data agree reasonably well, arsenic and selenium are unlikely to suffer serious sorption losses. This is probably related to the fact that both elements, in contrast to silver, cadmium, and zinc, form oxy acids, which are partly dissociated, leading to negatively charged ions.

CONCLUSION

In spite of the availability of a wealth of information on sorption phenomena occurring under more or less realistic conditions of trace determinations, adoption of comprehensive rules for specific analytical problems remains a ticklish matter. The sorption behaviour of trace elements depends on a variety of factors which, taken together, make sorption losses rather difficult to predict. However, the data from this study and from the literature indicate for which elements sorption losses may be expected as a function of a number of factors, such as trace element concentration, container material involved, pH, and salinity. Table 4 lists some literature references on sorption losses of the five elements considered in this study and 37 additional elements.

As is shown above, reduction of contact time and specific surface may be helpful in lowering sorption losses, and acidification with a strong acid will generally prevent the problems of losses by sorption. However, it must be emphasized that the use of acids may drastically change the initial composition of the aqueous sample, making unambiguous interpretation of the analytical results cumbersome or even impossible [40].

For cases of sample storage where losses cannot be excluded a priori, some sort of check is required. This should be done under conditions which are representative of the actual sampling, sample storage, and sample analysis. As this study indicates, the use of radiotracers is helpful in making such checks.

The various factors involved in sorption losses may be classified into four

TABLE 4

Survey on sorption of trace elements from aqueous solution on various materials

Element	Matrix	pH Range	Material[a]	Reference
Ag	Distilled water	5—11	B, M	1
	Distilled water	2—6	B, PE, PP	2
	Distilled water	7	B, PP, T, PS	3, 4[b]
	Distilled water	1.5—4	B, PE, T, B + desicote	5
	Distilled water	7	B, PE, T, B + desicote	6
	Sea-water		B	7
	Sea-water	1.5; 8	B, PE	8
Al	Synth. and natural water	1.5—8	B, PE	14
	Natural water	6.7	PE	22
	0.5% NaCl	1.5—12	B	13
Au	0.5% NaCl	1.5—11	B	10
	Sea-water		PE	41
Ba	Distilled water	1—7	B, PE	11[b]
	Hard water	4—7	B, PP	19
	0.5% NaCl	1.5—11	B	10
Be	Distilled water	1—7	B, PE	11[b]
Ca	0.5% NaCl	1.5—12	B	13
Cd	Distilled water	2—6	B, PE, PP	2
	Distilled water	1—7	B, PE	11[b]
	Distilled water	6—10	B, PE, PP, PVC	20
	Distilled water	1—10	B, PE	21[b]
	Synth. and natural water	1.5—8	B, PE	14
	River water	7.5—8	PE	12
	0.5% NaCl	1.5—11	B	10
Ce	Distilled water	5—11	B, M	1
	Hard water	4—7	B, PE	19
	Natural water	6.7	PE	22
Co	Synth. and natural water	1.5—8	B, PE	14
	Natural water	6.7	PE	22
	0.5% NaCl	1.5—12	B	13
	Sea-water		B	7
	Sea-water	1.5; 8	B, PE	8
Cr	Distilled water		B, PE	23[b]
	Synth. and natural water	1.5—8	B, PE	14
	Natural water	6.7	PE	22
	Sea-water		B	7
	Sea-water		B, PE, PP	24[b]
Cs	Hard water	4—7	B, PP	19
	Sea-water	1.5; 8	B, PE	8
	Sea-water		B	7
Cu	Distilled water	7.5—8	PE	12
	Synth. and natural water	1.5—8	B, PE	14
	0.5% NaCl	1.5—12	B	13
	Estuarine water		PE, T	25[b]
Eu	Distilled water	2—11	B, PE, PP, PS, PVC, T	26
Fe	Distilled water	0—13	B	27
	Distilled water	0—13	PE	28
	Synth. and natural water	1.5—8	B, PE	14

TABLE 4 (continued)

Element	Matrix	pH Range	Material	Reference
	Natural water	6.7	PE	22
	0.5% NaCl	1.5—12	B	13
	Estuarine water		PE, T	25[b]
	Sea-water	1.5; 8	B, PE	8
Hg	Distilled water	0—14	PE	29
	Distilled water	0—14	B	30
	Distilled water	0—7	PE	31
	Distilled water		PE, PP	32
	Distilled water		B, PE	33
	Creek water		PE	34
	Natural water	2; 7	B, PE, PVC	35
	Ice and river water		PE	36
	River water	5—8	PE	37
	River water	7.5—8	PE	12
	Sea-water		PE	15
I	Distilled water	5—11	B, M	1
	Hard water	4—7	B, PP	19
In	0.5% NaCl	1.5—11	B	10
	Sea-water	1.5; 8	B, PE	8
La	Hard water	4—7	B, PP	19
	Natural water	6.7	PE	22
Li	0.5% NaCl	1.5—11	B	10
Mg	0.5% NaCl	1.5—12	B	13
Mn	Distilled water	4—14	B	38
	Distilled water	1—7	B, PE	11[b]
	Synth. and natural water	1.5—8	B, PE	14
	Natural water	6.7	PE	22
	0.5% NaCl	1.5—12	B	13
Na	Distilled water	5—11	B, M	1
Ni	Distilled water	2—6	B, PE, PP	2
	Synth. and natural water	1.5—8	B, PE	14
	0.5% NaCl	1.5—12	B	13
Pb	Distilled water	2—6	B, PE, PP	2
	Distilled water	1—7	B, PE	11[b]
	Distilled water	1—7	B, PE	21[b]
	HNO_3 and H_2O_2		B, PE	39
	Synth. and natural water	1.5—8	B, PE	14
	0.5% NaCl	1.5—12	B	13
Pd	0.5% NaCl	1.5—11	B	10
Pt	0.5% NaCl	1.5—11	B	10
Rb	Sea-water	1.5; 8	B, PE	8
Rh	Hard water	4—7	B, PP	19
	0.5% NaCl	1.5—11	B	10
Ru	Hard water	4—7	B, PP	19
	0.5% NaCl	1.5—11	B	10
Sb	0.5% NaCl	1.5—11	B	10
	Sea-water		B	7
	Sea-water	1.5; 8	B, PE	8
Sc	Natural water	6.7	PE	22
	Sea-water	1.5; 8	B, PE	8

TABLE 4 (continued)

Element	Matrix	pH Range	Material	Reference
Se	Distilled water	0—7	B, PE	17
	Natural water	1.5—7.2	B, PE	18
	Sea-water		B	7
Sn	0.5% NaCl	1.5—11	B	10
Sr	Synth. and natural water	1.5—8	B, PE	14
	Hard water	4—7	B, PP	19
	0.5% NaCl	1.5—12	B	13
	Sea-water	1.5; 8	B, PE	8
Ti	0.5% NaCl	1.5—12	B	13
Tl	0.5% NaCl	1.5—11	B	10
U	Sea-water	1.5; 8	B, PE	8
V	0.5% NaCl	1.5—12	B	13
Y	Hard water	4—7	B, PP	19
Zn	Distilled water	2—6	B, PE, PP	2
	Distilled water	1—7	B, PE	11[b]
	Synth. and natural water	1.5—8	T	14
	0.5% NaCl	1.5—12	B	13
	Sea-water		B	7
	Sea-water	1.5; 8	B, PE	8
	Sea-water		PE	15
	Sea-water	5.0—8.6	B, PE	16
Zr	Hard water	4—7	B, PP	19

[a]B = borosilicate glass, PE = polyethylene, T = polyfluoroethylene, M = metal surfaces, PP = polypropylene, PS = polystyrene, PVC = polyvinylchloride. [b]Complexing agents were also considered.

categories. The first category is concerned with the analyte itself, especially chemical form and concentration. The second category includes the characteristics of the solution, such as the presence of acids (pH), dissolved material (e.g., salinity, hardness), complexing agents, dissolved gases (especially oxygen, which may influence the oxidation state), suspended matter (competitor in the sorption process) and microorganisms (e.g., trace element take-up by algae). The third category comprises the properties of the container, such as its chemical composition, surface roughness, surface cleanliness, and, as this study demonstrates, the specific surface. Cleaning by prolonged soaking in 8 M nitric acid [41] is to be recommended. The history of the containers (e.g., age, method of cleaning, previous samples, exposure to heat) is of importance because it may be of direct influence on the type and number of active sites for sorption. Finally, the fourth category consists of external factors, such as temperature, contact time, access of light, and occurrence of agitation. All of these factors must be considered in assessing the likelihood of sorption losses during a complete analysis.

REFERENCES

1 J. W. Hensley, A. O. Long and J. E. Willard, Ind. Eng. Chem., 41 (1949) 1415.
2 A. W. Streumpler, Anal. Chem., 45 (1973) 2251.
3 F. K. West, P. W. West and F. A. Iddings, Anal. Chem., 38 (1966) 1566.
4 F. K. West, P. W. West and F. A. Iddings, Anal. Chim. Acta, 37 (1967) 112.
5 W. Dyck, Anal. Chem., 40 (1968) 454.
6 R. A. Durst and B. T. Duhart, Anal. Chem., 42 (1970) 1002.
7 D. F. Schutz and K. K. Turekian, Geochim. Cosmochim. Acta, 29 (1965) 259.
8 D. E. Robertson, Anal. Chim. Acta, 42 (1968) 533.
9 E. D. Goldberg and J. P. Riley, in J. P. Riley and G. Skirrow (Eds.), in Chemical Oceanography, Academic Press, London, 1965.
10 A. E. Smith, Analyst, 98 (1973) 209.
11 A. D. Shendrikar, V. Dharmarajan, H. Walker-Merrick and P. W. West, Anal. Chim. Acta, 84 (1976) 409.
12 J. Gardiner, Water Res., 8 (1974) 157.
13 A. E. Smith, Analyst, 98 (1973) 65.
14 K. S. Subramanian, C. L. Chakrabarti, J. E. Sueiras and I. S. Maines, Anal. Chem., 50 (1978) 444.
15 Y. Dokiya, H. Ashikawa, S. Yamazaki and K. Fuwa, Spectrosc. Lett., 7 (1974) 551.
16 Y. M. Petrov, Zh. Anal. Khim., 29 (1974) 686.
17 A. D. Shendrikar and P. W. West, Anal. Chim. Acta, 74 (1975) 189.
18 V. Cheam and H. Agemian, Anal. Chim. Acta, 113 (1980) 237.
19 G. G. Eichholz, A. E. Nagel and R. B. Hughes, Anal. Chem., 37 (1965) 863.
20 W. G. King, J. M. Rodriguez and C. M. Way, Anal. Chem., 46 (1974) 771.
21 W. C. Hoyle and A. Atkinson, Appl. Spectrosc., 33 (1979) 37.
22 P. Benes and E. Steines, Water Res., 9 (1975) 741.
23 A. D. Shendrikar and P. W. West, Anal. Chim. Acta, 72 (1974) 91.
24 T. R. Gilbert and A. M. Clay, Anal. Chim. Acta, 67 (1973) 289.
25 R. E. Pellenbarg and T. M. Church, Anal. Chim. Acta, 97 (1978) 81.
26 F. Ichikawa and T. Sato, Radiochim. Acta, 12 (1969) 89.
27 P. Benes, J. Smetana and V. Majer, Collect. Czech. Chem. Commun., 33 (1968) 3410.
28 P. Benes and J. Smetana, Collect Czech. Chem. Commun., 34 (1969) 1360.
29 P. Benes and I. Rajman, Collect. Czech. Chem. Commun., 34 (1969) 1375.
30 P. Benes, Collect. Czech. Chem. Commun., 35 (1970) 1349.
31 J. H. Lo and C. M. Wai, Anal. Chem., 47 (1975) 1869.
32 R. W. Heiden and D. A. Aiken, Anal. Chem., 51 (1979) 151.
33 C. Feldman, Anal. Chem., 46 (1974) 99.
34 R. V. Coyne and J. A. Collins, Anal. Chem., 44 (1972) 1093.
35 R. M. Rosain and C. M. Wai, Anal. Chim. Acta, 65 (1973) 279.
36 H. V. Weiss, W. H. Shipman and M. A. Guttman, Anal. Chim. Acta, 81 (1976) 211.
37 K. I. Mahan and S. E. Mahan, Anal. Chem., 49 (1977) 662.
38 P. Benes and A. Garbe, Radiochim. Acta, 5 (1966) 99.
39 H. J. Issaq and W. L. Zielinski, Anal. Chem., 46 (1974) 1328.
40 T. M. Florence and G. E. Batley, CRC Critical Reviews in Anal. Chem., August (1980) 219.
41 R. W. Karin, J. A. Buone and J. L. Fasching, Anal. Chem., 47 (1975) 2296.

Analytica Chimica Acta, 127 (1981) 195—198
Elsevier Scientific Publishing Company, Amsterdam — Printed in The Netherlands

Short Communication

HIGHLY SENSITIVE LASER FLUORIMETRY OF EUROPIUM(III) WITH 1,1,1-TRIFLUORO-4-(2-THIENYL)-2,4-BUTANEDIONE

SUNAO YAMADA, FUMIHIRO MIYOSHI, KOJI KANO and TEIICHIRO OGAWA*

Department of Molecular Science and Technology, Kyushu University, Hakozaki, Fukuoka 812 (Japan)

(Received 10th December 1980)

Summary. The detection limit for tris(1,1,1-trifluoro-4-(2-thienyl)-2,4-butanediono)-europium(III) is established as 2 pg l^{-1}. A highly sensitive fluorimetric system consisting of a nitrogen laser and a pulse-gated photon counter is used.

Fluorimetric analysis is a very powerful method for the determination of fluorescent molecules at trace levels. A laser excitation technique coupled with a pulse-gated photon counting method has reduced the detection limit substantially [1, 2]; the detection limit of fluorescein in aqueous solution is 20 pg Tl^{-1} [2], which clearly indicates the potential of the method for ultratrace determinations of fluorescent molecules.

Europium(III) β-diketonates are highly luminescent, and their emission lifetimes are much longer than those of organic molecules [3, 4]. Furthermore, these complexes have larger Stokes shifts than organic molecules [3]. In this communication, an application of a highly sensitive laser fluorimetric system for the measurement of ultratrace concentrations of tris(1,1,1-trifluoro-4-(2-thienyl)-2,4-butanediono)europium(III), $Eu(TTA)_3$, is described.

Experimental

Materials. $Eu(TTA)_3$ was prepared by an established procedure [5]. 1,1,1-Trifluoro-4-(2-thienyl)-2,4-butanedione (HTTA) was purchased from Dojindo Laboratories.

Optical measurements. The absorption spectrum was taken on a JASCO UVIDEC-505 spectrophotometer. The fluorescence spectra were recorded on a Hitachi 650-10 spectrofluorimeter.

Instrumentation. The basic components of the experimental apparatus for time-resolved spectrometry are a nitrogen laser and an emission detecting equipment with a pulse-gated photon counter (Fig. 1). The nitrogen laser was constructed according to the design reported previously [1], and was operated at a repetition rate of 15—25 Hz. Its output power and pulse width were about 0.5 mJ and 10 ns, respectively. Photoemission was focused onto the entrance slit of a JE-25 monochromator or onto an interference

0003—2670/81/0000—0000/$02.50

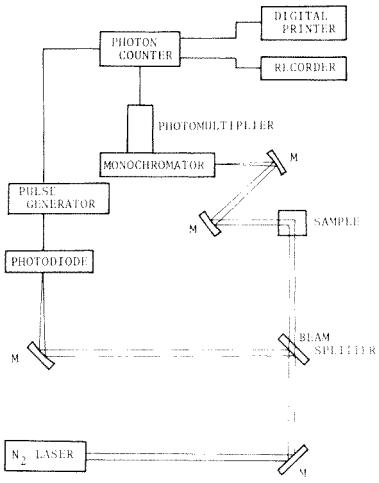

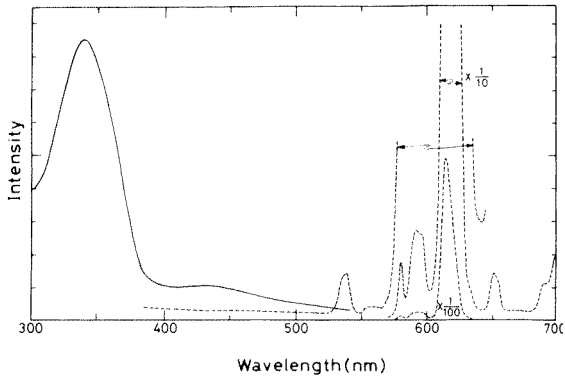

Fig. 1. Schematic diagram of the instrumentation.

Fig. 2. Absorption (——) and emission (- - - -) spectra of $Eu(TTA)_3$ in ethanol at room temperature.

filter. The photons were detected with a photomultiplier (HTV R-649), and the signals were amplified by an HTV C-716 amplifier. A photodiode (LSD 39A; rise time 0.35 ns) triggered a pulse generator (HP 214B) in order to control the time delay. The sampling gate was delayed for 3 μs from the laser pulse in order to remove the electrical noise from the discharge of a gap switch. The sampling gate time and the reference delay time were adjusted to 1.5 and 10 ms, respectively. The signal pulse was counted by a NF PC-545A photon counter (10 MHz), which also controlled the sampling gate time. The output signal was recorded either on a NADA DP-102C digital printer or on a RDK R-22 recorder.

Analytical procedure. In the measurement of the analytical curve, an emission signal was obtained by an integration over 100 laser pulses, and 10 runs measured under identical conditions were accumulated. Three cells (A, B, C) were used in order to correct for variation in the laser power and the optical characteristics of the quartz cells. The signals were measured for concentrations of $Eu(TTA)_3$ in the range $0—2.6 \times 10^{-14}$ M in cell A, while the concentrations in cells B and C were constant, 1.3×10^{-14} M and 0 M, respectively. Reference to the signals of cells B and C gave the ratio of emission signals, n(A)/n(B). The detection limit is defined at which S/N = 2.

Results

Spectra of $Eu(TTA)_3$. It is well known that sharp-line emissions of certain lanthanide β-diketonates are dependent both on the substituents of the β-diketones and on the presence of adducts. $Eu(TTA)_3$ is one of the Eu^{3+} β-diketonates to show very intense emission [6]. The absorption and emission

TABLE 1

Detection limits for europium

Analytical method	Detection limit ($ng\ l^{-1}$)	Ref.
Flame atomic emission spectrometry	200	[7]
I.c.p. emission spectrometry	60	[8]
Fluorimetric analysis		
Xe lamp — d.c. amplifier	10	This work
N_2 laser — pulse-gated photon counter	0.002	This work

spectra (excited at 337 nm) of $Eu(TTA)_3$ are shown in Fig. 2. The absorption maximum is 339 nm ($\epsilon = 8.2 \times 10^4$ l mol^{-1} cm^{-1}), whereas the emission bands appear at 540, 580, 593, 595, 614, 652, 690, and 700 nm, respectively. The coordinated ligands dissociate at least partially in highly dilute ethanolic solution; therefore, the emission spectra and the detection limit of $Eu(TTA)_3$ were measured in the presence of excess of ligand. The detection limit was determined to be 1×10^{-11} M by steady-state fluorimetry.

The absorption spectrum shows that a nitrogen laser is a good excitation source for this complex. The emission lifetime of the complex in ethanol at room temperature was measured to be 420 μs. An emission spectrum of $Eu(TTA)_3$ could be measured with the present apparatus even at 2×10^{-14} M.

Determination of detection limit by a filter system. The Stokes shift observed for $Eu(TTA)_3$ is more than 200 nm. Thus, an optical filter can be more useful for the measurements of weak photoemission than a monochromator. The emission signals around the strongest band (614 nm) were measured by a filter (λ_{max}, 614.5 nm; T_{max}, 40.5%; $\Delta\lambda_{1/2}$, 15.5 nm). The analytical curves of $Eu(TTA)_3$ were linear over a wide range and the detection limit was determined to be 2×10^{-15} M (2 pg l^{-1}).

Discussion

In ultratrace analysis, the residual fluorescent organic impurities and Raman signals of the solvent [2] as well as the electrical noise from the laser and the scattered light at cell surfaces strongly influence the detection limit. Most organic molecules have fluorescence lifetimes of the order of nanoseconds. In contrast, the emission lifetime of $Eu(TTA)_3$ is 420 μs. Therefore, the unwanted signals are effectively removed by the 3-μs delay used here.

A possible impurity may be $Sm(TTA)_3$; its emission intensity at 614 nm in ethanol is 2×10^{-3} times less than that of $Eu(TTA)_3$. None of emission bands of $Sm(TTA)_3$ was detected, and thus, the effect of $Sm(TTA)_3$ on the detection limit of $Eu(TTA)_3$ must be negligible.

The emission maximum of $Eu(TTA)_3$ was observed at 614 nm for an excitation at 337 nm. The Stokes shift of $Eu(TTA)_3$ is larger than those

of most organic molecules. The large Stokes shift is suitable for a filter detection system.

The detection limits for europium determined by several methods are listed in Table 1. It can be concluded that laser fluorimetry with a pulse-gated photon counter is a very sensitive analytical tool. Coprecipitation techniques combined with laser fluorimetry have been developed for ultra-trace measurements of lanthanide ions, and the detection limit for erbium was found to be 25 ng l^{-1} [9]. In the case given here, however, the sample is in solution, and the procedures are simple. The detection limit of $Eu(TTA)_3$ obtained in this work is 2×10^{-15} M, which is, to the best of our knowledge, the lowest value for fluorimetry in a solution state.

The present study was partially supported by a Grant-in-Aid for Special Project Research from the Ministry of Education.

REFERENCES

1 T. Imasaka, T. Ogawa and N. Ishibashi, Anal. Chem., 51 (1979) 502.
2 N. Ishibashi, T. Ogawa, T. Imasaka and M. Kunitake, Anal. Chem., 51 (1979) 2096.
3 R. E. Whan and G. A. Grosby, J. Mol. Spectrosc., 8 (1962) 315.
4 Y. Matsuda, S. Makishima and S. Shionoya, Bull. Chem. Soc. Jpn., 41 (1968) 1513; 42 (1969) 356.
5 L. R. Melby, N. J. Rose, E. Abramson and J. C. Caris, J. Am. Chem. Soc., 86 (1964) 5117.
6 H. G. Brittain, J. Chem. Soc. Dalton Trans., (1979) 1187.
7 H. Haraguchi, Kagaku no Ryoiki, 32 (1978) 313.
8 P. W. J. M. Boumans and R. M. Barnes, ICP Inf. Newsl., 3 (1978) 445.
9 F. J. Gustafson and J. C. Wright, Anal. Chem., 49 (1977) 1680.

Analytica Chimica Acta, 127 (1981) 199—201
Elsevier Scientific Publishing Company, Amsterdam — Printed in The Netherlands

Short Communication

DETERMINATION OF ZINC AND CADMIUM BY FLOW INJECTION ANALYSIS AND CHEMILUMINESCENCE

J. L. BURGUERA* and M. BURGUERA

Departmento de Quimica, Facultad de Ciencias, Universidad de Los Andes, Merida (Venezuela)

ALAN TOWNSHEND

Chemistry Department, University of Hull, Hull HU6 7RX (Gt. Britain)

(Received 22nd January 1981)

Summary. Zinc (10—100 ng ml^{-1}) and cadmium (20—200 ng ml^{-1}) are successively eluted from an ion-exchange column and determined by their inhibition of the cobalt-catalyzed chemiluminescence generation from luminol.

Flow injection analysis is very suitable for the determination of organic and inorganic species based on chemiluminescence measurements [1, 2]. Metal ions, in particular, may be determined by their catalytic effect on the oxidation of luminol [3, 4], or by their inhibiting effect on the catalyzed oxidation [5, 6]. In order to measure the transient emissions, the design of the system and the flow rates of the solutions should be chosen to ensure that maximum emission is generated whilst the emitter is in view of the detector [1, 2].

Zinc and cadmium have been found to inhibit the cobalt-catalyzed oxidation of luminol with hydrogen peroxide. This communication gives a preliminary assessment of the use of a small anion-exchange column in a flow system for the retention of zinc and cadmium as their chloro-complexes and subsequent sequential release, followed by their determination based on this inhibiting effect. Zinc is eluted first with an alkaline chloride solution, followed by cadmium with a nitric acid—chloride solution.

Experimental

The chemiluminescent measurements were carried out in the flow system shown in Fig. 1; 1-mm i.d. tygon tubing was used throughout, unless otherwise stated. The Amberlite IRA-400 resin (chloride form) was held in a glass tube (2 cm long, 3-mm i.d.). The sample and eluting solutions were injected from a glass syringe, through a self-sealing rubber septum, into the "solvent" stream of 0.1 M hydrochloric acid—0.5 M sodium chloride. The final solution flows through a 0.5-ml cell with a 10-mm optical path, positioned in front of the detector of a Shimatzu spectrophotometer.

The optimal conditions were: 100 μl of sample; 500 μl of 2 M sodium

0003—2670/81/0000—0000/$02.50

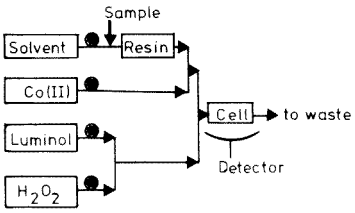

Fig. 1. Flow injection apparatus used for chemiluminescence measurements.

hydroxide and 1 M nitric acid, both 0.5 M in sodium chloride, for eluting zinc and cadmium, respectively; 0.01 M luminol in pH 11.0 carbonate buffer; cobalt(II) chloride (10 μg Co ml^{-1}) in 0.1 M hydrochloric acid—0.5 M sodium chloride. The flow rate was 1.0 ml min^{-1} in each primary line. The emission intensity was measured at 425 nm as a function of time over a period of 3 min. Alkaline eluent was injected 0.5 min after sample injection; acidic eluent was injected when the emission intensity had risen to the base-level after completion of the zinc response.

Results

When zinc or cadmium was added to the system, the otherwise constant emission intensity for the cobalt-catalyzed reaction was decreased. Thus sequential release of zinc and cadmium into the system from the anion-exchange column gave negative peaks, as shown in Fig. 2. Under the optimized conditions described above, the maximum decrease in intensity was linearly dependent on inhibitor concentration for 10—100 ng Zn ml^{-1} and 20—200 ng Cd ml^{-1}. The 2σ limits of detection were 5 ng Zn ml^{-1} (0.5 ng Zn) and 3 ng Cd ml^{-1} (0.3 ng Cd). The coefficient of variation for 6 determinations of a mixture of 10 ng each of zinc and cadmium was 2.0% for each element. Some other cations, such as copper(II), iron(II) and manganese(II) at the 80 ng ml^{-1} level enhanced the emission and interfered with the determination of 20 ng Zn ml^{-1}, but did not affect the determination of 20 ng Cd ml^{-1}. Nickel and cobalt(II) at the 80 ng ml^{-1} level did not affect the zinc

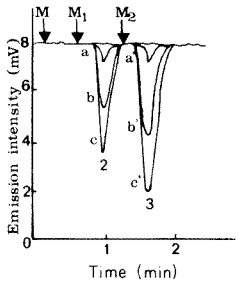

Fig. 2. Responses obtained from the system cobalt(II)—luminol—hydrogen peroxide, after injection of sample solution at M, zinc eluent at M_1 and cadmium eluent at M_2. Sample solutions contained: (a, a') 2 ng; (b, b') 10 ng; (c, c') 15 ng of each analyte.

determination, but slightly increased the intensity and thus interfered in the determination of cadmium.

The absorption and subsequent sequential release of zinc and cadmium in a flow injection system is thus capable of determining the two metals in admixture, in a sensitive and precise manner. The method is rapid (< 3 min per sample), and could undoubtedly be used for a wide range of other combinations of metal ions, as well as for improving selectivity [7]. The chemiluminescent detection system provides great sensitivity, but other means of monitoring the presence of the metals could also be used.

J. L. Burguera thanks C.D.C.H., Universidad de Los Andes, Merida, Venezuela, for financial support.

REFERENCES

1 J. L. Burguera and A. Townshend, Proc. Anal. Div. Chem. Soc., 16 (1979) 263.
2 J. L. Burguera, A. Townshend and S. Greenfield, Anal. Chim. Acta, 114 (1980) 209.
3 V. Isacsson and G. Wettermark, Anal. Chim. Acta, 68 (1974) 339.
4 D. B. Paul, Talanta, 25 (1978) 377.
5 A. T. Pilipenko, E. V. Mitropolitska and N. M. Lukovskaya, Ukr. Khim. Zh. (Russ. Ed.), 41 (1975) 1196.
6 L. J. Dubovenko and V. A. Bilochenko, Ukr. Khim. Zh. (Russ. Ed.), 40 (1974) 423.
7 W. R. Seitz and D. M. Hercules, Int. J. Environ. Anal. Chem., 2 (1973) 273.

Analytica Chimica Acta, 127 (1981) 203—207
Elsevier Scientific Publishing Company, Amsterdam — Printed in The Netherlands

Short Communication

A SIMPLE RELATIONSHIP BETWEEN THE HAMMETT ACIDITY FUNCTION, H_0, AND THE THERMODYNAMIC pK_a VALUES OF UNSUBSTITUTED AROMATIC CARBOXAMIDES

MICHAEL W. LOVELL and STEPHEN G. SCHULMAN*

College of Pharmacy, University of Florida, Gainesville, FL 32610 (U.S.A.)

(Received 27th October 1980)

Summary. The well-known failure of the Hammett H_0 function to describe the prototropic reaction isotherms of aromatic carboxamides can be corrected by taking account of the hydration requirements of the prototropic reactions of the carboxamides relative to the hydration requirements of the dissociations of the primary amines used as indicators to establish the H_0 scale. This approach has been successfully applied to benzamide and the naphthamides. For up to a 4:1 molar ratio of water to sulfuric acid, the amide acidity scale, H_A, and the H_0 scale are simply related by $H_A = H_0 - 2 \log a_w$, where a_w is the activity of water.

The Hammett acidity function, H_0, is based upon the ionization of substituted primary aromatic amines. It is well known that this function often fails to describe quantitatively the equilibrium prototropic behaviour [1—5] of other types of acids and bases, even when they are of the same charge type (singly positive acid, BH^+, neutral conjugate base, B) as the Hammett indicators [1]. Of particular interest here are the unsubstituted primary aromatic carboxamides, uncharged weak bases which fail to conform to the Hammett acidity relationship [6—9],

$$H_0 = pK_a + \log [B]/[BH^+] \quad (1)$$

According to Hammett and Deyrup's original definition [2]

$$h_0 = \text{antilog}(-H_0) = a_{H^+} f_B / f_{BH^+} \quad (2)$$

where a_{H^+} is the activity of the protonating species and f_B/f_{BH^+} is the ratio of the activity coefficients of B and BH^+.

In work related to the kinetics of acid hydrolysis of certain esters, Bunnett [10] redefined h_0 to include water as a reactant,

$$h_0 = a_{H^+} f_B / a_w^n f_{BH^+} \quad (3)$$

where a_{H^+} is the activity of the protonating species and f_B/f_{BH^+} is the ratio of the activity coefficients of B and BH^+.
and B (n is the difference between the number of water molecules hydrating B and H^+ and the number hydrating BH^+). A strong connection exists between the hydration requirement, n, of a protrotropic reaction and the failure of

neutral bases to conform to eqn. (1). Although tested unsuccessfully for tertiary amines [11], this connection has not been actively pursued for other classes of compounds. Rather, most attention has been focused on the lack of equivalence, resulting from structural differences, of the activity coefficient ratio, f_B/f_{BH^+}, for the Hammett indicators and other types of bases [12—19]. As a result, acidity functions were established for several classes of compound [6—9] including the H_A scale for aryl carboxamides [20—22]. The H_A scale is related to the activity of the hydrogen ion and the activity coefficients f_{HA^+} and f_A of the protonated and neutral amides by

$$h_A = \text{antilog}\,(-H_A) = a_{H^+}\, f_A/f_{HA^+} \tag{4}$$

Although relationships between H_0 and other acidity functions such as H_A have been explored on a more or less empirical basis [12—19, 23, 24], no obvious relationship to the molecular details of the various prototropic reactions of interest appears to have been established. Thus, in the present work, the variations of the electronic absorption spectra of benzamide and the naphthamides with the H_0 function were investigated at 25°C in sulfuric acid. In these, isosbestic points were observed for benzamide at 212 nm, for 1-naphthamide at 228 nm and for 2-naphthamide at 240 nm. However, at values of H_0 just beyond where the HA^+ species were isolated, the spectra tended to red-shift with loss of the isosbestic points, indicating either a general medium effect or a specific change in the solvation of the cations.

Results and discussion

It was decided to consider the possibility that eqn. (3) would correctly describe the relationship of the h_0 function to the dissociations of the primary ammonium ion indicators used to establish h_0 over the range of acidity studied, that the activity coefficient ratios, f_B/f_{BH^+} and f_A/f_{HA^+}, were equivalent for similar charge types, and that the dissociation constants of the primary aryl carboxamides would be given by

$$K_a = (a_{H^+}/a_w^r)(f_A/f_{HA^+})([A]/[HA^+]) \tag{5}$$

corresponding to the reaction $HA^+ + r\ H_2O \rightleftharpoons H^+ + A$. In this treatment, the degrees of hydration of H^+, HA^+, A, BH^+ and B are unimportant as long as they are invariant over the inflection regions of the spectrophotometric titrations. Combination of eqns. (3) and (5) yields

$$K_a/h_0 = a_w^{n-r}\,[A]/[HA^+] \tag{6}$$

In logarithmic form, eqn. (6) becomes

$$H_0 - \log\,[A]/[HA^+] = pK_a + (n—r)\log a_w \tag{7}$$

A plot of $H_0 - \log\,[A]/[HA^+]$ vs. $\log a_w$ should be linear, with slope $(n - r)$ and intercept pK_a.

Bascombe and Bell (25) have suggested that n = 4 with all four water molecules being associated with the hydration of the proton. The experiments of Teng and Lenzi [26] indicated that n = 3. Rosenthal and Dwyer

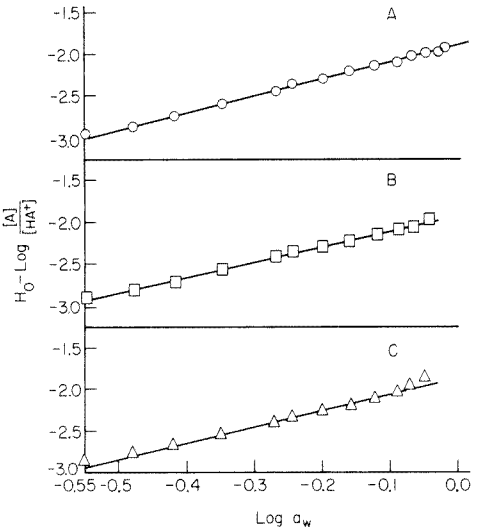

Fig. 1. Experimental data for (A) benzamide, (B) 1-naphthamide, (C) 2-naphthamide in aqueous sulfuric acid.

	Slope	Intercept	Standard error	Correlation coefficient
Benzamide (A)	2.01 ± 0.02	−1.89 ± 0.01	0.02	0.999
1-Naphthamide (B)	1.84 ± 0.01	−1.92 ± 0.01	0.03	0.999
2-Naphthamide (C)	2.05 ± 0.02	−1.84 ± 0.01	0.03	0.999

TABLE 1

Values of pK_a for benzamide and the naphthamides[a]

Amide	pK_a[b]	pK_a[c]
Benzamide	−1.89 ± 0.01	−1.89 ± 0.02
1-Naphthamide	−1.92 ± 0.01	−1.89 ± 0.02
2-Naphthamide	−1.84 ± 0.02	−1.85 ± 0.02

[a]For the reaction $HA^+ + rH_2O \rightleftharpoons A + H^+$. [b]Using (n − r) = 2.01, 1.84 and 2.05 for benzamide, 1-naphthamide and 2-naphthamide, respectively. [c]Using (n − r) = 2.

[27] found that a value of n = 2 fitted their experimental data better than n = 4 for HCl and LiCl, whereas a nonintegral value of n was required to give reasonable values for perchloric acid. However, since in eqn. (7) only the difference, (n − r), between the hydration requirements of the Hammett indicators and those of the carboxamides is important, it is not really necessary to know n explicitly.

Values of log [A]/[HA^+] were calculated for several values of H_0 around the inflection point of the appropriate titration curve. Values of a_w were taken from a curve constructed from the data of Giauque et al. [28], and plots of H_0 − log [A]/[HA^+] vs. log a_w were made for benzamide, 1-naph-

thamide, and 2-naphthamide as shown in Fig. 1. The intercepts of these plots were −1.89, −1.92 and −1.84, respectively. The slopes were 2.01, 1.84 and 2.05. If calculations of the pK_a values were made from eqn. (7) using integral values other than 2 for (n − r) the values showed a progression with increasing acidity. In the most dilute acid solutions, where $a_w \rightarrow 1$, all the calculated pK_a values converged on the mean value obtained for (n − r) = 2. The pK_a values of the protonated amides, as presented in Table 1, are in fair agreement with those reported for benzamide and the naphthamides [22] as determined by using the H_A function. The results imply that two fewer water molecules are involved in the dissociation reactions of the protonated amides than in the dissociations of the ammonium ions used in the establishment of the H_0 function. If the hydration numbers of the hydrogen ion and of the neutral and protonated amides in the moderately concentrated acid media are identical to those in water, the pK_a values in Table 1 should correspond to the thermodynamic values at infinite dilution.

The form of eqn. (7) suggests that the H_0 and H_A scales should be related by $H_A = H_0 - 2 \log a_w$. By using the tabulations of Boyd et al. [1], this was found to be the case up to about 55% (w/w) sulfuric acid—water mixtures. At higher sulfuric acid concentrations, (n − r) tends towards unity. Since at such concentrations there are fewer than 4 moles of water per mole of sulfuric acid, the breakdown in eqn. (7) seems likely to be due to the occurrence of a variety of hydrates of H^+ and perhaps of the indicator species. This statement is supported by the experiments of Ojeda and Wyatt [29] which demonstrated that a stepwise decrease in the hydration of the proton occurred with increasing concentration of neutral electrolytes.

The value of pK_a determined here for benzamide is in excellent agreement with the value determined by Vinnik [30] from the acidity dependence of the hydrolysis kinetics of benzamide in acidic media. Conceivably, the approach employed in the present work will be of use in the quantitative evaluation of the kinetics and mechanisms of other acid-catalyzed reactions.

REFERENCES

1 R. H. Boyd, F. F. Coetzee and C. D. Ritchie, Solute—Solvent Interactions, M. Dekker, New York, 1969, Ch. 3.
2 L. P. Hammett and A. J. Deyrup, J. Am. Chem. Soc., 54 (1932) 2721.
3 M. A. Paul and F. A. Long, Chem. Rev., 57 (1957) 1.
4 M. J. Jorgensen and D. R. Hartter, J. Am. Chem. Soc., 85 (1963) 878.
5 K. Yates and H. Wai, J. Am. Chem. Soc., 84 (1964) 5408.
6 A. R. Katritzky, A. J. Waring and K. Yates, Tetrahedron, 19 (1963) 465.
7 J. T. Edward and I. C. Wang, Can. J. Chem., 40 (1962) 966.
8 R. B. Homer and R. B. Moodie, J. Chem. Soc., (1963) 4377.
9 R. J. Gillespie and T. Birhall, Can. J. Chem., 41 (1963) 148.
10 J. F. Bunnett, J. Am. Chem. Soc., 83 (1961) 4956; 4968; 4973; 4978.
11 E. M. Arnett and G. W. Mach, J. Am. Chem. Soc., 86 (1974) 2671.
12 J. F. Bunnett and F. P. Olsen, Chem. Commun, (23) (1965) 601; Can. J. Chem., 44 (1966) 1899, 1917.

13 N. C. Marziano, G. M. Cimino and R. C. Passerini, J. Chem. Soc., Perkin II, (1973) 1915.
14 N. C. Marziano, P. Traverso and R. C. Passerini, J. Chem. Soc., Perkin II, (1977) 306.
15 N. C. Marziano, P. Traverso, A. Tomasin and R. C. Passerini, J. Chem. Soc., Perkin II, (1977) 309.
16 J. T. Edward and S. C. Wong, Can. J. Chem., 57 (1979) 1980.
17 R. A. Cox and K. Yates, J. Am. Chem. Soc., 100 (1978) 3861; Can. J. Chem., 57 (1979) 2944.
18 R. A. Cox, C. R. Smith and K. Yates, Can. J. Chem., 57 (1979) 2952.
19 R. A. Cox, M. F. Goldman and K. Yates, Can. J. Chem., 57 (1979) 2960.
20 K. Yates, J. B. Stevens and A. R. Katritzky, Can. J. Chem., 42 (1964) 1957.
21 C. D. Johnson, A. R. Katritzky and N. Shakir, J. Chem. Soc., 13 (1967) 1235.
22 K. Yates and J. B. Stevens, Can. J. Chem., 43 (1965) 529.
23 E. M. Arnett and G. W. Mach, J. Am. Chem. Soc., 88 (1966) 1177.
24 N. G. Zarakani, P. P. Nechaev and G. E. Zaikov, Ivz, Akad. Nauk SSSR, Ser. Khim., 3 (1978) 568.
25 K. N. Bascombe and R. P. Bell, Discuss. Faraday Soc., 24 (1957) 158.
26 T. T. Teng and F. Lenzi, Can. J. Chem., 50 (1972) 3283.
27 D. Rosenthal and J. S. Dwyer, Can. J. Chem., 41 (1963) 80.
28 W. F. Giauque, E. M. Hornung, J. E. Kunzler and T. R. Rubin, J. Am. Chem. Soc., 82 (1960) 62.
29 M. Ojeda and P. A. H. Wyatt, J. Phys. Chem., 68 (1964) 1857.
30 M. I. Vinnik, Ivz. Akad. Nauk SSSR, Ser. Khim., 4 (1978) 799.

Analytica Chimica Acta, 127 (1981) 209—212
Elsevier Scientific Publishing Company, Amsterdam — Printed in The Netherlands

Short Communication

SEPARATION OF CADMIUM FROM A LARGE AMOUNT OF ZINC BY CHLOROFORM EXTRACTION WITH ETHYLXANTHATE

YOSHIAKI SASAKI

Department of Chemistry, Faculty of Science, Yamaguchi University, Yoshida, Yamaguchi-shi, Yamaguchi 753 (Japan)

(Received 3rd November 1980)

Summary. Traces of cadmium are quantitatively extracted with potassium ethylxanthate into chloroform from 0.25 mol dm^{-3} ammonia buffer (pH 9.5), which masks zinc.

Alkylxanthates (*o*-alkyldithiocarbonates) react with many metal ions giving chelates which are sparingly soluble in water and soluble in organic solvents such as chloroform [1]. Xanthates, therefore, have been used for the solvent extraction of metal ions [2]. The chloroform extraction behavior of cadmium [3, 4] and zinc [3—5] xanthate complexes has been investigated and the compositions, overall formation constants and distribution coefficients for the complexes have been determined.

Consideration of these results suggested the possibility of the separation of cadmium from zinc by chloroform extraction with ethylxanthate (which was more suitable than other alkyl- and benzyl-xanthates). The optimum conditions for the extraction of cadmium and zinc with ethylxanthate were pH 6.5—10.5 and 4.5—7.5, and ethylxanthate concentrations 10^{-4}—10^{-2} mol dm^{-3} and 10^{-2}—10^{-1} mol dm^{-3}, respectively. Therefore, extraction from an ammoniacal aqueous solution containing a low level of xanthate gave a satisfactory separation of cadmium from a large amount of zinc.

Experimental

Reagents. Potassium ethylxanthate was synthesized and purified as described previously [4]. Its solution was freshly prepared daily. Stock solutions (10^{-2} mol dm^{-3}) of cadmium and zinc were prepared by dissolving their nitrates in 0.1 mol dm^{-3} nitric acid, and were standardized by titration with EDTA. The buffer solution was prepared by dissolving 1 mol of ammonium nitrate in water, adding aqueous ammonia until the pH reached 9.5, and diluting to 1 dm^3 with water.

Apparatus. A Shimadzu Model AA-610 atomic absorption spectrometer (air—acetylene flame) was used for the determination of cadmium and zinc. A Toa Model HM-5A pH meter with glass electrode was used for pH measurements.

Procedure. Cadmium and zinc were extracted into chloroform from the

aqueous solution containing pH 9.5 buffer and ethylxanthate. The chloroform phase was separated, back-extracted (if necessary), and evaporated to dryness. The residue was treated with concentrated nitric acid to decompose the metal xanthate complexes, and this solution was evaporated to dryness. The nitrates obtained were dissolved in 0.1 mol dm^{-3} hydrochloric acid and cadmium and zinc were determined by atomic absorption spectrometry.

Results and discussion

Effect of concentrations of buffer and xanthate. The effect of the concentration of pH 9.5 buffer and ethylxanthate on the extraction of cadmium and zinc was investigated under the following conditions. The aqueous phase was adjusted to pH 9.5; the initial concentrations of cadmium and zinc were both 2×10^{-5} mol dm^{-3} and the volumes of aqueous and chloroform phases were both 20 cm^3.

Ammonium concentrations of 0.10—0.35 mol dm^{-3} gave good results for the mutual separation, as shown in Fig. 1. Zinc was not masked completely at buffer concentration below 0.1 mol dm^{-3} whereas cadmium was also partly masked as the ammine at buffer concentrations above 0.35 mol dm^{-3}. The final ammonium concentration in buffer, therefore, was fixed at 0.25 mol dm^{-3} in all following experiments.

Xanthate in the range 1×10^{-3}—6×10^{-3} mol dm^{-3} was most suitable for the extraction of cadmium alone, as shown in Fig. 2. At lower concentrations ($<10^{-3}$ mol dm^{-3} xanthate), the extraction of cadmium was incomplete owing to competition from ammine formation. Zinc was slightly extracted at $\geqslant 8 \times 10^{-3}$ mol dm^{-3} xanthate.

Separation of cadmium from large amounts of zinc. The extractive separation of cadmium from large amounts of zinc was done with 2×10^{-3} mol dm^{-3} potassium ethylxanthate, and 0.25 mol dm^{-3} ammoniacal buffer. The volumes of both phases were 20 cm^3.

The separation of zinc from cadmium by a simple extraction is shown in Table 1. When the mole ratio of zinc to cadmium in the original aqueous

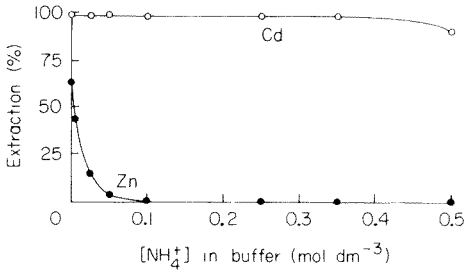

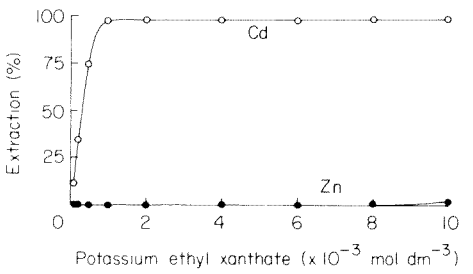

Fig. 1. Effect of the ammonium concentration of the pH 9.5 buffer on the extraction of cadmium and zinc with 10^{-3} mol dm^{-3} potassium ethylxanthate.

Fig. 2. Effect of ethylxanthate concentration on the extraction of cadmium and zinc. $[NH_4^+]$ in buffer = 0.25 mol dm^{-3}; other conditions as Fig. 1.

TABLE 1

Extractive separation of cadmium (2×10^{-5} mol dm^{-3}) from large amounts of zinc (without back-extraction)

[Zn] added (mol dm^{-3})	[Zn]/[Cd]	Extraction (%)		[Zn]/[Cd] in extract
		Cd	Zn	
5×10^{-5}	2.5	97.7	0.4	0.01
1×10^{-4}	5.0	97.6	0.3	0.02
2.5×10^{-4}	12.5	97.0	0.3	0.04
5×10^{-4}	25.0	96.3	0.3	0.07
1×10^{-3}	50	96.9	0.3	0.18
2×10^{-3}	100	97.4	0.3	0.32
3×10^{-3}	150	96.2	0.3	0.47
4×10^{-3}	200	96.4	0.3	0.67
5×10^{-3}	250	96.4	0.4	0.97

phase was 12.5, it was decreased to 0.04 in the organic phase after a single extraction. The separation was less complete in the presence of larger amounts of zinc. In such cases back-extraction of zinc was necessary.

After extraction with two 10-cm^3 portions of chloroform, the organic phase was back-extracted with 10 cm^3 of the 0.25 mol dm^{-3} ammoniacal buffer, 2×10^{-3} mol dm^{-3} in potassium ethylxanthate. The results obtained are shown in Table 2. Cadmium could be satisfactorily separated from zinc at up to a 10 000-fold molar ratio. By this method, cadmium could be quantitatively extracted at initial concentrations up to 5×10^{-4} mol dm^{-3} (Table 3); the positive errors at the lowest concentrations are probably due to reagent contamination. The coefficient of variation for the determination of cadmium after extraction was 0.9% (10 measurements) at the 2×10^{-5} mol dm^{-3} level.

Cadmium ethylxanthate can be easily decomposed to metal ion, carbon disulfide and ethanol by the addition of mineral acids such as nitric acid. The carbon disulfide and ethanol can easily be removed from the mixture by heating because of their volatility. Thus, cadmium can be recovered as a

TABLE 2

Extractive separation of cadmium (4×10^{-6} mol dm^{-3}) from a large amount of zinc (with back-extraction)

[Zn] added (mol dm^{-3})	[Zn]/[Cd]	Extraction (%)		[Zn]/[Cd] in extract
		Cd	Zn	
5×10^{-3}	1250	102	3×10^{-4}	0.0039
1×10^{-2}	2500	102	2×10^{-4}	0.0039
2×10^{-2}	5000	101	2×10^{-4}	0.012
4×10^{-2}	10000	104	5×10^{-4}	0.046
1×10^{-1}	25000	Precipitation of $Zn(OH)_2$		

TABLE 3

Extraction of cadmium

[Cd] added (mol dm^{-3})	Extraction (%)	[Cd] added (mol dm^{-3})	Extraction (%)
1×10^{-6}	108	5×10^{-5}	96
2×10^{-6}	108	1×10^{-4}	98
5×10^{-6}	102	2×10^{-4}	97
1×10^{-5}	102	5×10^{-4}	99
2×10^{-5}	101		

simple inorganic salt which is advantageous for the succeeding analytical procedure.

The author expresses his appreciation to Dr. K. Hayashi, Professor of Yamaguchi University, for helpful comments.

REFERENCES

1 S. R. Rao, Xanthates and Related Compounds, M. Dekker, New York, 1971.
2 E. M. Donaldson, Talanta, 23 (1976) 417.
3 K. Hayashi, Y. Sasaki and S. Furusho, Bunseki Kagaku, 24 (1975) 151.
4 Y. Sasaki, J. Inorg. Nucl. Chem., in press.
5 K. Hayashi, Y. Sasaki and H. Nojima, Bunseki Kagaku, 19 (1970) 325.

Analytica Chimica Acta, 127 (1981) 213—218
Elsevier Scientific Publishing Company, Amsterdam — Printed in The Netherlands

Short Communication

HIGH-PERFORMANCE LIQUID CHROMATOGRAPHIC SEPARATION OF THE FAT-SOLUBLE VITAMINS IN COD LIVER OIL AND FEEDS

R. R. ELTON-BOTT* and C. I. STACEY

Department of Chemistry, Western Australian Institute of Technology, South Bentley, Western Australia 6102 (Australia)

(Received 27th October 1980)

Summary. A MicroPak-CN column with a methylene chloride—chloroform—n-hexane (3:2:15) mobile phase separates the fat-soluble vitamins in cod liver oil and formulated feed. Powdered feed samples are dissolved in n-hexane—chloroform—ethanol (6:3.5:0.5) and centrifuged before injection. The oil is dissolved in the extraction solvent or mobile phase before injection. The naturally occurring vitamins are identified from their absorption spectra by stopped-flow scanning of the individual vitamins.

The resolution, identification and measurement of the fat-soluble vitamins contained in cod liver oil and formulated feeds is complicated by the complex biological matrix, and the physicochemical properties of the vitamins and their isomers. The saturated triglycerides invariably present tend to be retained strongly on reversed-phase chromatographic packings [1] because of their low solubility in the mobile phase used. Contamination problems on the octadecylsilane type of bonded stationary phase by lipids [2] seemed to preclude their application to vitamins. The triglycerides can be effectively removed by saponification, but hydrolysis of the vitamins to easily oxidised forms such as retinol and tocopherol would occur. Tocopherol, with its acidic phenolic group, would be vulnerable to losses during any alkaline phase separation. Recent reports [1—7] have tended to avoid saponification. Bayfield [5] extracted vitamin A directly from liver with 1:1 acetone—light petroleum with α-tocopherol as antioxidant after grinding with silica.

Normal-phase chromatography on silica gel can cause decomposition and catalytic isomerisation of the all-*trans* retinyl acetate and retinol [8]. Pilkiewicz et al. [9] used nitrile-modified silica packing with 1:99 diethyl ether—n-hexane to separate all-*trans* retinal and the three mono-*cis* isomers of retinal.

The great selectivity offered by the alkylnitrile-bonded packing together with a carefully selected mobile phase is shown here to permit the isocratic separation of the fat-soluble vitamins A, D, E and K_3 in formulated feed without prior saponification. The naturally occurring vitamins in cod liver oil

*Permanent address: Government Chemical Laboratories, Agricultural Chemistry Division, 30 Plain Street, Perth, Australia.

are resolved and identified from their absorption spectra by stopped-flow scanning of the individual peaks.

Experimental

Chemicals. The vitamin standards used were all-*trans* retinyl palmitate (BDH, Poole, England); all-*trans* retinyl acetate (Hoffman-La Roche);crystalline cholecalciferol and ergocalciferol (USPC, Rockville, MD); D-α-tocopheryl acetate and menadione (Sigma Chemical, MO).

Samples. Cod liver oil samples were obtained from F. H. Faulding and Co. Ltd., Adelaide and Vita-Valu Laboratories, Sydney. The pelletised poultry feed sample fortified with the fat-soluble vitamins as a dry stabilized concentrate was obtained from a local manufacturer.

Extraction. A sample (25 g) of ground feed (Tecator cyclone mill) was ground further to a fine powder with a mortar and pestle. Duplicate portions (10 g each) were transferred to glass centrifuge tubes fitted with ground-glass stoppers. The sample was mixed intimately with 10 ml of extraction solvent (spectrograde n-hexane, chloroform and ethanol in the volume ratio 6:3.5:0.5) in a vortex stirrer, and placed in the dark for 16 h (overnight). The mixture was shaken vigorously for a few minutes, and the solvent layer was separated by centrifugation at 3000 rpm for 15 min. A portion (3—4 ml) was transferred to a stoppered glass vial containing some anhydrous sodium sulphate.

Cod liver oil (250—500 mg) was transferred to a 25-ml volumetric flask and dissolved in the mobile phase before injection (20 or 100 μl) onto the column.

Equipment and operating conditions. A Varian-Techtron model 8500 liquid chromatograph equipped with a stop-flow pump was used with a variable wavelength detector (Varichrom model 635) and a double pen recorder at a chart speed of 0.5 cm min^{-1}.

The operating conditions were as follows: stainless-steel column (25 cm × 4.6 mm i.d.) with MicroPak-CN packing material (10 μm; Varian Assoc.); flow rate 20 ml h^{-1} (pressure 500 psi); ambient temperature; u.v. detector at 254 nm; mobile phase, methylene chloride—chloroform—n-hexane (3:2:15).

Results and discussion

Resolution of vitamin standards. The resolving capacity of the chromatographic system was good; the chromatograms for the pure compounds (Fig. 1) showed not only the main isomers but other isomers. The retention data are recorded in Table 1. 13-*cis*-Retinyl acetate (neo-vitamin A) is the predominant isomer of all-*trans* retinyl acetate [8, 10], which isomerises in solution on exposure to light. Isomers of D-α-tocopheryl acetate [4] were similarly detected. The pre-cholecalciferol peak was formed by isomerisation of cholecalciferol on heating the solution at 90°C. As reported by Krol et al. [11] who utilised a Vydac TM column, cholecalciferol could not be separated from ergocalciferol even at low flow rates.

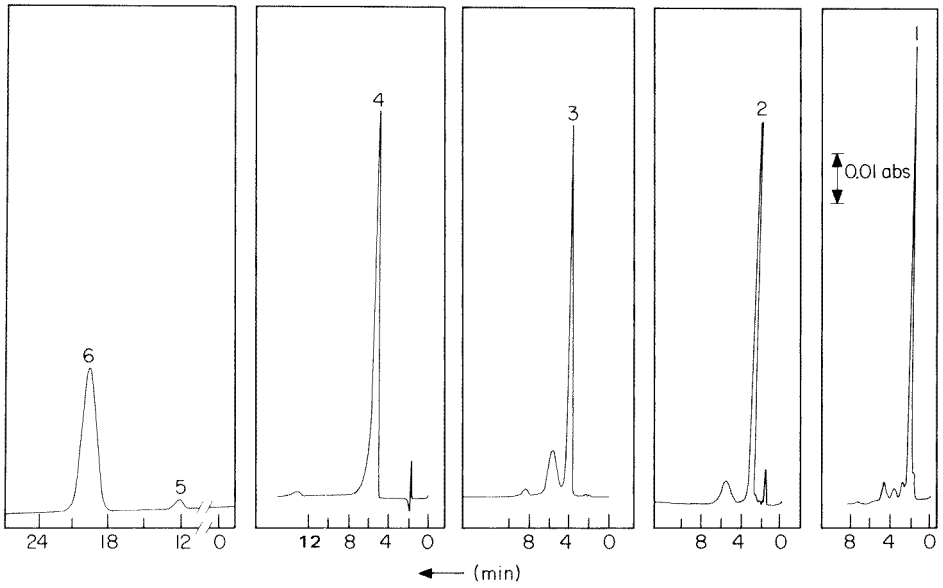

Fig. 1. High-performance liquid chromatogram of single vitamin standards showing the presence and resolution of their geometric isomers. Peak identity: (1) all-*trans* retinyl palmitate; (2) D-α-tocopheryl acetate; (3) all-*trans* retinyl acetate; (4) menadione; (5) pre-cholecalciferol; (6) cholecalciferol. Chromatographic conditions as in Experimental.

TABLE 1

Retention times (t_R) and absorption data for the vitamin compounds in n-hexane—methylene chloride—chloroform (15 : 3 : 2) mobile solvent system
(Retention values are the means of six separate injections)

Compound	t_R (min)	Relative retention	Sample size (μg)	λ_{max} (nm)
All-*trans* Retinyl palmitate	2.0	1.0	0.16	350, 325
D-α-Tocopheryl acetate	2.8	1.4	10	284
All-*trans* Retinyl acetate	3.6	1.8	0.12	325
Menadione	4.6	2.3	15	250
13-*cis*-Retinyl acetate	5.0	2.5	0.12	325
Pre-cholecalciferol	12.1	6.0	0.40	265
Cholecalciferol	19.3	9.6	0.40	265

Figure 2A illustrates separation of the mixture of lipophilic vitamins under the recommended conditions. The vitamin components are well resolved and are eluted within 18 min.

Influence of mobile phase composition. The mobile phase composition has a strong influence on solute retention. Decreasing the concentrations of chloroform and methylene chloride improved peak resolution but retention times became excessive. The addition of small amounts (0.5—2% v/v) of the

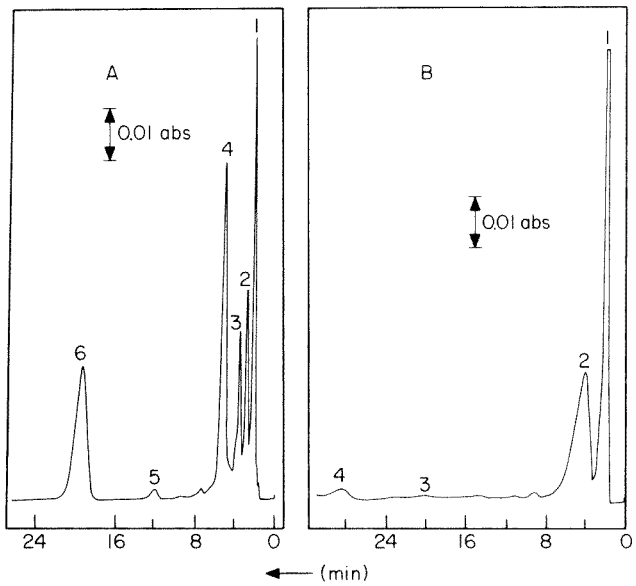

Fig. 2. (A) Chromatogram of mixed vitamin standards containing all-*trans* retinyl palmitate (1), D-α-tocopheryl acetate (2), all-*trans* retinyl acetate (3), menadione (4), precholecalciferol (5), and cholecalciferol (6). (B) Separation of vitamins in cod liver oil: (1) all-*trans* retinyl palmitate; (2) 3,4-didehydroretinyl ester (vitamin A_2 ester); (3) cholecalciferol; (4) pro-cholecalciferol. Conditions as in Experimental.

very polar ethanol decreased the column efficiency, and the vitamins were eluted close to the solvent front.

Separation and identification of vitamins in cod liver oil. Figure 2B shows a chromatogram of cod liver oil, and its separation was studied to identify the naturally occurring vitamins and to demonstrate the feasibility of avoiding saponification. Peak 1 was identified as all-*trans* retinyl palmitate from its retention time (t_R) of 2.0 min, and from the composition of cod liver oil reported in the literature [12, 13]. Its spectrum, scanned at 50 nm min^{-1} over the range 280—370 nm under stopped-flow conditions, was identical to the spectrum of all-*trans* retinyl palmitate standard, with $E_{350}/E_{325} = 1.34$ for both. Peak 2 ($t_R = 4.2$ min) was scanned similarly; the characteristic maxima at 287 nm and 350 nm identified this peak as being vitamin A_2 ester (3,4-didehydroretinyl ester) and the spectrum was very similar to those recorded in the literature [14]. The ratio $E_{350}/E_{287} = 3.1$ indicated higher purity of the fraction than the value of 2.0 found earlier [14]. Peak 4 ($t_R = 28.5$ min) was likewise scanned; its absorption spectrum showed $\lambda_{max} = 265$ nm. When the cod liver oil was subjected to sunlight for 4 h, peak 3 ($t_R = 19.3$ min) increased at the expense of peak 4. Peak 4 was thus identified as being provitamin D_3 (7-dehydrocholesterol).

Selection of internal standards. Several compounds were examined for suitability as an internal standard. Three compounds which satisfied the

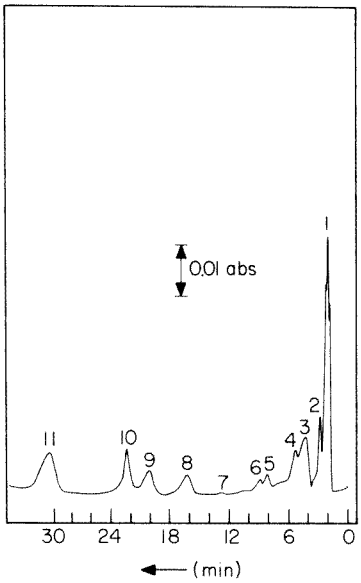

Fig. 3. Separation of vitamins in poultry feed extract: (1) all-*trans* retinyl palmitate; (2) α-tocopheryl acetate; (3) 13-*cis* retinyl acetate; (4) menadione; (5) mono-*cis* isomer of retinyl acetate; (6) unknown; (7) pre-cholecalciferol; (8) unknown; (9) cholecalciferol; (10) unknown; (11) phenol (internal standard). Conditions as in Experimental.

requirements were thymol, phenol, and benzyl alcohol with retention times of 9.6 min, 30.2 min, and 36.8 min, respectively.

Application to fat-soluble vitamins in poultry feed. Figure 3 shows a chromatogram of the extract of poultry feed with phenol as internal standard. The vitamins were identified from their retention times, and also by spiking with standards. As the response ratio of a compound at two wavelengths under fixed conditions is usually characteristic for that compound, the peaks were also examined for conformity with the ratios for the pure standards at 254 nm and the appropriate wavelengths of maximum absorption.

The all-*trans* retinyl acetate peak was absent from the chromatogram, but its 13-*cis* isomer (t_R = 5.0 min) was present to an appreciable degree. This is in agreement with Egberg et al. [15] who demonstrated the presence of the 13-*cis* isomer in several food products with a reversed-phase procedure. The hydrolysis and oxidation of added vitamin A esters, during storage, to the aldehyde form (λ_{max} = 373 nm) is a possibility, and should be considered because the bio-activity of retinal is essentially the same as that of crystalline vitamin A [13]. The addition of vitamin K_3 to poultry feed as its water-soluble form, menadione sodium hydrogensulphite, would require treatment of the sample with sodium hydroxide solution to precipitate menadione. The menadione could then be extracted into hexane—chloroform. Tomkins and Tscherne [16] have described the extraction of vitamins from gelatin-protected beadlets by dispersion of the sample in warm dimethylsulphoxide.

Conclusions

The normal-phase isocratic separation of the vitamins as described has several advantages, chiefly those of speed, economics and long-term stability of the chromatographic system. The vitamins are not subjected to heat or hydrolysis so that their stability is not affected. The column is easily regenerated after constant use, with a mobile phase consisting of 19:1 n-hexane—isopropanol.

A limitation of the method is its inability to separate and identify vitamin D_3 from vitamin D_2, which has been achieved with reversed-phase systems [17, 18]. However, the reversed-phase system does not separate the vitamins from their provitamin forms [18]. Sobel et al. [19] described conditions for measuring combined vitamin D_2 and D_3, and for distinguishing spectrophotometrically the vitamins and their provitamins after reaction with glycerol 1,3-dichlorohydrin in the presence of acetyl chloride. This reaction should perhaps be restudied.

We thank Messrs. J. Jago, S. C. Baseden, A. M. Rowley (Government Chemical Laboratories); Mr. S. Blackbourn (Department of Pharmacy); and Ms. N. Ho (Department of Community Health Science) for kind donation of poultry feed sample and vitamin standards. We are also grateful to Dr. J. W. Hosking for useful discussions, and to Messrs. G. Ozsdolay and R. Levitt for helpful assistance with h.p.l.c. equipment.

REFERENCES

1 N. A. Parris, J. Chromatogr., 157 (1978) 161.
2 W. A. Widicus and J. R. Kirk, J. Assoc. Off. Anal. Chem., 62 (1979) 637.
3 S. A. Barnett and L. W. Frick, Anal. Chem., 51 (1979) 641.
4 J. F. Cavins and G. E. Inglett, Cereal Chem., 51 (1974) 605.
5 R. F. Bayfield, Anal. Biochem., 64 (1975) 403.
6 C. Mackay, J. Tillman and D. Thornburn Burns, Analyst., 104 (1979) 626.
7 R. Vanhaelen-Fastre and M. Vanhaelen, J. Chromatogr., 153 (1978) 219.
8 M. Vecchi, J. Vesly and G. Oesterhelt, J. Chromatogr., 83 (1973) 447.
9 F. G. Pilkiewicz, M. J. Pettei, A. P. Yudd and K. Nakanishi, Exp. Eye Res., 24 (1977) 421.
10 J. E. Paanakker and G. W. T. Groenendijk, J. Chromatogr., 168 (1979) 125.
11 G. J. Krol, C. A. Mannan, F. Q. Gemmil, Jr., G. E. Hicks and B. T. Kho, J. Chromatogr., 74 (1972) 43.
12 W. H. Sebrell and R. S. Harris (Eds.), The Vitamins, Academic Press, New York, 2nd edn., Vol 1, 1971.
13 The Merck Index, M. Windholz (Ed.), Merck, Rahway, NJ, 9th edn., 1976, p. 1287.
14 See, e.g., F. Bro-Rasmussen, W. Hjarde and O. Porotnikoff, Analyst, 80 (1955) 418.
15 D. C. Egberg, J. C. Heroff and R. H. Potter, J. Agric. Food Chem., 25 (1977) 1127.
16 D. F. Tomkins and R. J. Tscherne, Anal. Chem., 46 (1974) 1602.
17 R. A. Wiggins, Chemy. Ind., (1977) 841.
18 M. Osadca and M. Araujo, J. Assoc. Off. Anal. Chem., 60 (1977) 993.
19 A. E. Sobel, A. Margot Meyer and B. Kramer, Anal. Chem., 17 (1945) 160, in M. G. Mellon (Ed.), Analytical Absorption Spectroscopy, J. Wiley, New York, 1950, p. 415.

Analytica Chimica Acta, 127 (1981) 219—222
Elsevier Scientific Publishing Company, Amsterdam — Printed in The Netherlands

Short Communication

ABTRENNUNG VON WISMUT DURCH CHLOROFORMEXTRAKTION MIT *N*-BENZOYL-α-AMINOBUTTERSÄURE†

S. DULLNIG und R. PIETSCH*

Institut für Anorganische und Analytische Chemie der Universität Graz (Österreich)

(Eingegangen den 9. September 1980)

(Separation of bismuth by extraction with N-benzoyl-α-butanoic acid into chloroform.)

Summary. Extractive separation of bismuth in nitric acid solutions from many metal ions is possible after simple pH adjustment. A specially designed separating funnel is useful. Alloys and pharmaceutical preparations are easily analyzed.

Zusammenfassung. Es wird über die Möglichkeit der Wismutextraktion aus salpetersaurer Lösung berichtet. Die Abtrennung des Wismut von vielen Metallen ist durch einfache pH-Einstellung der wäßrigen Lösung möglich. Die Anwendbarkeit der Methode auf die Analyse von Legierungen und pharmazeutischen Präparaten wurde untersucht.

An der Aminogruppe benzoylierte, geradkettige α-Aminosäuren eignen sich zur extraktiven Abtrennung verschiedener Metallionen mit Chloroform als Extraktionsmittel. Vor einiger Zeit wurde bereits über die Abtrennung von Wismut und Blei mit *N*-Benzoyl-α-Aminocapronsäure in Chloroform berichtet [1].

Die *N*-Benzoyl-α-Aminobuttersäure bietet gegenüber der längerkettigen analog substituierten Capronsäure den Vorteil noch besserer Abtrennungsmöglichkeiten für Wismut. Die *N*-Benzoyl-α-Aminobuttersäure (BB) wurde erstmals von Fischer und Mouneyrat [2] synthetisiert. Die in dieser Arbeit benötigten größeren Mengen wurden nach der sinngemäß angewandten Methode von Steiger [3] hergestellt.

Bei den Voruntersuchungen, die einen allgemeinen Überblick über die mit BB erzielbaren Metallextraktionen in Chloroform geben sollten, wurden 0,4 mmol der zu untersuchenden Metalle in Form ihrer Nitrate in 40 ml salpetersaurer wäßriger Lösung, einmal mit 40 ml Chloroform, das $2{,}0 \times 10^{-3}$ Mol BB enthielt, bei verschiedenen pH-Werten der wäßrigen Lösung ausgeschüttelt. Der Gehalt der Chloroformphase an extrahiertem Metall wurde in geeigneter Weise quantitativ bestimmt. Die mit den untersuchten Metallen erhaltenen Ergebnisse zeigt Tab. 1.

Arbeitsmethode

Der für diese Extraktionen angefertigten Scheidetrichter von 100 ml

†Herrn Professor Dr. Gustav Zigeuner zum 60. Geburtstag gewidmet.

0003—2670/81/0000—0000/$02.50

TABELLE 1

Extraktionsergebnisse verschiedener Metalle
(0,4 mmol Metall in 40 ml H_2O: 2,0 × 10^{-3} Mol BB in 40 ml $CHCl_3$ bei einmaliger Extraktion)

Metall	Extraktionsbereich in pH	pH der Maximalextrakt.	Maximalextrakt. (%)	Metall	Extraktionsbereich in pH	pH der Maximalextrakt.	Maximalextrakt. (%)
Na	—	—	—	Cr/Cr^{3+}	4—6	5	11
Ca	—	—	—	Bi	2—5	3	94
Mg	—	—	—	In	2—5	4	86
Cu	4—5	4,5	12	La	>4	5	39
Ni	—	—	—	Be	4—6	5	50
Co	>4	>8	25	Ag	—	—	—
Mn	—	—	—	Au	3—5	4	1
Zn	>8	>8	3	Pt	—	—	—
Ba	—	—	—	Pd	2—8	4	27
Cd	>8	>8	1	V	—	—	—
Pb	>3	6	72	W	—	—	—
U/UO_2^{2+}	3—9	4	70	Mo	—	—	—
Fe/Fe^{3+}	2—5	3	60	Zr	1—4	3,5	42
Al	3—6	4	22	Th	2—7	4	26

Gesamtvolumen trägt einen 29-mm Normalschliff, durch den es leicht möglich ist, einen mit Motor angetriebenen Propellerrührer so einzuführen, daß die maximale Durchmischung der Phasen an der Grenzschichte der oberen wäßrigen und der unteren Chloroformphase, die das Reagens BB enthält, eintritt. Gleichzeitig kann durch diesen großen Schliff die Zugabe von verdünnter Ammoniaklösung zur pH-Einstellung der wäßrigen Phase erfolgen. Durch eine seitlich angesetzte Schliffhülse (NS 14,5) wird eine kombinierte Glaselektrode (EA 121, Metrohm, Herisau, Schweiz) so eingesetzt, daß die Kugel und der Asbestfaden der Glaselektrode in der oberen, wäßrigen Schicht liegen. In Verbindung mit dem zugehörigen pH-Meter E 520 der gleichen Firma kann die Aciditätsänderung der wäßrigen Phase leicht verfolgt werden. Bei entsprechend raschem Lauf des Rührers erfolgt eine intensive Phasendurchmischung und damit rasche Extraktion.

Die das Wismut in rund 40 ml schwach salpetersaurer wäßriger Lösung enthaltende Probe wird im oben beschriebenen Scheidetrichter mit 40 ml einer Reagenslösung von 10 g BB in 1 l Chloroform versetzt. Durch rasches Rühren wird das Reagens gut verteilt und gleichzeitig durch Zugabe von verdünnter Ammoniaklösung der pH auf 3,0—3,5 eingestellt. Hierauf wird so lange durch rasches Rühren weiterextrahiert, bis die Chloroformphase völlig klar ist. Die das Wismut enthaltende Chloroformphase wird nun in einen Titrierkolben abgelassen und der Scheidetrichter mit reinem Chloroform quantitativ nachgespült. Danach wird noch dreimal mit je 10 ml Reagenslösung nachextrahiert.

Die gesammelten Chloroformextrakte werden mit 150 ml einer 0,14 M

TABELLE 2

Ergebnisse von Wismuttrennungen

Bi gegeben (mg)	Begleitmetall (mg)	Bi gefunden (mg)	Begleitmetall im Extrakt (mg)
20,5	Al 156,0	20,5	0,0
34,2	Pb 270,4	34,2	1,3
68,3	Cr 11,4	68,5	2,0
68,3	La 139,4	68,2	0,3
68,3	Zn 201,8	68,2	0,6
68,3	Cd 856,0	68,1	0,6
68,3	Co 209,2	68,1	0,2
68,3	Ni 598,2	68,3	4,9
68,3	Cu 206,4	68,3	1,1
68,3	Ag 254,3	68,2	0,0
68,3	Ca 505,0	68,3	1,8
68,3	Mg 265,6	68,1	0,2

Salpetersäure überschichtet, und unter starkem Rühren mittels Magnetrührer mit Äthylendiaminotetraessigsäure gegen Xylenolorange [4] als Indikator auf den Umschlag von rot nach reingelb titriert.

Um die Extrahierbarkeit des Wismut mit BB sicherzustellen, wurden zuerst reine, salpetersaure wäßrige Wismutnitratlösungen in der angegebenen Weise extrahiert und das Wismut wie oben angeführt bestimmt. Wismutmengen zwischen 20,5 mg und 101,1 mg wurden in den Extrakten mit einem Fehler von ±0,2% des Wertes wiedergefunden, wobei zu bemerken ist, daß dieser Fehler in der Größenordnung des Titrierfehler liegt.

Trennungsergebnisse

Tabelle 1 zeigt die gute Abtrennbarkeit des Wismut von den meisten Metallen. Lediglich die Trennung von begleitendem dreiwertigen Eisen ist infolge analoger Extraktionsbereiche durch genaue pH-Einstellung allein nicht möglich. Kleine Eisenmengen können aber erfolgreich mit Sulfosalicylsäure maskiert werden. Von 12 Metallen aus Tab. 1 wurden quantitative Trennungen vorgenommen, wobei auch die im Chloroformextrakt enthaltenen Begleitmetalle quantitativ bestimmt wurden, was in Tab. 2 veranschaulicht wird.

Nach der angegebenen Arbeitsmethode läßt sich Wismut einfach und gut von begleitendem Magnesium, Calzium, Kupfer, Nickel, Zink, Cadmium und Lanthan bei pH 3,0 abtrennen. Aluminium, Blei, Silber, und Kobalt sollten in nicht zu großer Menge als Begleitmetalle vorhanden sein, da sonst Wismutfällungen auftreten, die die Extraktionsausbeute vermindern.

Interessant ist die Abtrennung des Wismut von dreiwertigem Chrom. Chrom allein ist bei pH 3,0 überhaupt nicht extrahierbar. In Gegenwart von Wismut jedoch wird das Chrom bei pH 3,0 mitextrahiert, was an der Grün-

färbung der Chloroformphase deutlich erkennbar ist. Das Ausmaß der Mitextraktion steigt mit der Menge des neben Wismut vorhandenen Chroms prozentual an.

Die praktische Anwendbarkeit der Abtrennung des Wismut mit BB wurde auch an einigen Testanalysen überprüft. So wurde das Wismut in einer Legierung bestimmt, die neben 36,1% Wismut noch 23,2% Sn und 40,6% Pb enthielt. Gefunden wurden 35,9% Bi. In einem Kupfermetall, das nur 0,003% Bi, neben 91,8% Cu, 7,8% Sn und kleineren Mengen an Sb, Pb, Fe, Mn, Ni, Al, Mg, Zn, Cd und Ag enthielt, wurden rasch und ohne Schwierigkeiten durch die große Kupfermenge 0,002% Bi gefunden.

In einem pharmazeutischen Präparat, das 18,8 mg Bi in Form von Wismutaluminat pro Tablette enthielt, neben größeren Mengen Aluminiumglycinat, Succ. Liquiritiae, Magnesiumcarbonat, und Äthylpapaverin, wurden nach Lösen in verdünnter Salpetersäure und Extraktion mit BB 18,7 mg Bi mit einer Genauigkeit von —0,5% gefunden. Eine direkte Wismutbestimmung aus der salpetersauren, dunkelbraunen wäßrigen Lösung mittels Titration mit Äthylendiaminotetraessigsäure war nicht zielführend.

LITERATUR

1 R. Pietsch, Anal. Chim. Acta, 115 (1980) 379.
2 E. Fischer und A. Mouneyrat, Ber. Dtsch. Chem. Ges., 33 (1900) 2390.
3 R. Steiger, J. Org. Chem., 9 (1944) 399.
4 Komplexometrische Bestimmungsmethoden mit Titriplex, E. Merck, Darmstadt, S. 51.

Analytica Chimica Acta, 127 (1981) 223—226
Elsevier Scientific Publishing Company, Amsterdam — Printed in The Netherlands

Short Communication

THE DETERMINATION OF CHROMIUM IN WATER-SOLUBLE POLYMERS BY GAS CHROMATOGRAPHY

GARY G. HAWN*
Alcolac Inc., 3440 Fairfield Road, Baltimore, MD 21226 (U.S.A.)
CHARLES P. TALLEY
GAF Corp., 1361 Alps Road, Wayne, NJ 07470 (U.S.A.)
ALVIN BROWN
Calgon Corp., P.O. Box 1346, Pittsburgh, PA 15230 (U.S.A.)
(Received 17th February 1981)

Summary. Water-soluble polymers have found increasing use in the areas of water treatment, paper production and oil recovery, and the determination of heavy metals in such materials is important from an environmental standpoint. Heavy metal contamination could result from redox catalysts in the polymerization system, raw materials or stainless steel storage facilities.

Many types of polymers have been analyzed for heavy metals, primarily by atomic absorption methods [1—3]. Henn [3] showed that electrothermal atomic absorption spectrometry was a very sensitive method; detection limits for copper, chromium and iron were established to be 500 pg. Other conventional techniques, such as u.v.-visible spectrophotometry, cannot approach this sensitivity.

Gas chromatography of metals, after formation of volatile metal chelates and extraction into an organic solvent, has proved to be a rapid, sensitive technique [4—8]. The purpose of this work was to show that gas chromatography is a useful tool for measuring trace amounts of chromium (and possibly other metals) in water-soluble polymers via the *tris*(trifluoroacetylacetone)chromium(III) complex. To test the complete method, two polymers, polyacrylamide and a copolymer of acrylamide/acrylic acid, were prepared after a known amount of chromium had been added to the monomer mixes. The resultant polymers were analyzed by both atomic absorption spectrometry and gas chromatography. Recovery of the metal and comparison between methods were excellent.

Experimental

Chromatography. All chemicals were reagent grade and were used without further purification. A Hewlett-Packard Model 5720-A gas chromatograph, equipped with a flame ionization detector, was used. A glass coiled column

0003—2670/81/0000—0000/$02.50

(2 m × 2 mm i.d.) packed with 3% OV-1 on GasChrom Q was used to effect the separation. The oven temperature was held at 135°C while the injector and detector were kept at 200°C. A Hewlett-Packard Model 3354-A Laboratory Data System was used to collect and analyze the data. The chromium content was quantified by using standard additions of a prepared standard. This standard was prepared by dissolving in toluene an appropriate amount of *tris*(trifluoroacetylacetone)chromium(III), synthesized and purified by a known procedure [9].

Atomic absorption spectrometry. A Perkin-Elmer Model 305B spectrometer equipped with an HGA-2100 heated graphite atomizer with a pyrolytically coated graphite tube and background correction, was used for atomic absorption measurements. The instrumental conditions were as follows: 357.9 nm (u.v. range), slit 4, damping 1, ABS mode and function; heating cycle (s/°C), dry (30/100), char (30/1000), atomize (10/2500); argon purge gas at setting 40; sample size 25 μl.

Samples. Homopolyacrylamide and a copolymer of acrylamide/acrylic acid (72.5:27.5 mol%, initial monomer charge) were prepared by using standard polymerization techniques [10]. Chromium was added to the monomer mixes, as $Cr(NO_3)_3 \cdot 9H_2O$, to yield a final product which contained 0.08 mg of chromium per gram of polymer.

Procedures. A stock solution of each polymer was prepared by dissolving 1.00 ± 0.01 g of polymer in 1 l of water. This solution was used directly for atomic absorption measurements. For gas chromatography, a 25.0 g aliquot was weighed into a 50-ml volumetric flask, followed by 5 ml of acetate buffer (pH 5.2; 0.25 mol of sodium acetate trihydrate and 2.5 ml of glacial acetic acid diluted to 200 ml with water), 5 ml of aqueous sodium sulfite and 1.0 ml of 0.2 M trifluoroacetylacetone (tfa) in toluene. The flask was capped and shaken mechanically for 2 h. Distilled water was added to bring the toluene layer into the neck of the flask and a 2-μl aliquot was injected for gas chromatography.

Results and discussion

Chromium was chosen as a representative metal because many other matrices have been assayed for chromium at low levels [11—14]. The metal chelate forms rapidly, is quantitatively extracted from aqueous solution, and is stable, and there are definite possibilities for the presence of chromium in polymers.

Initially, many types of water-soluble polymers, nonionic, anionic and cationic were analyzed but no chromium was detected, although the gas chromatographic procedure had been shown to be satisfactory for standard chromium(III) solutions added at low concentrations to the polymer solutions. It was decided to fortify the monomer mix with chromium to provide polymers with known amounts of chromium. Homopolyacrylamide was chosen because of its widespread applications, and the copolymer of acrylamide/acrylic acid was chosen because an anionic polymer should present the most

difficult situation for extracting chromium(III). Chromium was fortified into the monomer mixes to yield a level of 0.08 mg g^{-1} of polymer, i.e., 80.0 ppm. The results of atomic absorption (a.a.s.) and gas chromatographic (g.c.) measurements, summarized in Table 1, agreed very well with the amount of chromium that was added and between the two assays.

The conventional method of standard additions was used to quantify the chromium in the a.a.s. measurements, account being taken that 1 g of polymer was diluted with 1 l of water. For the g.c. measurements, an external standard of *tris*(trifluoroacetylacetone)chromium(III) in toluene was used for quantification. Calculation for the amount of chromium must take into account not only the dilution factor of 1 g of polymer in 1 l of water, and the concentration factor in extracting into 1 ml of toluene, but also the molecular weight ratio of chromium metal to the chromium chelate.

The optimum conditions for extraction of the metal chelate occurred at about pH 5 with mechanical shaking for 2 h [12]. The sodium sulfite solution was used to reduce any Cr(VI) to Cr(III) because chromium(VI) does not form the chelate. Actually, $Cr(tfa)_3$ forms *cis* and *trans* geometrical isomers in a ratio of 1:4. In this work, quantification was based on the *trans* isomer. A sample chromatogram is shown in Fig. 1. The absolute detection limit is approximately 500 pg of chromium as Cr(III). The sensitivity could be enhanced further by extracting a larger portion of sample or by using a more sensitive detector (electron capture).

TABLE 1

Comparison of results obtained for fortified polymers
(Results are averages of duplicate analyses)

	Cr added (mg)	Cr found by a.a.s. (mg)	Recovery (%)	Cr found by g.c. (mg)	Recovery (%)
Polyacrylamide	0.080	0.085	106	0.073	91
Acrylamide/acrylic acid	0.080	0.065	81	0.068	85

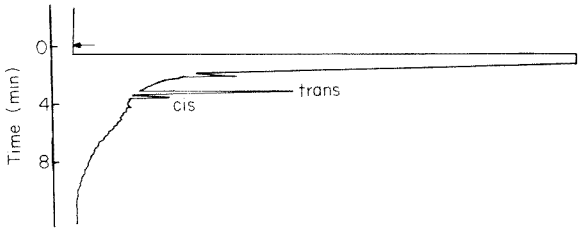

Fig. 1. Chromatogram of the toluene extract of the polyacrylamide sample, depicting both the *trans* and *cis* isomers of [$Cr(tfa)_3$]. Chromatographic conditions are outlined in the Experimental Section.

The charge on the polymer had no effect on the assay, as shown by the consistent recoveries for both the neutral homopolymer and the anionic copolymer. Steric influences, ligand field effects and other factors [15, 16] favor the formation of a metal chelate. Because of the number of available chelating agents which have been used to form stable, volatile metal chelates [4—6], it should be possible to analyze for many metals in aqueous polymer solutions. The simplicity and the sensitivity of this assay could be an important advantage over more conventional methods.

The authors thank Mr. Robert Faust, Calgon Corp., for all the atomic absorption assays.

REFERENCES

1 W. Slavin, At. Absorpt. Newsl., 4 (1965) 192.
2 M. Olivier, At. Absorpt. Newsl., 10 (1971) 12.
3 E. L. Henn, Anal. Chim. Acta, 73 (1974) 273.
4 R. W. Moshier and R. E. Sievers, Gas Chromatography of Metal Chelates, Internation Series of Monographs in Analytical Chemistry, Vol. 23, Pergamon, New York, 1965.
5 G. Guiochon and C. Pommier, Gas Chromatography in Organics and Organometallics, Ann Arbor Science Publishers, Ann Arbor, 1973.
6 J. A. Rodriguez-Vazquez, Anal. Chim. Acta, 73 (1974) 1.
7 H. Kawaguchi, T. Sakamoto and A. Mizuiki, Talanta, 20 (1973) 321.
8 P. C. Uden, D. E. Henderson and C. A. Burgett, Anal. Lett., 7 (1974) 807.
9 R. C. Fay and T. S. Piper, J. Am. Chem. Soc., 85 (1963) 500.
10 H. Warson, The Applications of Synthetic Resin Emulsions, E. Benn, London, 1972.
11 M. S. Black and R. E. Sievers, Anal. Chem., 48 (1976) 1872.
12 R. J. Lovett and G. Fred Lee, Environmental Science and Technology, 10 (1973) 67.
13 W. R. Wolf, M. L. Taylor, B. M. Hughes, T. O. Tiernan and R. E. Sievers, Anal. Chem., 44 (1972) 616.
14 C. Gentry, C. Honin, P. Malherbe and R. Schott, Anal. Chem., 43 (1971) 235.
15 F. A. Cotton and G. Wilkinson, Advanced Inorganic Chemistry, Interscience, New York, 3rd edn., 1972.
16 C. J. Hawkins, Absolute Configuration of Metal Complexes, Wiley—Interscience, New York, 1971.

Analytica Chimica Acta, 127 (1981) 227—231
Elsevier Scientific Publishing Company, Amsterdam — Printed in The Netherlands

Short Communication

MOLECULAR EMISSION CAVITY ANALYSIS
Part 19. Improved Procedure for the Determination of Boron

M. BURGUERA[a]

Chemistry Department, Birmingham University, P.O. Box 363, Birmingham, B15 2TT (Gt. Britain)

ALAN TOWNSHEND*

Chemistry Department, University of Hull, Hull HU6 7RX (Gt. Britain)

(Received 12th December 1980)

Summary. Boron is converted to trimethylborate, which is volatilized into an oxy-cavity in a hydrogen—nitrogen flame. Insertion of a trap at —50°C decreases the methanol background, allowing 0.05—20 μg of boron to be determined.

Boron compounds give rise to a green BO_2 emission [1, 2] when introduced into hydrogen-based flames. However, because many inorganic boron compounds are broken down in such flames only with difficulty, prior conversion to more labile species is usually essential. This has been achieved either by extraction of borate with 2-ethylhexane-1,3-diol [3—6] or by conversion to volatile trimethyl borate [4, 7, 8] or boron trifluoride [9—11].

Such procedures were also found to be necessary for the determination of boron by molecular emission cavity analysis (m.e.c.a.). The extraction procedure, combined with the use of an oxy-cavity, gave a linear calibration graph for 5—80 ng of boron in 10 μl of extract [4]. The 2σ detection limit was 0.16 μg ml^{-1}, and only fluoride interfered. The use of a flame generated entirely within a cavity gave a similar sensitivity and detection limit [5]. In both instances, the detection limit was governed by the flame background emission. The generation of trimethyl borate and transport of the vapour to an oxy-cavity gave a linear calibration graph for 2—30 μg of boron in 1.5 ml of solution [4]. No interferences were detected. The relatively poor sensitivity and detection limit (ca. 1 μg) arose from the considerable flame background emission caused by volatilization of some of the excess of methanol from the reaction mixture. Preliminary experiments on boron trifluoride vapourization gave a detection limit of 0.6 μg of boron [11]. Background problems also limit other flame procedures for boron [3, 5].

This communication reports the development of an improved procedure for the determination of boron by m.e.c.a. based on volatilization of trimethyl borate. It involves more rapid volatilization than previously, and a considerably decreased background emission.

[a]Present address: Departmento de Quimica, Facultad de Ciencias, Universidad de Los Andes, Merida, Venezuela.

Experimental

Equipment. The m.e.c.a. spectrometer and oxy-cavity previously described [12] were used without modification. The trimethyl borate generator was a glass vial (4.5 cm long × 1.5 cm i.d.) screwed into a rulon cap, and sealed with a silicone rubber septum. Three holes were drilled through the cap. Two stainless-steel tubes were inserted for passing nitrogen into the reaction mixture, and removing the evolved gases, respectively, and a chromatograph injection port was welded onto the top of the cap to coincide with the central third hole. The exit tube from the generator was connected, when stated, to a glass tube (10 cm long × 1.0 cm i.d.) filled with a molecular sieve, or a coiled 30 cm long × 4 mm i.d. teflon tube (for immersion in a cold bath), and thence by further stainless-steel tubing to the inlet to the cavity. The generator tube and the steel tubing to the cavity could be heated electrically at 80°C.

Some preliminary experiments were carried out in a 10 cm long × 1.5 cm i.d. polypropylene generator.

Reagents. All water used was twice distilled from an all-glass apparatus. A boron solution (1000 μg ml^{-1}) was prepared by dissolving 2.860 g of analytical-grade boric acid in 500 ml of methanol. The methanol and 98% sulphuric acid required to prepare methylating mixtures were mixed daily by vigorous stirring in a bath of cold water.

Recommended procedure. To the anhydrous sample containing 0.05—20 μg of boron in the cold generator tube were added 1 ml of methanol and 1 ml of (1 + 1) methanol—sulphuric acid, and the cap was attached. Alternatively, methanolic standard solutions (1 ml) were injected through the port onto 1 ml of the methylating mixture. Nitrogen was bubbled through at 10 ml min^{-1}, the teflon coil immersed in a bath of solid carbon dioxide in (1 + 1) chloroform—carbon tetrachloride at —50°C, and the flame (2.0 l H_2 min^{-1}, 5.0 l N_2 min^{-1}, 80 ml O_2 min^{-1} to the cavity) ignited. After 5 min, the generator was heated to 80°C, and the evolved gases were retained in the coil. When this was complete, the coil was immersed in water at 80°C and the emission produced by the vapours transported by the nitrogen carrier gas was measured at 518 nm (slit width 0.2 mm ≡ 11 nm) as a function of time.

Determination of boron in ferro-boron. An accurately weighed sample (ca. 0.1 g) was dissolved in 20 ml of (1 + 1) concentrated sulphuric acid—hydrochloric acid by gentle warming. The solution was transferred to a 100-ml volumetric flask and diluted to volume with water. Various volumes (0.25—1 ml) of this solution were pipetted into the glass vials used as generators, and the water evaporated on a hotplate. To the cool residue, 1 ml of methanol and 1 ml of (1 + 1) methylating mixture were added, and the boron was determined as above.

Determination of boron in mild steel. An accurately weighed sample (0.1—0.5 g) was dissolved in 10 ml of 12.5% (w/v) sulphuric acid. The solution was carefully evaporated to ca. 1 ml and transferred to a generator tube. The evaporation was continued until fumes were observed. Boron was determined as described above.

Results

Some preliminary experiments were carried out using the larger generator and no trap. Spectral measurements (Fig. 1) show the BO_2 emission bands and the underlying emission produced by methanol. Although the peak at 546 nm is the highest, the blank is also near its maximum at this wavelength, and so the peak at 518 nm was used for further study. In general, the BO_2 and background intensity increased with flame temperature. As a result of flame composition optimization studies, a flame of 2.0 l H_2 min^{-1} and 5.0 l N_2 min^{-1} was selected for further use.

The effect of the methanol:sulphuric acid ratio on the rate and extent of trimethyl borate generation was studied. Stahl [7] recommended a (5 + 1) mixture, below 60°C. This was used in the previous m.e.c.a. study [4]. However, this mixture was found to give relatively small emission responses, and a long heating time was needed for evolution of trimethyl borate (Fig. 2). Mixtures containing a smaller proportion of methanol were studied. The results obtained (Fig. 2) showed that fastest generation occurred with the (2 + 1) methanol:sulphuric acid, although the ultimate intensity was slightly lower than the (1 + 1) mixture. This slight decrease probably arises from the noticeably exothermic reaction that occurs on adding the methanolic boron solution to the (2 + 1) methylating mixture, causing early volatilization of some boron. Thus the (1 + 1) mixture is to be preferred; in the procedure an equal volume of methanol is added to this mixture before heating.

When these optimized conditions were used, a linear calibration graph

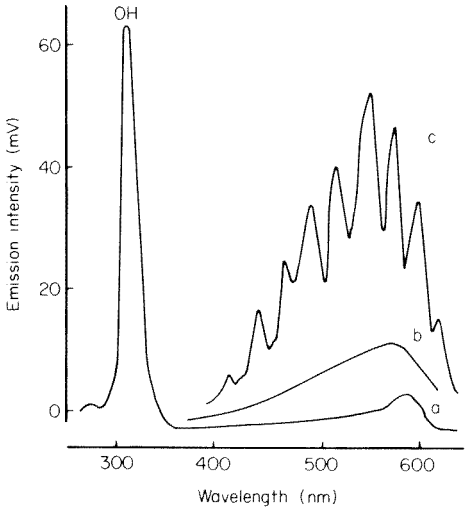

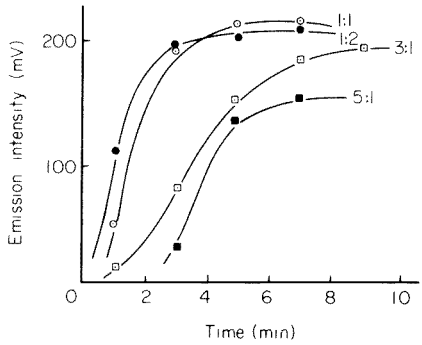

Fig. 1. Spectra from: (a) flame; (b) methanol blank; (c) boron. Flame: 1.8 l H_2 min^{-1}, 5.5 l N_2 min^{-1}, 80 ml O_2 min^{-1} to cavity; slit 0.2 mm ≡ 11 nm.

Fig. 2. Effect of ratio of methanol: 98% sulphuric acid in methylating mixture on emission generated by 20 μg of boron after various reaction times at 80°C (peak height measurement).

based on peak height was obtained for 5—20 μg of boron. The 2σ detection limit was 0.2 μg, a slight improvement over that obtained previously [4].

Attempts to decrease the blank signal. As the detection limit was governed by the emission originating from methanol, attempts were made to decrease this emission by trapping methanol, either by a molecular sieve or by freezing. The small generator was used for these and all subsequent experiments, as it gave faster trimethyl borate generation.

Molecular sieves 4A, 5A and self-indicating 13X were investigated for trapping methanol during the determination of 10 μg of boron. All the materials eliminated the methanol blank, but also considerably decreased (by 80—96%) the boron signal as well, indicating appreciable trapping of trimethyl borate. In addition, the time needed for deaerating the system was considerably increased, to 15 min.

The use of a cold trap capable of condensing methanol (b.p. 65°C) and trimethyl borate (b.p. 68°C) was also investigated. Because of the very small differences in their boiling points, complete separation of the two gases by this means was not expected. Nevertheless, when a trap containing solid carbon dioxide suspended in a mixture of equal volumes of chloroform and carbon tetrachloride (—50°C) was used, and the recommended procedure followed, the blank response was decreased by an order of magnitude to 6—7 mV, compared to a peak height of 53 mV for 5 μg of boron under the same conditions. Much of the methanol seemed to condense in the small portion of the tube between the generator and the cold trap, and was not subsequently volatilized with the trimethyl borate. The trap and associated tubing should be completely cleaned and dried between experiments.

Calibration and applications. The range of linearity with the cold trap procedure was 0.05—20 μg of boron (0.8—151 mV). The mean blank intensity was 6.4 mV (s.d. 0.2, 9 measurements), the 2σ detection limit was 30 ng of boron, and the relative standard deviation for six consecutive measurements of 1.0 μg of boron was 5.2%.

The technique was applied to the determination of boron in a steel and in ferroboron. The results are given in Table 1. Although the samples contained a little more sulphuric acid at the generation stage than the standard (methanolic boric acid), the results are accurate.

Conclusions

The improved procedure enables 0.05—20 μg of boron to be determined in 1-ml samples. Larger volumes can readily be accommodated by evaporation. The detection limit is 30 times better than that obtained previously by m.e.c.a. [4]. The lack of interferences, established previously [4], enables the method to be applied directly to steels and other samples. The use of methanolic boric acid solution for standards eliminates the need to evaporate aqueous standards to dryness.

TABLE 1

Results for the determination of boron in a mild steel and ferroboron

Sample	Amount used	Net emission intensity (mV)	Amount of boron (μg)	Conc. of boron (%)	
				Found	Certified
Ferroboron	1.00[a]	118	15.3	15.3	
B.C.S. 373	0.50[a]	61	7.6	15.2	15.1
	0.25[a]	35.1	3.8	15.2	
				Mean 15.2	
Steel	0.50[b]	45	5.0	0.0010	
B.C.S. 456	0.30[b]	30	3.0	0.0010	0.0010
	0.10[b]	12	0.95	0.0009	
				Mean 0.0010	

[a]Volume (ml) taken from the 100 ml. [b]Weight (g) of steel analyzed.

M. Burguera thanks FONINVES, Venezuela, for the provision of a research scholarship.

REFERENCES

1 A. A. Mal'tsev, V. K. Matveer and V. M. Tatevskii, Dokl. Akad. Nauk SSR, 137 (1961) 123.
2 W. E. Kaskan and R. C. Milliken, J. Chem. Phys., 32 (1960) 1273.
3 Y. C. M. Pau, E. E. Pickett and S. R. Koirtyohann, Analyst, 97 (1972) 860.
4 R. Belcher, S. A. Ghonaim and A. Townshend, Anal. Chim. Acta, 71 (1974) 255.
5 S. L. Bogdanski, E. Henden and A. Townshend, Anal. Chim. Acta, 116 (1980) 93.
6 Y. R. Melton, W. L. Hoover, P. A. Howard and Y. L. Ayers, J. Assoc. Off. Anal. Chem., 53 (1970) 682.
7 W. Stahl, Fresenius Z. Anal. Chem., 83 (1930) 268; 101 (1935) 342, 348.
8 H. C. Weber and R. D. Jacobson, Ind. Eng. Chem., Anal. Ed., 10 (1978) 273.
9 H. Gilbert, Z. Angew. Chem., 6 (1893) 531.
10 V. Lenher and J. S. C. Wells, J. Am. Chem. Soc., 21 (1899) 417.
11 M. Burguera, Ph.D. Thesis, Birmingham University, 1978.
12 M. Burguera, A. Townshend and S. L. Bogdanski, Anal. Chim. Acta, 117 (1980) 247.

Analytica Chimica Acta, 127 (1981) 233—238
Elsevier Scientific Publishing Company, Amsterdam — Printed in The Netherlands

Short Communication

THE INFLUENCE OF THE SURFACTANT IN A PERFLUORINATED EMULSION ON THE DETERMINATION OF THALLIUM, LEAD AND CADMIUM BY ANODIC STRIPPING VOLTAMMETRY

J. GEORGES

Laboratoire de Chimie Analytique III (E.R.A. 0474), Université Claude Bernard, 43, Boulevard du 11 Novembre 1918, 69622 Villeurbanne Cedex (France)

(Received 1st December 1980)

Summary. The effects of the Pluronic F-68 surfactant in the emulsion are described. A study of the two electrode processes in the measuring cycle shows that the deposition stage is not affected provided that the deposition potential is negative enough. The peak potentials for Pb^{2+} and Cd^{2+} are slightly shifted and the stripping currents are seriously decreased when the differential pulse (d.p.) mode is used, but the inhibition is independent of metal ion concentration and deposition time, and the d.p. mode is suitable for quantitative work. The performance of hanging drop and film mercury electrodes is compared.

The presence of surfactants in the measuring system gives rise to serious interference in analysis for metals by anodic stripping voltammetry (a.s.v.) at the hanging mercury drop electrode (HMDE) or the mercury film electrode (MFE) and the behaviour of these organic compounds must be considered [1, 2]. Adsorption of a surfactant on the electrode may have an important effect on the height and the potential of the stripping peaks. The surfactant may affect the electrolytic deposition stage or the stripping step or even both [3, 4]. The purpose of the work described here was to study the influence of a non-ionic surfactant (Pluronic F-68) in a perfluorinated emulsion (Fluosol-43) when a.s.v. techniques were used for thallium(I), lead(II) and cadmium(II) determinations. In previous work [5] it was shown that the polarographic reduction of lead(II) and cadmium(II) in such a medium is strongly affected and that the inhibition of the electrode process depends only on the monomer form of the surfactant present in the emulsion. It seemed therefore worthwhile to examine if this inhibition occurs in a.s.v., and to evaluate the contributions of the deposition and stripping stages to the total effect of the surfactant. Different factors, like metal ion concentration and deposition time, which could alter the magnitude of the inhibitory effect were investigated to determine if the analytical utilization of a.s.v. is possible in such a medium. Surfactant influence on interference effects was also examined and compared at the HMDE and the MFE.

Experimental

Cyclic, normal pulse and anodic stripping voltammograms were obtained

0003—2670/81/0000—0000/$02.50

with a Princeton Applied Research Model 174 polarographic analyser and recorded with a Sefram TRP x-y recorder. The operating modes were as follows. For linear sweep voltammetry, the scan rate was 100 mV s^{-1} for cyclic voltammograms and 10 mV s^{-1} for the stripping mode. For normal pulse polarograms, the scan rate was 2 mV s^{-1} and the drop time 2 s. For the differential pulse stripping mode, the pulse modulation was 25 mV, the scan rate 2 mV s^{-1} and the pulse repetition 0.5 s.

The HMDE was a Metrohm E410 model with a drop size corresponding to 3 divisions of the micrometer. The MFE was a glassy carbon electrode with a 0.3 cm diameter disc, onto which the mercury film was plated in situ by adding 2×10^{-5} M mercury(II) nitrate to the sample solution [6]. Before each assay, the electrode was cleaned with a soft paper. Solutions were stirred during the deposition period with a magnetic stirrer for HMDE studies and by electrode rotation (2000 rpm) for MFE studies. Stirring was stopped and the solution held at the deposition potential for 20 s before the anodic stripping scan was initiated. The auxiliary electrode was a platinum wire; the reference was a saturated calomel electrode to which all the potentials are referred.

Fluosol-43 emulsion (25% perfluorotributylamine and 3.2% Pluronic F-68 in distilled water) was supplied by the Green Cross Corporation (Osaka, Japan). Its pH is about 3.

The solutions used were prepared from analytical reagents. All solutions were deoxygenated with nitrogen and all measurements were made at 25°C.

Results and discussion

Surfactant effects on reduction and re-oxidation processes. These aspects were studied by cyclic voltammetry (c.v.) at the HMDE and by normal pulse polarography (p.p.) at the dropping mercury electrode. In these two polarographic modes, the metal analgam formed during the deposition period, cathodic scan (in c.v.) or initial cathodic potential application (in p.p), is dissolved during the stripping step, linear-sweep anodic scan (in c.v.) or pulse anodic scan (in p.p.) [7]. Figures 1 and 2 confirm and extend previous observations [5]: the inhibitory effect of the surfactant for the reduction stage increases in the order $Tl^+ < Pb^{2+} < < Cd^{2+}$. The stripping step is unchanged for thallium(I); for lead(II) and cadmium(II), the anodic peaks (c.v.) or waves (p.p.) in the emulsion are very similar to those corresponding to the reversible system in pure water. Peak or wave potentials are slightly shifted towards anodic values, but their heights are equal, when the lower values of the diffusion coefficients in the emulsion [5] are taken into account. These results suggest that if the surfactant slows down the deposition process, the inhibition does not seem to occur in the quantity of metal amalgam formed, provided that the deposition potential is negative enough and corresponds to the polarographic diffusion plateau of the irreversible system, i.e. about −0.7 V for lead(II) and −1.2 V (vs. SCE) for cadmium(II). This is emphasized by Table 1 where three stripping modes are compared in water and in

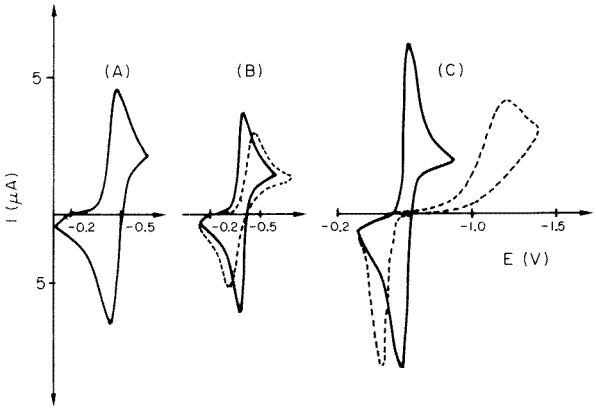

Fig. 1. Cyclic voltammograms at the HMDE in water +0.1 M $LiClO_4$. pH 3 (——) and in emulsion +0.1 M $LiClO_4$ (----) for (A) 5×10^{-4} Tl^+; (B) 5×10^{-4} M Pb^{2+}; (C) 5×10^{-4} M Cd^{2+}. Scan rate 100 mV s^{-1}.

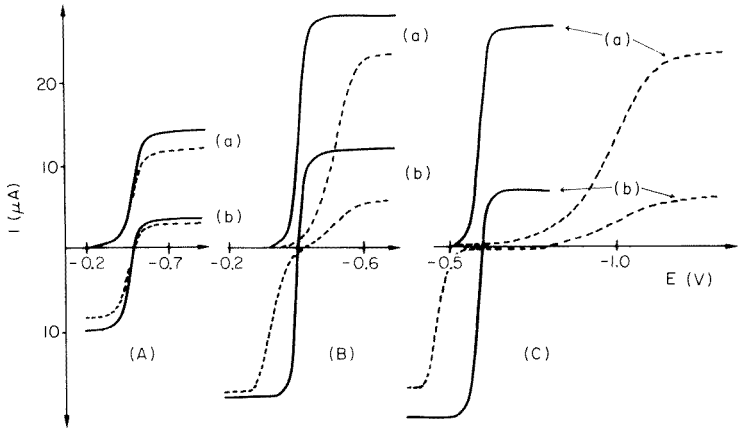

Fig. 2. Cathodic (a) and anodic (b) pulse polarograms at the DME in water +0.1 M $LiClO_4$, pH3 (——) and in emulsion +0.1 M $LiClO_4$ (----) for (A) 5×10^{-4} M Tl^+; (b) 5×10^{-4} M Pb^{2+}; (C) 5×10^{-4} M Cd^{2+}. Scan rate 2 mV s^{-1}; drop time 2 s.

emulsion for 5×10^{-7} M Tl^+, Pb^{2+} or Cd^{2+}. It can be seen that the stripping currents in the linear-sweep and normal pulse modes are practically unchanged in the emulsion and that the electrolysis yield is not lessened at the potentials mentioned. In contrast, the currents obtained in the differential pulse mode are decreased significantly in the emulsion for lead(II) and cadmium(II), but it can be asserted confidently that this is connected only with the stripping step.

Analytical aspects. Despite the above observations, the differential pulse (d.p.) stripping mode at the HMDE is the most versatile method for quantitative work. Figure 3 shows the linear calibration graphs obtained in pure

TABLE 1

Peak or wave currents[a] (nA) at the HMDE for 5×10^{-7} M Tl^+, Pb^{2+} and Cd^{2+} in water and in emulsion for different stripping modes
(Deposition time 100 s; deposition potential —0.7 V for Tl^+ and Pb^{2+}, and —1.2 V for Cd^{2+})

Metal ion	Linear sweep		Pulse		Differential pulse	
in 0.1 M $LiClO_4$	Water	Emulsion	Water	Emulsion	Water	Emulsion
Tl^+	110	105	175	170	47	45
Pb^{2+}	270	260	400	395	180	45
Cd^{2+}	200	190	320	310	140	35

[a]Average value for 3 assays.

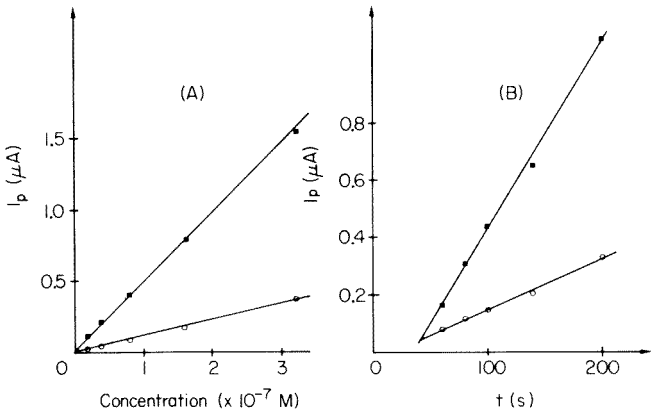

Fig. 3. Peak currents versus concentration (A) and deposition time (B) for cadmium(II) using the d.p. stripping mode at the HMDE in water + 0.1 M $LiClO_4$ (▪) and in emulsion + 0.1 M $LiClO_4$ (○).

water and in emulsion for cadmium(II) in the range 2×10^{-8}—3.5×10^{-7} M. Similar straight lines were obtained when peak currents were plotted versus deposition time between 60 and 200 s for the same cadmium ion concentration (4×10^{-8} M). The average ratio between peak currents in water and in emulsion was about 0.25. These results suggest that the amplitude of the inhibition, which occurs during the d.p. stripping stage, is independent of the quantity of metal amalgam deposited, and that the method is suitable for analytical applications in such a medium.

Surfactant effects on interferences. The most important interference in a.s.v. occurs when two stripping peaks have similar potentials. The influence of Pluronic F-68 in the emulsion, expressed by shifts of peak potentials is shown in Table 2 where the d.p. stripping mode at the HMDE is compared with the rapid d.c. stripping mode at the MFE. The results listed show first the fundamental difference between the peak potentials at the HMDE and the MFE, as predicted from the electrode equations [8]. In water, resolution

TABLE 2

Stripping peak potentials at the HMDE and the MFE in water and in emulsion

Metal ion in 0.1 M $LiClO_4$	$E_{1/2}$ [5]		E_p			
	Water	Emulsion	MFE[a]		HMDE[b]	
			Water	Emulsion	Water	Emulsion
Tl^+	−0.470	−0.470	−0.800[c]	−0.800[c]	−0.490	−0.490
Pb^{2+}	−0.400	−0.435	−0.520	−0.510	−0.410	−0.360
Cd^{2+}	−0.590	−0.850	−0.700	−0.670	−0.600	−0.510

[a]Linear sweep, 10 mV s^{-1} scan rate. [b]Differential pulse mode, 25 mV amplitude. [c]First scan after cleaning the electrode.

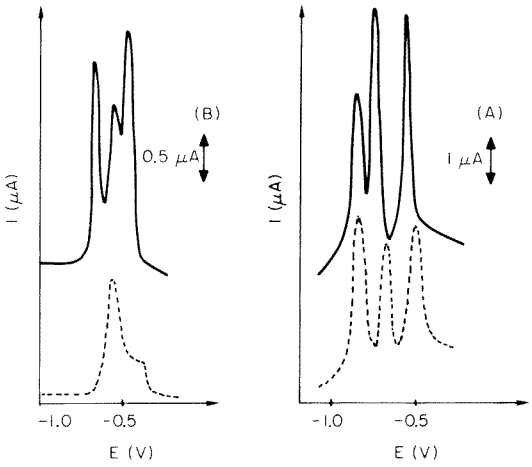

Fig. 4. Stripping peaks for 10^{-6} M Tl^+, 10^{-6} M Pb^{2+} and 10^{-6} M Cd^{2+} at pH3 in water + 0.1 M $LiClO_4$ (——) and in emulsion + 0.1 M $LiClO_4$ (----). Deposition time 100 s, deposition potential −1.2 V, scan from −1.0 V (vs. SCE). (A) Linear sweep at MFE, 10 m V s^{-1} scan; (B) differential pulse at HMDE, 25 mV amplitude, 2 mV s^{-1} scan.

of Tl^+ and Cd^{2+} is poor at the MFE and good at the HMDE, whereas resolution of Tl^+ and Pb^{2+} is poor at the HMDE and good at the MFE. In the emulsion, the peak potentials for lead and cadmium are shifted towards anodic values and so the resolution becomes better for the three cations at the MFE but worse at the HMDE (Table 2 and Fig. 4). Nevertheless the thallium—cadmium interference at the HMDE can be overcome by decreasing the deposition potential to a value where cadmium ions are not reduced. This operation is easier in the emulsion because the surfactant increases the difference between the half-wave potentials of thallium(I) and cadmium(II) (Table 2). For a deposition potential of −0.7 V (vs. SCE), therefore, the yield of thallium electrolysis is a maximum whilst the reduction of cadmium ions would be negligible. This inhibitory effect can be used in some analyses for impurities

in the presence of a large amount of matrix element without preliminary separation as in determinations of lead and thallium in cadmium salts [9].

The author is grateful to S. Desmettre for experimental assistance.

REFERENCES

1 Z. Lukaszewski and M. K. Pawlak, Chem. Anal., 24 (1979) 221.
2 G. E. Batley and T. M. Florence, J. Electroanal. Chem., 72 (1976) 121.
3 Z. Lukaszewski, M. K. Pawlak and A. Ciszewski, J. Electroanal. Chem., 103 (1979) 217.
4 Z. Lukaszewski and M. K. Pawlak, J. Electroanal. Chem., 103 (1979) 225.
5 J. Georges, Anal. Chim. Acta, 121 (1980) 29.
6 T. M. Florence, J. Electroanal. Chem., 27 (1970) 273.
7 K. B. Oldham and E. P. Parry, Anal. Chem., 42 (1970) 229.
8 G. E. Batley and T. M. Florence, J. Electroanal. Chem., 55 (1974) 223.
9 Z. Lukaszewski, M. K. Pawlak and A. Ciszewski, Talanta, 72 (1980) 181.

Analytica Chimica Acta, 127 (1981) 239—243
Elsevier Scientific Publishing Company, Amsterdam — Printed in The Netherlands

Short Communication

SYNCHRONIZATION OF SIGNAL SAMPLING WITH LIQUID PULSATION IN SYSTEMS WITH PERISTALTIC PUMPS

F. OPEKAR and A. TROJÁNEK*

The J. Heyrovský Institute of Physical Chemistry and Electrochemistry, Jilská 16, 110 00 Prague 1 (Czechoslovakia)

(Received 29th December 1980)

Summary. Method and electronic circuitry are described for synchronization of analytical signal sampling with pulsation of liquid flow in systems with a peristaltic pump. The technique is illustrated for cathodic stripping voltammetry of manganese.

Peristaltic pumps are used to pump solutions of samples and reagents in flow-through apparatus. Roller pumps frequently produce marked liquid pulses in the tubing, and these in turn cause pulsation in the measured signal. These pulses, which are especially marked in signals from amperometric and potentiometric detectors, considerably complicate signal measurement and treatment.

In practice, current and potential pulses are usually damped by passive RC components; these are either electronic (placed between the detector and the recorder), hydrodynamic (placed between the pump and the detector) or both. An increase in the rate of pumping and a decrease in the internal diameter of the tube as recommended by Opheim and Lund [1] is a type of passive damping exploiting the natural time constant of the system.

These damping methods produce signals with pulse amplitudes so decreased that the signal can easily be recorded and used. Incompletely removed pulses, whose amplitudes do not prevent analog recording of the measured signal, can, however, produce considerable complications in data treatment. For example, signal differentiation is practically impossible because even small pulses have a frequency (depending on the pumping rate and type of pump) which is usually greater (sometimes much greater) than the changes in the measured signal. This is a major disadvantage of simple methods of pulse suppression. Further complications can result from possible distortion of the recorded signal, worsening of the hydrodynamic conditions in the liquid circuit, and lengthening of the response time of the detector; this last effect depends on the ratio of the time constants of the damping components and of the process studied.

An analogous problem occurs in the damping of current oscillations when dropping mercury electrodes are used [2]; a very useful (though more complex) method here involves current sampling at a certain instant in the life of

0003—2670/81/0000—0000/$02.50

the mercury drop [3, 4]. An analogous sampling technique can be used to eliminate signal pulses in systems with peristaltic pumps. The application and uses of this approach, which have not previously been described, are the subject of this communication.

Experimental

A suitable synchronizing signal must be obtained if the sampling of the measured signal is to be synchronized with the pulses of the liquid flow. The most suitable method is to use the pressure changes in the tubing beyond the pump produced by the movement of the pump rollers; various pressure sensors can be employed. In this work, a common telephone microphone with a membrane was used as a pressure sensor. A thin-walled tube of flexible material of suitable diameter, forming part of the tubing of the measuring apparatus was led through a hole in the top of the microphone so that it formed a loop pressing lightly on the membrane in the space at the top of the microphone (Fig. 1). A compressing element (e.g., a capillary) can be placed at the outlet of this sensor, to amplify the pressure changes; frequently, however, the hydrodynamic resistance of the subsequent section of the liquid circuit is sufficient. The whole sensor must be acoustically and mechanically isolated from the rest of the apparatus.

Changes in the resistance of the microphone can be sensed by an operational amplifier with a suitable gain (Fig. 1). The residual component of the voltage at the amplifier output corresponding to the normal resistance of the microphone can be compensated by an auxiliary voltage E_a. A bridge-type connection of the microphone can also be employed. After modification of

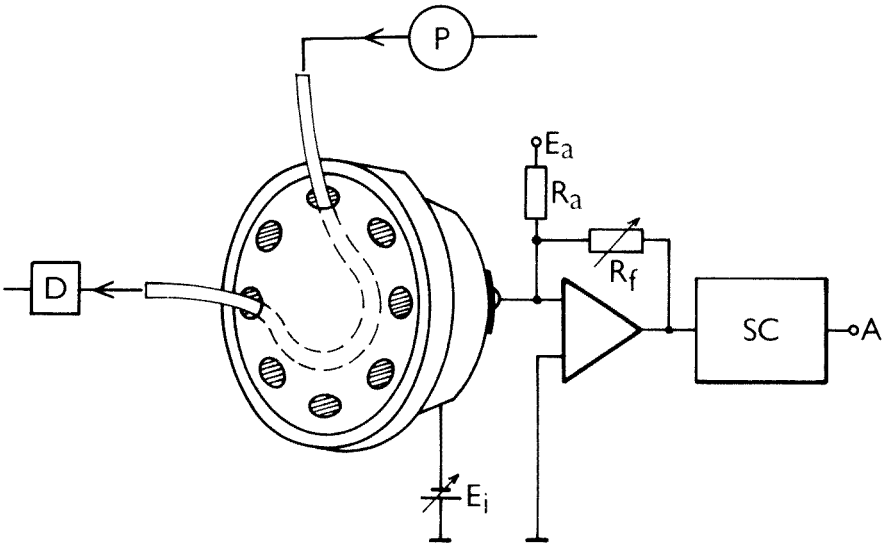

Fig. 1. Microphone pressure sensor: P, pump; D, detector; SC, shaping circuit; A, output of the synchronizing signal.

their amplitude and shape, the resultant synchronizing pulses can be used to control other parts of the apparatus.

The pulses in synchronized sampling of the measured signal can be eliminated by integrating the signal [5] during the sampling period, rather than by simple sampling. A suitable circuit is depicted in Fig. 2(a); its principle is apparent from the course of the impulses controlling the switches. Synchronizing signal A controls the instant of initiation of sampling. When switch S1 is closed and S3 opened, the sampled signal is integrated over time t_{int}. Then the signal from the output of the integrator is transferred to memory M and the integrating capacitor C is short-circuited through switch S3. The impulses controlling the switches are derived from the synchronizing signal using monostable flip-flop circuits (MS1 and MS2) and a NOR gate (G). The time constant RC of the integrator and of the flip-flop circuits must reflect the character of the sampled signal and rate of sampling.

Results

As an illustration of the sampled signal, Fig. 2(b) depicts the stripping curves for the determination of manganese by the cathodic stripping voltammetry (c.s.v.) [6] method. The curves correspond to optimal damping by the

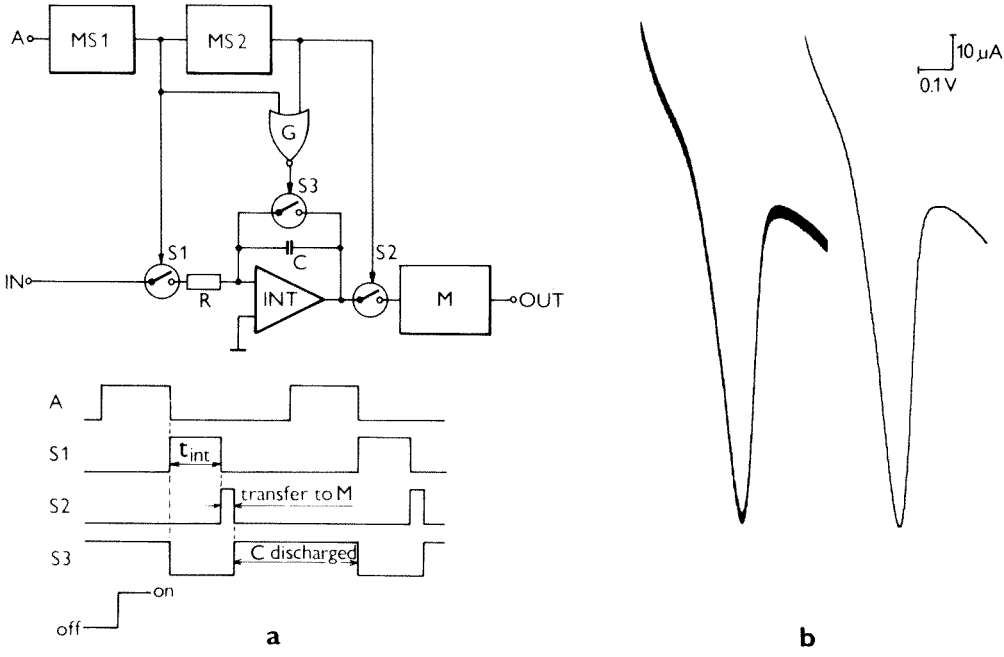

Fig. 2. Circuit for pulse elimination by synchronized sampling of the signal from the detector: (a) electronic connection; (b) damped and sampled stripping *I—E* curve for the determination of Mn^{2+} by the c.s.v. method (5×10^{-6} M Mn^{2+} in acetate buffer pH 5.4, 60-s electrolysis at +1.0 V vs. s.c.e., flow rate 0.22 ml s^{-1}, polarization rate 15 mV s^{-1}, Zalimp 304 pump (Poland) with 6 rollers, rate 45 rpm).

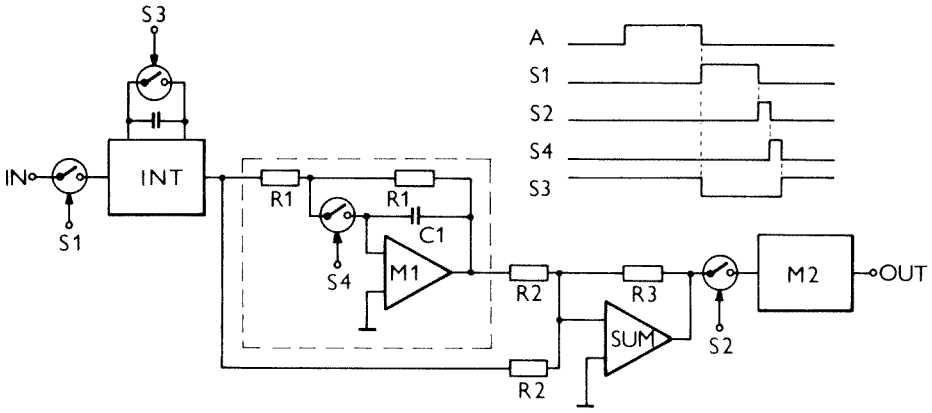

Fig. 3. Circuit for differentiation of the output signal.

RC filter and to the sampled curve. The residual current pulses on the damped curve cannot be eliminated without substantial distortion of the curve shape.

In the chronopotentiometric determination of manganese by the c.s.v. method with automatic reading of the transition times [6], the stripping E—t curves were differentiated. This could not be done by an analog method because of the residual potential pulses; the relatively high pulse frequency was an obstacle, even though the pulse amplitude was considerably decreased by filtration. The derivative curve was thus constructed by using the difference between two successive values of the potential sampled synchronously with the liquid pulses. A scheme of the apparatus and the shape of the pulses controlling the necessary switches are depicted in Fig. 3. (The first part of the circuit with the integrator was the same as in Fig. 2(a).) Analog memory M1 contains the $(n-1)$th sampled potential value. As an inverting operational amplifier circuit is employed in the memory, the signal at its output has the opposite sign to that at the output of the INT integrator. Thus the SUM circuit produces the difference between the $(n-1)$th and the nth sampled value. This difference is stored in the final memory M2 and then fed to the apparatus for automatic measurement of the transition times [7]. The temporal resolution for the differentiated $E-t$ curves is equal to the reciprocal of the number of potential values sampled per second. The time constants of the analog memories must be chosen according to the duration of the corresponding signals controlling switches S2 and S4.

Conclusions

The proposed method of synchronizing signal sampling with liquid pulses in systems with peristaltic pumps permits practically complete elimination of signal pulses without curve distortion. Curve evaluation is thus simplified, as is further treatment in the measuring apparatus. It is possible to synchronize other functions of the apparatus with sampling of the measured quantity, e.g., application of voltage or current pulses, addition of reagent, etc.

REFERENCES

1 L. N. Opheim and W. Lund, Anal. Chim. Acta, 90 (1977) 245.
2 W. Lund and L. N. Opheim, Anal. Chim. Acta, 82 (1976) 245.
3 H. B. Hanekamp, W. H. Voogt and P. Bos, Anal. Chim. Acta, 118 (1980) 73.
4 A. Trojánek and I. Holub, Anal. Chim. Acta, 110 (1979) 161.
5 R. Kalvoda and A. Trojánek, J. Electroanal. Chem., 75 (1977) 151.
6 A. Trojánek and F. Opekar, Anal. Chim. Acta, 126 (1981) 15.
7 F. Opekar, M. Herout and R. Kalvoda, Chem. Listy, 74 (1980) 542.

Analytica Chimica Acta, 127 (1981) 245—249
Elsevier Scientific Publishing Company, Amsterdam — Printed in The Netherlands

Short Communication

RAPID DETERMINATION OF PHENYLALANINE WITH IMMOBILIZED *LEUCONOSTOC MESENTEROIDES* AND A LACTATE ELECTRODE

TADASHI MATSUNAGA, ISAO KARUBE, NOBUAKI TERAOKA and SHUICHI SUZUKI

Research Laboratory of Resources Utilization, Tokyo Institute of Technology, 4259 Nagatsuta-cho, Midori-ku, Yokohama, 227 (Japan)

(Received 15th December 1980)

Summary. A linear relationship is obtained between current decrease and log (phenylalanine concentration) from 5×10^{-5} to 10^{-7} g ml^{-1}. The assay was complete in 90 min with a standard deviation of ca. 6%. Phenylalanine was determined accurately in human blood serum.

Microbioassay has often proved to be advantageous because of its specificity, sensitivity and ability to yield many replicate results almost simultaneously, with very small amounts of samples. Microbioassays are usually based on turbidimetry or titrimetry, but these methods require a long incubation and are affected by contamination with other micro-organisms [1]. Moreover, colored samples cannot be used for the turbidimetric microbioassay. A faster microbioassay by using a lactate electrode has been reported recently [2]. The contaminating bacteria usually do not produce lactate as a metabolite, and so the microbioassay was performed by determining the amount of lactate produced. Phenylalanine could be determined within 6 h.

In recent years, techniques for immobilizing intact micro-organisms have been developed. Several microbial sensors based on such micro-organisms and electrochemical devices have been reported [3—7]. These immobilized micro-organisms can grow and are active for a month in a polymer gel matrix [8, 9]. *Leuconostoc mesenteroides* requires phenylalanine for growth, and produces mainly lactate as a metabolite. A rapid method for determination of phenylalanine by using immobilized bacteria and a lactate electrode is described here.

Experimental

The basic assay medium (Takara Kosan Co.) had the composition listed previously [2]. L-Phenylalanine (Nippon Rikagaku Pharmaceutical Co.), cigarette filters (Japan Monopoly Corporation) and lactate oxidase (Toyo Jyozo Co.) were used. Other reagents were of analytical-reagent or laboratory grade. Deionized water was used in all procedures.

Culture of micro-organisms. L. mesenteroides ATCC 8042 was employed for the assay of L-phenylalanine. It was maintained in peptone—yeast agar and transferred to a fresh medium (pH 6.8) containing 2.5 g of meat extract,

0003—2670/81/0000—0000/$02.50

2.5 g of peptone, 1.0 g of sodium chloride and 1.8 g of glucose. The cells were centrifuged at 5°C and 10,000 *g* for 10 min and washed twice with physiological saline.

Immobilization of micro-organisms. Bacteria were immobilized on an acetylcellulose filter with agar as follows: 20 mg of agar was dissolved in 900 μl of physiological saline in a test tube at 120°C and cooled to 52°C. Physiological saline (100 μl) containing 10 mg of wet intact cells of *L. mesenteroides* was added. The acetylcellulose filter (diameter 1.3 cm, thickness 4 mm) was dipped into the agar solution described above for 20 s, cooled to 5°C and washed with physiological saline. To these immobilized bacteria in a test tube, 1 ml of assay medium (pH 6.8) was added and the test tube was kept at 37°C for 16 h.

Lactate electrode and apparatus. These were as described previously [2].

Assay procedure. Aliquots (0.5 ml) of the double-strength basic assay medium and 0.5-ml aliquots of sample solutions were placed in test tubes with immobilized bacteria (filter gel) prepared as described above. As a blank test, 1 ml of the assay medium was placed in another test tube with another filter gel. All these test tubes were incubated at 37°C for 90 min, and 100-μl of each medium was injected into the measurement system. The currents were continuously displayed on a recorder (Riken Denshi, Model SP-J5C), and the peak currents measured. The differences between the peak currents obtained from sample and blank were calculated.

Determination of phenylalanine in human sera. This was carried out by an automatic amino acid analyzer as described previously [2]. For microbioassay, sera were added directly to the assay medium.

Results

The principle of the lactate electrode has been described previously [2]. A linear relationship is obtained between the current decrease and the lactate concentration (5×10^{-5}—8×10^{-4} g ml^{-1}) at optimum conditions (pH 7.0, 37°C).

L. mesenteroides requires phenylalanine for its growth, and produces mainly lactate as a metabolite. When the lactate produced by immobilized *L. mesenteroides* was determined in a medium containing phenylalanine, the current decrease was greater than that obtained from the blank medium, the current decreasing more with increasing phenylalanine concentration (Fig. 1). The current difference between sample and blank was proportional to the logarithm of the phenylalanine concentration.

Optimum conditions for immobilization. L. mesenteroides was immobilized on acetylcellulose filter with agar gel. The effect of bacterial concentration in the agar gel on the current difference is shown in Fig. 2. The optimum bacterial concentration (wet cells) was 10 mg ml^{-1}. The current difference became very small at high concentrations of bacteria.

As previously reported [6], the concentration of agar employed for immobilization affects the growth of bacteria in the gel matrix. Therefore,

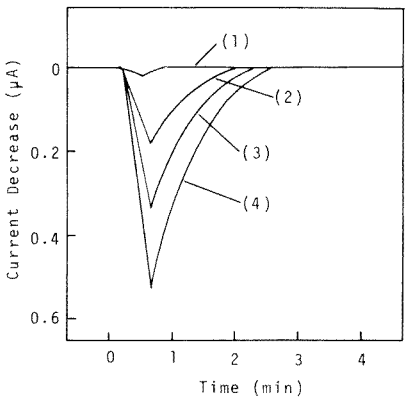

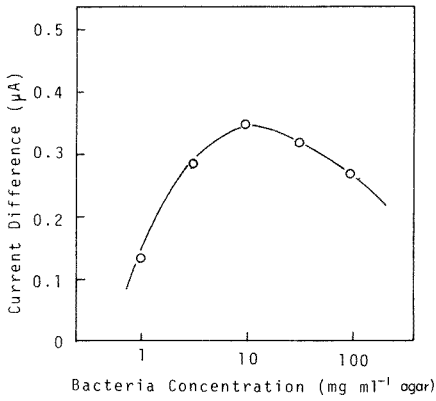

Fig. 1. Response curves of the lactate electrode in the microbioassay medium incubated for 90 min with immobilized *L. mesenteroides* under the recommended conditions. Phenylalanine concentrations (1) 0 (the blank); (2) 10^{-6} g ml^{-1}; (3) 10^{-5} g ml^{-1}; (4) 10^{-4} g ml^{-1}.

Fig. 2. Effect of bacterial concentration on the current difference. The medium contained 10^{-5} g of phenylalanine per ml. The agar concentration was 2% (w/v). The currents were measured after incubation for 90 min at 30°C.

the effect of agar concentration on the current difference was also examined. The maximum current difference was observed at agar concentrations between 2% and 2.5% (w/v); outside that range, changes in the agar gel concentration decreased the current difference.

Time course of the reaction. This is shown in Fig. 3. The current difference first increased linearly with increasing incubation time but approached a plateau after incubation for 90 min. An incubation time of 90 min was therefore selected for the assay of L-phenylalanine.

Calibration. The plot of current difference and logarithm of L-phenylalanine concentration was linear for 1×10^{-7}—5×10^{-5} g of L-phenylalanine in the 1-ml aliquot added with a slope of ca. 0.13 μA per decade. The relative standard deviation was 6% for 20 determinations of 5×10^{-5} g ml^{-1} of phenylalanine.

Application to human sera. The microbioassay system was applied to the determination of phenylalanine in human sera which were also analyzed by the amino acid AutoAnalyzer. For concentrations of 0.01—5×10^{-5} g ml^{-1}, the linear correlation coefficient between the two methods (20 points) was 0.90, the conventional method giving the slightly higher results, probably because of lactate already in human sera.

Storage stability of the immobilized bacteria. Immobilized bacteria were stored in the assay medium. Phenylalanine was determined at 5-day intervals with the stored bacteria. The current difference obtained from each experiment was constant for 20 days. The bacteria immobilized in acetylcellulose with agar are, therefore, active for 20 days.

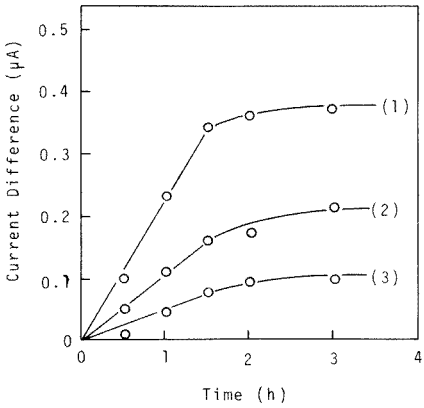

Fig. 3. Effect of time on current difference (10 mg of wet cells per ml, other experimental conditions as for Fig. 2 except for incubation time). Phenylalanine concentrations were: (1) 10^{-5} g ml^{-1}; (2) 10^{-6} g ml^{-1}; (3) 10^{-7} g ml^{-1}.

Discussion

Determination of phenylalanine is required for proper management of phenylketonuria [2]. The serum of phenylketonuremic patients contains more than 6×10^{-5} g ml^{-1} of phenylalanine; for normal individuals, the level is about 1×10^{-5} g ml^{-1} [10]. Phenylketonuria can be detected by the conventional semiquantitative microbioassay [11], but confirmation is required by an amino acid analysis when presumptive positive phenylketonuria is detected, and this requires 3—10 ml of deproteinized serum [12]. In contrast, the calibration graph for the present electrochemical method covers the range 10^{-7}—10^{-5} g ml^{-1}. Therefore, only 50 μl of serum is usually required for the rapid microbioassay with a lactate electrode.

As previously reported [2, 5], a large injection of bacteria shortened the time required for the microbioassay. However, the minimum time was still 6 h, and increased injections did not shorten the incubation time further. The bacteria cannot grow in a medium containing a large amount of the bacteria, yet they can grow in a gel containing a large amount of bacteria. The number of cells increased 1.2—2.0 times during 90-min incubation in the medium containing phenylalanine. Without phenylalanine, bacteria did not grow in the gel. Thus, this microbioassay system is based on the rapid growth of *L. mesenteroides* in the gel. Chloramphenicol is known as an inhibitor of protein synthesis in bacteria. The current difference was very small when chloramphenicol was added to the medium containing phenylalanine, as would be expected.

The diffusion rate of substrates and products through the gel matrix is low [13]. Lactate production by gel-entrapped whole cells occurs mainly at the surface of the gel. Therefore, agar containing *L. mesenteroides* was embedded in an acetylcellulose filter. As this agar-acetylcellulose filter is very porous, the medium and lactate easily permeate through it. Agar is

a natural material with ill-defined crosslinkage, and bacterial growth depends on the pore size of the interstitial spaces. These spaces become filled with bacteria at high concentrations of bacteria, so that further growth becomes impossible and smaller current differences are obtained. An optimal agar concentration (2% w/v) can be explained similarly; further increase above 2% decreases the pore size, and the bacteria cannot grow so well under these conditions.

In conclusion, the determination of phenylalanine is possible within 90 min by using immobilized *L. mesenteroides* and a lactate electrode. This general method can also be applied to the determination of other amino acids, vitamins and antibiotics.

REFERENCES

1 T. M. Berg and H. A. Behagen, Appl. Microbiol., 23 (1972) 531.
2 I. Karube, T. Matsunaga, N. Teraoka and S. Suzuki, Anal. Chim. Acta, 119 (1980) 271.
3 I. Karube, T. Matsunaga and S. Suzuki, J. Solid-Phase Biochem., 2 (1977) 97.
4 I. Karube, T. Matsunaga, S. Mitsuda and S. Suzuki, Biotechnol. Bioeng., 19 (1977) 1534.
5 T. Matsunaga, I. Karube and S. Suzuki, Anal. Chim. Acta, 98 (1978) 25.
6 T. Matsunaga, I. Karube and S. Suzuki, Anal. Chim. Acta, 99 (1978) 233.
7 M. Hikuma, T. Kubo, T. Yasuda, I. Karube and S. Suzuki, Anal. Chim. Acta, 109 (1979) 33.
8 I. Karube, T. Matsunaga, S. Tsuru and S. Suzuki, Biochim. Biophys. Acta, 444 (1976) 338.
9 Y. Morikawa, K. Ochiai, I. Karube and S. Suzuki, Antimicrob. Agents Chemother., 15 (1979) 126.
10 H. A. Harper, Review of Physiological Chemistry, Lange Medical Publications, Los Altos, 1975, p. 401.
11 R. Guthrie, J. Am. Med. Assoc., 178 (1961) 863.
12 D. H. Spackman, Method in Enzymology, Academic Press, New York, 1967, Vol. 11, p. 3.
13 T. Matsunaga, I. Karube and S. Suzuki, Biotechnol. Bioeng., 22 (1980) 2601.

Analytica Chimica Acta, 127 (1981) 251—255
Elsevier Scientific Publishing Company, Amsterdam — Printed in The Netherlands

Short Communication

DETERMINATION OF TIN IN THE PRESENCE OF LEAD BY STRIPPING VOLTAMMETRY WITH COLLECTION AT A ROTATING MERCURY-FILM DISC-RING ELECTRODE

P. KIEKENS, R. M. H. VERBEECK, H. DONCHE and E. TEMMERMAN*

Laboratory for Analytical Chemistry, Ghent University, J. Plateaustraat 22, 9000 Ghent (Belgium)

(Received 28th October 1980)

Summary. Stripping voltammetry with collection at a rotating mercury-film disc-ring electrode is applied for the determination of tin in glassy-carbon methanolic hydrobromic acid solution. The limit of determination is 20 nM (2.3 ng ml^{-1}). Lead does not interfere when the lead/tin concentration ratio is less than ca. 500.

When tin is determined by anodic stripping voltammetry, a serious difficulty is caused by the overlap of the stripping peaks of tin and lead in most electrolytes. Moreover, in many samples lead is present in excess. For this reason, preliminary separations are needed or unusual electrolytes are employed [1—6]. It has been shown [7] that tin can be detected down to ca. 0.2 μM concentrations in the presence of 50-fold amounts of lead by stripping voltammetry with collection (s.v.w.c.) at a glassy-carbon rotating ring-disc electrode. As tin can be easily determined by stripping from a mercury film deposited on a polished glassy-carbon electrode [4], it was thought worthwhile to investigate this technique in combination with collection at a ring electrode.

Stripping voltammetry with collection was introduced by Johnson and Allen [8, 9] and, besides the advantages mentioned by these authors, the technique has been proved to give excellent results [7, 10]. An in situ mercury-plated glassy-carbon disc electrode [11] with a glassy-carbon ring was used here. This mode of preparation of a mercury film was found to give more reproducible results than a preplated film.

Tin(II), leaving the disc as a result of the linearly varying stripping scan, can be detected at an appropriate positive ring potential, where it is oxidized to tin(IV). Lead is also oxidized to lead(II) at the disc but is not electro-active at any positive ring potential used in this study, and consequently does not interfere.

From the Levich equation [12] the charge equivalent to the oxidation current of the electro-active species collected at the ring is given [8] by $Q_r = 0.62\,N\,A\,n\,F\,\nu^{-1/6}\,\omega^{1/2}\,D^{2/3}\,C_b\,T_{dep}$, where N is the collection efficiency [13, 14], A the electrode surface (cm^2), ν the kinematic viscosity ($cm^2\ s^{-1}$), n

0003—2670/81/0000—0000/$02.50

the number of electrons involved, D the diffusion coefficient ($cm^2\ s^{-1}$), ω the rotation speed (rad s^{-1}), C_b the bulk concentration of the analysed species (mol ml^{-1}) and T_{dep} the accumulation time (s).

Experimental

The supporting electrolyte used was 1 M HBr in methanol (30% v/v) [4]. Solutions were prepared with Merck reagent-grade products and water freshly generated by a Milli-Q system (Millipore). Stock solutions of tin(IV) were prepared by mixing the required volume of a warm tin tetrabromide solution with concentrated hydrobromic acid. The tin(IV) solutions were standardized by reduction to tin(II) with zinc amalgam, and titration with a potassium iodate solution. Lead(II) solutions were obtained by dissolving lead chloride in 0.1 M hydrochloric acid. Nitrogen containing less than 1 ppm of oxygen served for deaeration of the test solutions. A mercury film was deposited in situ by adding Hg(II) to the cell solution from a mercury(II) nitrate stock solution (pH 2).

The glassy carbon ring-disc electrode, cell assembly, apparatus and other equipment have been described elsewhere [7]. The disc radius of the electrode was 0.262 cm while the inner and outer ring radii were 0.273 and 0.330 cm, respectively.

The glassy carbon electrode system was polished in the usual way, the final polishing being done with 0.05 μm alumina on Buehler microcloth to a mirrorlike finish. The electrode was rinsed with water and activated in 1 M HBr by cycling the potential between 0.7 and −1.0 V vs. SCE at a scan rate, v, of 0.030 V s^{-1} until a reproducible and very low background was obtained. Then the electrode was transferred to the deaerated test solution. No special treatment of the ring was necessary. An initial potential of 0.6 V vs. SCE was applied to the disc electrode. This potential was maintained for 2 min between successive runs to remove the mercury film. Pre-electrolysis was started by applying the required deposition potential, E_{dep}, to the disc; to obtain a homogeneous mercury film, E_{dep} was fixed at −1 V vs. SCE. During deposition, the potential of the ring, E_r, was held at 0.0 V and switched to the appropriate collection potential 1 min before the end of T_{dep}. At the end of the deposition, the potential of the disc was scanned to +0.6 V. After collection, E_r was returned to 0.0 V. The blank was taken as the charge or peak current obtained for $T_{dep} = 0$, immediately after a scan with finite deposition time.

Results and discussion

Stripping voltammetric curves for tin and lead in 30% methanolic 1 M HBr solution with simultaneous collection of tin(II) at the ring are shown in Fig. 1. The ionization current at the disc arises from the reactions $Pb(0) \rightarrow Pb(II) + 2e^-$ and $Sn(0) \rightarrow Sn(II) + 2e^-$. The peak current appears at approximately −0.53 V vs. SCE. The small displacement of the ring collection peak, where the reaction $Sn(II) \rightarrow Sn(IV) + 2e^-$ occurs, indicates the finite time necessary

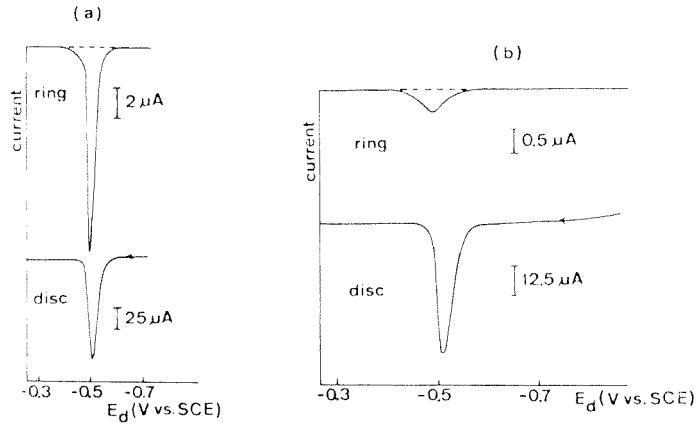

Fig. 1. Current—potential curves for s.v.w.c. in 1M HBr at a glassy carbon-based mercury-film electrode with 0.1 mM Hg(II) and 0.5 μM Pb(II). $E_{dep} = -1$ V vs. SCE; $E_r = 0.7$ V vs. SCE; $T_{dep} = 300$ s; $\upsilon = 0.05$ V s^{-1}; $\omega = 315$ rad s^{-1}. The base-line is indicated by the dashed line. (a) 1 μM Sn(IV); (b) 0.05 μM Sn(IV).

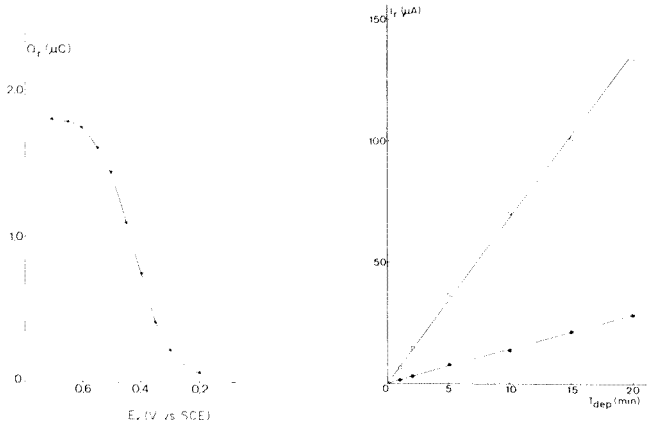

Fig. 2. Dependence of Q_r on E_r for 1 μM Sn(IV) and 0.05 mM Hg(II). E_{dep}, υ and ω as for Fig. 1; $T_{dep} = 60$ s.

Fig. 3. Dependence of I_r on electrolysis time. E_{dep}, E_r, υ, and ω as for Fig. 1. (•) 0.1 mM Hg(II), 0.5 μM Sn(IV), 1 μM Pb(II); (○) 0.05 mM Hg(II), 2 μM Sn(IV).

for the tin species stripped from the disc, to reach the ring. The base-line at the ring is easily evaluated. The best results were obtained with 1—2 M hydrobromic acid as the supporting electrolyte; other electrolytes and other HBr concentrations were less satisfactory. The addition of methanol (30% v/v) considerably improved the reproducibility as already noted by Florence and Farrar [4].

A plot of Q_r as a function of E_r at constant E_{dep} is shown in Fig. 2. The optimal collection potential at the ring was found to be 0.7 V; at more

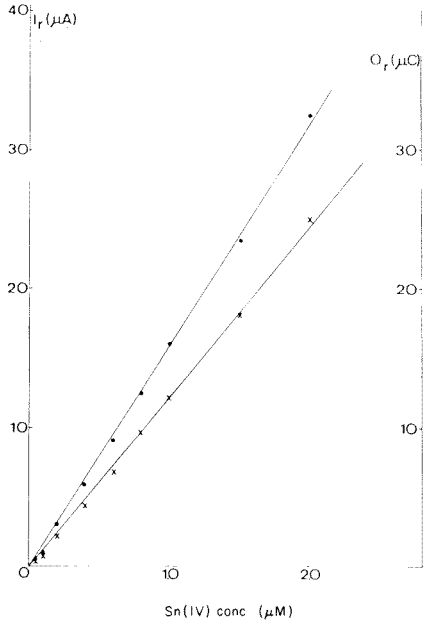

Fig. 4. Dependence of Q_r (×) and I_r (•) on the concentration of Sn(IV) in solution containing 0.1 mM Hg(II), 0.5 μM Pb(II). E_{dep}, E_r, T_{dep}, v and ω as for Fig. 1.

positive values, bromide was oxidized. At this potential, the I_r/I_d and Q_r/Q_d ratios are equal to the collection efficiency N, in the absence of lead.

According to the Levich equation, Q_r is predicted to be proportional to $\omega^{1/2}$ and to be independent of scan rate; this was confirmed experimentally. Figure 3 illustrates the linear dependence of I_r on T_{dep} up to 20 min. The dependence of I_r and Q_r on the concentration of tin(IV) is linear for the range 0.05—2 μM (Fig. 4). The straight lines extrapolate to the coordinate origin and so the standard addition technique is preferred to the use of calibration curves. The relative standard deviations based on four experiments for each concentration given in Fig. 4 varied from 1.1 to 9.5%.

As the aim of this work was to develop a fast method of determining tin in the presence of lead, the influence of adding a large amount of lead was examined. Lead did not interfere significantly when the Pb(II)/Sn(IV) concentration ratio was less than about 500. The collection peaks were not influenced, thus only those peaks need to be recorded and a single pen recorder can be used. The detection limit for tin(IV) was 0.02 μM. More than one ring stripping peak of tin occurred when the amount of lead exceeded the 500:1 ratio, compared to 50:1 on a bare glassy carbon electrode [7]. On glassy carbon a solid lead—tin mixture is present and it is clear that interaction between the metals is considerably weakened when they are stripped from a mercury film. This can be explained by the dilution of the metals in the amalgam and the fact of amalgam formation.

Compared to the previous results with the glassy carbon system [7] the detection limit has decreased by over an order of magnitude. The presence of the mercury on the electrode significantly reduces the difficulties in the electrolytic deposition of ions from very dilute solutions and excellent sensitivity can be attained. In the present case, it has the additional advantage of eliminating, or at least considerably diminishing, interactions between the simultaneously deposited metals so that the voltammetric curves are not distorted during electrodissolution.

P. K. thanks the NFWO for financial support.

REFERENCES

1 Analytical Methods Committee, Analyst, 92 (1967) 320.
2 K. Z. Brainina, Talanta, 18 (1971) 513.
3 V. P. Portretnyi, V. F. Malyuta and V. T. Chuiko, Zh. Anal. Khim., 28 (1973) 1337.
4 T. M. Florence and Y. J. Farrar, J. Electroanal. Chem., 51 (1974) 191.
5 A. Hitchen, Talanta, 26 (1978) 369.
6 S. Glodowski and Z. Kublik, Anal. Chim. Acta, 104 (1979) 55.
7 P. Kiekens, H. Verplaetse, L. de Cock and E. Temmerman, Analyst, 107 (1981) 305.
8 D. C. Johnson and R. E. Allen, Talanta, 20 (1973) 305.
9 R. E. Allen and D. C. Johnson, Talanta, 20 (1973) 799.
10 D. Laser and M. Ariel, J. Electroanal. Chem., 49 (1974) 123.
11 T. M. Florence, J. Electroanal. Chem., 27 (1970) 273.
12 V. G. Levich, Physicochemical Hydrodynamics, Prentice Hall, Englewood Cliffs, NJ, 1962, p. 69.
13 W. J. Albery and S. Bruckenstein, Trans. Faraday Soc., 62 (1966) 1920.
14 D. T. Napp, D. C. Johnson and S. Bruckenstein, Anal. Chem., 39 (1967) 481.

Analytica Chimica Acta, 127 (1981) 257—261
Elsevier Scientific Publishing Company, Amsterdam — Printed in The Netherlands

Short Communication

ELECTROCHEMICAL DETERMINATION OF SULFIDE AND SULFITE IONS BY PNEUMATOAMPEROMETRY

DANTON D. NYGAARD

Environmental Protection Agency — National Enforcement Investigations Center, Building 53, Box 25227, Denver Federal Center, Denver, CO 80225 (U.S.A.)

(Received 8th January 1981)

Summary. Sulfide and sulfite ions in aqueous solution are converted through acidification to hydrogen sulfide and sulfur dioxide, which are purged from solution with nitrogen carrier gas. The volatile species are detected through oxidation in 1 M sulfuric acid at an anodically polarized platinum electrode separated from the gas stream by a gas-permeable polymer membrane. Mixtures of sulfide and sulfite are separated and determined independently through pH control during acidification. Interferences from metal ions, which form sulfide precipitates, and other anions, which form volatile species on acidification, are discussed.

Pneumatoamperometry is a term which has been coined recently [1—3] to describe the general analytical procedure in which some dissolved non-volatile substance is converted to a volatile form through chemical reaction; the volatile form is then purged from solution with a carrier gas and detected electrochemically through oxidation or reduction, with the resulting current being related to the concentration of the original substance in solution. Sulfide and sulfite ion are readily determined by such an analytical procedure, because only acidification is required to convert them to hydrogen sulfide and sulfur dioxide, both of which can be detected through oxidation in acidic medium [4—6] at an anodically polarized platinum electrode. This work utilizes a membrane-covered electrode to bring the gas phase into contact with the electrode and electrolyte.

Experimental

Reagents. All solutions were prepared from ACS Reagent Grade chemicals and deionized, distilled water. Stock sulfide and sulfite solutions were prepared with nitrogen-purged water to minimize oxidation losses, made 0.1 M in sodium hydroxide to minimize volatilization losses, and standardized periodically by titrimetry [7]. Water-pumped, compressed nitrogen was the purge gas.

Apparatus. The purge cell and electrochemical detector are shown in Fig. 1. The purge cell (A) is a 30-ml midget impinger, which is fitted with a medium-porosity fritted glass sparge tube, and to which a screw-capped, septum-covered sidearm is attached. The three-electrode detection cell (B) is a

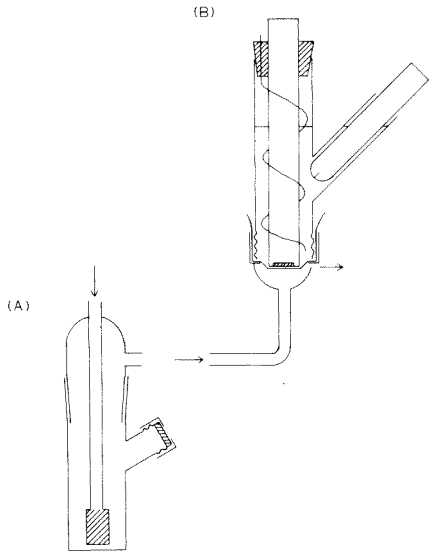

Fig. 1. Reaction purge cell (A) and membrane-covered electrode detector (B). Arrows indicate the direction of purge gas flow.

2 × 9-cm glass tube, which is threaded at one end for a plastic screw cap, and to which a sidearm is attached. The working electrode (Corning Platinum Inlay, 0.5-cm diameter) and counter electrode (12 cm of 15 gauge platinum wire) are inserted through the open end of the tube and held in place with a neoprene stopper. The reference electrode [Corning fiber junction type saturated calomel electrode (SCE)] is inserted through the sidearm. The plastic screw cap is drilled to produce a 1.5-cm diameter hole. A glass flow-through cell (5-ml internal volume) is cemented to the screw cap. A 0.9-mil polyethylene membrane is fitted over the threaded end of the glass tube, pulled snug against the platinum working electrode, wrapped with teflon tape around the threads, and held firmly in place with the screw cap. The cell is filled with 1 M H_2SO_4 electrolyte. The purge cell and detector are connected with a short piece of teflon tubing.

The electrochemical detector is polarized, and the resulting current amplifield; a cyclic voltammetry instrument (Bioanalytical Systems, Inc., model CV-1A) was used. The amplified current was displayed on an Esterline Angus Speed Servo II strip chart recorder. The purge-gas flow rate was monitored with a Matheson No. 602 float type flowmeter, and controlled with a two stage regulator and needle valve. A glass syringe with teflon plunger and teflon-coated needle was used to inject reagents into the purge cell.

Procedure for sulfide. The sample (10 ml) containing sulfide and/or sulfite ion is placed in the midget impinger and made 0.1 M in NaOH to prevent volatilization losses. The detector electrode is polarized at +0.85 V vs. SCE, and the nitrogen purge-gas flow rate is adjusted to 150 ml min^{-1}. A sulfamic

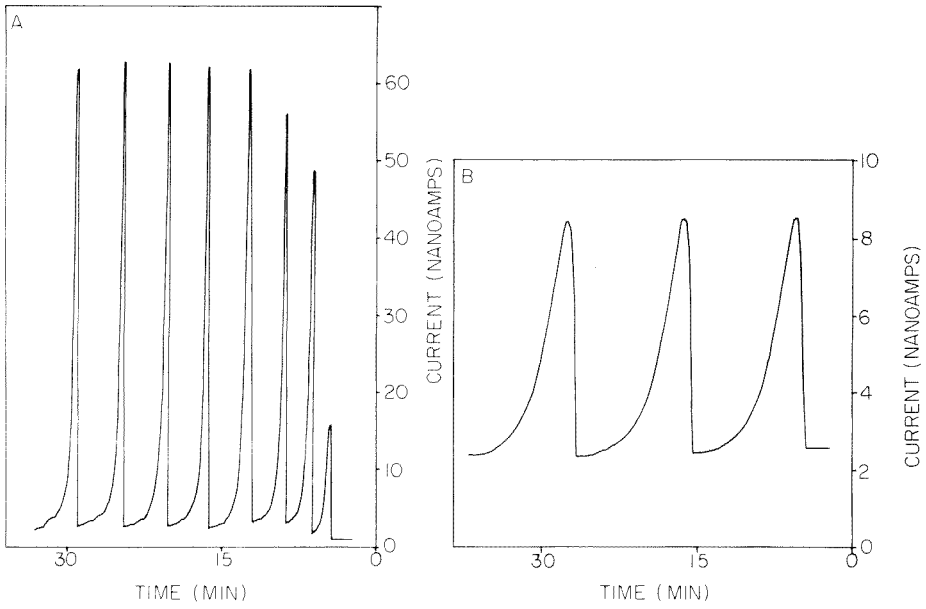

Fig. 2. Detector responses: (A) to eight consecutive samples, each containing 0.5 μmol sulfide ion; (B) to three consecutive samples, each containing 1.0 μmol sulfite ion.

acid solution (1 ml of 0.6% w/v) is added through the sidearm septum to eliminate any nitrite ion present. After a detector baseline current is established, the sample is brought to pH 4.5 by injecting 1 ml of 0.6 M tartaric acid through the sidearm septum. The detector peak current resulting from H_2S evolution is measured and plotted against sulfide ion concentration.

Procedure for sulfite. After all the H_2S has been evolved (but see below), the purge-gas flow rate is increased to 300 ml min^{-1}, and the sample is made 2 M in sulfuric acid by injecting 2 ml of 12 M H_2SO_4 through the sidearm septum. The detector peak current resulting from SO_2 evolution is measured and plotted against sulfite ion concentration.

Metal ion interferences. Possible metal ion interferences were examined by treating samples containing 1 μmol of sulfide and 1 μmol of sulfite with a 10-fold molar excess of the following metal ions: Hg^{2+}, Cu^{2+}, Cd^{2+}, Pb^{2+}, Zn^{2+}, Ni^{2+}, Fe^{2+}, and Mn^{2+}. The above sulfide/sulfite procedure was then applied to each sample.

Results and discussion

Sulfide determination. At the beginning of each day, the detector response to H_2S increases with each succeeding sample until it reaches a constant response after 4—5 samples. At the same time, the background current increases with each sample until it reaches a constant value. This is shown in Fig. 2A. When the detector is allowed to stand without exposure to H_2S for a long time, the baseline current slowly returns to its initial value, and the detector

loses its sensitivity to H_2S (approximately a 10% decrease per hour). Similar results have been reported for an electrochemical gas chromatographic detector for H_2S utilizing a gold electrode [8]. These results are consistent with the literature hypothesis [4, 5] that H_2S is oxidized to sulfur through an adsorbed platinum sulfide intermediate. No sulfide-induced passivation of the electrode has been observed at the polarizing potential used in this work, which is also consistent with the literature [5].

Once the detector has been sensitized by exposure to H_2S, a linear response is observed over the range 0.01—10 μmol of sulfide. For 20 samples in this range, the regression equation is $I_p = (120 \pm 1)\, n_s + 7 \pm 2$ with standard error of 7.6 nA and a correlation coefficient of 0.9996 where I_p is peak current in nA and n_s is the micromoles of sulfide. A relative standard deviation of 0.6% was obtained for five replicate determinations at the 0.5 μmol sulfide level. The detection limit, defined as three times the peak-to-peak background noise, is approximately 0.8 nmol of sulfide.

Other anions such as cyanide, sulfite, and carbonate produce volatile products when acidified (HCN, SO_2, and CO_2, respectively) and nitrite ion is unstable in acidic solution, undergoing disproportionation to nitrate ion and nitric oxide. Of these possibly interfering products, only HCN and CO_2 are evolved at the pH used for sulfide determination, and neither of these is electroactive at platinum in acidic medium [9].

The sulfide ion present in suspended precipitates is detected only if the precipitates dissolve at pH 4.5. Of the metals studied, Hg^{2+}, Cu^{2+}, Cd^{2+} and Pb^{2+} totally suppress H_2S evolution, and Zn^{2+} decreases the rate of H_2S evolution. The other metals produce no effect on sulfide ion.

Sulfite determination. The detector response to SO_2 from sulfite is not complicated by any activation or sensitization effect. A linear response to sulfite is observed over the range 0.1—10 μmol of sulfite. The regression equation for 10 samples in this range is $I_p = (6.0 \pm 0.02)\, n_{SO_3^{2-}} + 1.5 \pm 0.6$ with standard error of 1.4 nA and a correlation coefficient of 0.9999. A relative standard deviation of 0.9% was obtained for six replicate determinations at the 1 μmol sulfite level. The detection limit, defined as above, is approximately 16 nmol of sulfite ion.

The lower sensitivity observed for sulfite as compared to sulfide is due in part to the smaller partition coefficient between the gas and solution phases for SO_2 compared to H_2S (0.01 for SO_2 vs. 0.3 for H_2S). The smaller partition coefficient for SO_2 also results in a longer response time (Fig. 2B). It is to reduce the response time to a reasonable value that the purge-gas flow rate is increased from 150 to 300 ml min^{-1} during sulfite determinations. The relative insensitivity of the method to sulfite ion, combined with the slowly decreasing background current which results after exposure of the electrode to H_2S, makes the sequential determination of sulfide and sulfite ion at the same detector difficult. If determination of both sulfide and sulfite is desired, it is suggested that two detectors be used, one reserved for sulfide and one reserved for sulfite, with the purge gas diverted to the appropriate detector during each determination.

All of the possibly interfering volatile species listed above for sulfide are produced under the acidic conditions employed for SO_2 evolution, and, of course, any sulfide remaining in solution will result in H_2S evolution. Of these, only H_2S and nitric oxide are electroactive, H_2S being oxidized to sulfur as above, and nitric oxide being oxidized to nitrate ion [10]. Nitrite produces not only a positive interference due to evolution of nitric oxide, but it also produces a negative interference by oxidizing sulfite to sulfate ion under acidic conditions. Both positive and negative interferences from nitrite ion are eliminated by addition of 1 ml of 0.6% (w/v) sulfamic acid to the sample prior to acidification [11].

The sulfide procedure (acidification to pH 4.5 and nitrogen purge) eliminates sulfide interference on sulfite, except when lead or cadmium sulfide precipitates are suspended in solution. These precipitates are insoluble at pH 4.5, but dissolve to liberate H_2S under the acidic conditions used for sulfite determination (2 M H_2SO_4). The only recourse in such a case is to remove the precipitates. None of the metal ions studied produces any interference on sulfite determinations. There is tentative evidence that a slight improvement in the sensitivity ratio of sulfite to sulfide could be achieved by measuring peak areas rather than peak heights.

REFERENCES

1 D. D. Nygaard, Anal. Chem., 52 (1980) 358.
2 P. R. Gifford and S. Bruckenstein, Anal. Chem., 52 (1980) 1024.
3 P. Beran and S. Bruckenstein, Anal. Chem., 52 (1980) 2207.
4 E. Najdeker and E. Bishop, J. Electroanal. Chem. Interfacial Electrochem., 41 (1973) 79.
5 M. Faroque and T. Z. Fahidy, J. Electrochem. Soc., 125 (1978) 544.
6 D. T. Sawyer and E. T. Seo, J. Electroanal. Chem., 7 (1964) 184; Electrochim. Acta, 10 (1965) 239.
7 Standard Methods for the Examination of Water and Wastewater, 14th edn., American Public Health Association, Washington, DC, 1976, pp. 505 and 508.
8 J. R. Stetter, J. M. Sedlak and K. F. Blurton, J. Chromatogr. Sci., 15 (1977) 125.
9 D. T. Sawyer and R. J. Day, J. Electroanal. Chem., 5 (1963) 195.
10 D. Dutta and D. Landolt, J. Electrochem. Soc., 119 (1972) 1320.
11 F. P. Scaringelli, B. E. Saltzman and S. A. Frey, Anal. Chem., 39 (1967) 1709.

Analytica Chimica Acta, 127 (1981) 263—269
Elsevier Scientific Publishing Company, Amsterdam — Printed in The Netherlands

Short Communication

POTENTIOMETRIC TITRATION OF FREE ACID IN SALT SOLUTIONS AFTER ADDITION OF POTASSIUM OXALATE AS A COMPLEXING AGENT

P. PAKALNS

Australian Atomic Energy Commission Research Establishment, Lucas Heights, N.S.W., 2234 (Australia)

(Received 30th September 1980)

Summary. An intersect method was used to determine free acid in the presence of Al^{3+}, Hg^{2+}, Fe^{3+}, VO_3^- and Zr^{4+}. Hydrolysis at higher pH values can be overcome by titrating solutions containing Bi(III), Ce(IV), Sb(III), Sn(II), UO_2^{2+} and VO_2^+ to a predetermined pH of 6.05 in potassium oxalate media, if phosphate is absent. The presence of sodium salts requires the use of sodium oxalate.

In the early 1950s, great interest was shown in the determination of free acid in the presence of hydrolyzable cations. Various organic acids, including oxalic acid, were examined as complexing agents for the determination of free acid in inorganic salts used in pharmaceutical preparations [1]. However, it was observed [2] that in some cases if the end-point was taken to be the mid-point of that portion of the potentiometric titration curve having the steepest slope, the results were low. Various modifications were made to improve the detection of the end-point [3—5].

On closer examination, it was apparent that, in the case of aluminium, the potentiometric titration curves were not of the usual S-shape; beyond the point of the steepest slope there was a sudden break. If the top section of the S-curve and the parallel line were extrapolated, then the intersect gave the correct titre of sodium hydroxide required to neutralize the free acid present in potassium oxalate solution. The free acid in salt solutions was determined, according to the behaviour of individual cations, by one of two methods: either by the usual potentiometric titration, or by the intersect plot.

The more suitable sodium oxalate was also investigated as an alternative complexing agent to overcome cation hydrolysis which sometimes takes place in potassium oxalate solutions when the end-point occurs at higher pH values (7.8—9.0), and to determine free acid in ammonium and sodium salt solutions when the amount exceeds 1 mmol per titration. Phosphate must be absent when titrations are carried out at pH 6.05.

Experimental

Apparatus and reagents. A Philips digital pH meter with a combined electrode was used. After each titration, the electrode was immersed for 5 min

in an aqueous solution of pH approximately 1.4 and then for a further 5 min at pH 4.0—5.0. A saturated solution of 200 g of dipotassium oxalate (Merck) in 580 ml of distilled water was prepared (pH ca. 8.3).

Recommended procedure. Transfer a sample containing not more than 1 mmol of cation to a 150-ml beaker. Add 60 ml of potassium oxalate solution and dilute to ca. 80 ml. (For salt solutions containing less than 1 mmol of ammonium ions per titration, add 14 g of potassium oxalate.) If the sample is only slightly acidic or acid-deficient, add 10.00 ml of 0.100 M hydrochloric acid. Insert the electrodes and titrate with 0.100 M sodium hydroxide, while stirring mechanically. In the region of the end-point add the titrant in 0.10-ml increments. Plot the results against the volume of standard base added.

If the potentiometric titration curve has the characteristic S-shape, the end-point is taken as the mid-point of that portion of the curve with the

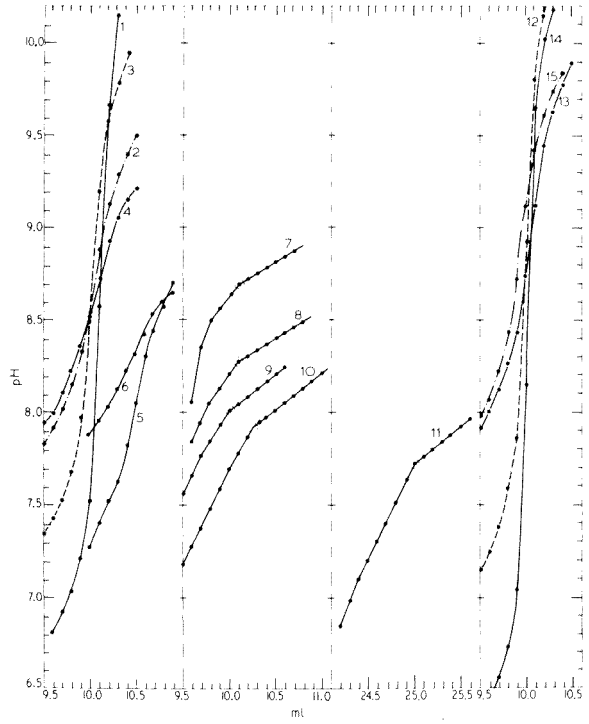

Fig. 1. Titration curves obtained by titrating free acid with 0.1 M sodium hydroxide after addition of potassium oxalate. 10.00 ml of 0.1 M HCl added to salts represented by curves 1, 3, 7, 10, 12 and 14; 10.50 ml to 5; 30.00 ml to 9; and 25.00 ml to 11. 10.00 ml of 0.1 M KH_2PO_4 added to salts represented by curves 2, 4, 8, 13 and 15; 10.50 ml added to 6. 1 mmol of salts used, except for (12—15) where 1 g was added. (1,2) $Ca(NO_3)_2 \cdot 4H_2O$; (3,4) $Th(NO_3)_4 \cdot 4H_2O$; (5,6) NH_4Cl; (7,8) $Al(NO_3)_3 \cdot 9H_2O$; (9) NH_4VO_3; (10) $Fe(NO_3)_3 \cdot 9H_2O$; (11) $ZrOCl_2 \cdot 8H_2O$; (12,13) KCl; (14,15) NaCl in sodium oxalate solution (2 g per 100 ml).

steepest slope. But if a sudden flattening of the curve is observed, add at least an additional 0.80 ml of the titrant to establish the correct slope for this straight line. The end-point is given by the intersect between the top section of the S-curve and the straight line (Fig. 1).

Determine the blank by taking 10.00 ml of 0.100 M hydrochloric acid through the whole procedure. Generally, the addition of 60 ml of potassium oxalate solution will give a slightly smaller sodium hydroxide titre (less than 0.05 ml). Some cations require slightly different complexing procedures; this is discussed below.

Results and discussions

Free acid and acid deficiency. The recommended procedure will titrate the hydrogen ions of hydrochloric, nitric and perchloric acids and the first and second hydrogen ions of sulphuric and phosphoric acids; 1 mol of sulphuric or phosphoric acid will require 2 mol of sodium hydroxide. These free acids can be titrated individually or in various mixtures, and the free acid or acid deficiency can be expressed only as milliequivalents or normality, because the first and second hydrogen ions of an acid cannot be differentiated by this method. The acid deficiency is generally present in one of two forms, either as a metal oxide in a salt, e.g. $HgO \cdot 2Hg(NO_3)_2$, or as solutions to which certain amounts of base have been added, e.g. 1 N acid-deficient aluminium nitrate salting-out solution, $Al(OH)_{0.37}(NO_3)_{2.63}$.

End-point detection. The usual S-shape potentiometric titration curves were obtained for singly- and most doubly-charged ions, and for some triply-charged ions and metal oxyanions. The ions examined were K^+, Na^+, NH_4^+, Ca^{2+}, Cd^{2+}, Co^{2+}, Cr^{3+}, Cu^{2+}, Fe^{2+}, La^{3+}, MoO_4^{2-}, Th^{4+}, WO_4^{2-} and Zn^{2+} (Fig. 1, curves 1—6 and 12,13). The method of intersect was used to determine the free acid in the presence of Al^{3+}, Hg^{2+}, Fe^{3+}, VO_3^- and Zr^{4+} (Fig. 1, curves 7—11). In the case of the intersect method, the end-point is indicated by an abrupt drop in the increase in the pH (about 0.02—0.05) for the addition of 0.1 ml of the titrant. A straight line is drawn through these points on the plot of pH versus titrant volume (Fig. 1, curves 7—11); to obtain the intersect, a second straight line should be drawn through three or four points on the curve closest to the first line. In the titration of free acid with alkali, there is always competition between the metal oxalate complex and the hydroxide, which tends to form when the alkali comes in contact with solutions containing a metal. After the end-point, as determined by the method of intersect, addition of alkali will cause a small increase in the pH because of the formation of hydroxy—oxalate complexes.

When the free acid was determined in salt mixtures containing metals from different end-point detection groups, e.g. Ca + Al, the end-point was determined by the intersect method.

Results for the free acid in various salts using either of these two end-point detection methods are shown in Table 1.

Variations in the procedure. Ammonium ions interfere with the end-point. The effect of up to 1 mmol of ammonium per titration is overcome by the

TABLE 1

Free acid determined in various salts

Salt	Free acid (meq per mmol of salt)	pH at end-point	Salt	Free acid (meq per mmol of salt)	pH at end-point
$Al(NO_3)_3 \cdot 9H_2O$	0.010[a]	8.7	$La(NO_3)_3 \cdot 6H_2O$	0.000	8.6
$Ca(NO_3)_2 \cdot 4H_2O$	0.010	8.6	NaCl	0.000[f]	8.2
$CdCl_2 \cdot 2.5H_2O$	0.000	8.3	$Na_2HPO_4 \cdot 12H_2O$	0.000[f]	9.0
$Co(NO_3)_2 \cdot 6H_2O$	0.000	8.8	$Na_2MoO_4 \cdot 2H_2O$	0.000	9.1
$CrCl_3 \cdot 6H_2O$	0.030	8.6	$Na_2WO_4 \cdot 2H_2O$	0.000	8.3
$CuSO_4 \cdot 5H_2O$	0.000	8.8	NH_4Cl	0.000[g]	8.0
$FeCl_3$ soln.	0.050[b]	8.2	NH_4VO_3	2.00[h]	8.0
$Fe(NO_3)_3 \cdot 9H_2O$	0.025[b]	8.0	$Th(NO_3)_4 \cdot 4H_2O$	0.010	8.8
$Fe(SO_4)_2 \cdot 7H_2O$	0.080[c]	8.0	$ZnSO_4 \cdot 7H_2O$	0.000	8.6
$HgO \cdot 2Hg(NO_3)_2$	2.07[d]	8.2	$ZrOCl_2 \cdot 8H_2O$	0.000[i]	7.7
K_2HPO_4	0.000[e]	8.9			

[a]The same results obtained by method used in [8]. [b]The same results obtained by method used in [9]. [c]Some Fe(II) oxidized to Fe(III); acid-deficient. [d]Sample 0.25 mmol; acid-deficient. [e]Determined on 1 g of sample plus 30 ml of potassium oxalate solution. [f]Determined on 1 g of sample dissolved in sodium oxalate solution (2 g per 100 ml). [g]Determined on 1 g sample by the sodium oxalate method to pH 6.05. [h]30.00 ml of 0.1 M HCl added; acid-deficient. [i]25.00 ml of 0.1 M HCl added.

addition of an extra 14 g of potassium oxalate to the titration solution. The saturated potassium oxalate solution decreases the solubility of ammonium salts and results in good titrations (Fig. 1, curves 5 and 6). A very good end-point can be obtained (phosphate must be absent) if the free acid in an ammonium salt solution (0.5 ml) is titrated in saturated sodium oxalate solution to a pH of 6.05; this is closer to the pH of ammonium oxalate (6.5). When acid deficiency was determined in 1 N acid-deficient aluminium nitrate solution, interference by the ammonium ion in potassium oxalate solution was successfully overcome by the addition of 14 g of potassium oxalate. Then 10.00 ml of 0.1 M hydrochloric acid was added and the excess of acid back-titrated with standard alkali.

Sodium ions in large amounts (>1 mmol) interfere with the true end-point giving a negative error, and the free acid in sodium salts can only be determined by dissolving the salt in sodium oxalate solution at its natural pH of 9.3. To achieve this, 0.5—1.0 g of sodium salt is added to the titration beaker, followed by 2 g of sodium oxalate and 100 ml of water; after dissolution, the titration is done to the potentiometric end-point with 0.1 M sodium hydroxide solutions (Fig. 1, curves 14 and 15).

Calcium and cadmium ions form precipitates after the addition of potassium oxalate. Only 30 ml of the potassium oxalate is required; larger amounts give poor end-points. Chromium(III) forms the oxalate complex very slowly; after the addition of potassium oxalate solution, the solution must be

brought to the boil, and then cooled to room temperature before titration. Mercury(II) hydrolyzes easily near the end-point, but 0.25 mmol could be complexed satisfactorily with 60 ml of potassium oxalate solution. Thorium(IV) hydrolysis near the end-point can be prevented by the addition of 14 g of potassium oxalate; the excess of oxalate forms a soluble thorium oxalate complex and the free acid is readily determined.

Vanadium(V) (VO_3^-) requires the addition of 30.00 ml of 0.1 M hydrochloric acid to 1 mmol of vanadium salt. After 34 g of potassium oxalate has been added, the solution is diluted to 80 ml with water and boiled to dissolve the salt; the solution is then cooled to room temperature, and the excess of acid is titrated with 0.1 M sodium hydroxide. Zirconium(IV) polymerizes in aqueous solutions hence depolymerization by heating with acid is required before it can be complexed with oxalate [6]. Any heating with potassium oxalate solution will reverse the depolymerization. The following procedure maintains zirconium(IV) in a depolymerized form: to 1 mmol of zirconium salt is added 25.00 ml of 0.1 M hydrochloric acid and the solution is brought to the boil, left to cool for 15 min, and then cooled to room temperature; 60 ml of potassium oxalate solution is added and the mixture is immediately titrated with 0.1 M sodium hydroxide (Fig. 1, curve 11).

Effect of metal ion hydrolysis on the end-point. Many metal ions, e.g., Bi(III), Ce(IV), Sb(III) and Sn(II), hydrolyze in water at pH 7, and stable solutions of these species must contain $\geqslant$1 M acid. On boiling with potassium oxalate in the presence of 10 ml of 0.1 M hydrochloric acid, clear oxalate solutions are formed. During titration, a small amount of precipitate was

TABLE 2

The effect of metal ion hydrolysis on the determination of free acid (10.00 ml of 0.1 M HCl added to salts)

Metal ion	Potassium oxalate method[a]		Sodium oxalate method	
	Maximum sample (mmol)	Free acid (meq per mmol of cation)	Maximum sample (mmol)	Free acid (meq per mmol of cation)
Bi(III)	0.5	0.14[b]	1.0	Nil[f]
Ce(IV)	0.25	1.1[c]	1.0	Nil
Sb(III)	0.5	1.1[d,e]	0.5	0.14[f]
Sn(II)	0.5	0.40[d]	1.0	0.01[f]
UO_2^{2+}	0.25	1.2	1.0	0.04
VO_2^{2+}	0.25	0.36	1.0	0.12

[a]End-point determined by intersect method. [b]Sample plus 60 ml of potassium oxalate boiled, then cooled. [c]60 ml of potassium oxalate solution and 14 g of potassium oxalate added. [d]Sample plus 60 ml of potassium oxalate boiled; then cooled. 14 g of potassium oxalate added. [e]End-point determined by the mid-point method. [f]Sample plus sodium oxalate heated to boil, then cooled to room temperature.

noticed when the titrant came into contact with the oxalate solution. Although the precipitate apparently dissolved, a metal hydroxide—oxalate complex had formed, giving a higher result than expected (Table 2). Such cations as UO_2^{2+} and VO_2^{2+} did not form sufficiently strong oxalate complexes, also giving high results. Phosphate ion interfered with the end-point detection to a varying degree; it must be absent when these easily hydrolyzable ions are present.

Hydrolysis at higher pH can be overcome by titrating solutions containing these ions to a lower pH end-point using sodium oxalate as a complexing agent. A modification of a published method [7] for the determination of free acid in the presence of uranyl ions was used. Sodium oxalate solution (100 ml of 0.15 M) was mixed with 2 g of sodium oxalate, and the solution was adjusted to pH 6.05 with 0.2 M hydrochloric acid, the volume of acid added being recorded. A sample aliquot and 10.00 ml of 0.1 M hydrochloric acid were then titrated with 0.1 M sodium hydroxide until pH 6.05 was reached. If necessary, the mixture was boiled and cooled before titration. Any large volume changes were compensated by adding the required amount of 0.2 M hydrochloric acid. Heating to boil was required for Bi(III), Sb(III) and Sn(II). This method is not suitable for the determination of free acid in the presence of phosphate. The results in Table 2 show a significant improvement on the potassium oxalate method because, at pH 6.05, little or no hydrolysis had taken place.

Titanium(IV) interfered by hydrolysis in both the potassium oxalate and sodium oxalate methods.

Conclusions

The determination of free acid in metal solutions by complexing the metal ion with oxalate was studied for several cations; the results show that the following approach is suitable. First, 1 mmol of the metal ion as neutral salt is treated with 10.00 ml of 0.1 M hydrochloric or nitric acid and 60 ml of potassium oxalate solution, and the solution is diluted to 80 ml and titrated with standard alkali. This titration should indicate the occurrence of hydrolysis and the end-point, using either the mid-point or intersect method. Then if the intersect method shows no sharp break in the titration curve, a smaller sample (ca. 0.25 mmol of cation) should be tried. Solutions containing ions which form the oxalate complex slowly must be brought to the boil and then cooled to room temperature. Easily hydrolyzable cations can be maintained in solution during the whole titration by adding more potassium oxalate or by titrating the free acid to pH 6.05 after addition of sodium oxalate.

This method is not applicable to solutions containing ions which do not form strong oxalate complexes, e.g. titanium(IV). Free acid in the presence of phosphate ion can be determined only in solutions containing metal ions which form strong complexes with potassium oxalate. Phosphate will interfere with the free acid determination in solutions containing easily hydrolyzable

cations which, in the potassium oxalate solution, form hydroxide—oxalate complexes near the end-point, and will produce low results when the titration is done in sodium oxalate media to the predetermined end-point at pH 6.05.

REFERENCES

1 P. Karsten and J. van der Spek, Pharm. Weekblad, 85 (1950) 725.
2 M. M. Seniavin and A. M. Sorochan, Tr. Kom. Anal. Khim. Akad. Nauk. SSR, 7 (1956) 246.
3 W. J. Blaedel and J. J. Panos, Anal. Chem., 22 (1950) 910.
4 G. L. Booman, M. C. Elliott, R. B. Kimball, F. O. Cartan and J. E. Rein, Anal. Chem., 30 (1958) 284.
5 USAEC Report TID-7015: 9-012205, 1953.
6 P. Pakalns, Anal. Chim. Acta, 44 (1969) 73.
7 USAEC Report TID-7022: 1.3.1.4, 1964.
8 ASTM Standards, Part 45: C799, 1976.
9 A. Moskowitz, J. Dasher and H. W. Jamison, Anal. Chem., 32 (1960) 1362.

ANALYTICA CHIMICA ACTA, Vol. 127 (1981)

AUTHOR INDEX

(continued from back cover)

Short Communications

Elsevier Scientific Publishing Company, 1981

Printed in The Netherlands.

CONTENTS

(continued on inside page of cover)